

Doctoral thesis

Doctoral theses at NTNU, 2024:5

Bahareh Tajiani

Analysis of Vibration Data and Investigation of Models to Support Maintenance Decision of Rotating Components

NTNU
Norwegian University of Science and Technology
Thesis for the Degree of
Philosophiae Doctor



Norwegian University of
Science and Technology

Bahareh Tajjani

Analysis of Vibration Data and Investigation of Models to Support Maintenance Decision of Rotating Components

Thesis for the Degree of Philosophiae Doctor

Trondheim, January 2024

Norwegian University of Science and Technology
Faculty of Engineering
Department of Mechanical and Industrial Engineering

NTNU

Norwegian University of Science and Technology

Thesis for the Degree of Philosophiae Doctor

Faculty of Engineering

Department of Mechanical and Industrial Engineering

© Bahareh Tajjani

ISBN 978-82-326-7610-1 (printed ver.)

ISBN 978-82-326-7609-5 (electronic ver.)

ISSN 1503-8181 (printed ver.)

ISSN 2703-8084 (online ver.)

Doctoral theses at NTNU, 2024:5

Printed by NTNU Grafisk senter

Preface

This thesis is submitted to the Norwegian University of Science and Technology (NTNU) for partial fulfillment of the requirements for the degree of Philosophiae Doctor. The work was carried out at the Department of Mechanical and Industrial Engineering at NTNU, in Trondheim, Norway. Professor Jørn Vatn from the Department of Mechanical and Industrial Engineering at NTNU was the main supervisor. Professor Anne Cecile Pénélope Barros and Senior Researcher Dr Rune Schlanbusch were the co-supervisors from 18.03.2019 to 03.07.2020 and 03.07.2020 to 29.05.2022 respectively. The Department of Mechanical and Industrial Engineering at NTNU funded the doctoral work.

The target audience of this work includes researchers and practitioners interested in the following areas: remaining useful life (RUL) prediction, accelerated life tests, signal-processing, vibration analysis, stochastic modelling, and maintenance optimization.

Bahareh Tajjani

Trondheim, August 2023

Acknowledgement

The three years of my PhD was full of learning, exploring, ups and downs, and enjoyable moments. I would like to take this moment to thank everyone who supported me during this journey. First, I would like to express my sincere gratitude to my main supervisor, Professor Jørn Vatn, for his constant support, patience, guidance, recommendations, and advice. I hope I can have collaborations with him in the future and learn more and more from him.

I would like to thank my co-supervisor, Senior Researcher Dr Rune Schlanbusch, for having great discussions about signal-processing and helping me understand more about this subject. I would also like to thank Professor Anne Cecile Pénélope Barros. She was one of the best teachers I had during my master's studies. I owe special thanks to her for all her support and encouragement in my academic journey. Furthermore, I thank Viggo Gabriel Borg Pedersen for assisting me in the RAMS laboratory when I started my PhD.

I wish to express my appreciation to my PhD fellows at NTNU, Ewa, Tianqi, Renny, Tom Ivar, Xinheng, Nanda, Arif, Shenae, and Gibran. Having lunch, coffee breaks, and short chats with these people were so heart-warming.

My deep appreciation goes to my colleagues at Equinor in Stjørdal and Bergen. Thank you all for the chats and following up with me. I feel very fortunate to start my professional career with all of you and I look forward to exciting collaborations with you in the future. Special thanks to my manager, Amund Myrseth, whose encouragement paved the way for me to pursue my PhD alongside my professional commitments.

I would also like to thank the administrative staff at MTP department, Kari Elise Dahle, Monica Høgsten, and Linn-Cecilie Felle Brattheim for all the help and assistance.

Warm thanks to all my friends in Trondheim for their friendship, happy, and fun moments together.

Finally, I would like to thank my uncle, Masoud, for supporting me, encouraging me in the toughest moments, and having belief in me. I am humbled and thankful for all your help. Above all, I would like to thank my parents and my little sister for their unconditional help and support. I am deeply grateful to my husband, my best friend, Mehdi, for his understanding and continued love. I feel very lucky to have you by my side.

Thank you,

Bahareh

Summary

This PhD project focuses on analysis of vibration data and investigation of mathematical models to support maintenance decision of rotating components and more specifically roller bearings. The PhD work generally consists of experimental work and mathematical modelling. There are 6 papers included in the thesis. The first 4 papers work on developing a laboratory vibration setup to run accelerated life tests, data-processing, and investigation of prognostic models, while Paper 5 uses the insights gained from previous papers to propose a maintenance optimization model to be able to support maintenance-decisions for systems subject to competing failures. Paper 6 by Alfarizi et al. (2022) studies a random forest technique as a machine learning algorithm for bearings and I contributed in data collection and data processing.

Analysis of vibration data and prognostic models for remaining useful life (RUL) prediction of bearings have been widely studied in recent literature. Bearings are critical components which are widely employed in industrial machines, power generation, and automotive systems. They are often operating in harsh and demanding environment conditions such as high temperature, heavy loads, and contaminated surroundings. Such factors can accelerate the bearings wear and tear, making RUL prediction crucial for an effective maintenance planning, safe operation, and proactive resource management.

RUL prediction of bearings is challenging due to noisy vibration signals, presence of low and high frequency components, nonlinearity of the signals, as well as diversity of fault types and their degradation patterns. In Papers 1-4, we collected the laboratory data, investigated time-domain and frequency-domain statistical features obtained from various signal-processing techniques, and developed deterministic and stochastic RUL prediction models to predict RUL of bearings. Additionally, a comparative analysis was carried out to highlight the benefits of frequency aspect of the vibration signals over time aspect, while the most appropriate health indicators (HI) were proposed for condition-monitoring. Different types of uncertainties were incorporated in the model to address the stochasticity of failure threshold and model parameters. In Paper 5, the findings from previous papers have been used and a numerical maintenance optimization model was proposed for continuously monitored systems that follow a Wiener process. The model is suitable for systems that experience random shocks in addition to internal degradation in their lifetime. A Monte-Carlo simulation-based approach is also developed to validate the results of the numerical model. The “run-to-failure” datasets were collected in Reliability, Availability, Maintainability, and Safety (RAMS) laboratory at NTNU and used in the papers to demonstrate the applicability of the proposed frameworks.

The thesis can serve as a basis for further research and engineering applications from different perspectives. The physical characteristics of bearings (i.e., fault signatures) can be integrated with stochastic models to enhance the RUL prediction performance. Machine learning algorithms such as pattern recognition can be implemented on faulty processed signals for both fault diagnosis and failure prognosis purposes. Moreover, it would be interesting to further improve the maintenance optimization model to consider different maintenance strategies, consider various sources of shocks with varying deterioration rate affected by a change of operating condition, as well as developing the model to take a system-level perspective.

Nomenclature

CBM	Condition-based Maintenance
CDF	Cumulative Distribution Function
CI	Condition Indicator
CM	Corrective Maintenance
CNN	Convolutional Neural Network
CRA	Cumulative Relative Error
EMD	Empirical Mode Decomposition
EUT	Expected Utility Theory
EWT	Empirical Wavelet Transform
FFT	Fast Fourier Transform
FPT	First Passage Time
FT	Failure Threshold
HE	Hilbert Energy
HHT	Hilbert Huang Transform
HI	Health Indicator
HPP	Homogeneous Poisson Process
IG	Inverse-Gaussian
IMF	Intrinsic Mode Function
MCS	Monte-Carlo Simulation
ML	Machine Learning
MLE	Maximum Likelihood Estimation
MRA	Multiresolution Analysis
MTP	Department of Mechanical and Industrial Engineering
NTNU	Norwegian University of Science and Technology
PbM	Physics-based Model
PC	Principle Component
PCA	Principle Component Analysis
PDF	Probability Density Function
PH	Prognostic Horizon
PHM	Prognostics and Health Management
RAMS	Reliability, Availability, Maintainability, and Safety
RMS	Root Mean Square
RPM	Revolutions Per Minute
RQ	Research Question
RUL	Remaining Useful Life
SIF	Stress Intensity Factor
STFT	Short-time Fourier Transform
SVM	Support Vector Machine
TF	Time - Frequency domain
WT	Wavelet Transform

Table of Contents

Chapter 1. Introduction	1
1.1 Problem background.....	1
1.2 Research objectives	4
1.3 Thesis outline	4
1.4 List of Publications	6
1.5 A short summary of the papers	7
1.6 Declaration of Authorship.....	8
Chapter 2. Review of Research Background	11
2.1. Prognostics and Health Management (PHM)	11
2.2. Data Acquisition	12
2.3. Fault Diagnostics and Failure Prognostics.....	16
2.4. Health Management to Support Decision-Making	19
Chapter 3. Research Approach, Materials, and Methods.....	21
3.1. Overview of research approach.....	21
3.2. Experimental Setup.....	21
3.3. Data Description	22
3.4. Methodology.....	23
3.4.1. Signal-processing and RUL Prediction.....	23
3.4.2. Maintenance Optimization	27
3.5. Challenges and lessons learned	27
Chapter 4. Results and Discussion	29
4.1. Paper 1	29
4.2. Paper 2	33
4.3. Paper 3	35
4.4. Paper 4	38
4.5. Paper 5	44
4.6. Summary of Results	47
Chapter 5. Conclusions and Further Work.....	49
References	55
Appended papers.....	65

Chapter 1. Introduction

This chapter provides an introduction to the PhD work. It includes problem background with current challenges, research objectives, thesis outline, a list of publications included in the thesis, and a short summary of the papers.

1.1 Problem background

Recently, a lot of research has been carried out on prognostics and health management (PHM) which is a computation-based paradigm that is gaining interest from both academia and industry. Most of the recent research studies have been within the field of machinery PHM which leads to the development of algorithms for this particular application. The majority of these algorithms focus on common rotary machinery components such as gears and bearings (Lee et al. 2014). Bearings in rotating machinery account for 45% to 55% of the rotating equipment failures and are widely used in many industrial systems such as high-speed trains, aircraft and wind turbine generators (Rai and Upadhyay 2016; B. Zhao et al. 2021; Peng et al. 2022). In PHM, physical knowledge, information, and data must be integrated with model-based and data-driven approaches for anomaly detection, prediction of the behavior, and evolution of systems and components to anticipate and prevent upcoming failures, aiming at a higher reliability and safer operation and maintenance (Zio 2022).

The two key links in PHM are fault diagnosis and failure prognostics. Unlike fault diagnosis which is a well-developed area and it is widely studied in literature, failure prognostics and RUL prediction is still in development with several challenges ahead since they entail significant uncertainty (S. Liu and Fan 2022).

According to the standard ISO 13381-1:2004, prognostics is the “estimation of time to failure and risk for one or more existing and future failure modes” (ISO 2004). However, what we mean by failure here is important to discuss. A commonly understood definition of failure is “inability of a system or component to perform its required functions within specified performance requirements” (Del Frate 2013). The interpretation of failure and determination of failure threshold can vary based on customer needs, the specific application, and context in which a system or component is used. For instance, different systems can have different performance requirements. For one system, a slight degradation might be acceptable and not considered a failure, while for another system even a small degradation from the expected performance can be deemed as failure.

RUL in the same standard is defined as: “remaining time before system health falls below a defined failure threshold”. In other words, it refers to the remaining time until the system reaches a point where it can no longer meet the required performance standards, although it has not completely failed yet. RUL is often a stochastic variable and can vary depending on degradation mechanism, current age of the asset, environmental conditions, and observed health information (Ahmadzadeh and Lundberg 2014). Due to such uncertainties, RUL prediction is often integrated with statistical and probabilistic approaches, and it deals with predicting the entire probability density function (PDF) of RUL rather than a single point estimate. This is particularly important in maintenance optimization to increase reliability, avoid unplanned downtime, and effective decision-making. In literature, two terms of RUL

estimation and RUL prediction are widely used. However, the term “RUL prediction” is a more appropriate term since it is more aligned with the probabilistic nature of RUL. RUL prediction involves various categories of models to predict the probability distribution of upcoming failures. As stated in (Refaee, n.d.), estimation in statistical inference is about using sample data to estimate the model parameters, while prediction refers to using the sample data to predict a new future observation and stochastic variables. An accurate and robust RUL prediction can significantly improve system reliability and operational safety, reduce maintenance costs, and decrease unplanned breakdowns (M. Zhao, Tang, and Tan 2016).

The main focus of this PhD study is the prognostics aspect of PHM to support maintenance decision-making for bearings which its first step is acquiring condition-monitoring data (i.e., vibration data) and its interpretation (W. Wang and Gu 2000).

Different kinds of measurements are considered for condition-monitoring and RUL prediction of bearings such as acoustic, pressure, and temperature. Among them, vibration measurements data is the most common since it is easy to measure and analyze, and it is measured by mounting a sensor on the bearing to sample signals (Wu, Li, and Qiu 2017). Since vibration data from sensors are often contaminated by noise, they can be unusable for direct fault diagnosis and prognostics. A common approach to obtain meaningful data from noisy vibration signals is extracting features (also called characteristics or signatures). Features are generally detected using three main categories of signal-processing techniques: Time-domain, frequency domain, and time-frequency domain (TF) (Yang, Mathew, and Ma 2003).

One of the challenges here is extraction of fault features from the bearing signals and identification of the fault frequency characteristics. The three main groups of TF techniques are Fast Fourier Transform (FFT), Hilbert Huang Transform (HHT), and Wavelet Transform (WT) which are able to turn the signal into a more informative view or domain (Puliafito, Vergura, and Carpentieri 2017). The features extracted from such techniques have a physical meaning and can provide a more detailed representation of the signals by analyzing their frequency content over time, while a single time-based feature cannot comprehensively reflect the true degradation stage of bearings (J. Zhou et al. 2022). The root mean square (RMS) and kurtosis from time-domain are the two widely used features in both academia and industry for fault diagnosis and prognostics. One main disadvantage with simple time-domain features is that, in some applications, they have no obvious variation tendency until the incipient fault or severe fault occurs. Moreover, some features are only effective for a certain type of defect and at a certain stage of the bearing lifetime (M. Zhao, Tang, and Tan 2016). However, the features extracted based on FFT, HHT, and WT have received significant interest due to their effectiveness in analyzing non-stationary and transient vibration signals. The features processed by such techniques can be used further to construct a robust health indicator (HI) for deterioration modeling.

When it comes to prognostics or more specifically RUL prediction of bearings, the approaches are roughly classified into model-based approaches, data driven approaches, and hybrid models (Q. Li et al. 2022). The first group of models exploits the domain knowledge of the system and its failure mechanisms and focuses on stochastically modelling the system degradation in discrete or continuous time. Data-driven methods, rather than relying on the domain knowledge of the system, use a large amount of sensor data to train algorithms to capture degradation trends (Liao and Köttig 2016). Hybrid models is a combination of both data-driven methods

and model-based approaches. Wiener process and Gamma process are the two widely used stochastic models appropriate for degradation modeling which accounts for inherent randomness in the degradation process (Yan et al. 2021).

Another main challenge for both researchers and maintenance employees in industries is determination of a proper failure threshold (FT) for deterioration modelling and RUL prediction which needs a lot of industrial expertise and knowledge. Even if the bearings are of the same size and type, and work under the same operating condition, the type and time of failure may not be the same for all of them. Therefore, HI values of different bearings may have large variations at failure time. One of the reasons for this variation is different degradation curves which can correspond to different fault locations and failure modes such as outer race, inner race, rollers, and cage failure and different incipient fault sizes. Therefore, investigation of a probabilistic FT needs to be emphasized further since it can lead to a more reliable operation of rotating machines (C. Zhao et al. 2020s; Behzad et al. 2020). A number of recent studies focused on developing a stochastic failure threshold for RUL prediction models. Tang et al. (2016) is one of the few researchers who developed a Wiener-based RUL prediction model with a random failure threshold following truncated Normal distribution (TND). However, the uncertainty in the degradation parameters was not considered in their work.

In addition, bearings in rotating machinery, similar to most industrial systems and real-life machines, are often subject to variable operating patterns which includes change of operating parameters and different sources of degradation (Heng et al. 2009). In other words, they are not only suffering from internal deterioration caused by tear and wear, but also, they can be exposed to extreme environment variables and different operational states such as speed and load (Tao et al. 2020).

However, the majority of prediction models in literature are applicable for systems which are exposed to internal degradation (i.e., due to aging), while they do not consider the effect of external events on the system performance (J. Wen, Gao, and Zhang 2018; Y. Li et al. 2021; Liu and Fan 2022). Thus, it is important to incorporate these stochastic factors in modeling the system degradation and maintenance optimization. In this regard, new approaches and models are required to model the system degradation caused by both internal and external causes, while also accounting for the change of operating parameters throughout the system lifetime.

Recent research studies focusing on shock models to find the optimal maintenance policy, can generally be divided into two groups: the first group are the ones that work with systems with continuous states (X. Zhao et al. 2018; Castro, Caballé, and Pérez 2015) and the second group who focused on systems with discrete states (Byon, Ntaimo, and Ding 2010; Gan, Hu, and Coit 2023; Juybari, Hamadani, and Ardakan 2023). However, in literature within the first group, there was a lack of extensive discussion with respect to Wiener-based maintenance models that incorporate lead time into the model, while accounting for both fatal and non-fatal shocks. Although non-fatal shocks will not cause a direct system failure, they can still negatively affect system performance to a great extent. In addition, the impact of maintenance lead time was not discussed in many literature studies while it is significantly important since long lead time can infer several challenges such as critical spare parts unavailability to carry out maintenance and huge production loss (Godoy, Pascual, and Knights 2013; Sarada and Shenbagam 2021; Wakiru et al. 2018).

Given the challenges and discussion above, this PhD research focuses on addressing these gaps by answering the following questions.

1.2 Research objectives

The main goal of this PhD research study is to establish a framework for analysis of bearings vibration data and investigate models to support their maintenance decisions. The main research goal is narrowed down by formulating the following research questions (RQs):

RQ1. How to perform accelerated life tests on roller bearings as one of the most critical rotating components to deal with the lack of run-to-failure data?

RQ2. How can time-frequency signal processing techniques benefit RUL prediction compared to traditional time-domain techniques?

RQ3. How to develop an adaptive RUL prediction framework for bearings that can handle nonlinearity and nonstationary characteristics of vibration signals and treat different kinds of uncertainties?

RQ4. How to propose a maintenance optimization model which can deal with external stochastic shocks in addition to system degradation?

Table 1 shows how the peer-reviewed papers 1 – 6 filled the research gaps and answered the research questions:

Table 1, Link between the papers and the research questions

	Paper 1	Paper 2	Paper 3	Paper 4	Paper 5	Paper 6
RQ1	×		×			
RQ2		×	×			
RQ3				×		×
RQ4					×	

To answer the above research questions, the main sub-objectives of this study are as follows:

- To design and set up an experimental vibration setup which is used to perform accelerated life tests on roller bearings in laboratory operating condition.
- To develop a two-phase numerical framework for feature extraction, deterioration modelling and RUL prediction of bearings and present how frequency-based methods can benefit RUL prediction in comparison with time-based methods.
- Numerical optimization of the maintenance alarm threshold for systems that are exposed to both internal degradation and external stochastic shocks in presence of lead time.

1.3 Thesis outline

Chapter 1 gives an introduction to PHM, the two main aspects of PHM with a focus on prognostics and RUL prediction of roller bearings. It also provides the current challenges faced

by bearings failure prognostics, the outline of the thesis, a list of publications, as well as a short summary of the papers.

Chapter 2 is a review of research background and also presents some important points about our own research work.

Chapter 3 presents research approach, materials, and methods. It also describes the experimental setup and data used in this project. A more detailed literature overview of the signal-processing methods used in the papers is provided in this chapter as well.

Chapter 4 presents the results and discussion of the papers.

Chapter 5 states the conclusion and puts forward some ideas and recommendations for the future.

1.4 List of Publications

Table 2, List of publications

Number	Publications	Status
Paper 1	Tajjani, Bahareh, Jørn Vatn, and Viggo Gabriel Borg Pedersen. 2020. “Remaining Useful Life Estimation Using Vibration-Based Degradation Signals.” In <i>The 30th European Safety and Reliability Conference and the 15th Probabilistic Safety Assessment and Management Conference (ESREL2020 PSAM15)</i> , edited by Piero Baraldi, Francesco Di Maio, and Enrico Zio. Venice, Italy. https://www.rpsonline.com.sg/proceedings/esrel2020/pdf/4793.pdf	Published
Paper 2	Tajjani, Bahareh, and Jørn Vatn. 2020. “Degradation Modelling of Roller Bearings Using Two Different Health Indicators.” In <i>The 30th European Safety and Reliability Conference and the 15th Probabilistic Safety Assessment and Management Conference (ESREL2020 PSAM15)</i> , edited by Piero Baraldi, Francesco Di Maio, and Enrico Zio. Venice, Italy. https://www.rpsonline.com.sg/proceedings/esrel2020/pdf/5812.pdf	Published
Paper 3	Tajjani, Bahareh, and Jørn Vatn. 2021. “RUL Prediction of Bearings Using Empirical Wavelet Transform and Bayesian Approach.” In <i>31st European Safety and Reliability Conference (ESREL 2021)</i> , edited by Bruno Castanier, Marko Cepin, David Bigaud, and Christophe Berenguer. Angers, France. https://www.rpsonline.com.sg/proceedings/9789811820168/pdf/475.pdf	Published
Paper 4	Tajjani, Bahareh, Jørn Vatn. 2023. “Adaptive Remaining Useful Life Prediction Framework with Stochastic Failure Threshold for Experimental Bearings with Different Lifetimes Under Contaminated Condition”, <i>International Journal of System Assurance Engineering and Management</i> . https://doi.org/10.1007/s13198-023-01979-0	Published
Paper 5	Tajjani, Bahareh, Jørn Vatn, Masoud Naseri, “Maintenance Optimization of Systems with Lead Time Subject to Natural degradation and Stochastic Shocks”, Submitted to <i>Reliability Engineering and System Safety journal (RESS)</i> .	Under review
Paper 6	Muhammad Gibran Alfarizi, Bahareh Tajjani, Jørn Vatn, Shen Yin. 2022. “Optimized Random Forest Model for Remaining Useful Life Prediction of Experimental Bearings”, <i>IEEE Transactions on Industrial Informatics</i> . https://doi.org/10.1109/TII.2022.3206339	Published

This thesis is based on the above papers. The papers not included in the thesis are as follows:

1. Tajjani, Bahareh, Razieh Amiri, and Jørn Vatn. 2021. “Risk Assessment of Fires in

Residential Buildings-A Case Study in Norway.” In *31st European Safety and Reliability Conference (ESREL 2021)*, edited by Bruno Castanier, Marko Cepin, David Bigaud, and Christophe Berenguer. Angers, France.

Reasons for exclusion: This paper focuses on a quantitative risk assessment of fires in residential buildings and uses the real data of fires in dwellings in Norway from 2015 to 2020. The paper is not in line with the objective of this PhD study and thus is excluded from the thesis.

2. Liu, Jie, Bahareh Tajiani, Jørn Vatn. 2022. “A comparison study for bearing remaining useful life prediction by using standard stochastic approach and digital twin”, *International Journal of reliability and Safety (IJRS)*

Reasons for exclusion: The paper discusses the RUL prediction of bearings using two stochastic models: Wiener process and Geometric Brownian motion. In this paper, my contribution was in data collection and laboratory work. I assisted the first author to collect experimental data in the laboratory, reviewed the manuscript and gave comments. The contribution is reflected in Paper 1 in Table 2. Thus, this paper is excluded from the thesis.

1.5 A short summary of the papers

This thesis has 6 appended papers which are either published or under review. A short summary of the papers is provided below.

Paper 1

The aim of this paper is to design a vibration setup and implement a set of real-time accelerated life tests on roller bearings for deterioration modelling and developing RUL prediction models. It also demonstrates how to use different time-domain features such as kurtosis, RMS, crest factor, etc., as condition indicators (CI) for bearings’ RUL prediction and how to apply feature selection methods to propose an HI. The RUL of experimental bearings are estimated using two deterministic models and a Wiener process as a continuous-time stochastic model.

Paper 2

The main contribution in this paper is to utilize two different energy-based representative features which are RMS from time-domain and Hilbert energy from HHT signal-processing technique for degradation modelling and failure prognostics of bearings. The performance of features was demonstrated and compared at different stages of bearings’ lifetime and factors influencing the RUL prediction such as the bearing lifespan were discussed.

Paper 3

The goal of this paper is to predict the RUL of bearings using empirical wavelet transform (EWT) and a stochastic Wiener process. The parameters of the Wiener process were assumed to be unknown while they were updated using the bearings’ prior information continuously. The RUL prediction uncertainty has reduced throughout the degradation process using the Bayesian inference approach.

Paper 4

In this paper, a numerical two-stage RUL prediction framework is developed for experimental bearings under contaminated condition. The framework consists of feature extraction stage for building up a health indicator and modelling stage for predicting RUL of bearings while the model's parameters were updated iteratively at each time instant using Bayesian Inference method. At the first phase, various signal-processing approaches have been applied and compared in terms of prediction accuracy and the second phase focuses on stochastically modelling the bearing degradation to predict RUL. The model considers the uncertainty of failure threshold.

Paper 5

The main contribution in this paper is to propose a numerical optimization model to find the optimal maintenance alarm threshold for systems that are exposed to random shocks with stochastic magnitudes in addition to internal degradation. The shock magnitude can be large enough to result in a direct failure where the system goes beyond the failure threshold immediately or it can be smaller and simply increase the degradation level by a random extent. The probability of system failure due to a fatal shock increases as the system approaches the failure threshold. The proposed model is compared with Monte-Carlo simulation (MCS) using a numerical example and a bearings' experimental dataset collected in the laboratory. The optimal maintenance alarm threshold is obtained by minimizing the total expected cost.

Paper 6

This paper proposes an optimized random forest model as a machine learning algorithm for RUL prediction of bearings. It also evaluates the prediction results by comparing the developed method with traditional machine learning algorithms.

1.6 Declaration of Authorship

The declaration of authorship or the contribution to the appended papers is given as follows:

Paper 1: Bahareh Tajiani collected the experimental data, proposed the idea, conceptualized the paper, and wrote the manuscript. Viggo Gabriel Pedersen assisted in developing the vibration setup to collect data. Jørn Vatn provided valuable comments, revised the manuscript, and supervised the work.

Paper 2: Bahareh Tajiani collected the experimental data, analysed the data, proposed the idea, organized, and wrote the manuscript. Jørn Vatn provided valuable comments, revised the manuscript, and supervised the work.

Paper 3: Bahareh Tajiani collected the experimental data, analysed the data, proposed the idea, conceptualized the paper, and wrote the manuscript. Jørn Vatn provided comments, revised the manuscript, and supervised the work.

Paper 4: Bahareh Tajiani collected the experimental data, analysed the data, proposed the idea, organized and wrote the manuscript. Jørn Vatn provided feedback, revised the manuscript, and supervised the work.

Paper 5: Bahareh Tajiani proposed the idea, conceptualized the paper with help from Jørn Vatn, did the data analysis and mathematical modelling, and wrote the manuscript. Masoud

Naseri reviewed the manuscript, provided feedback to the modelling and writing. Jørn Vatn helped with the methodology, supervised the work, revised the manuscript, and gave comments in scientific discussion.

Paper 6: Bahareh Tajiani provided the real-time vibration signals of bearings and preprocess them using a signal-processing approach. The processed data was then delivered to the first author and they were used as inputs to the proposed prediction model. Muhammad Gibran Alfarizi proposed the idea, developed the proposed machine learning approach, organized and wrote the manuscript. Jørn Vatn and Shen Yin supervised the work and gave comments. Bahareh has also written “data description” and “health indicator” sections in the paper, reviewed the manuscript, and commented on that.

Chapter 2. Review of Research Background

2.1. Prognostics and Health Management (PHM)

Prognostics and health management (PHM) is an integrated technology which takes data, information, and knowledge of system's performance, operation, and maintenance as input for anomaly detection and fault diagnosis, as well as predicting the future health state of the system and RUL prediction to dynamically support maintenance decisions (Hu et al. 2022). Adopting PHM enables engineers to proactively take measures to maintain the required availability of systems, improve reliability and safety while reducing cost of maintenance and unplanned downtime (Meng and Li 2019).

Back in time, corrective maintenance (CM) (also called reactive, unplanned, or breakdown maintenance) was the first generation of maintenance which is carried out when the failure has already occurred. The second generation of maintenance which is time-based preventive maintenance (also called planned maintenance) uses the predetermined periodic intervals to prevent upcoming failures regardless of the system health state. However, it may not be very cost-effective when there are a lot of components that have not reached their end of life but get replaced at certain intervals. Thus, to reduce the maintenance and inspection cost, while maintaining a desirable reliability and safety, condition-based maintenance (CBM) has appeared to be the most promising solution. CBM is a new maintenance strategy which repairs the damaged parts based on the actual condition of the equipment and is a key enabling technology of PHM. Figure 1 shows the evolution of maintenance strategies (Kim, Choi, and An 2016).

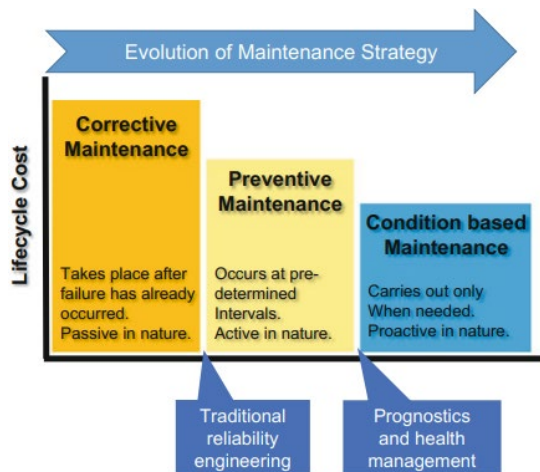


Figure 1, Evolution of maintenance strategies (Kim, Choi, and An 2016)

As discussed before, PHM is a well-established concept for mechanical components such as gears, bearings, and valves, while it has also been extended to more complex systems such as wind turbines and engines. There are different interpretations of PHM framework steps. However, the general PHM framework consists of 4 main steps which are: data acquisition, diagnostics, prognostics, and health management. Figure 2 presents the PHM framework which is adapted from Moradi and Growth (2020).

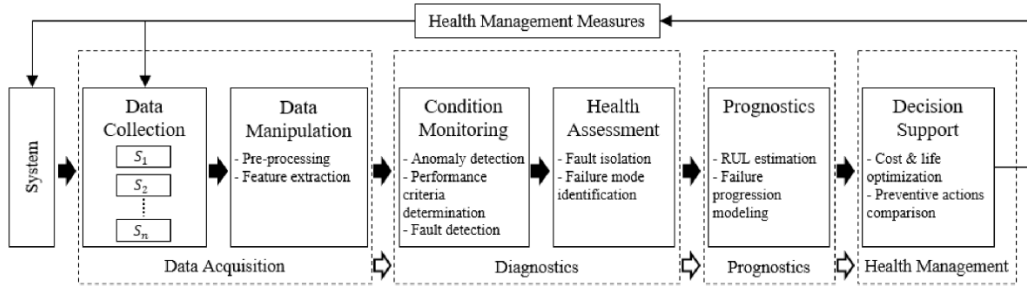


Figure 2, General PHM framework (Moradi and Groth 2020)

2.2. Data Acquisition

There are different datasets of bearings used by researchers for the purpose of developing RUL prediction and prognostics. The most popular one is “IEEE PHM 2012 prognostic challenge dataset” which is publicly open for researchers in both academia and industry to challenge them to come up with diagnostic and prognostic models for RUL prediction of bearings. In this dataset, the experimental platform called Pronostia was used to perform accelerated degradation tests on bearings under controlled operating conditions. The bearings health condition was measured by temperature and vibration in both horizontal and vertical directions. To accelerate the degradation process of bearings, a load is applied on the bearings. As a result, the vibration and temperature data of 7 bearings were collected under the first operating condition (1800 revolutions per minute (rpm), 4000N), 7 bearings dataset under the second operating condition (1650 rpm, 4200N), and 3 bearings under the third operating condition (1500 rpm, 5000N) (Nectoux et al. 2012).

Another bearing dataset is collected by University of Agder (UiA) in Norway and is accessible in (Klausen et al. 2017). The test is carried out within 35 days of continuous driving until the complete failure of the bearing while only the last 7 days of operation is available in the dataset. The degradation mechanism was radial and axial loads applied to the bearing, and the experiment was conducted under low speed.

Another example is NASA bearing dataset provided by the Centre for Intelligent Maintenance Systems (IMS), University of Cincinnati. Three datasets are provided and each dataset describes a test-to-failure experiment. The collected data are vibration signals snapshot recorded at specific intervals (mostly 10 minutes). At the end of experiments, outer race and inner race failures could be observed on a couple of bearings. The motor speed for the experiments was 2000 rpm and a radial load was applied to the shaft and the bearings to accelerate the experiments (Qiu et al. 2006).

XJTU-SY bearing datasets are provided by the institute of design science and basic component at Xi’an Jiaotong university (XJTU) in China (B. Wang et al. 2020). The experiments are conducted on 15 roller bearings and 15 run-to-failure datasets were gathered as a result. Every batch of 5 bearings were operated under a specific radial load and motor speed. The dataset is open to everyone for validation of prognostics algorithms of rolling-element bearings.

As it can be seen from the examples above, applying axial and radial loads or force to the bearing is a common approach to conduct accelerated life tests on such components, since

loading factor can speed up the experiment process to a great extent. However, there are other mechanisms that can cause a bearing failure such as corrosion, particle contamination, and wrong lubrication. According to literature, a large part of bearings failures arises from contamination. Figure 3 shows different percentage contributions of failures in roller bearings where 48% of failures in bearings are caused by particle contamination which is mostly caused by foreign substances from external sources in the bearing lubricant (Khan et al. 2022).



Figure 3, Failure causes of roller bearings (Khan et al. 2022)

There are different sensor measurements for monitoring the health condition of bearings such as acoustic measurements, temperature, and vibration in which the vibration is the most widely used technique in industries that can detect more than 90% of the bearings defects (Malla and Panigrahi 2019). In this PhD work, sensor vibration measurements were collected from bearings which were degraded by contamination of bearings oil.

The acquired data needs to be processed before it can be used for fault diagnosis and failure prognostics. Data processing is required to transform the data into a more structured and clearer format and consequently improve the data quality. As mentioned before, the vibration data have measurement errors and are contaminated with noise. Pre-processing techniques are useful to process the signals and transform them into a number of representative features. Below, the three time-frequency transformation techniques for signal-processing of bearings are briefly discussed.

- **Fast Fourier Transform**

Fast Fourier transform (FFT) and Short-time Fourier transform (STFT) have traditionally been used for anomaly detection and fault diagnosis since they are easier to apply and have a shorter computational time compared to other approaches. FFT gives the frequency spectrum of a signal while the change of frequency ranges in the Fourier spectrum is useful for detecting anomaly in bearings. A possible physical explanation for this frequency change, is the initiation of crack, spall, or other defects on the bearing surface. This method has been used by the center for advanced life cycle engineering (CALCE) in their winning entry for the IEEE 2012 PHM data challenge competition. The anomalies detected by FFT were treated as the degradation starting points for RUL prediction of bearings (Sutrisno et al. 2012). In Xia et al. (2019), the authors developed a two-stage automated approach for prediction of bearings RUL using deep neural network. The input to train the neural network was the frequency coefficients extracted from the frequency spectrum, obtained by applying FFT to the time-domain vibration signals.

A combined method for bearing RUL prediction and fault diagnosis using STFT and convolutional neural network (CNN) is also proposed in (S. Zhou et al. 2020) where the STFT is implemented on raw unprocessed vibration data effectively to avoid the loss of fault characteristics.

However, there are some drawbacks in Fourier transform which makes it less attractive for researchers. For instance, bearing rotor systems have some characteristics such as friction, uneven clearances, and nonlinear stiffness terms which result in nonlinearity in their signals while they are also nonstationary in nature. Non-linear signals are best analyzed in time-frequency domain, where along with frequency content, time information is also retained. However, Fourier transform is not a very efficient method to analyze bearings nonlinear and nonstationary defective signals. In addition, it is also less efficient for detecting inner race faults in bearings which emit very attenuated vibration during the incipient stage of bearings lifetime (V. K. Rai and Mohanty 2007).

In this PhD work, in Paper 4, Fourier transform is employed on the experimental data collected at the laboratory to extract the defective frequency of the signals for feature extraction and degradation modelling. The sensitive frequency band was selected based on variation of frequency in frequency spectrum of the signals which represents the signal energy distribution as a function of frequency.

- **Hilbert Huang Transform**

Hilbert-Huang transform (HHT) is used as an effective method for processing nonstationary and nonlinear vibration signals for RUL prediction of bearings (Huang and Wu 2008). Empirical mode decomposition (EMD) as a part of HHT is a self-adaptive approach which uses the empirical time-based signals to perform the decomposition process. Due to its empirical characteristics, it can reveal the real physical significance of data and thus it is useful to construct health indicators. FFT and wavelet transform (WT) methods need parameter-setting and in some cases, it can be challenging how to select the input parameters and functions (Bian et al. 2022).

There are several research works that use HHT for fault diagnosis and prognosis of roller bearings. However, most of them combine such transformations with machine learning (ML) algorithms. For instance, C Cheng et al. (2022) proposed a failure prognostics framework for bearings by combining HHT and CNN. A nonlinear degradation indicator, called degradation energy indicator (DEI), is extracted from the raw vibration signals using HHT and it has been used as the label for training dataset. The DEI was calculated based on marginal Hilbert spectrum which is a function of bearing defect frequencies (i.e., inner race, outer race, balls, and cage frequencies). In their study, the Pronostia dataset was used to illustrate the proposed framework. Soualhi, Medjaher, and Zserhouni (2014) focused on extracting health indicators using HHT for tracking the bearings degradation, while different degradation states were detected by a supervised classification technique for prognostics. Merainani et al. (2022) developed an indicator, called spectral shape factor (SSF), inspired by spectral kurtosis, then extracted relevant features from SSF, and treated as input to Elman Neural Network.

In terms of fault diagnosis, Thakker et al. (2020) detected different types of bearings faults (inner race, outer race, cage, and ball bearing faults) using a combination of HHT and a fault classification method as an ML algorithm. V. K. Rai and Mohanty (2007) claims that the

conventional FFT may only be sufficient for condition monitoring of bearings. However, for fault detection, it is necessary to employ more advanced signal-processing techniques such as HHT to obtain intrinsic mode functions (IMFs), and apply FFT on the IMFs, to improve the fault detection process. They have argued that the combination of HHT and FFT can increase the effectiveness of this technique in detection of different defects in roller bearings robustly. This is useful to gain insight into the dominant frequency associated with each intrinsic function while enhancing the time-frequency resolution.

- **Wavelet Transform**

Wavelet transform (WT) is useful in converting the complex vibration signals into more simplified signals with higher resolution as well as determining the frequency with defect characteristic in bearings. WT examines acceleration signals using several wavelet basis functions. The selection of this function and the number of decomposition levels in the denoising process are crucial factors for extracting the fault features and affect the performance of fault detection process (Lin and Qu 2000).

Empirical Wavelet Transform (EWT) was proposed by Jerome Gilles (2013) for the first time to enhance the performance of conventional WT. Unlike EMD, EWT focuses on decomposing signals based on their frequency domain and it segments the Fourier spectrum of the signal, instead of the signal itself (Chen et al. 2016). The statistical features from wavelet coefficients can then be fed into ML algorithms such as support vector machine (SVM) and artificial neural networks (ANN) (Kankar, Sharma, and Harsha 2011). Among recent literature that used this method, Wenbo Wang, Zhao, and Ding (2022) proposed an improved EWT and one-dimension CNN to overcome the problem of too many spectrum division in conventional EWT process. In this method, first, the mutual information value was used to redetermine the frequency band boundaries obtained from EWT and keep the ones that are highly correlated. Secondly, the effective coefficients from improved EWT are selected based on kurtosis index to extract multi-dimensional features and train CNN algorithm for RUL prediction. Zhu, Chen, and Peng (2019) focused on RUL prediction of bearings where the time-frequency representation of the acquired time-series signals was extracted using WT and were further regarded as inputs to deep learning models. In addition, Guo et al. (2022) developed a hybrid RUL prediction framework for roller bearings by integrating long short-term memory (LSTM) and EWT to improve the prediction accuracy or reduce the deviation between the actual RUL and the predicted RUL. The framework consisted of three main steps. Firstly, the raw vibration signals were stationarily decomposed into IMFs. Secondly, the representative IMFs with the most degradation characteristics were selected based on weighted energy entropy criteria, and thirdly the selected IMFs were regarded as inputs to the network model. In all the aforementioned studies, Pronostia dataset was used as a real-time case study to illustrate the works, and RUL prediction models were based on neural network variations and other ML approaches. Liu and Chen (2019) provides a general review of recent advancements in EWT and its applications. In Paper 3 and Paper 4 in this thesis, EWT approach was employed for feature extraction and modelling the stochastic deterioration of bearings with different lifetime.

In existing literature, the joint combination of stochastic approaches and signal processing transformation techniques is rare. The majority of research focused on employing machine learning and neural network algorithms to address fault classification, diagnosis, and RUL prediction of rotating components (Zhu, Chen, and Peng 2019; J. Liu et al. 2021; X. Li, Ding,

and Sun 2018), while in few other studies, statistical models such as linear regression and exponential model have been applied or the authors worked on stochastic models such as non-linear Wiener process while they did not consider the frequency aspect of vibration signals (Ahmad et al. 2019; Thoppil, Vasu, and Rao 2021; J. Wen, Gao, and Zhang 2018). Thus, in Paper 4, we combine the wiener-based stochastic model with the three different frequency-based signal-processing techniques for predicting the RUL of experimental bearings, while the uncertainty of failure threshold and the key parameters of the model are also incorporated in the model. Additionally, in Paper 2, the Hilbert energy which presents the energy of the signals in frequency domain has been used and compared with simple time-based RMS feature in terms of RUL prediction. Although, the data in this paper was so limited, it could shed some lights on the performance of HHT in RUL prediction in comparison with time-domain technique at different stages of the bearing lifetime.

2.3. Fault Diagnostics and Failure Prognostics

Fault diagnostics and failure prognostics are the two important aspects of the general PHM framework. Fault diagnostics means the process of fault detection and isolation of faults and failures while failure prognostics focuses on estimating the system future state based on the historical and current condition of the systems (Ly et al. 2009). There are different techniques for fault diagnostics and RUL prediction which is the core of failure prognostics. Since fault diagnostics is out of the scope in this PhD work, we only focus on the prognostics part. An, Kim, and Choi (2015) classifies the prognostic models into three categories of: data-driven, physic-based, and hybrid models as presented in Figure 4.

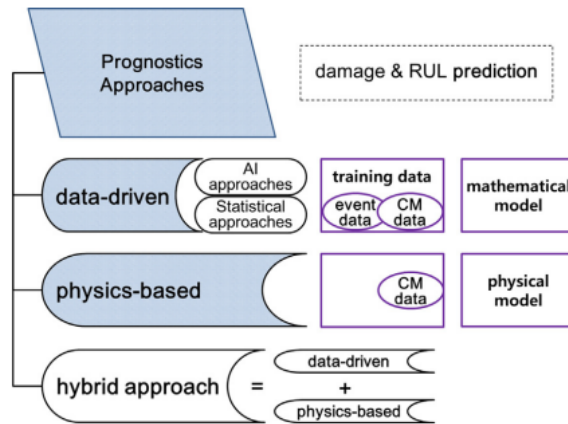


Figure 4, Classifications of prognostic methods (An, Kim, and Choi 2015)

- **Data-driven Approaches**

Data-driven models track the dynamic behaviour of roller bearings in real-time using condition-monitoring sensor data to identify the characteristics of its damage behaviour and predict the future degradation process. Data-driven approaches are divided into: 1- statistical and stochastic models that include Gamma process, hidden Markov model, and regression-based model such as Gaussian process (GP) regression and least square regression, and 2- machine learning and AI algorithms that include neural networks and fuzzy logic (An, Kim, and Choi 2013).

Statistical and stochastic models use a dataset to fit a degradation model to the item's condition from a healthy state to the failed state. Some examples of this classification are deterministic trend models and stochastic processes (José and Torres 2022). To depict the random impact from internal and external environment, stochastic models are good candidates for deterioration modelling. Recent literature has shown that Wiener process, Gamma process, and Inverse Gaussian (IG) process are the most suitable and widely used models for failure prognostics (Ye, Chen, and Shen 2015). Gamma process is suitable for degradation modelling of systems that have monotonic sample paths while a distinct feature in Wiener process is that its sample path is not necessarily monotone (Ye and Chen 2014).

Unlike statistical and stochastic approaches, machine-learning techniques aim to use data with an automated model building, they often need massive data to train the prediction model, and have a relatively high calculation cost (Cui et al. 2020). However, they gained significant attention due to development of sensors, sensors network, and computing systems. A key difference compared to statistical and stochastic models is that here the PDF of RUL is not estimated, while the prediction uncertainty is evaluated using the error estimated based on validation dataset (José and Torres 2022).

There have been extensive research works regarding RUL prediction of roller bearings with data-driven techniques. Ren et al. (2018) proposed a new RUL prediction method for bearings using deep convolutional neural network where a new feature extraction method named spectrum-principle-energy-vector is used to obtain the eigenvector of the signals. The new method based on deep CNN has improved the prediction accuracy significantly. Nie et al. (2022) also developed a RUL prediction framework for bearings by using a one-dimension CNN method and similarity feature fusion. The similarity feature is extracted based on the correlation between time-series data and the statistical features. The eligible features are then used to construct a HI, and the HI is utilized to train the RUL prediction model. Cheng et al. (2020) developed a data-driven framework for RUL prediction of bearings by combining the HHT method to extract a nonlinear degradation indicator and CNN to reveal the hidden pattern between the energy indicator and the raw vibration data.

With respect to statistical and stochastic models, Le Son et al. (2013) proposed a health indicator based on principle component analysis (PCA) and modelled the degradation of bearings using Wiener process where the failure threshold is assumed to be constant. The 2008 PHM challenge dataset has been used to illustrate the effectiveness of the proposed method. The HI built on PCA was based on time-domain data where the frequency domain of the vibration data was not considered. Wang, Liao, and Ma (2022) developed a stochastic multi-phase modelling and health condition monitoring method for multi-component systems based on degradation branching processes which basically follow a Wiener process. The gradient of RMS was used as the HI and the failure threshold was a constant value in degradation modelling. The importance of each component in terms of its effect on the system's performance and safety has been reflected using a weight scoring function. Wang et al. (2022) proposed a data-model-fusion prognostic framework which consists of three main steps to predict the RUL of bearings. The first stage was dedicated to detection of abnormal fluctuations in time-series data and the second stage focused on determination of the starting prediction time while stage three predicted RUL using exponential degradation model. The prediction was based on the period of life from when the degradation has started until it crosses the failure threshold. However, the authors did not address the frequency aspect of vibration signals as

well as the stochasticity in model parameters and failure threshold. In (Y. Wen et al. 2018), the authors developed a multiple change-point Wiener process to consider the various phases of bearing degradation process while a full Bayesian approach was applied to account for the randomness of the model parameters. They also used time-domain RMS as the HI for RUL prediction.

Within the prognostic models, this PhD work focused on statistical and stochastic processes category. More specifically, variants of Wiener process are used in the appended papers 1-5, while Paper 6 applies a machine learning algorithm for RUL prediction of bearings.

- **Physics-based Models**

Physics-based models (PbM) are the ones that use degradation models based on the physical laws, rules, and a set of equations derived from engineering and science knowledge, which describe the damage behaviour of the systems. The Performance of PbM depend on their capability to accurately represent the failure and degradation phenomena. Cubillo, Perinpanayagam, and Esperon-Miguez (2016) gives a detailed review of physics-based models for fault diagnosis and prognostics of rotating bearings and gears. Normally, for diagnostics of bearings and gears, the faults are detected by comparing the output from PbM and the real measurements from the system. For instance, to classify the bearing defects, the natural defect frequencies which are obtained from knowledge of the physics of the bearing can be compared with the system's real measurements to find out deviations. In their review article, they also discuss different prognostic models for bearings depending on various degradation mechanisms such as fatigue, creep, wear, and excessive load. Paris law is one of the widely used physics-based models for crack growth detection and prediction in mechanical materials (Qian, Yan, and Gao 2017). The empirical crack growth model based on stress intensity factor (SIF) was first proposed by Paris, Director, and Erdogan (1963) and is described as follows:

$$\frac{dl}{dN} = C_0(\Delta K)^n \quad (1)$$

where l is the crack length, N is the fatigue life, ΔK is the amplitude of SIF, and C_0 and n are material constants which depend on environment, stress ratio, temperature, and frequency and are obtained empirically (José and Torres 2022).

One of the constraints in physics-based models is that they require explicit analytical understanding of the system damage evolution which can be challenging in complex equipment. In addition, from a time-scale perspective, PbM describes the physical state evolution on a slow time-scale (i.e., focusing on the long-term behaviour of the system) while data-driven techniques gather real-time data from sensor measurements and thus reflects the characteristics of a dynamical system on a fast-scale (i.e., focusing on short-term variations) (F. K. Wang and Mamo 2019).

- **Hybrid Models**

Hybrid models combine the aforementioned categories to improve the prediction performance. Developing a hybrid approach can combine the strength of both data-driven and physics-based techniques to model the deterioration of a dynamical system consisting of both fast and slow time-scales (F. K. Wang and Mamo 2019). There are several research studies that worked on

hybrid models particularly for rotating bearings. For instance, P. Wang, Long, and Wang (2020) developed a hybrid RUL prediction model for bearings in wind turbines. They extracted time-domain and frequency-domain features, selected the most appropriate features for degradation modelling based on Spearman correlation analysis, and fused the selected features using PCA to come up with a single HI. The RUL is then estimated using an exponential degradation model. PCA helps to reduce features dimension and fuse the features by combining them as a linear function which captures the maximum variance in the data. B. Wang et al. (2020) also proposed a hybrid approach by integrating relevance vector machine (RVM), exponential degradation model, and a Fréchet distance to accurately predict RUL of roller bearings.

2.4. Health Management to Support Decision-Making

According to de Almeida and Bohoris (1995), decision theory is concerned with identification of an action which is expected to provide maximum benefits to a decision-maker. Decision-making process is derived based on the objective of the decision-maker and the knowledge of the problem. In decision-making process, a framework is provided where the ideas of the decision-maker get critically evaluated and modified, especially when new information should be incorporated to the problem.

Maintenance optimization supports maintenance decision-making which is the final step of PHM and consists of using different mathematical models to find an optimum balance between the costs and benefits of doing maintenance, while taking all different constraints into account (Dekker 1996). In existing literature, the objective function for maintenance optimization is often based on minimization of asymptotic expected cost rate, while some researchers work on utility function. The asymptotic cost rate is defined as the expected total cost in one renewal cycle divided by the length of the cycle. For instance, Ko and Byon (2017) proposed an analytical method to schedule maintenance activities for a large-scale system with many homogeneous units based on minimizing asymptotic cost rate. Their proposed method is specifically suitable for units with discrete states. In (Cao, Luo, and Dong 2023), the authors develop a framework for condition-based maintenance optimization for systems with discrete states that suffer from both hard and soft failures where the dependency between the failure processes is taken into account. They develop a Monte-Carlo simulation to find the optimal maintenance action times with respect to minimum inspection cost. Another research work is (Koutras, Malefaki, and Platis 2017) in which the authors develop a generic model for optimization of inspection time in multi-state systems where the inspection is carried out regularly to determine whether minor or major imperfect maintenance needs to be performed based on type of failure or degradation level. The minor maintenance means the system goes back to its previous state and major maintenance means the system returns to as good as new state.

Although minimizing expected cost rate is often reasonable for most cases and it leads to minimization of the long run cost given the ability to absorb any losses, some people use expected utility theory (EUT) for optimization problems. EUT is a framework to take into account risk attitudes when there are different possible alternatives with uncertain outcomes. In cases when there are severe consequences for various alternatives, optimizing maintenance based on minimizing expected cost rate is not very desirable (Pedersen and Vatn 2022). Vatn and Aven (2009) also developed an overall model for maintenance optimization which

considers different aspects for decision-making such as maintenance costs, loss of production cost, and environmental effects. Such a general global model needs expertise from reliability managers, risk analysts, and decision-makers and needs a good communication to ensure that they come into an agreement to make the decision and fully understand why one decision is preferred to another. The objective of such a global approach can be based on utility in net profit within a certain time interval.

Optimization of maintenance policy can get more complicated in presence of random delays in engineering systems (X. Zhao et al. 2018). Random delay (also called lead time or logistic delay time) is the time needed to mobilize the necessary resources such as personnel and spare parts to complete the maintenance action. Lead time accounts for a large part of maintenance time and maintenance cost in some assets. An example is offshore wind turbines where the cost of having personnel and spare parts readily available is quite high depending on location of spare parts (e.g., central or distributed warehouses) and means of transport for personnel (e.g., boat or helicopter) (Pedersen and Vatn 2022). Considering lead time in deriving maintenance optimization model is very important since long lead time can infer several challenges such as huge production loss and unavailability of the system (Sarada and Shenbagam 2021; Godoy, Pascual, and Knights 2013).

Furthermore, since maintenance decision-making is based on the system's degradation information, it is important to come up with a model which can represent the real degradation process of the system with less uncertainty. In reality, the majority of real industrial systems inevitably suffer from external shocks. In the example of offshore wind turbines, the shocks can be caused by harsh marine environment such as icing, wind, and wave shocks (Shafiee, Finkelstein, and Bérenguer 2015). Some research studies involved external shocks in maintenance optimization (Shafiee, Finkelstein, and Bérenguer 2015; Gan, Song, and Zhang 2022; Qi and Huang 2023). Among the existing literature, a number of researchers including (Gan, Hu, and Coit 2023), worked on systems with multistate degradation process using variations of Markov processes. The recent stream of articles that studied maintenance optimization of continuously monitored systems were mostly based on Gamma process (X. Zhao et al. 2018; Dong et al. 2020). For instance, Jin et al. (2023) focused on simulating the equipment condition following Gamma process, taking multiple stochastic external events into account to propose a model for maintenance optimization.

Following the above discussion, in Paper 5, we developed a numerical maintenance optimization model based on expected asymptotic cost rate for systems that are continuously monitored and exposed to external random shocks to find the optimal maintenance alarm threshold. The shocks can either have large magnitudes and lead to a direct system failure or they can have small magnitudes and simply increase the degradation level by a random extent. The model considers a constant lead time before maintenance implementation. Monte-Carlo simulation was used to validate the proposed model, while a numerical example and the laboratory dataset were used to show the applicability of the proposed framework.

Chapter 3. Research Approach, Materials, and Methods

3.1. Overview of research approach

There were different activities and phases in this PhD work which resulted in different outcomes. During the first half of the PhD period, the focus was on PhD mandatory courses, literature review, and regular supervision meetings with my supervisor to clarify the way forward. The literature review was conducted mostly based on academic articles from journals and conference proceedings on maintenance modelling, RUL prediction, accelerated life tests, and maintenance optimization. Relevant textbooks were also used to read and learn the different methods in more detail. This has resulted in formulating the problem and developing ideas, approaches, as well as the experimental dataset. Throughout the project, the ideas and results were shared through RAMS seminars at NTNU and conferences to discuss with others and get feedback on the work. In addition, the experimental setup was redesigned to fit the research purpose and the experiments were conducted in RAMS laboratory. During the second half of the work, the focus has gradually shifted towards writing papers for academic journals, as well as having discussion and collaboration with other PhD students. Figure 5 presents the overview of the overall PhD research approach.

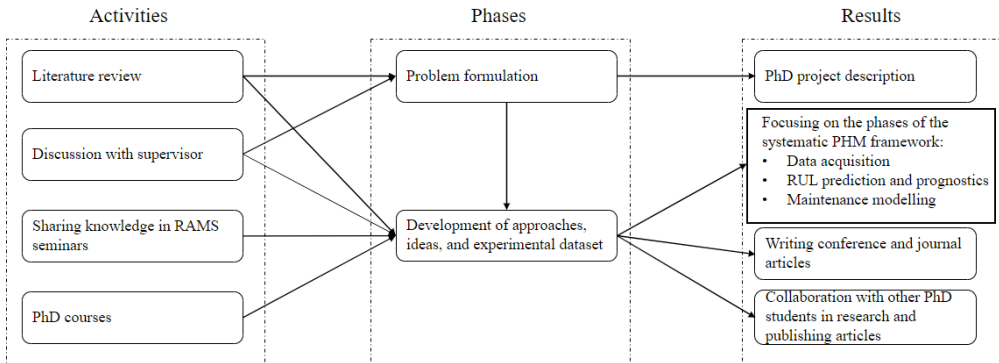


Figure 5, Overall Research Approach (inspired by (Zikrullah 2022))

Below, there is a summary of the experimental setup, data description, and the research methods in more detail.

3.2. Experimental Setup

The vibration setup is called “Bently Nevada (system 1) Rotor Kit, model RK4” which has been designed for training purpose in RAMS laboratory at NTNU. It has been used as a part of this PhD to conduct accelerated life tests on roller bearings and investigate RUL prediction models. The main components of this setup are an amplifier (type 5134B), 10-nm-long bearing shaft, bearing houses mounted on the two sides of the shaft, and the accelerometers (type 8702B100). The bearing house on the left side of the shaft is used to hold the experimental bearing which runs until failure. Following ISO 10816-7: 2009, the two miniature accelerometers are mounted radially and axially to measure acceleration over time in both horizontal and vertical directions. The data are then transformed to the central system which

visualizes the data on the screen. The rotating part of this setup is an asynchronous motor, which is used as an actuator that allows the inner race, rollers/balls, and the bearing cage to rotate through the entire system. The setup is mounted on an aluminium platform with a safety cover to be used while running experiments for safety issues. The maximum rotational speed that the motor can handle is about 10^4 rpm.

According to ISO 15243:2017, the two important failure mechanisms in bearings are wrong lubrication and contamination. In this work, the contamination has been selected as the degradation mechanism to degrade the bearings, since it can speed up the experiment process. Contamination is mixing solid Silicon Carbide (called BW F240, Coulter particles, with the average size of $50 - 52 \mu m$) and lubricant oil to pour into the bearing at predefined time intervals (i.e., every 25 minutes) until the acceleration amplitude reaches $10g$. Running experiments with the acceleration above $10g$ can cause damage to the vibration setup. Thus, in light of the discussion surrounding RUL prediction in Section 1.1, $10g$ is arbitrarily selected assuming that the bearing has reached its operational lifespan, where the bearing “useful” life has surpassed, and it can no longer fulfill its intended purpose. Figure 6 and Figure 7 show an overview of the vibration setup used for this PhD work and its main components, respectively.

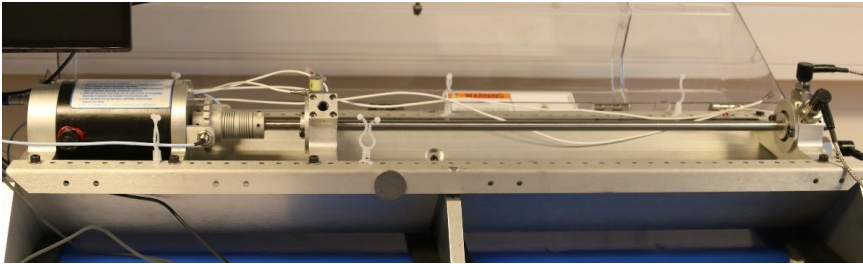


Figure 6, Overview of the experimental vibration setup

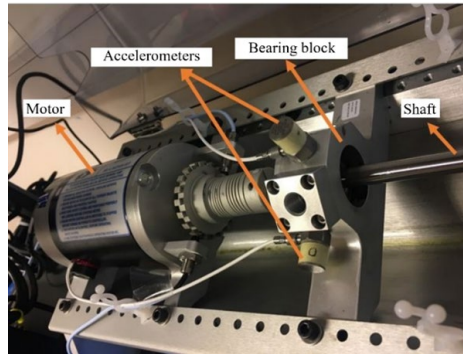


Figure 7, The main components of the vibration setup

3.3. Data Description

The data is collected in CSV format and includes horizontal and vertical acceleration in time, motor speed, and the date and time of data collection. The bearing has 10 rollers and its diameters are listed in Table 3. In this research, horizontal acceleration data are used since bearings generate vibrations predominantly in horizontal direction and the acceleration in

vertical direction are affected by the gravity and thus, they may not be accurate enough for condition-monitoring.

Table 3, Geometric characteristics of the bearing

Type of bearing	Open roller/ball bearing (R10)
Number of balls	10 balls
Pitch diameter (mm)	70
Ball diameter (mm)	4.7
Inner diameter (mm)	15.9
Outer diameter (mm)	34.9

3.4. Methodology

This section presents the methodology used in the appended papers to meet the goal of this PhD thesis. Figure 8 shows how the main goal is addressed through papers 1-5. Since the contribution in Paper 6 has overlap with Paper 4, it is not presented in Figure 8.

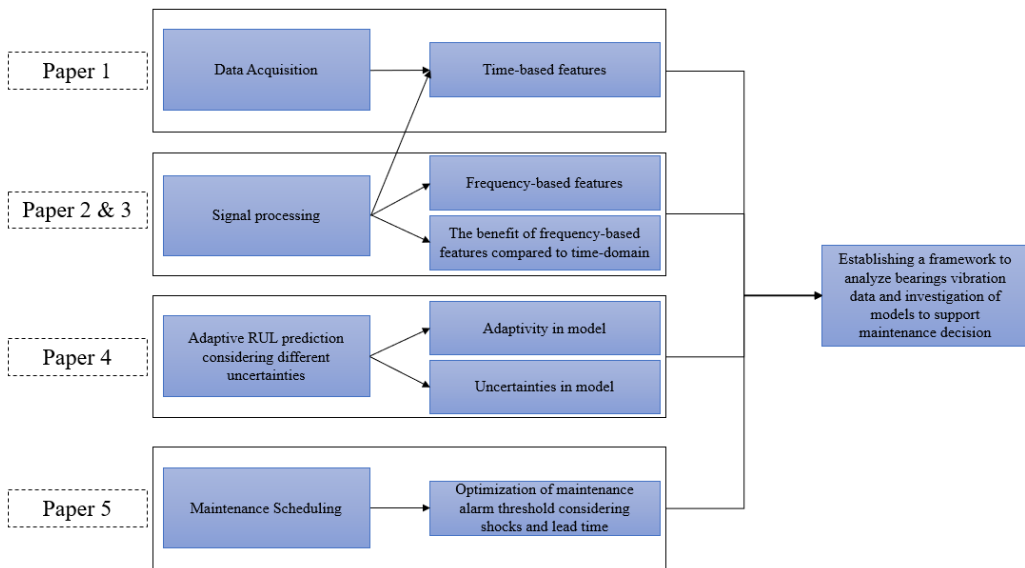


Figure 8, Addressing the PhD goal through papers 1-5

The methods used in the papers is particularly a combination of two subjects: signal processing and RUL prediction, and maintenance optimization.

3.4.1. Signal-processing and RUL Prediction

In Paper 1, the focus was on setup design, data collection, and studying the traditional time-based processing methods. In Paper 2 and Paper 3, the focus has shifted to frequency aspect of the data and frequency-based processing techniques. This includes extracting frequency spectrum of the vibration signals, looking for physical characteristics and localized faults on frequency domain, as well as stochastic modelling for RUL prediction. In Paper 4, the signal processing techniques have been studied in more detail and they have been implemented on the real-time data while the RUL-prediction model has been developed further to consider

uncertainty of model parameters and the failure threshold using Bayesian Inference approach. The methods focusing on signal-processing are explained below.

- **Fast Fourier Transform**

FFT transforms a time-based signal into a frequency-based and generates the frequency spectrum of the signal which includes all the constituent frequencies (fundamental and its harmonics). The discrete Fourier transformation (DFT) of a time-based signal $x(t)$ is defined as:

$$Y(k) = \sum_{j=1}^M x_j e^{\frac{-2\pi i(j-1)(k-1)}{M}} \quad (2)$$

where M is the number of acceleration readings or the signal length, $e^{\frac{-2\pi i}{M}}$ is the M th root of unity, and k is the number of points in DFT, or the new length of the Fourier-transformed signal, which is obtained from $2^{2^k \geq |M|}$ and is used to improve the visual frequency resolution and performance of FFT. $Y(k)$ is the k th Fourier coefficient, which is a complex number comprising an imaginary part and a real part (Wald, Khoshgoftaar, and Sloan 2011; Wu, Li, and Qiu 2017).

- **Hilbert Huang Transform**

EMD as the main part of HHT is a self-adaptive approach which uses the empirical signals data to perform the decomposition process. Let us assume that we have an arbitrary time-series signal $x(t)$. If $y(t)$ is the hilbert transformation of this time-series data, the analytic signal can be built as follows:

$$z(t) = x(t) + iy(t) = a(t) e^{i\theta(t)} \quad (3)$$

where

$$a(t) = \sqrt{x^2(t) + y^2(t)} \quad (4)$$

and

$$\theta(t) = \arctan\left(\frac{y(t)}{x(t)}\right) \quad (5)$$

where $a(t)$ is the instantaneous amplitude and $\theta(t)$ is the phase of the signal. From the instantaneous phase, instantaneous frequency can be derived as:

$$\omega(t) = \frac{d(\theta(t))}{dt} = \frac{\dot{y}(t)x(t) - y(t)\dot{x}(t)}{x^2(t) + y^2(t)} \quad (6)$$

To effectively construct frequency spectrum of a time-series vibration signal $x(t)$ that consists of multiple-frequency components, EMD can be applied on the signal $x(t)$ to obtain mono-component functions. The IMF must satisfy two conditions. First, the number of local extrema and the number of zero crossings must differ at most by one. Second, at any point in the IMF, the mean value of the local minima and local maxima must be zero. Algorithm 1 is adopted from (Cho, Shahriar, and Chong 2014) and shows how to perform an EMD. We used piecewise cubic Hermite interpolating polynomial (PCHIP) in step 4 of the algorithm to find the mean of

the local extrema of the signals, since it is suitable for interpolating non-smooth signals and can handle abrupt changes.

Algorithm 1 EMD on Vibration signals

Input: A time-series vibration signal $x(t)$

- 1- Initialize with $r_i = x(t)$, and $i = 1$
- 2- Extract the i th IMF
- 3- Initialize $h_{i(k-1)} = r_i$, $k = 1$
- 4- Use pchip interpolation to determine the mean of the upper and the lower envelopes of $h_{i(k-1)}$ called $m_{i(k-1)}$
- 5- $h_{i(k)} = h_{i(k-1)} - m_{i(k-1)}$
- 6- If $h_{i(k)}$ meets the two conditions of IMF, then $IMF_i = h_{i(k)}$, else go to step 3 and set $k = k + 1$
- 7- Define $r_{i+1} = r_i - IMF_i$
- 8- If the decomposition stopping criteria is met, stop and r_{i+1} will be the residue of the signal, else go to step 2 and set $i = i + 1$

Output: The output is a collection of IMF_i (for $i = 1, 2, \dots, n$) of signal $x(t)$ and a residue r_n which the summation of them gives the signal $x(t) = \sum_{i=1}^n IMF_i + r_n$

Extracted features from IMFs of the signals serve as condition indicators and are inputs to the prognostic model.

• **Wavelet Transform**

While EMD decomposes the time-based domain signals, EWT as an extension to WT focuses on decomposing signals based on their frequency domain. Therefore, it segments the Fourier spectrum of the signal, instead of the signal itself. The intention is to separate different portions of the spectrum which correspond to modes that are centered around a specific frequency. Assume that the signal's Fourier support should be segmented into N contiguous segments. This means that there are $N + 1$ boundaries which need to be identified. Assuming that the first and the last boundaries are $\omega^0 = 0$ and $\omega^N = \pi$ respectively, $N - 1$ extra boundaries should be detected.

The original EWT method follows the following procedure to detect the boundaries (Jerome Gilles 2013):

- Finding all the local maxima in the Fourier spectrum and sort them in a decreasing order (0 and π are excluded).
- Assuming that the algorithm found M maxima. If the number of detected maxima is M , two situations can arise:
 - o $M > N$, then only the first $N - 1$ are kept.
 - o $M < N$, then all the detected maxima are kept, and N is reset to the appropriate value.
- Now that we have the set of maxima plus 0 and π , the set of boundaries $\Omega = \{\omega^n\}$, $n = 0, 1, \dots, N$ can be found by:

$$\omega^0 = 0, \omega^N = \pi, \omega^n = \frac{\omega_n + \omega_{n-1}}{2}, \text{ for } 1 \leq n \leq N - 1 \quad (7)$$

This approach can cause 2 challenges called “flat-picked modes issue” and “global versus local modes” (Jérôme Gilles, Tran, and Osher 2014; Geetikaverma and Singh 2018).

To describe the flat-picked modes issue in more detail, let us consider that there are two close consecutive modes where one has a wide support and the other one has a narrow support (see Figure 9). According to the above algorithm, the solid line shows the segmentation where the corresponding boundary ω^n will fall into the larger support of the first mode. This means that the dashed area in Figure 9 belong to the second mode while it is apparent that it belongs to the first mode. A good segmentation is shown with a dashed line instead of the solid line.

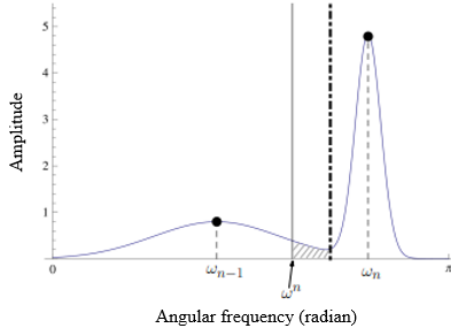


Figure 9, Flat-Picked modes issue (Jérôme Gilles, Tran, and Osher 2014)

Another situation is when there are several local maxima in the same mode, and they are larger than other modes (see Figure 10). According to the above algorithm, the square boxes show the local maxima, and the solid lines represent the Fourier spectrum boundaries. However, it is more reasonable to consider ω^1 and ω^2 as parts of the same mode and then keep ω^3 as the other mode. The dashed line shows a reasonable segmentation in this case. This challenge is due to the fact that we only consider the local maxima points and do not consider the spectrum global trend.

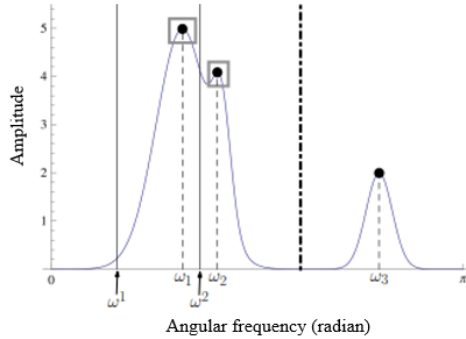


Figure 10, Global versus local modes (Jérôme Gilles, Tran, and Osher 2014)

To overcome these two challenges, we used the method proposed by Jérôme Gilles, Tran, and Osher (2014) and Jerome Gilles (2013), where the local minima points in the logarithm of the spectrum are used instead of the local maxima in spectrum. If U_n is the set of all local minima between ω_{n-1} and ω_n , then the Fourier boundaries are derived as:

$$\omega^0 = 0, \omega^N = \pi, \text{ and } \omega^n = \arg_{\omega} \min U_n \text{ for } 1 \leq n \leq N - 1 \quad (8)$$

The different frequency modes obtained from EWT can then be used for further feature extraction and RUL prediction model.

3.4.2. Maintenance Optimization

In Paper 5, the focus was more on maintenance optimization modelling for systems which their failure originates from both internal degradation and external shocks. The model has been developed to support maintenance decisions in cases where there is a lead time. Lead time was defined as a deterministic delay from when the maintenance request is placed until it is actually carried out. The model was developed numerically with good precision without the need for Monte-Carlo simulation. The model is explained in more detail in the paper.

3.5. Challenges and lessons learned

- *Lack of collaboration with industry:* Since this PhD research work was internally funded by the Mechanical and Industrial Engineering (MTP) department at NTNU, there was lack of collaboration with industry in this project. Collaboration between industry and academic provides a myriad of benefits to both parties. For academics, these benefits could include opportunity to address research questions with real-world applications, gain access to new skills, data, equipment, and get a better understanding of the challenges they have. On the other hand, companies can invest in research to improve new technologies, and extend their capabilities and expertise. This limitation gave me the idea to carry out accelerated life tests in RAMS laboratory at NTNU. Although the number of experiments were limited, it could shed lights on how the vibration setup can be designed, and how the experiments characteristics such as the length of dataset can affect the degradation process and prognostics. In addition, the experiments consider a degradation mechanism which is a common failure mechanism for rotating components in industry, but yet not focused before in available datasets in literature. Additionally, it brings the opportunity to students and future researchers at NTNU to work on this open dataset in the future for signal-processing analyses and investigation of maintenance models. This addresses the RQ1.
- *Covid pandemic:* Around 2 years of this research period (early 2020 – early 2022) was affected by the Covid pandemic. The pandemic resulted in having online seminars and conferences instead of attending physically (in person). The first conference in my PhD was held online. It was also not possible to attend summer schools and have exchange opportunities due to Covid and the limited budget of this PhD position. The experimental part of the PhD work was also affected by the pandemic. The laboratory was closed and there was no possibility to conduct experiments for some time. Overall, the pandemic situation had reduced benefits from different aspects. During the time that there was no or limited access to the laboratory, I focused on literature review to get a better understanding of different techniques to process signals, feature extraction methods, analysis of the frequency spectrum of the signals, and the prognostic models. Although my background from my master's program was far from this, I could find the right balance between the depth of knowledge I gained in Signal-processing and employing this knowledge into maintenance modelling and RUL prediction. This is connected to RQ2 and RQ3 where there is a link between time- and frequency-based features and RUL prediction using stochastic wiener process and Bayesian approach.

- *Laboratory access:* The vibration setup could only be used during the day, and it was not possible to run the experiments overnight. Therefore, the experiments were conducted in consecutive days. Due to this challenge and time limitation, the tests were stopped at a certain threshold and could not be continued for a long time to observe the real defects on the bearings (i.e., outer race, inner race, cage, and rollers defects). However, the length of the tests were long enough to show the deterioration trend of the bearings over time.

Chapter 4. Results and Discussion

4.1. Paper 1

Title: Remaining useful life estimation using vibration-based degradation signals (Tajiani, Vatn, and Gabriel Borg Pedersen 2020)

Motivation:

In the first semesters, I reviewed several bearing datasets which were published online to encourage researchers to develop innovative solutions towards prognostics and RUL prediction. The common factor in those datasets was the degradation mechanism (i.e., loading factor) they used to degrade the bearings. The motivation in the first paper was to conduct accelerated life tests on the vibration setup by contamination which is also a common failure mode in rotating components in industry, however it could not be found in online available datasets. In addition, degrading bearings using contamination could make the experiment time shorter. Thus, the main focus in this paper was real-time data acquisition and RUL prediction using deterministic and stochastic models. In addition, the time-domain features such as kurtosis, crest factor, and shape factor were also investigated to understand how effective they are in bearings RUL prediction.

Results:

The vibration setup was used to run the experiments and collect horizontal acceleration data to track the bearings degradation process. Two experiments were carried out under a constant operating condition which is the motor speed 3050 rpm and the room temperature. The sampling frequency is 12860 Hz, each sample has a duration of 0.158 seconds and has 2032 datapoints. The acceleration samples are taken every 6 minutes. B1 and B2 have 86 and 100 samples respectively. Figure 11 and Figure 12 show the first and the last samples of B1 for illustration.

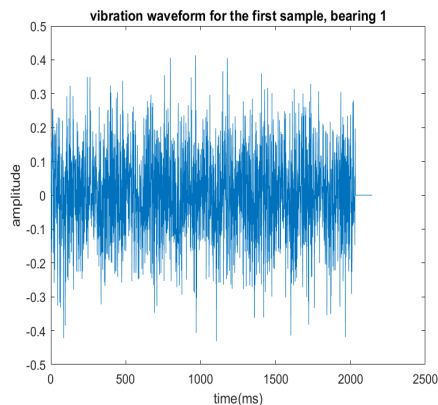


Figure 11, The first sample of B1

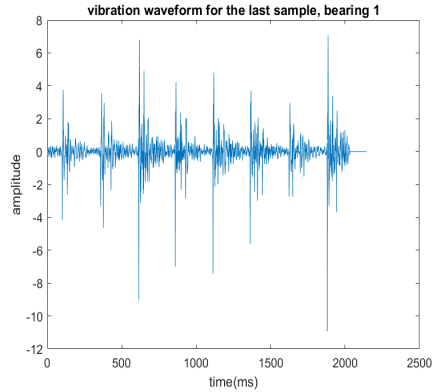


Figure 12, The last sample of B1

The lifetime of a bearing is a number of collected acceleration samples obtained every 6 minutes. Figure 13 is a schematic picture of a bearing lifetime.

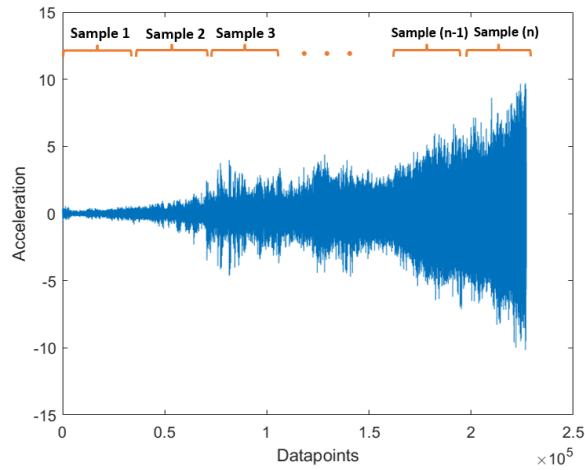


Figure 13, A schematic picture of a bearing lifetime tested in the laboratory

The next step was to extract condition indicators from the acceleration signals. Statistical time-domain features were calculated for the two bearings, mean-centred, and normalized in order to be in the same scale. The moving-average filter has also been applied to smooth the acceleration signals. The window size for the moving average was selected as 5 datapoints. Figure 14 presents the time-domain features calculated for bearing 2 from the healthy state to the failed state.

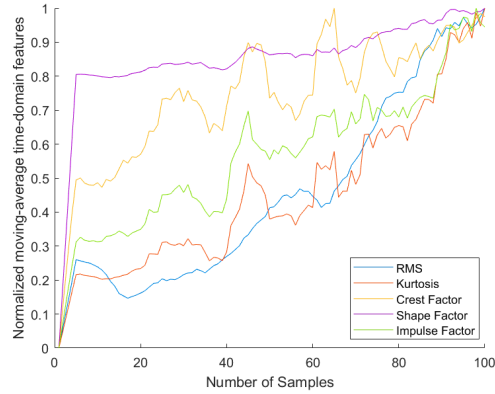


Figure 14, Time-domain features degradation behaviour for B2

To select the health indicator from the extracted features, Spearman’s correlation coefficient and PCA have been used. First, the correlation between different features and the original acceleration sample from the failed state was calculated to find the highly correlated features. As it is shown in Table 4, crest factor and impulse factor have a correlation of 0.7, and thus they were not selected for further analysis. In addition, PCA has been employed on the remaining features to find out how able the features are to explain the variation in the data. In B1, the first two principal components explain 96 percent of the variance of the data, while in B2, the first principal component explains 94 percent of the data variation. Therefore, sum of the loading scores for the first 2 PCs in B1 and the first PC in B2 are calculated to understand which feature has the highest impact in explaining the data variation. The results in Table 5 showed that kurtosis is the dominant one considering Spearman’s correlation and PCA and thus it was used as the HI to model the bearings degradation and RUL prediction.

Table 4, Spearman's correlation coefficient for different time domain features

Time-domain Features	B1	B2
kurtosis	0.7377	0.9124
RMS	0.8917	0.9391
Crest Factor	0.5933	0.7681
Shape Factor	0.8606	0.9318
Impulse Factor	0.6810	0.8814

Table 5, Loading scores for the rest of the features

Loading scores	B1	B2
kurtosis	1.3609	0.5737
Shape factor	0.8154	0.5879
RMS	1.1241	0.5703

Figure 15 shows the degradation paths for the two bearings which is the normalized moving-average kurtosis over time.

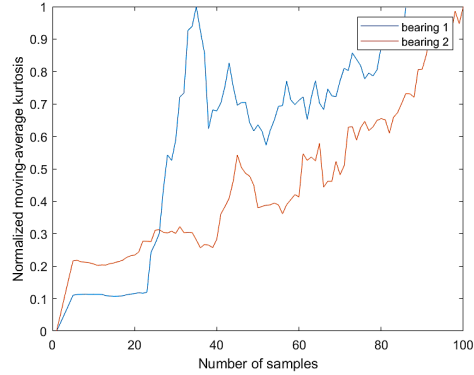


Figure 15, Normalized moving-average kurtosis for the two bearings

Wiener process as a continuous-time stochastic model and the three time-series deterministic models were then employed to model the two bearings deterioration. The deterministic models were fitted on the normalized moving-average kurtosis degradation paths of the bearings, and the R-squared value corresponding to the three models were calculated. Table 6 gives the R-squared values of the deterministic models.

Table 6, Goodness of fit of the trend models

Number	Deterministic Models	B1	B2
1	$y = aexp(bt)$	0.7902	0.9729
2	$y = aexp(bt^2)$	0.7006	0.9599
3	$y = at + b$	0.8488	0.9473

The parameters of the Wiener process were estimated using maximum likelihood estimation (MLE) and they are listed in Table 7.

Table 7, Drift and diffusion parameters of the Wiener process

	Drift Parameter	Diffusion Parameter
Bearing 1	0.0080	0.0553
Bearing 2	0.0101	0.0370

The first passage time (FPT) or the first time that degradation level reaches the predefined failure threshold were estimated for the deterministic models and the stochastic model for the two bearings. For deterministic models, different parametric distributions were fitted on the models' coefficients to figure out which distribution describes the coefficients best. Weibull distribution was selected due to the lowest negative log-likelihood value among others. Then a Monte-Carlo simulation (MCS) was applied to simulate a sufficiently large number of degradation paths by generating random samples from the Weibull distribution shape and scale parameters in order to predict the bearings RUL. The expected values of RUL for the three models were 71, 75, and 69 samples respectively. Since the time interval between two samples is 6 minutes, RUL can also be interpreted in terms of time (minutes). While in Wiener process, the FPT distribution is analytically known as Inverse Gaussian (IG) distribution. Thus, as presented in Figure 16, the cumulative distribution function (CDF) of FPT was computed and plotted against number of samples.

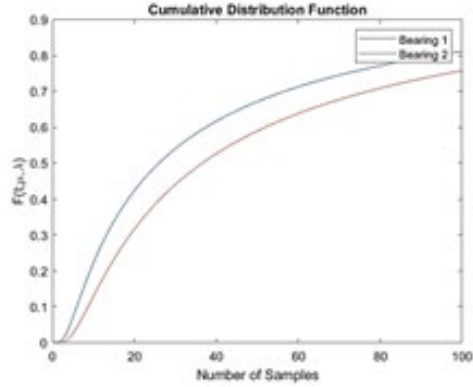


Figure 16, CDF of FPT for the two bearings

Concluding remarks:

The aim of the paper was to develop an approach for conducting accelerated life tests on roller bearings and investigate time-domain features and feature selection techniques for RUL prediction of bearings which was in line with RQ1. One of the limitations with respect to Paper 1 is the limited number of available datasets. Distribution fitting and statistical analysis in this paper are again based on limited datasets. Lack of sufficient data introduces a high uncertainty in the prediction results and makes it challenging to draw a robust and reliable conclusion. However, this paper could still demonstrate the possibility of conducting accelerated life tests for further analysis. It could also give insight on possible time-based features, how to compare them, and how to utilize features for degradation modelling.

4.2. Paper 2

Title: Degradation modelling of roller bearings using two different health indicators (Tajjani and Vatn 2020)

Motivation:

When I did more research on signal processing, I realized that although time domain features are easy to extract and reliable in some applications, most studies work with frequency-based features due to their capability in analysing localized faults in nonlinear and nonstationary signals. Thus, I have dedicated more attention to frequency aspect of acceleration signals. The motivation of Paper 2 was to compare the performance of energy-based features from time-domain and frequency domain in RUL prediction of bearings to find out how different they are, and whether the frequency domain features can outperform traditional time-domain features. Empirical mode decomposition (EMD) was selected to process the signals and divide them into different modes which correspond to different frequencies. The reason to choose EMD to compare with time-domain features was the fact that the basic principle in EMD approach is the time-domain characteristics of the signals. In other words, it uses the empirical time-based acceleration signals, and their associated local maxima and minima points to find the boundaries in the signals and decompose them into a number of intrinsic mode functions (IMFs).

Results:

In Paper 2, two other experiments were conducted using the vibration setup as presented in Table 8.

Table 8, Collected data in paper 2

Bearing	Number of samples	Number of datapoints in each sample	Sample duration (millisecond)
B1	104	2064	0.161
B2	34	8192	0.639

EMD as the fundamental part of HHT has been used to break down the signals into different IMFs with various frequencies. Figure 17 presents the IMFs and the residue of the first sample of B1 when the bearing is in healthy state.

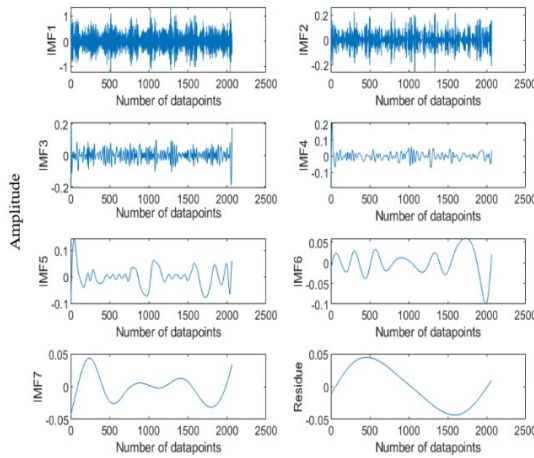


Figure 17, IMFs and the residue of sample 1 in B1

To identify the IMF with the most defect information, EMD was applied on the lifetime signal of the bearings. Afterwards, the Pearson correlation coefficient and the energy of its associated IMFs were calculated and compared to understand which IMF is suitable for degradation modelling. Table 9 presents the result for B1.

Table 9, The energy and correlation values calculated for different IMFs of B1

IMF	Energy	Pearson correlation coefficient
1	3.2e5	0.9460
2	2.5e4	0.2463
3	8.6e3	0.1147
4	1.5e3	0.0189
5	2.9e3	0.06
6	637.13	0.0158
7	130.73	0.0014
8	46.5	0.0014
9	52.15	0.000006

According to previous literature, although the first IMF was highly correlated with the original signal and had the highest energy, it is recognized as the IMF with high-frequency noise

components while it may not capture the low-frequency trend of the signal, and it can be misleading to select that for feature extraction. The 2nd IMF contains intermediate frequencies which are generally associated with fault-related phenomena and can be indicative of the system health condition. Thus, the second IMF was chosen to calculate Hilbert energy (HE). The HE from the 2nd IMF of all the vibration samples and the traditional time-domain RMS feature were used as the two energy-representative HIs for RUL prediction. The RUL was predicted using Wiener process at different samples or different stages of bearings' lifetime. Table 10 presents the RUL prediction results for the two bearings at different samples.

Table 10, Comparison of the expected RUL by Wiener process divided by the actual RUL using two different HIs for the two bearings

Sample number	RMS, B1	RMS, B2	HE, B1	HE, B2
8	84%	97%	86%	46%
10	86%	95%	84%	49%
20	97%	85%	75%	64%
30	94%	39%	65%	71%
40	96%		58%	
50	86%		48%	
60	82%		46%	
70	51%		32%	
80	36%		22%	
90	30%		10%	

Concluding remarks:

The conclusion and remarking points showed that both RMS and Hilbert energy were most informative at the early stage of bearing lifetime while they could not perform well in the deterioration stage. In addition, HE is dependent on the length of the dataset, since it was not able to predict RUL of B2 with 34 samples accurately at the beginning of the degradation while at the end, the prediction was better than time-based RMS feature. Therefore, different time and frequency energy-based features may have different RUL prediction capability depending on the length of the dataset and failure modes. The results of Paper 2 could highlight the importance of considering the frequency aspect of vibration signals in RUL prediction for bearings which have a short lifetime. This was in line with RQ2. In addition to lack of sufficient data as a limitation, the uncertainty of model parameters and failure threshold were not considered in this paper. The parameters of Wiener process were constant throughout the whole degradation process while in real-life applications, the degradation rate often change over time due to aging or external factors. Although the model's uncertainty was disregarded in this paper, it could provide a comparative analysis of the features performance in RUL prediction. Another area for further investigation was the choice of IMF for feature extraction. In this paper, we relied on the findings of previous studies (Cho, Shahriar, and Chong 2014) and selected the 2nd IMF to extract features. However, more research on this topic could be beneficial to make a more informed decision. For instance, setting thresholds on IMFs to eliminate the ones with low-energy or high-noise content.

4.3. Paper 3

Title: RUL Prediction of Bearings using Empirical Wavelet Transform and Bayesian Approach (Tajiani and Vatn 2021)

Motivation:

As described before in Paper 2, EMD approach has been selected for extraction of features from acceleration signals. In the method used in Paper 2, the time-based empirical signals were directly used to find the boundaries of the IMFs. The motivation for Paper 3 was to investigate EWT which has several benefits over EMD. Compared to EMD approach, EWT is able to decompose the signals based on their frequency domain. It can reduce the effect of mode-mixing issue and can thus provide more accurate separation of signal components. The base function in EWT is better adapted to capture features from non-smooth signals with abrupt changes and discontinuities. Thus, I conducted more research on this technique for analysis of vibration signals. In EWT, the frequency spectrum logarithm of the signals is first obtained using Fourier transform and then the decomposition boundaries are identified for extracting features and CIs. The aim in Paper 3 was to combine EWT and Wiener process with Bayesian approach to propose a RUL-prediction model for the bearings. The challenges of EWT approach and the methods to overcome those challenges were reviewed from literature and applied in the paper.

Results:

In this paper, first an overview of different time-frequency signal-processing techniques was provided from the literature to give an insight into the method selection process to readers. Table 11 shows the comparison of these techniques.

Table 11, A comparison of time-frequency signal-processing techniques

	Fourier	Wavelet	Hilbert	EWT
Presentation	Energy-frequency	Energy-time-frequency	Energy-time-frequency	Energy-time-frequency
Nonlinear	No	No	Yes	Yes
Nonstationary	No	Yes	Yes	Yes (to some extent)
Theoretical basis	Theory complete	Theory complete	Empirical	Theory complete

A higher number of accelerated life tests were conducted and used in Paper 3. Table 12 shows the dataset in this paper.

Table 12, Bearings and number of samples

Bearing	Number of samples
B1	110
B2	35
B3	146
B4	106
B5	77
B6	248
B7	150
B8	143
B9	114

The acceleration samples collected from different bearings were decomposed into different wavelet sub-bands using EWT approach to filter out the irrelevant frequencies and find out the most sensitive-to-defect frequency band. To divide the signals into frequency modes, the first step was to obtain the logarithm of Fourier spectrum of the signals. The local minimum method and the Fourier spectrum logarithm were used to tackle the challenges of “flat-picked modes issue” and “global versus local modes”. Once the acceleration samples were decomposed into

wavelet sub-bands, time-domain features were extracted from each sub-band and compared in terms of monotonicity, prognosability, and trendability metrics in which the RMS from the first wavelet sub-band was the dominant feature in the three metrics among all. Thus, it has been selected as the HI for RUL prediction. Figure 18 shows the degradation paths of different bearings.

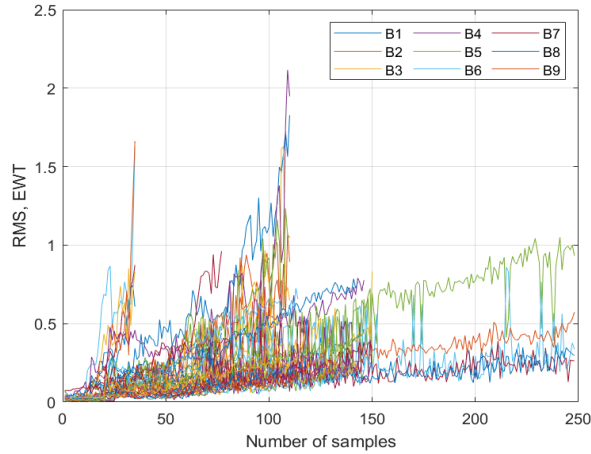


Figure 18, RMS degradation paths of experimental bearings

The RUL of bearings were predicted using Bayesian inference approach. In this paper, to obtain the prior parameters for each bearing, other bearings as reference were considered to build the prior knowledge. Figure 19 presents the three-dimension plot showing the RUL of B1 at different samples. It shows how the standard deviation or uncertainty of RUL decreases, while more observations of degradation measurement are available. The red dots connected together represent the expected values of PDFs. The details of Wiener process parameters and RUL prediction plots of all the bearings are provided in the paper.

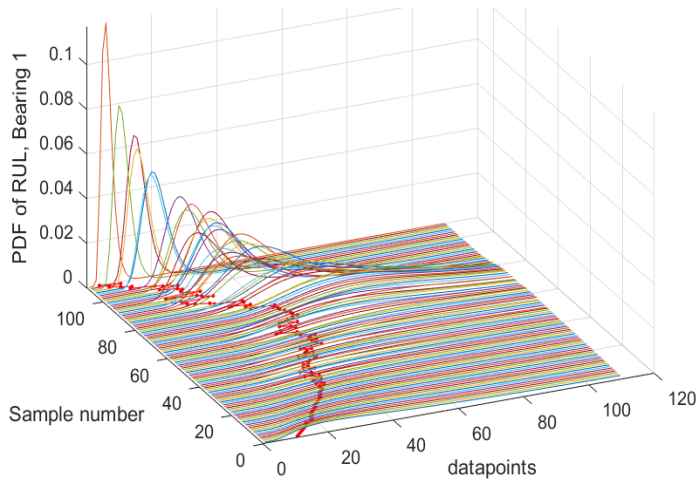


Figure 19, PDF of RUL of B1. The Wiener process parameters are updated continuously from the health state (sample 1) to the failed state (sample 110)

Concluding remarks:

In conclusion, the EWT approach performed well in extracting features from the acceleration signals. For most of the bearings, the predicted RUL values fall within 30% confidence intervals, while the predictions were also more accurate when the bearings were in steady state and close to the failure limit where the RUL prediction and maintenance planning is often more important compared to the bearings' early life stage. Paper 3 addressed RQ1 and RQ2 where the uncertainty in the model's parameters was also taken into account.

4.4. Paper 4

Title: Adaptive Remaining Useful Life Prediction Framework with Stochastic Failure Threshold for Experimental Bearings with Different Lifetimes Under Contaminated Condition (Tajiani and Vatn 2023)

Motivation:

In recent literature about failure prognostics of roller bearings, most studies focused on two research categories: machine learning algorithms combined with frequency-based techniques, and stochastic or statistical models integrated with traditional time-based techniques. Thus, it was interesting to explore the integration of frequency-based approaches along with stochastic modelling, as this combination can offer potential possibilities for enhanced signal analysis methodologies. Due to the linear non-monotonic behaviour of the bearings' degradation paths, a Wiener process was used for degradation modelling. The failure threshold was also assumed to be a stochastic parameter following a truncated Normal distribution to reflect the threshold variability while the key parameters of the prediction model were consecutively updated over time. The numerical framework in this paper was applied to the 10 bearing datasets collected in the laboratory.

Results:

Figure 20 presents the framework in paper 4.

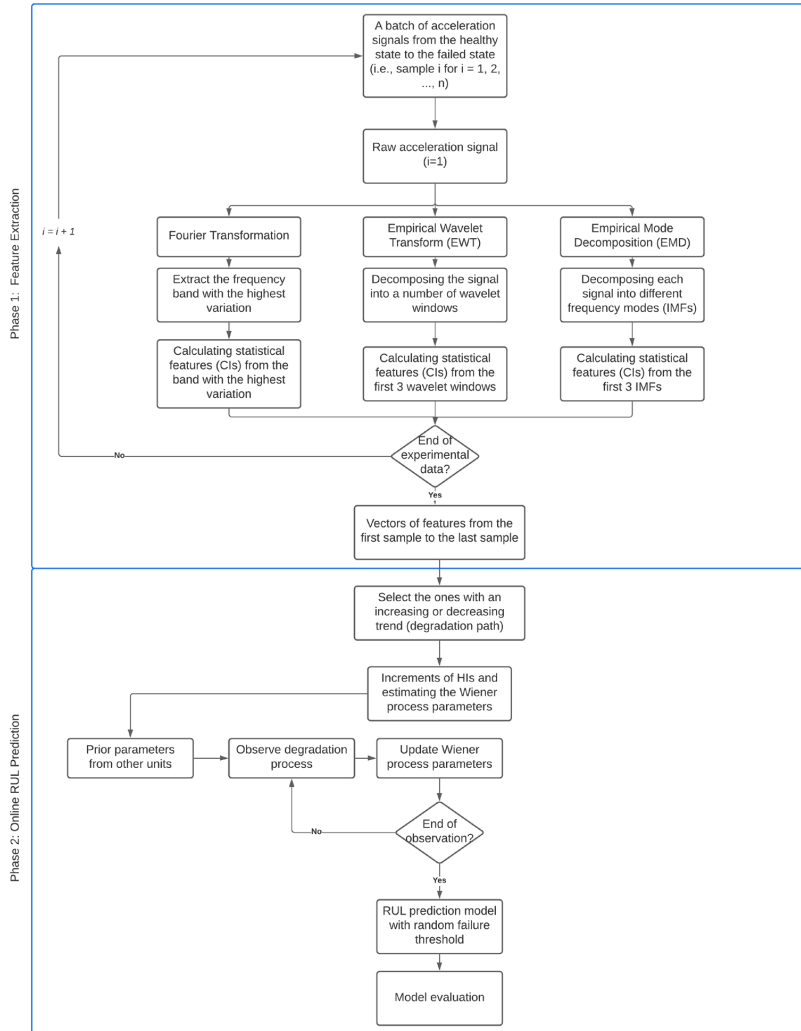


Figure 20, Proposed framework for RUL prediction of bearings

The dataset used in this paper is the same dataset in Paper 3, in addition to a bearing with 115 acceleration samples tested under the same laboratory operating condition. To start with phase 1, the features were extracted using three main time–frequency transformation functions which are Fourier transform (FT), EMD in HHT, and EWT. The fault-prone frequency band of acceleration signals in FT was identified by calculating frequency variation throughout the bearing lifetime. Figure 21 and Figure 22 illustrate the frequency variation and the optimal frequency band for the 10 bearings.

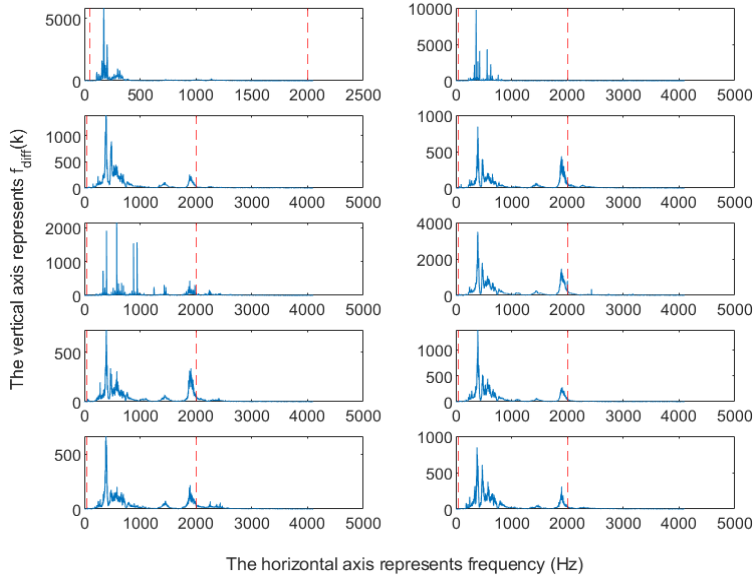


Figure 21, Frequency variation throughout the bearings lifetime

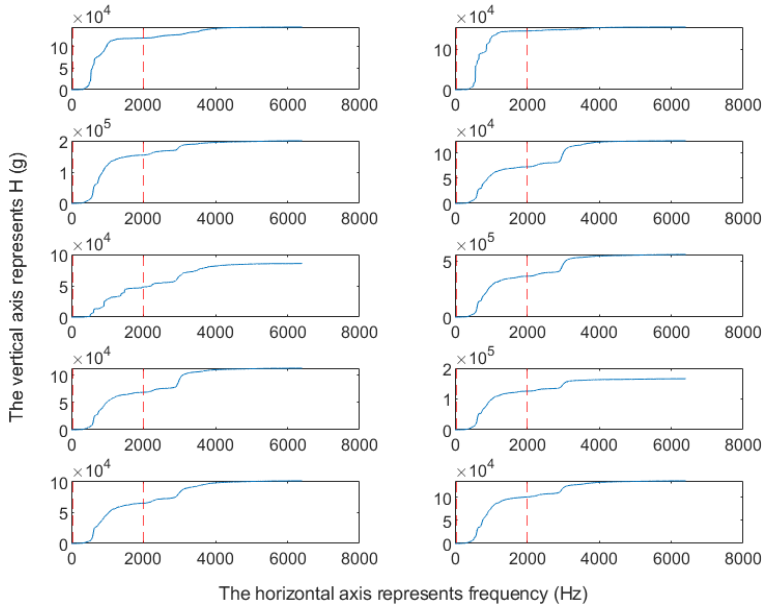


Figure 22, Optimal frequency band using FT, [50 - 2000] Hz

In addition to Fourier transform, EMD and EWT have been implemented to process the acceleration signals by decomposing them into a number of frequency bands. Figure 23 shows the statistical features from the optimal frequency band [50 - 2000] Hz of Fourier transform compared with the features from the first intrinsic mode function in EMD, and the first frequency window (called multiresolution analysis (MRA)) in EWT.

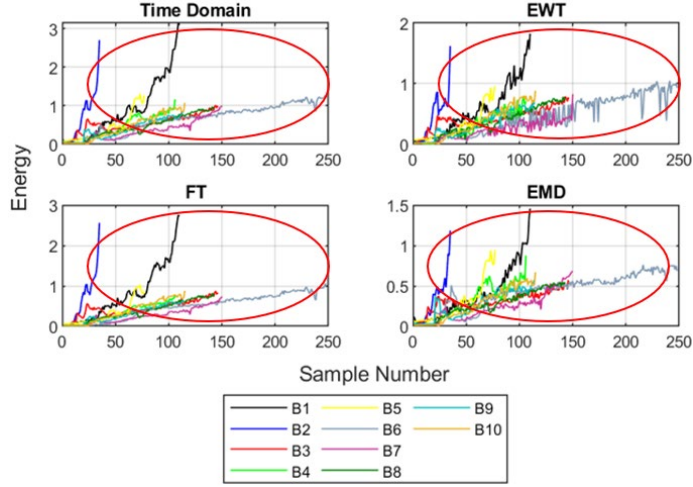


Figure 23, Energy degradation trajectories using different signal-processing approaches

It was shown that the time-frequency signal-processing techniques have a better sensitivity to defects compared to traditional time-based approach and they present more variation at the degradation stage of bearings lifetime. In other words, EWT and EMD could reveal the complex variations in signals which were not evident in traditional time-domain technique. The focus of phase 2 was the modelling of bearings degradation and RUL prediction considering different uncertainties. For this purpose, the numerical RUL prediction approach was developed where the model key parameters and the failure threshold were updated throughout the whole degradation process. Table 13 provides the parameters of the truncated Normal distribution which is used to show the uncertainty of failure threshold. The parameters of Wiener process and RUL prediction of bearings with different feature extraction techniques using constant and stochastic failure threshold are summarized in Table 14. The results have shown that considering a stochastic failure threshold can increase the accuracy of RUL prediction to a large extent specially when the bearings are in steady state. In addition, the results illustrated that the RUL prediction of bearings depends heavily on both failure threshold setting and the length of bearings lifetime. Calculating different RUL prediction performance metrics such as cumulative relative error (CRA) shows that the RMS feature from the first IMF with the highest frequency in EMD has the best performance and thus is a more suitable health indicator for modelling the degradation of experimental bearings.

Table 13, Normal distribution parameters of stochastic failure threshold (i. e., $L \sim TND(\mu_L, \sigma_L)$)

	EWT (MRA 1)	EMD (IMF 1)	FT [50–2000]	Time domain
μ_L	1.0470	0.8570	1.3350	1.4540
σ_L	0.3871	0.2975	0.7891	0.7510

Table 14, Wiener process and prior parameters for B1

	EWT (MRA 1)	EMD (IMF 1)	FT [50–2000]	Time domain
μ	0.0166	0.0132	0.0270	0.0280
σ_B	0.0976	0.0599	0.1823	0.0884
μ_0	0.0110	0.0089	0.0144	0.0163
σ_0	0.0127	0.0092	0.0213	0.0218

$\rho_0(\times 10^4)$	0.6174	1.1736	0.2200	0.2110
α_0	1.7926	3.6000	2.9186	2.5573
β_0	142.2290	176.3439	109.5286	179.5783
$\kappa_0(\times 10^5)$	11.078	7.9595	1.2562	2.4337

Figure 24 and Figure 25 show the $\alpha - \lambda$ plot of predicted RUL versus the actual RUL for different bearings using the stochastic and constant failure thresholds.

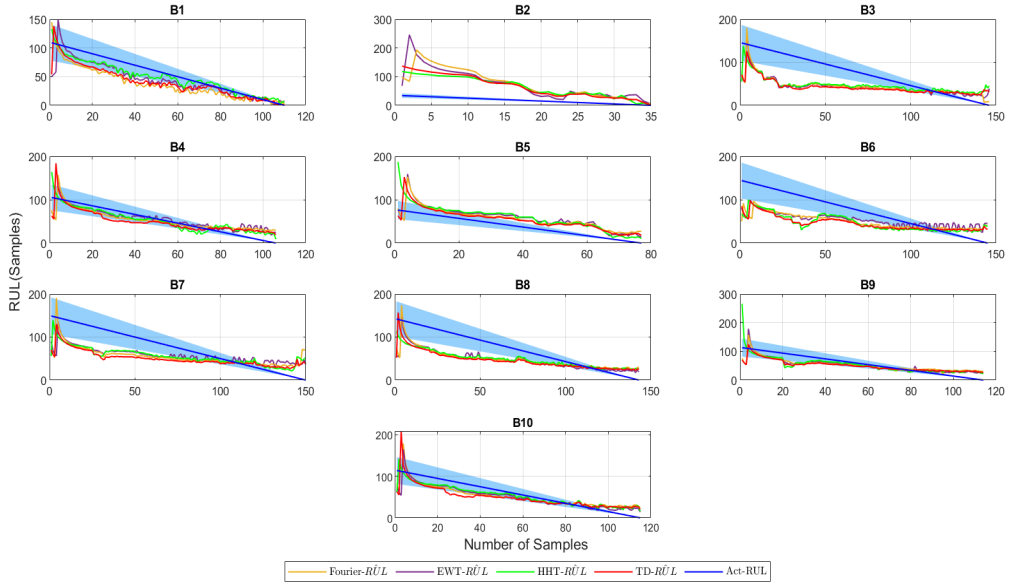


Figure 24, RUL prediction using stochastic failure threshold and different techniques

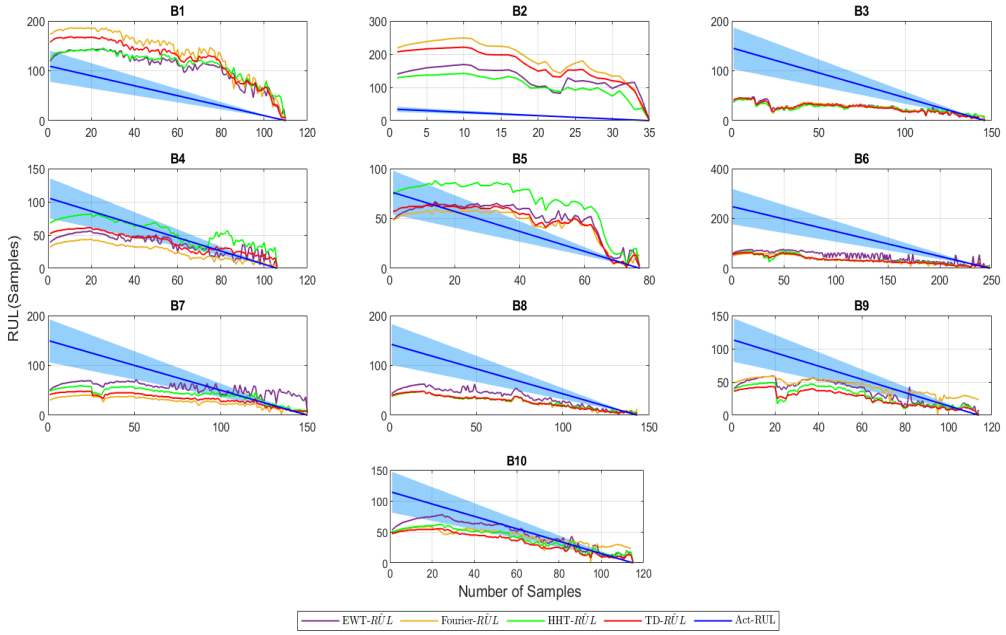


Figure 25, RUL prediction using a constant failure threshold and different techniques

Concluding remarks:

Paper 4 could provide insight into how to develop an adaptive RUL prediction numerical framework for bearings and how the frequency aspect of acceleration signals can offer advantages in fault diagnosis and failure prognostics which are in line with RQ2 and RQ3. With respect to RQ2, the time-frequency methods to process the signals could outperform the traditional time-domain approach and provide features with higher sensitivity and variation at the deterioration stage while they also result in a more accurate and realistic RUL prediction especially for bearings with an average length of lifetime. With respect to RQ3, if the uncertainties in the model were disregarded, a conventional Wiener process could easily be applied, and the RUL could be estimated analytically by IG distribution (similar to Paper 2). However, to incorporate the uncertainties of failure threshold, drift, and diffusion parameters of the Wiener process, we solved the model numerically. Taking the randomness of failure threshold into account improved the prognostic horizon (PH) significantly which means the model could estimate the end of life of a bearing earlier in the deterioration process. Overall, the results also suggest that the RMS feature from EMD technique can be a more suitable HI candidate for condition-monitoring compared to others. This result has been used as a basis in Paper 6 where the random forest as a machine learning algorithm was employed for RUL prediction.

A possible approach to show the effectiveness of the numerical model is Monte-Carlo simulation (MCS). MCS is generally more computationally expensive compared to numerical discretization approach. The prediction accuracy in MCS depends on the sample size which may require a trade-off between the sample size and the computation time. Numerical discretization approach is commonly used in solving continuous mathematical problems and is more efficient compared to MCS. However, its efficiency and stability depend on the

discretization step. This was one of the constraints in Paper 4 which could be further investigated.

4.5. Paper 5

Title: Maintenance Optimization of Systems with Lead Time Subject to Natural degradation and Stochastic Shocks, *Submitted to Reliability Engineering and System Safety (RESS)*

Motivation:

In this paper, the focus is more on maintenance optimization modelling. According to the existing literature, bearings used in different equipment such as wind turbines, drills, and electric motors suffer from both natural degradation and shocks caused by external factors (Bozbulut and Eryilmaz 2020). The motivation in this paper was to propose a maintenance optimization model for single-component systems that are subject to competing failures in presence of a deterministic lead time before maintenance implementation. In the developed model, the stochastic shocks occur randomly during the degradation process and can either lead to direct system failure (i.e., fatal) or simply increase the degradation level by a random extent (i.e., non-fatal) depending on their magnitudes and the system's age. A numerical approach was proposed to find the optimal maintenance alarm threshold (i.e., M^*) for hard-time maintenance and the result was compared with MCS. A numerical example was used to illustrate the model and the bearings' dataset in Paper 4 was employed to show the effectiveness of the proposed model on real case study. The model has also been compared with linear Wiener process and it was shown that the shock model is more realistic in terms of system failure probability, risk perspective, and decision-making.

Results

There are two cases described in the paper: 1. Modelling; Natural degradation, 2. Modelling; Natural degradation and shocks. In case 1, assuming that the system degradation follows a Wiener process, and the system is only exposed to internal degradation, maintenance optimization model can easily be found by IG distribution. However, we develop the numerical model for case 1, so that we can extend it later on for case 2 when the additional features (i.e., external stochastic shocks) are incorporated into the model. Figure 26 presents the expected cost per cycle $C(M)$ versus maintenance alarm threshold M for our numerical example in case 1.

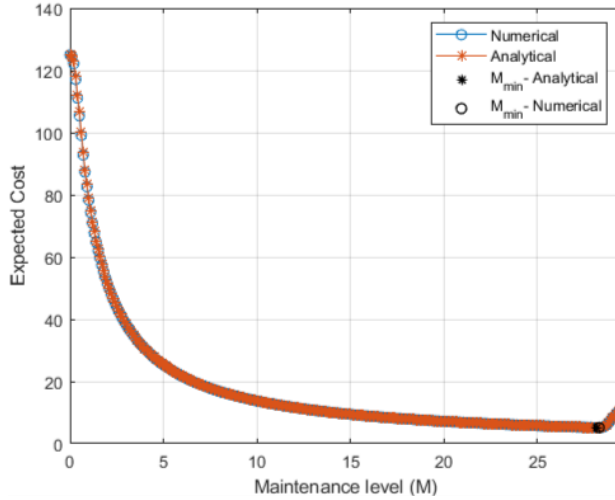


Figure 26, Expected total cost versus maintenance alarm threshold

The Wiener process was then extended to the shock model by including the external shocks with stochastic magnitudes. The shocks arrive to the system according to a Homogeneous Poisson Process (HPP) while the magnitudes follow a Gamma distribution. In this case, it is challenging to develop the analytical solution. Thus, we compared our numerical approach with MCS. Figure 27 shows the expected cost for maintenance alarm threshold M considering different time steps (i.e., $dt = 0.3$, $dt = 0.4$, $dt = 0.5$, and $dt = 1$). Although there is a small deviation in numerical solution and MC simulation due to numerical stability challenge, the optimal maintenance threshold M^* , rounded with one decimal place, is the same in both approaches (i.e., $M^* = 23$) while our numerical technique is more efficient and gives a good level of accuracy in calculation of M^* .

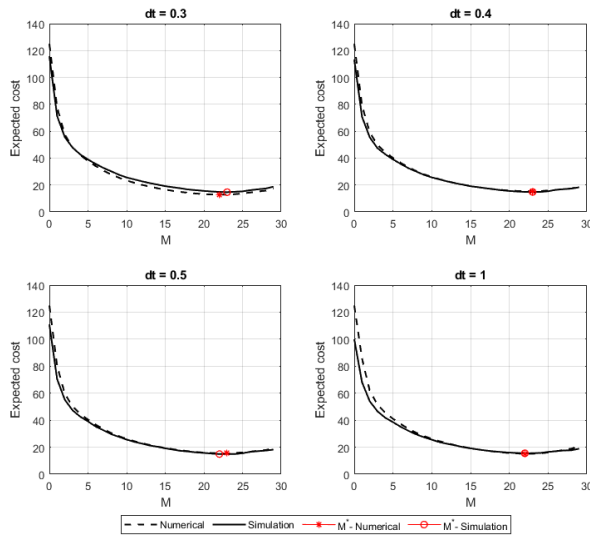


Figure 27, Expected cost versus maintenance alarm threshold considering different time steps

The system failure probability in lead time was compared in the two cases. As it is shown in Figure 28, having external shocks leads to significant changes in probability of failure while the pure Wiener process cannot capture the impact of external shocks and thus underestimates the system’s failure probability. In other words, since the shock model can account for unexpected events, it gives a more reliable estimation of failure probability, and thus is more appropriate to model the real-world degradation behaviour of systems while the pure Wiener process can make it challenging to accurately assess risk and make effective maintenance decisions.

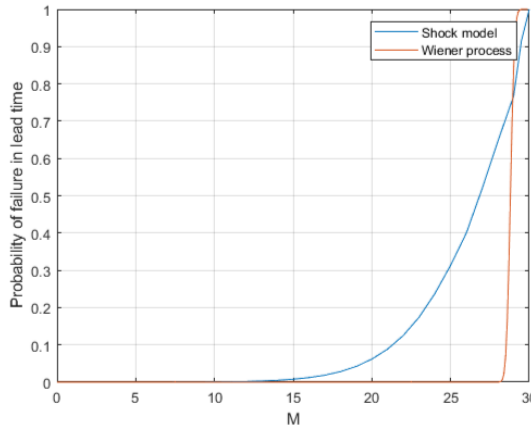


Figure 28, Probability of failure in lead time for Wiener process (case 1) and shock model (case 2)

Additionally, the framework has been employed on a real-life bearing dataset which were collected in the laboratory. Since particles contamination has been used to accelerate the bearings degradation, it was a bit challenging to detect whether the particles contributed to shocks or not. In addition, in a more controlled environment like a laboratory, the experiments are carried out under the same operating condition and the influence of some external random shocks such as extreme weather conditions are minimized. In real-life applications, there are various approaches to identify shocks such as checking the historical work orders, maintenance records, and comparing degradation patterns at different time periods. In our case study, it is assumed that the degradation increments exceeding 2σ , where σ is the standard deviation of the degradation increments, correspond to the external shocks while the others arise from system’s internal degradation.

Determining an appropriate threshold to detect shocks depends on the context, data characteristics, and desired risk tolerance. In some systems, if missing a shock has severe consequences, defining a more conservative threshold is required to capture a broader range of potential significant events. Figure 29 presents the expected cost over maintenance threshold M for different bearings assuming 2σ and 1.5σ .

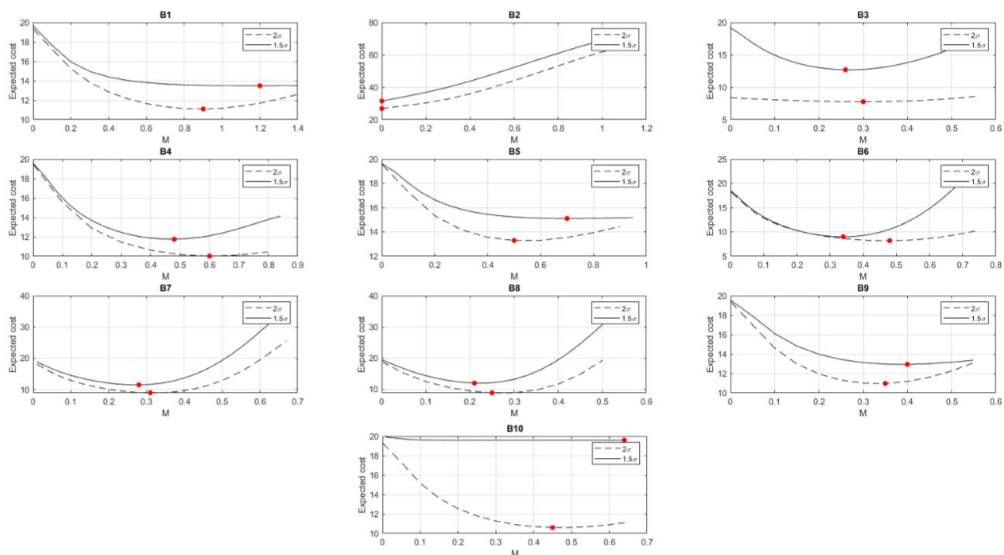


Figure 29, Expected cost over maintenance threshold for the experimental bearings

The different model parameters and the lifetime of the bearings lead to different maintenance strategies (i.e., run-to-failure, request maintenance early at the life stage, etc.). For instance, in B2, the lead time is large compared to the bearing lifetime which gives a higher probability of failure during lead time. Therefore, the optimal maintenance threshold to place the maintenance request is at the beginning of the experiment. However, in B10, the maintenance strategy according to 1.5σ is “run to failure” which means that the bearing can be operated until it fails or breaks down while according to 2σ threshold the optimal maintenance threshold is 0.45 where more than half of the bearing lifespan has elapsed.

Concluding remarks

Paper 5 could answer RQ4 with the help of some analysis from the previous papers. A numerical approach was proposed to find the optimal maintenance alarm threshold to place the maintenance request in single-component continuously monitored systems. The model accounts for significant random events or shocks that attribute to the system degradation. The result can be further used for an effective maintenance planning, decision-making, and replacement and maintenance optimization.

In Paper 5, there are several possibilities to improve the maintenance optimization model. For instance, incorporating diverse maintenance strategies such as imperfect repair in addition to replacement can make the model more applicable to real-life scenarios. In addition, another interesting point is to consider a system-level perspective where the interdependencies and interactions between several components are taken into account.

4.6. Summary of Results

To sum up, Table 15 lists the main results of the 6 appended papers and presents the link between the papers and the research questions. The research questions are repeated below for the ease of the readers.

RQ1. How to perform accelerated life tests on roller bearings as one of the most critical rotating components to deal with the lack of run-to-failure data?

RQ2. How can time-frequency signal processing techniques benefit RUL prediction compared to traditional time-domain techniques?

RQ3. How to develop an adaptive RUL prediction framework for bearings that can handle nonlinearity and nonstationary characteristics of vibration signals and treats different kinds of uncertainties?

RQ4. How to propose a maintenance optimization model which can deal with external stochastic shocks in addition to system degradation?

Table 15, Main results of the appended papers and how they are linked to the research questions

Papers	Main results	Research question
Paper 1	Design and development of the vibration setup to conduct accelerated life tests on roller bearings	RQ1
Paper 2 & Paper 3	Implementation of signal-processing techniques (i.e., Hilbert and Wavelet transformation functions) to involve frequency aspect of vibration signals and present how they differ in RUL prediction compared to traditional time-based approach. The uncertainty of model parameters was taken into account.	RQ2
Paper 4 & Paper 6	In Paper 4, a RUL prediction framework is developed in which the model parameters were updated through the degradation process and the uncertainty of failure threshold was considered. It was shown that the frequency-based processing techniques are more sensitive to faults and defects and thus more suitable for prognostics. In Paper 6, a random forest machine learning algorithm was proposed for RUL prediction of the experimental bearings.	RQ3
Paper 5	A numerical maintenance optimization model is proposed for systems that are subject to both internal degradation and external stochastic shocks. The internal degradation is modelled by a Wiener process. A Monte-Carlo Simulation-based approach is used to validate the model.	RQ4

Chapter 5. Conclusions and Further Work

The research carried out in this PhD work was following the general PHM framework in Figure 2 while the difference is that we did not focus on diagnostics in this PhD. Four dimensions to consider are: data acquisition, signal processing, prognostics, and maintenance optimization to support maintenance decisions. To conclude, we present the 4 dimensions on a radar chart, also known as spider chart, where each dimension is self-evaluated from 2 perspectives: “the current state of my research” and “the status of the industry”. To be able to evaluate the work, several questions are asked, discussed, and the scores are given from 1 to 5 based on the discussion, where 1 is the lowest or less developed, and 5 is the highest or well-developed. The score for “the status of the industry” is given based on my limited work experience in energy industry in Norway.

- **Data acquisition**

Table 16, Data Acquisition

Questions	My research	Industry
a. How good is the data collection method?	3	5
b. How diverse and comprehensive is the collected data?	3	5
c. How is the data quality?	4	3
d. Are there any limitations or biases in the data?	4	4
e. How much data is collected (i.e., data quantity)?	2	5
f. Are the data accessible and can they be shared with others?	5	2.5
g. Does the data cover various scenarios and conditions?	2	5
h. Are the data reliable and accurate?	3	3
Average	3.25	4.06

- The data collection in this PhD work was done manually. In other words, a bearing was mounted on the vibration setup, and the snapshot of vibration samples were stored as CSV files at regular time intervals manually. However, the industry has access to real-time condition-monitoring data continuously and data collection is easier and more advanced.
- The degradation mechanism used to degrade the bearings was “contamination”. There are other important failure mechanisms that could be implemented such as overloading. However, it was not within the scope of this project due to time limitation. In industry, bearings are used in various equipment, and they experience different failure modes in their outer race, inner race, cage, and rollers. Thus, the data in industry are more diverse and different types of measurements from temperature sensors, acoustic sensors, and wear debris sensors are available.
- Data quality is a main challenge in both academia and industry. It depends on data accuracy, lack of missing data, and relevance to the research objective. In my research, there is a gap between every two samples taken in the laboratory. The data are relevant to my research objectives since “run-to-failure” tests are carried out which are suitable for condition-monitoring and conducting RUL prediction models. Additionally, data collected in a controlled laboratory condition, have no interactions with other equipment and have generally less impurities. On the other hand, in industry, the bearings can interact with other

systems and thus are more affected, while missing data is also a common issue in industry due to sensor failures, human error, or problem in data transmission systems.

- d. Data collection has limitations and biases in both academia and industry. For instance, in industry, the data bias can be due to different operating conditions, human inputs, sensor malfunctions, and wrong labels which can result in misleading bearing condition monitoring. In laboratory environment, one limitation is lack of enough samples. The experiments could only be conducted in daytime. Thus, it was not possible to run the experiments until complete failure where the defect is visible on the bearing. Some physics-based methods to find the bearings localized faults failed to provide meaningful results due to this limitation.
- e. The data is very limited in my research compared to the data in industry.
- f. In terms of accessibility and sharing data with others, industry has to comply with several regulations and often the data is confidential. Although the collected data in my research is limited, it is accessible and can be openly shared with future researchers.
- g. The data in my research does not cover several real-life scenarios and it is only representative for bearings degraded by particle contamination. However, the data collected from industrial bearings are exposed to various real scenarios.
- h. Generally, data is more reliable and accurate in controlled laboratory environment compared to industrial data, but the measurement errors and noises are inevitable in both cases.

- **Signal-processing**

Table 17, Signal-processing

Questions	My research	Industry
a. How effective are the signal-processing methods used to process acceleration signals?	4	2.5
b. How is the quality of data after processing?	4	3
c. How adoptable and scalable are the used signal-processing techniques to other datasets?	4	3
d. Can the signal-processing methods be integrated with other technologies?	5	5
e. How computationally expensive are the methods?	5	5
Average	4.4	3.7

- a. To the best of my knowledge, among different signal-processing methods, Fourier transform is widely used in industry to process vibration signals. The data are transformed from time domain into frequency domain, while the deviations and discrepancies from the system's normal state can be detected by monitoring the frequency domain and considering several deterministic critical thresholds. The signal-processing techniques in my research are applicable to both non-linear and non-stationary signals. In addition, Hilbert transform is an empirical approach and provides the analytic signal having both magnitude and phase information. Wavelet transform also gives a multi-resolution analysis of a signal by decomposing it in different levels, making it possible to focus on low-frequency and high-frequency components of the signal. Furthermore, it was presented in Paper 4 that EWT and EMD were more sensitive to deviation and thus more suitable for condition-monitoring.

- b. One of the approaches to assess the quality of data after processing is to evaluate how effective they were for RUL prediction. By assessing the RUL prediction results in Paper 4, we found that the energy feature from EMD technique has a better performance compared to Fourier-extracted feature in terms of prediction error. Therefore, this can show that the quality of data has improved after being processed.
- c. As mentioned earlier, EMD and EWT are both adoptable to systems with non-linear and non-stationary signals, while FT fails to adopt to non-linear signals. EMD has a time-based decomposition process, it is fully empirical, and needs no mathematical function.
- d. Within the field of fault diagnosis and failure prognostics, all methods have the possibility to be integrated with stochastic models, physics-based models, and machine-learning algorithms.
- e. Although the methods are different, they had almost the same computation time when applied on our dataset.

- **Prognostics**

Table 18. Prognostics

Questions	My research	Industry
a. Are the prognostic models able to predict RUL accurately?	4	2.5
b. Are the models realistic and adoptable to real-life scenarios?	4	3
c. Does the model include physical characteristics of the system (i.e., physics-based) or it is only data-driven?	3	4
d. Are the models robust, easy to be generalized, and implemented?	3.5	4
e. Are the models computationally expensive?	4	5
Average	3.7	3.7

- a. To my knowledge, the industry mainly uses simple first-principles, physics-based models, and deterministic models for failure prognostics, and they have different critical thresholds for condition monitoring. The continuous-time stochastic Wiener process used in my research has a number of advantages over the current models used in industry. The joint consideration of Wavelet and Hilbert transform, and Wiener process has given a good RUL prediction accuracy for bearings with different lifetimes while it accounts for the inherent randomness in the system degradation process.
- b. The model in our research takes into account the uncertainties of Wiener process parameters as well as the failure threshold which makes it adoptable to real-life scenarios. The drift and diffusion parameters show how the degradation process evolves and how quickly it progresses while they are not known with certainty in reality. There are various methods to include the uncertainties in the model such as Markov Chain Monte Carlo (MCMC), Bayesian modelling, and ensemble modelling. In this PhD work, we focused on Bayesian approach. However, the model in our research has not been tested on a large dataset, while the current existing models in industry have been developed and tested on real engineering complex systems for a long time but they do not consider parameters variability.
- c. The model in our research is data-driven and the physical characteristics of bearings is not considered. Due to the limited project time, we were not able to run the experiments until

total breakdown of the bearings. Thus, it was not possible to see the actual defect on the bearings which made it difficult to work with physics-based models and focus on the fault frequencies. While in industry, in most cases, there is a large amount of historical data, failure data, and maintenance records, which makes it easier to employ fault frequencies to find localized faults for diagnostics purpose compared to my research.

- d. The models can be generalized and implemented to other systems as long as their degradation follows a Wiener process with independent and normally distributed increments. Additionally, shocks can be integrated into the model, making it more applicable for systems that are exposed to varying operating conditions and affected by external factors. However, compared to existing models in industry, they have not been tested on large scale and they need to be validated.
- e. The numerical model in my research is more computationally expensive compared to the ones used in industry. Computation time also depends on the desired level of accuracy, and how efficient it has been developed (in terms of coding optimization and used numerical algorithms). Finding the right balance between accuracy and computational cost is crucial.

- **Maintenance optimization**

Table 19. Maintenance optimization

Questions	My research	Industry
a. Does the model focus on the right objective?	4	4.5
b. Can the model provide insight and maintenance decision support to maintenance personnel and planners?	4.5	2.5
c. Is the model adoptable to real-life scenarios? Can it be generalized?	3.5	4
Average	4	3.67

- a. The maintenance optimization model focuses on the expected total cost, which is a function of failure probability, expected downtime, mean time to reach maintenance threshold, and their associated costs. The model assumes that the system gets replaced once it has failed. There are some models in literature that focus on utility function for CBM optimization (Hong et al. 2014; Ait Mokhtar, Laggoune, and Chateauneuf 2016). Expected utility theory is a framework to consider attitudes towards risk when assessing different alternatives with uncertain outcomes (Pedersen and Vatn 2022). The utility function in this theory is used to embed the business desires and stakeholders' attitudes to enable the estimation of optimal policy (Bousdekis et al. 2018). Pedersen and Vatn (2022) proposed a model based on utility function for CBM optimization taking the risk preferences of a decision-maker. This is an appropriate approach for cases where the decisions can have severe consequences and minimization of expected cost as the objective function is not very desirable. However, use of the expected long run cost is well suited for less expensive components such as bearings and when the component's mean life is short compared to the planning horizon of the maintenance program (Pedersen and Vatn 2022). It would be interesting to extend the model based on multi-objective utility function as a further work. In industry, the maintenance planning is always integrated with expert judgement and human inputs. Since maintenance optimization models based on expected cost may not be very applicable to

complex engineering systems in industry, I gave score 4 to the research work and 4.5 to industry status.

- b. The model is capable to provide meaningful insights to maintenance personnel and decision-makers. It is suitable for continuously monitored systems with competing failures while there is a deterministic lead time before maintenance implementation. The current model is applicable for hard time maintenance where the system is returned to “as good as new” condition after it reaches the failure threshold. The existing models in industry also consider external factors when planning maintenance actions. However, the planning is often based on equipment’s failure history, maintenance records, and maintenance personnel opinions. Thus, it lacks a solid statistical background and needs some improvements to be more effective. Thus, I gave score 4.5 to the model in our research and 2.5 to the existing models in industry. Our model has potential to be improved from several perspectives as follows:
 - Include several maintenance strategies such as imperfect repair.
 - Incorporate shocks with a change of degradation rate in deterioration process for cases which experience a change of operating condition during their lifetime (e.g., wind turbines exposed to seasonal weather variations).
 - Sensitivity analysis with respect to maintenance and failure thresholds, Wiener process parameters, lead time distribution, and cost parameters.
- c. The model is not integrated with physical aspects of the system, and it is flexible enough to be adopted to industrial systems which their degradation has a behaviour similar to Wiener process. However, the computation time and the model complexity can pose a barrier, making it challenging to apply the model on real-world systems. On the other hand, although the existing models in industry require further improvements, they have been implemented for a long time and they work well on large-scale systems.

The discussion with respect to the four dimensions focused in this PhD work gives the following radar chart.

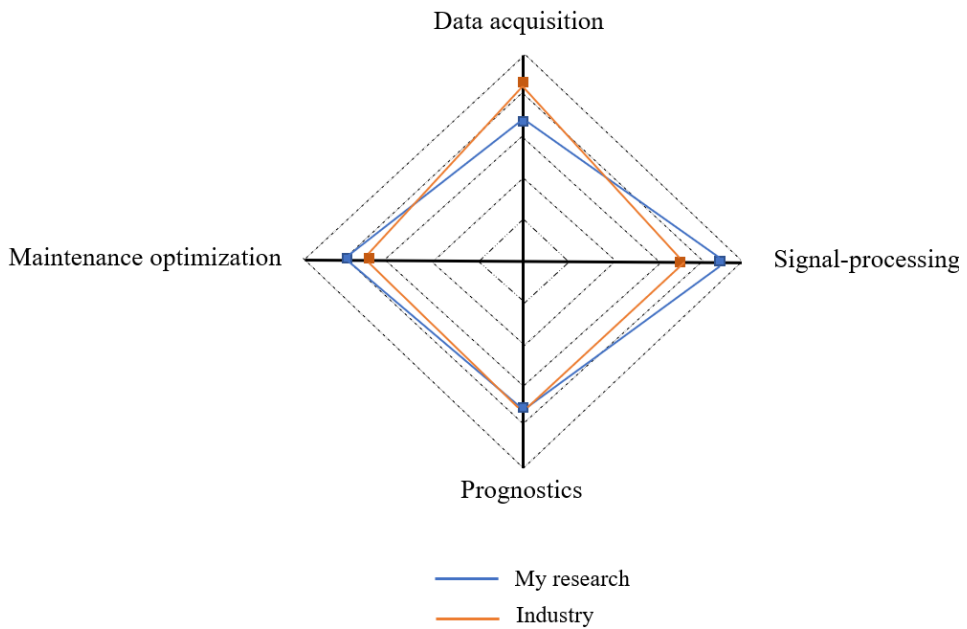


Figure 30, Radar chart comparing the PhD research work and current state of industry

Although the scores in Table 16 to Table 19 are determined through self-assessment and no survey has been conducted for this purpose, it provides insight into the contributions made by this PhD research.

References

- Ahmad, Wasim, Sheraz Ali Khan, M. M. Manjurul Islam, and Jong Myon Kim. 2019. "A Reliable Technique for Remaining Useful Life Estimation of Rolling Element Bearings Using Dynamic Regression Models." *Reliability Engineering & System Safety* 184 (April): 67–76. <https://doi.org/10.1016/J.RESS.2018.02.003>.
- Ahmadzadeh, Farzaneh, and Jan Lundberg. 2014. "Remaining Useful Life Estimation: Review." *International Journal of System Assurance Engineering and Management* 5 (4): 461–74. <https://doi.org/10.1007/S13198-013-0195-0/FIGURES/1>.
- Ait Mokhtar, El Hassene, Radouane Laggoune, and Alaa Chateaneuf. 2016. "Utility-Based Maintenance Optimization for Complex Water-Distribution Systems Using Bayesian Networks." *Water Resources Management* 30 (12): 4153–70. <https://doi.org/10.1007/S11269-016-1412-9/TABLES/4>.
- Alfarizi, Muhammad Gibran, Bahareh Tajiani, Jorn Vatn, and Shen Yin. 2022. "Optimized Random Forest Model for Remaining Useful Life Prediction of Experimental Bearings." *IEEE Transactions on Industrial Informatics*, September, 1–10. <https://doi.org/10.1109/TII.2022.3206339>.
- Almeida, A. T. de, and G. A. Bohoris. 1995. "Decision Theory in Maintenance Decision Making." *Journal of Quality in Maintenance Engineering* 1 (1): 39–45. <https://doi.org/10.1108/13552519510083138/FULL/HTML>.
- An, Dawn, Nam H. Kim, and Joo Ho Choi. 2015. "Practical Options for Selecting Data-Driven or Physics-Based Prognostics Algorithms with Reviews." *Reliability Engineering and System Safety* 133: 223–36. <https://doi.org/10.1016/J.RESS.2014.09.014>.
- An, Dawn, Nam Ho Kim, and Joo-Ho Choi. 2013. "Options for Prognostics Methods: A Review of Data-Driven and Physics- Based Prognostics." *Annual Conference of the PHM Society* 5 (1). <https://doi.org/10.36001/PHMCONF.2013.V5I1.2184>.
- Behzad, Mehdi, Sajjad Feizhoseini, Hesam Addin Arghand, Ali Davoodabadi, and David Mba. 2020. "Failure Threshold Determination of Rolling Element Bearings Using Vibration Fluctuation and Failure Modes." *Applied Sciences* 2021, Vol. 11, Page 160 11 (1): 160. <https://doi.org/10.3390/APP11010160>.
- Bian, Xihui, Mengxuan Ling, Yuanyuan Chu, Peng Liu, and Xiaoyao Tan. 2022. "Spectral Denoising Based on Hilbert–Huang Transform Combined with F-Test." *Frontiers in Chemistry* 10 (August). <https://doi.org/10.3389/FCHEM.2022.949461>.
- Bousdekis, Alexandros, Babis Magoutas, Dimitris Apostolou, and Gregoris Mentzas. 2018. "Review, Analysis and Synthesis of Prognostic-Based Decision Support Methods for Condition Based Maintenance." *Journal of Intelligent Manufacturing* 29 (6): 1303–16. <https://doi.org/10.1007/S10845-015-1179-5/FIGURES/3>.
- Bozbulut, Ali Riza, and Serkan Eryilmaz. 2020. "Generalized Extreme Shock Models and Their Applications." *Communications in Statistics: Simulation and Computation* 49 (1): 110–20. <https://doi.org/10.1080/03610918.2018.1476699>.
- Byon, Eunshin, Lewis Ntamo, and Yu Ding. 2010. "Optimal Maintenance Strategies for Wind Turbine Systems under Stochastic Weather Conditions." *IEEE Transactions on*

- Reliability* 59 (2): 393–404. <https://doi.org/10.1109/TR.2010.2046804>.
- Cao, Yingsai, Jianqiang Luo, and Wenjie Dong. 2023. “Optimization of Condition-Based Maintenance for Multi-State Deterioration Systems under Random Shock.” *Applied Mathematical Modelling* 115 (March): 80–99. <https://doi.org/10.1016/J.APM.2022.10.036>.
- Castro, I. T., N. C. Caballé, and C. J. Pérez. 2015. “A Condition-Based Maintenance for a System Subject to Multiple Degradation Processes and External Shocks.” *International Journal of Systems Science* 46 (9): 1692–1704. <https://doi.org/10.1080/00207721.2013.828796>.
- Chen, Jinglong, Jun Pan, Zipeng Li, Yanyang Zi, and Xuefeng Chen. 2016. “Generator Bearing Fault Diagnosis for Wind Turbine via Empirical Wavelet Transform Using Measured Vibration Signals.” *Renewable Energy* 89 (April): 80–92. <https://doi.org/10.1016/J.RENENE.2015.12.010>.
- Cheng, C, G Ma, Y Zhang, M Sun, ... F Teng - IEEE/ASME, and Undefined 2020. 2022. “A Deep Learning-Based Remaining Useful Life Prediction Approach for Bearings.” *Ieeexplore.Ieee.Org* C Cheng, G Ma, Y Zhang, M Sun, F Teng, H Ding, Y Yuan *IEEE/ASME Transactions on Mechatronics, 2020* *ieeexplore.Ieee.Org*. <https://ieeexplore.ieee.org/abstract/document/8982045/>.
- Cheng, Cheng, Guijun Ma, Yong Zhang, Mingyang Sun, Fei Teng, Han Ding, and Ye Yuan. 2020. “A Deep Learning-Based Remaining Useful Life Prediction Approach for Bearings.” *IEEE/ASME Transactions on Mechatronics* 25 (3): 1243–54. <https://doi.org/10.1109/TMECH.2020.2971503>.
- Cho, Sangjin, Md. Rifat Shahriar, and Uipil Chong. 2014. “Identification of Significant Intrinsic Mode Functions for the Diagnosis of Induction Motor Fault.” *The Journal of the Acoustical Society of America* 136 (2): EL72–77. <https://doi.org/10.1121/1.4885541>.
- Cubillo, Adrian, Suresh Perinpanayagam, and Manuel Esperon-Miguez. 2016. “A Review of Physics-Based Models in Prognostics: Application to Gears and Bearings of Rotating Machinery.” *Advances in Mechanical Engineering* 8 (8): 1–21. <https://doi.org/10.1177/1687814016664660>.
- Cui, Lingli, Xin Wang, Huaqing Wang, and Jianfeng Ma. 2020. “Research on Remaining Useful Life Prediction of Rolling Element Bearings Based on Time-Varying Kalman Filter.” *IEEE Transactions on Instrumentation and Measurement* 69 (6): 2858–67. <https://doi.org/10.1109/TIM.2019.2924509>.
- Dekker, Rommert. 1996. “Applications of Maintenance Optimization Models: A Review and Analysis.” *Reliability Engineering & System Safety* 51 (3): 229–40. [https://doi.org/10.1016/0951-8320\(95\)00076-3](https://doi.org/10.1016/0951-8320(95)00076-3).
- Dong, Wenjie, Sifeng Liu, Suk Joo Bae, and Yingsai Cao. 2020. “Reliability Modelling for Multi-Component Systems Subject to Stochastic Deterioration and Generalized Cumulative Shock Damages.” <https://doi.org/10.1016/j.res.2020.107260>.
- Frate, Luca Del. 2013. “Failure of Engineering Artifacts: A Life Cycle Approach.” *Science and Engineering Ethics* 19 (3): 913–44. <https://doi.org/10.1007/S11948-012-9360-0/FIGURES/5>.
- Gan, Shuyuan, Hengheng Hu, and David W. Coit. 2023. “Maintenance Optimization

- Considering the Mutual Dependence of the Environment and System with Decreasing Effects of Imperfect Maintenance.” *Reliability Engineering and System Safety* 235 (July). <https://doi.org/10.1016/J.RESS.2023.109202>.
- Gan, Shuyuan, Zhifang Song, and Lei Zhang. 2022. “A Maintenance Strategy Based on System Reliability Considering Imperfect Corrective Maintenance and Shocks.” *Computers & Industrial Engineering* 164 (February): 107886. <https://doi.org/10.1016/J.CIE.2021.107886>.
- Geetikaverma, and Vikramjit Singh. 2018. “Empirical Wavelet Transform & Its Comparison with Empirical Mode Decomposition: A Review.” *International Journal of Engineering Research and Technology*.
- Gilles, Jerome. 2013. “Empirical Wavelet Transform.” *IEEE Transactions on Signal Processing* 61 (16): 3999–4010. <https://doi.org/10.1109/TSP.2013.2265222>.
- Gilles, Jérôme, Giang Tran, and Stanley Osher. 2014. “2D Empirical Transforms. Wavelets, Ridgelets, and Curvelets Revisited.” *SIAM Journal on Imaging Sciences* 7 (1): 157–86. <https://doi.org/10.1137/130923774>.
- Godoy, David R., Rodrigo Pascual, and Peter Knights. 2013. “Critical Spare Parts Ordering Decisions Using Conditional Reliability and Stochastic Lead Time.” *Reliability Engineering and System Safety* 119: 199–206. <https://doi.org/10.1016/J.RESS.2013.05.026>.
- Guo, Runxia, Bo Gong, Runxia Guo, and Bo Gong. 2022. “Research on Remaining Useful Life of Rolling Bearings Using EWT-DI-ALSTM.” *MeScT* 33 (9): 095104. <https://doi.org/10.1088/1361-6501/AC6EC9>.
- Heng, Aiwin, Sheng Zhang, Andy C.C. Tan, and Joseph Mathew. 2009. “Rotating Machinery Prognostics: State of the Art, Challenges and Opportunities.” *Mechanical Systems and Signal Processing* 23 (3): 724–39. <https://doi.org/10.1016/J.YMSSP.2008.06.009>.
- Hong, H. P., W. Zhou, S. Zhang, and W. Ye. 2014. “Optimal Condition-Based Maintenance Decisions for Systems with Dependent Stochastic Degradation of Components.” *Reliability Engineering & System Safety* 121 (January): 276–88. <https://doi.org/10.1016/J.RESS.2013.09.004>.
- Hu, Yang, Xuewen Miao, Yong Si, Ershun Pan, and Enrico Zio. 2022. “Prognostics and Health Management: A Review from the Perspectives of Design, Development and Decision.” *Reliability Engineering & System Safety* 217 (January): 108063. <https://doi.org/10.1016/J.RESS.2021.108063>.
- Huang, Norden E., and Zhaohua Wu. 2008. “A Review on Hilbert-Huang Transform: Method and Its Applications to Geophysical Studies.” *Reviews of Geophysics* 46 (2). <https://doi.org/10.1029/2007RG000228>.
- ISO. 2004. Condition monitoring and diagnostics of machines, prognostics, part 1: General guidelines, International Standard, ISO 13381-1:2004, issued 2004.
- “ISO 15243:2017 - Rolling Bearings — Damage and Failures — Terms, Characteristics and Causes.” n.d. Accessed August 13, 2023. <https://www.iso.org/standard/59619.html>.
- Jin, Yuxue, Jie Geng, Chuan Lv, Ying Chi, and Tingdi Zhao. 2023. “A Methodology for Equipment Condition Simulation and Maintenance Threshold Optimization Oriented to

- the Influence of Multiple Events.” *Reliability Engineering and System Safety* 229 (January). <https://doi.org/10.1016/J.RESS.2022.108879>.
- José, Renny, and Arismendi Torres. 2022. “Piecewise Deterministic Markov Processes for Condition-Based Maintenance Modelling Applications to Critical Infrastructures.”
- Juybari, Mohammad N., Ali Zeinal Hamadani, and Mostafa Abouei Ardakan. 2023. “Availability Analysis and Cost Optimization of a Repairable System with a Mix of Active and Warm-Standby Components in a Shock Environment.” *Reliability Engineering and System Safety* 237 (September). <https://doi.org/10.1016/J.RESS.2023.109375>.
- Kankar, P. K., Satish C. Sharma, and S. P. Harsha. 2011. “Fault Diagnosis of Ball Bearings Using Continuous Wavelet Transform.” *Applied Soft Computing* 11 (2): 2300–2312. <https://doi.org/10.1016/J.ASOC.2010.08.011>.
- Khan, MA, B Asad, K Kudelina, T Vaimann, A Kallaste - Energies, and Undefined 2022. 2022. “The Bearing Faults Detection Methods for Electrical Machines—The State of the Art.” *Mdpi.Com*. <https://www.mdpi.com/1996-1073/16/1/296>.
- Kim, Nam Ho, Joo Ho Choi, and Dawn An. 2016. “Prognostics and Health Management of Engineering Systems: An Introduction.” *Prognostics and Health Management of Engineering Systems: An Introduction*, January, 1–345. <https://doi.org/10.1007/978-3-319-44742-1/COVER>.
- Klausen, A., R. W. Folgerø, K. G. Robbersmyr, and H. R. Karimi. 2017. “Accelerated Bearing Life-Time Test Rig Development for Low Speed Data Acquisition.” *Modeling, Identification and Control* 38 (3): 143–56. <https://doi.org/10.4173/MIC.2017.3.4>.
- Ko, Young Myoung, and Eunshin Byon. 2017. “Condition-Based Joint Maintenance Optimization for a Large-Scale System with Homogeneous Units.” <Http://Dx.Doi.Org/10.1080/0740817X.2016.1241457> 49 (5): 493–504. <https://doi.org/10.1080/0740817X.2016.1241457>.
- Koutras, V. P., S. Malefaki, and A. N. Platis. 2017. “Optimization of the Dependability and Performance Measures of a Generic Model for Multi-State Deteriorating Systems under Maintenance.” *Reliability Engineering & System Safety* 166 (October): 73–86. <https://doi.org/10.1016/J.RESS.2017.01.002>.
- Lee, Jay, Fangji Wu, Wenyu Zhao, Masoud Ghaffari, Linxia Liao, and David Siegel. 2014. “Prognostics and Health Management Design for Rotary Machinery Systems - Reviews, Methodology and Applications.” *Mechanical Systems and Signal Processing* 42 (1–2): 314–34. <https://doi.org/10.1016/J.YMSSP.2013.06.004>.
- Li, Qiang, Changfeng Yan, Guangyi Chen, Huibin Wang, Hongkun Li, and Lixiao Wu. 2022. “Remaining Useful Life Prediction of Rolling Bearings Based on Risk Assessment and Degradation State Coefficient.” *ISA Transactions* 129 (October): 413–28. <https://doi.org/10.1016/J.ISATRA.2022.01.031>.
- Li, Xiang, Qian Ding, and Jian Qiao Sun. 2018. “Remaining Useful Life Estimation in Prognostics Using Deep Convolution Neural Networks.” *Reliability Engineering & System Safety* 172 (April): 1–11. <https://doi.org/10.1016/J.RESS.2017.11.021>.
- Li, Yuxiong, Xianzhen Huang, Pengfei Ding, and Chengying Zhao. 2021. “Wiener-Based Remaining Useful Life Prediction of Rolling Bearings Using Improved Kalman Filtering

- and Adaptive Modification.” *Measurement: Journal of the International Measurement Confederation* 182 (September).
<https://doi.org/10.1016/J.MEASUREMENT.2021.109706>.
- Liao, Linxia, and Felix Köttig. 2016. “A Hybrid Framework Combining Data-Driven and Model-Based Methods for System Remaining Useful Life Prediction.” *Applied Soft Computing* 44 (July): 191–99. <https://doi.org/10.1016/J.ASOC.2016.03.013>.
- Lin, Jing, and Liangsheng Qu. 2000. “FEATURE EXTRACTION BASED ON MORLET WAVELET AND ITS APPLICATION FOR MECHANICAL FAULT DIAGNOSIS.” *Journal of Sound and Vibration* 234 (1): 135–48.
<https://doi.org/10.1006/JSVI.2000.2864>.
- Liu, Junqiang, Chunlu Pan, Fan Lei, Dongbin Hu, and Hongfu Zuo. 2021. “Fault Prediction of Bearings Based on LSTM and Statistical Process Analysis.” *Reliability Engineering & System Safety* 214 (October): 107646. <https://doi.org/10.1016/J.RESS.2021.107646>.
- Liu, Shujie, and Lexian Fan. 2022. “An Adaptive Prediction Approach for Rolling Bearing Remaining Useful Life Based on Multistage Model with Three-Source Variability.” *Reliability Engineering & System Safety* 218 (February): 108182.
<https://doi.org/10.1016/J.RESS.2021.108182>.
- Liu, Wei, and Wei Chen. 2019. “Recent Advancements in Empirical Wavelet Transform and Its Applications.” *IEEE Access* 7: 103770–80.
<https://doi.org/10.1109/ACCESS.2019.2930529>.
- Ly, Canh, Kwok Tom, Carl S Byington, Romano Patrick, and George J Vachtsevanos. 2009. “Fault Diagnosis and Failure Prognosis for Engineering Systems: A Global Perspective; Fault Diagnosis and Failure Prognosis for Engineering Systems: A Global Perspective.” <https://doi.org/10.1109/COASE.2009.5234094>.
- Malla, Chandrabhanu, and Isham Panigrahi. 2019. “Review of Condition Monitoring of Rolling Element Bearing Using Vibration Analysis and Other Techniques.” *Journal of Vibration Engineering & Technologies* 7: 407–14. <https://doi.org/10.1007/s42417-019-00119-y>.
- Meng, Huixing, and Yan Fu Li. 2019. “A Review on Prognostics and Health Management (PHM) Methods of Lithium-Ion Batteries.” *Renewable and Sustainable Energy Reviews* 116 (December): 109405. <https://doi.org/10.1016/J.RSER.2019.109405>.
- Merainani, Boualem, Sofiane Laddada, Eric Bechhoefer, Mohamed Abdessamed Ait Chikh, and Djamel Benazzouz. 2022. “An Integrated Methodology for Estimating the Remaining Useful Life of High-Speed Wind Turbine Shaft Bearings with Limited Samples.” *Renewable Energy* 182 (January): 1141–51.
<https://doi.org/10.1016/J.RENENE.2021.10.062>.
- Moradi, Ramin, and Katrina M. Groth. 2020. “Modernizing Risk Assessment: A Systematic Integration of PRA and PHM Techniques.” *Reliability Engineering and System Safety* 204 (December). <https://doi.org/10.1016/J.RESS.2020.107194>.
- Nectoux, Patrick, Rafael Gouriveau, Kamal Medjaher, Emmanuel Ramasso, Brigitte Chebel-Morello, Nouredine Zerhouni, Christophe Varnier, et al. 2012. “PRONOSTIA : An Experimental Platform for Bearings Accelerated Degradation Tests.” sur CD ROM (June): 1–8. <https://hal.science/hal-00719503>.

- Nie, Lei, Lvfan Zhang, Shiyi Xu, Wentao Cai, and Haoming Yang. 2022. "Remaining Useful Life Prediction for Rolling Bearings Based on Similarity Feature Fusion and Convolutional Neural Network." *Journal of the Brazilian Society of Mechanical Sciences and Engineering* 44 (8): 1–16. <https://doi.org/10.1007/S40430-022-03638-0/FIGURES/15>.
- Paris, P, Assistant Director, and F Erdogan. 1963. "A Critical Analysis of Crack Propagation Laws." http://asmedigitalcollection.asme.org/fluidsengineering/article-pdf/85/4/528/5763569/528_1.pdf.
- Pedersen, Tom Ivar, and Jørn Vatn. 2022. "Optimizing a Condition-Based Maintenance Policy by Taking the Preferences of a Risk-Averse Decision Maker into Account." *Reliability Engineering and System Safety* 228 (December). <https://doi.org/10.1016/J.RESS.2022.108775>.
- Peng, Fei, Li Zheng, Yongdong Peng, Congcong Fang, and Xianghui Meng. 2022. "Digital Twin for Rolling Bearings: A Review of Current Simulation and PHM Techniques." *Measurement: Journal of the International Measurement Confederation* 201 (September). <https://doi.org/10.1016/J.MEASUREMENT.2022.111728>.
- Puliafito, Vito, Silvano Vergura, and Mario Carpentieri. 2017. "Fourier, Wavelet, and Hilbert-Huang Transforms for Studying Electrical Users in the Time and Frequency Domain." *Energies* 2017, Vol. 10, Page 188 10 (2): 188. <https://doi.org/10.3390/EN10020188>.
- Qi, Faqun, and Meiqi Huang. 2023. "Optimal Condition-based Maintenance Policy for Systems with Mutually Dependent Competing Failure." *Quality and Reliability Engineering International*, March. <https://doi.org/10.1002/QRE.3316>.
- Qian, Yuning, Ruqiang Yan, and Robert X. Gao. 2017. "A Multi-Time Scale Approach to Remaining Useful Life Prediction in Rolling Bearing." *Mechanical Systems and Signal Processing* 83 (January): 549–67. <https://doi.org/10.1016/J.YMSSP.2016.06.031>.
- Qiu, Hai, Jay Lee, Jing Lin, and Gang Yu. 2006. "Wavelet Filter-Based Weak Signature Detection Method and Its Application on Rolling Element Bearing Prognostics." *Journal of Sound and Vibration* 289 (4–5): 1066–90. <https://doi.org/10.1016/J.JSV.2005.03.007>.
- Rai, Akhand, and S. H. Upadhyay. 2016. "A Review on Signal Processing Techniques Utilized in the Fault Diagnosis of Rolling Element Bearings." *Tribology International* 96 (April): 289–306. <https://doi.org/10.1016/J.TRIBOINT.2015.12.037>.
- Rai, V. K., and A. R. Mohanty. 2007. "Bearing Fault Diagnosis Using FFT of Intrinsic Mode Functions in Hilbert–Huang Transform." *Mechanical Systems and Signal Processing* 21 (6): 2607–15. <https://doi.org/10.1016/J.YMSSP.2006.12.004>.
- Refaei, Ali. n.d. "Introduction to Inference: Estimation and Prediction." In .
- Ren, Lei, Yaqiang Sun, Hao Wang, and Lin Zhang. 2018. "Prediction of Bearing Remaining Useful Life with Deep Convolution Neural Network." *IEEE Access* 6 (February): 13041–49. <https://doi.org/10.1109/ACCESS.2018.2804930>.
- Sarada, Y., and R. Shenbagam. 2021. "Optimization of a Repairable Deteriorating System Subject to Random Threshold Failure Using Preventive Repair and Stochastic Lead Time." *Reliability Engineering and System Safety* 205 (January).

<https://doi.org/10.1016/J.RESS.2020.107229>.

- Shafiee, Mahmood, Maxim Finkelstein, and Christophe Bérenguer. 2015. “An Opportunistic Condition-Based Maintenance Policy for Offshore Wind Turbine Blades Subjected to Degradation and Environmental Shocks.” *Reliability Engineering and System Safety* 142 (July): 463–71. <https://doi.org/10.1016/J.RESS.2015.05.001>.
- Son, Khanh Le, Mitra Fouladirad, Anne Barros, Eric Levrat, and Benoît Iung. 2013. “Remaining Useful Life Estimation Based on Stochastic Deterioration Models: A Comparative Study.” *Reliability Engineering & System Safety* 112 (April): 165–75. <https://doi.org/10.1016/J.RESS.2012.11.022>.
- Soualhi, Abdenour, Kamal Medjaher, and Noureddine Zerhouni. 2014. “Bearing Health Monitoring Based on Hilbert-Huang Transform, Support Vector Machine and Regression.” *IEEE Transactions on Instrumentation and Measurement*, 1–11. <https://doi.org/10.1109/TIM.2014.2330494i>.
- Sutrisno, Edwin, Hyunseok Oh, Arvind Sai, Sarathi Vasani, and Michael Pecht. 2012. “Estimation of Remaining Useful Life of Ball Bearings Using Data Driven Methodologies.” <https://doi.org/10.1109/ICPHM.2012.6299548>.
- Tajiani, Bahareh, Raziieh Amiri, and Jørn Vatn. 2021. “Risk Assessment of Fires in Residential Buildings-A Case Study in Norway.” In *31st European Safety and Reliability Conference (ESREL 2021)*, edited by Bruno Castanier, Marko Cepin, David Bigaud, and Christophe Berenguer. Angers, France. <https://doi.org/10.3850/978-981-18-2016-8>.
- Tajiani, Bahareh, and Jørn Vatn. 2020. “Degradation Modelling of Roller Bearings Using Two Different Health Indicators.” In *The 30th European Safety and Reliability Conference and the 15th Probabilistic Safety Assessment and Management Conference (ESREL2020 PSAM15)*, edited by Piero Baraldi, Francesco Di Maio, and Enrico Zio. Venice, Italy: Research Publishing: Singapore. <https://doi.org/10.3850/978-981-14-8593-0>.
- Tajiani, Bahareh, and Jørn Vatn. 2021. “RUL Prediction of Bearings Using Empirical Wavelet Transform and Bayesian Approach.” In *31st European Safety and Reliability Conference (ESREL 2021)*, edited by Bruno Castanier, Marko Cepin, David Bigaud, and Christophe Berenguer. Angers, France. <https://doi.org/10.3850/978-981-18-2016-8>.
- Tajiani, Bahareh, and Jørn Vatn. 2023. “Adaptive Remaining Useful Life Prediction Framework with Stochastic Failure Threshold for Experimental Bearings with Different Lifetimes under Contaminated Condition.” *International Journal of System Assurance Engineering and Management* 1: 3. <https://doi.org/10.1007/s13198-023-01979-0>.
- Tajiani, Bahareh, Jørn Vatn, and Viggo Gabriel Borg Pedersen. 2020. “Remaining Useful Life Estimation Using Vibration-Based Degradation Signals.” In *The 30th European Safety and Reliability Conference and the 15th Probabilistic Safety Assessment and Management Conference (ESREL2020 PSAM15)*, edited by Piero Baraldi, Francesco Di Maio, and Enrico Zio. Venice, Italy: Research Publishing: Singapore. <https://doi.org/10.3850/978-981-14-8593-0>.
- Tao, Y, J Zhao, S Feng - Journal of Mechanical Science and Technology, and undefined 2020. 2020. “A Reliability Assessment Model for Journal Bearing Based on Natural Degradation and Random Shocks.” *Springer* 34 (11): 4641–48.

<https://doi.org/10.1007/s12206-020-1022-6>.

- Thakker, H. T., V. Dave, V. Vakharia, and S. Singh. 2020. "Fault Diagnosis of Ball Bearing Using Hilbert Huang Transform and LASSO Feature Ranking Technique." *IOP Conference Series: Materials Science and Engineering* 841 (1). <https://doi.org/10.1088/1757-899X/841/1/012006>.
- Thoppil, Nikhil M., V. Vasu, and C. S.P. Rao. 2021. "Health Indicator Construction and Remaining Useful Life Estimation for Mechanical Systems Using Vibration Signal Prognostics." *International Journal of System Assurance Engineering and Management* 12 (5): 1001–10. <https://doi.org/10.1007/S13198-021-01190-Z>.
- Vatn, Jørn, and Terje Aven. 2009. "An Approach to Maintenance Optimization Where Safety Issues Are Important." <https://doi.org/10.1016/j.res.2009.06.002>.
- Wakiru, J., L. Pintelon, P. N. Muchiri, and P. Chemweno. 2018. "Maintenance Optimization: Application of Remanufacturing and Repair Strategies." *Procedia CIRP* 69: 899–904. https://doi.org/10.1016/J.PROCIR.2017.11.008/MAINTENANCE_OPTIMIZATION_A_APPLICATION_OF_REMANUFACTURING_AND_REPAIR_STRATEGIES.PDF.
- Wald, Randall, Taghi Khoshgoftaar, and John C. Sloan. 2011. "Fourier Transforms for Vibration Analysis: A Review and Case Study." *Proceedings of the 2011 IEEE International Conference on Information Reuse and Integration, IRI 2011*, 366–71. <https://doi.org/10.1109/IRI.2011.6009575>.
- Wang, Biao, Yaguo Lei, Naipeng Li, and Ningbo Li. 2020. "A Hybrid Prognostics Approach for Estimating Remaining Useful Life of Rolling Element Bearings." *IEEE Transactions on Reliability* 69 (1): 401–12. <https://doi.org/10.1109/TR.2018.2882682>.
- Wang, Fu Kwun, and Tadele Mamo. 2019. "Hybrid Approach for Remaining Useful Life Prediction of Ballbearings." *Quality and Reliability Engineering International* 35 (7): 2067–2511.
- Wang, Han, Haitao Liao, and Xiaobing Ma. 2022. "Stochastic Multi-Phase Modeling and Health Assessment for Systems Based on Degradation Branching Processes." *Reliability Engineering & System Safety* 222 (June): 108412. <https://doi.org/10.1016/J.RESS.2022.108412>.
- Wang, Han, Dongdong Wang, Haoxiang Liu, and Gang Tang. 2022. "A Predictive Sliding Local Outlier Correction Method with Adaptive State Change Rate Determining for Bearing Remaining Useful Life Estimation." *Reliability Engineering & System Safety* 225 (September): 108601. <https://doi.org/10.1016/J.RESS.2022.108601>.
- Wang, Ping, Zhiqiang Long, and Gao Wang. 2020. "A Hybrid Prognostics Approach for Estimating Remaining Useful Life of Wind Turbine Bearings." *Energy Reports* 6 (December): 173–82. <https://doi.org/10.1016/J.EGYR.2020.11.265>.
- Wang, W., and F. Gu. 2000. "Modeling Condition Based Maintenance Decision Support." *Proceedings of the 33rd International MATADOR Conference*, 159–64. https://doi.org/10.1007/978-1-4471-0777-4_25.
- Wang, Wenbo, Jiaojiao Zhao, and Guorong Ding. 2022. "RUL Prediction of Rolling Bearings Based on Improved Empirical Wavelet Transform and Convolutional Neural Network." *Advances in Mechanical Engineering* 14 (6). https://doi.org/10.1177/16878132221106609/ASSET/IMAGES/LARGE/10.1177_16878

132221106609-FIG20.JPEG.

- Wen, Juan, Hongli Gao, and Jiangquan Zhang. 2018. "Bearing Remaining Useful Life Prediction Based on a Nonlinear Wiener Process Model." *Shock and Vibration* 2018. <https://doi.org/10.1155/2018/4068431>.
- Wen, Yuxin, Jianguo Wu, Devashish Das, and Tzu Liang(Bill) Tseng. 2018. "Degradation Modeling and RUL Prediction Using Wiener Process Subject to Multiple Change Points and Unit Heterogeneity." *Reliability Engineering & System Safety* 176 (August): 113–24. <https://doi.org/10.1016/J.RESS.2018.04.005>.
- Wu, Bo, Wei Li, and Ming Quan Qiu. 2017. "Remaining Useful Life Prediction of Bearing with Vibration Signals Based on a Novel Indicator." *Shock and Vibration* 2017. <https://doi.org/10.1155/2017/8927937>.
- Xia, Min, Teng Li, Tongxin Shu, Jiafu Wan, Clarence W de Silva, Zhongren Wang, Jiafu M Wan Xia, T Li, and C W de Silva. 2019. "A Two-Stage Approach for the Remaining Useful Life Prediction of Bearings Using Deep Neural Networks; A Two-Stage Approach for the Remaining Useful Life Prediction of Bearings Using Deep Neural Networks." *J. Wan Is with the School of Mechanical and Automotive Engineer-Ing* 15 (6). <https://doi.org/10.1109/TII.2018.2868687>.
- Yan, Bingxin, Xiaobing Ma, Guifa Huang, and Yu Zhao. 2021. "Two-Stage Physics-Based Wiener Process Models for Online RUL Prediction in Field Vibration Data." *Mechanical Systems and Signal Processing* 152 (May): 107378. <https://doi.org/10.1016/J.YMSSP.2020.107378>.
- Yang, Hongyu, Joseph Mathew, and Lin Ma. 2003. "Vibration Feature Extraction Techniques for Fault Diagnosis of Rotating Machinery : A Literature Survey." *Asia-Pacific Vibration Conference*.
- Ye, Zhi Sheng, and Nan Chen. 2014. "The Inverse Gaussian Process as a Degradation Model." *Technometrics* 56 (3): 302–11. https://doi.org/10.1080/00401706.2013.830074/SUPPL_FILE/UTCH_A_830074_SM8965.PDF.
- Ye, Zhi Sheng, Nan Chen, and Yan Shen. 2015. "A New Class of Wiener Process Models for Degradation Analysis." *Reliability Engineering and System Safety* 139: 58–67. <https://doi.org/10.1016/J.RESS.2015.02.005>.
- Zhao, Bo, Xianmin Zhang, Zhenhui Zhan, and Qiqiang Wu. 2021. "A Robust Construction of Normalized CNN for Online Intelligent Condition Monitoring of Rolling Bearings Considering Variable Working Conditions and Sources." *Measurement* 174 (April): 108973. <https://doi.org/10.1016/J.MEASUREMENT.2021.108973>.
- Zhao, Chengying, Xianzhen Huang, Huizhen Liu, al -, Chong Chen, Tao Wang, and Ying Liu. 2020. "Bearing Remaining Useful Life Estimation Using an Adaptive Data-Driven Model Based on Health State Change Point Identification and K-Means Clustering You May Also like A Novel Bootstrap Ensemble Learning Convolutional Simple Recurrent Unit Method for Remaining Useful Life Interval Prediction of Turbofan Engines Spatial Attention-Based Convolutional Transformer for Bearing Remaining Useful Life Prediction." <https://doi.org/10.1088/1361-6501/ab6671>.
- Zhao, Minghang, Baoping Tang, and Qian Tan. 2016. "Bearing Remaining Useful Life Estimation Based on Time–Frequency Representation and Supervised Dimensionality

- Reduction.” *Measurement* 86 (May): 41–55.
<https://doi.org/10.1016/J.MEASUREMENT.2015.11.047>.
- Zhao, Xiujie, Shuguang He, Zhen He, and Min Xie. 2018. “Optimal Condition-Based Maintenance Policy with Delay for Systems Subject to Competing Failures under Continuous Monitoring.” *Computers and Industrial Engineering* 124 (October): 535–44.
<https://doi.org/10.1016/J.CIE.2018.08.006>.
- Zhou, Jianghong, Yi Qin, Dingliang Chen, Fuqiang Liu, and Quan Qian. 2022. “Remaining Useful Life Prediction of Bearings by a New Reinforced Memory GRU Network.” *Advanced Engineering Informatics* 53 (August): 101682.
<https://doi.org/10.1016/J.AEI.2022.101682>.
- Zhou, Shuang, Maohua Xiao, Petr Bartos, Martin Filip, and Guosheng Geng. 2020. “Remaining Useful Life Prediction and Fault Diagnosis of Rolling Bearings Based on Short-Time Fourier Transform and Convolutional Neural Network.”
<https://doi.org/10.1155/2020/8857307>.
- Zhu, Jun, Nan Chen, and Weiwen Peng. 2019. “Estimation of Bearing Remaining Useful Life Based on Multiscale Convolutional Neural Network.” *IEEE Transactions on Industrial Electronics* 66 (4): 3208–16. <https://doi.org/10.1109/TIE.2018.2844856>.
- Zikrullah, Nanda Anugrah. 2022. “Contributions to the Safety of Novel Subsea Technologies - Methods and Approaches to Support the Safety Demonstration Process.”
- Zio, Enrico. 2022. “Prognostics and Health Management (PHM): Where Are We and Where Do We (Need to) Go in Theory and Practice.” *Reliability Engineering & System Safety* 218 (February): 108119. <https://doi.org/10.1016/J.RESS.2021.108119>.

Appended papers

Paper 1

Remaining Useful Life Estimation Using Vibration-based Degradation Signals

Bahareh Tajiani

Department of Industrial and Mechanical Engineering, Norwegian University of Science and Technology (NTNU), Norway. E-mail: Bahareh.tajiani@ntnu.no

Jørn Vatn

Department of Industrial and Mechanical Engineering, Norwegian University of Science and Technology (NTNU), Norway. E-mail: jorn.vatn@ntnu.no

Viggo Gabriel Borg Pedersen

Department of Industrial and Mechanical Engineering, Norwegian University of Science and Technology (NTNU), Norway. E-mail: viggo.g.pedersen@ntnu.no

Roller bearing as one of the most critical components in rotating machinery can lead to many failures. Thus, condition-monitoring of them has gained immense attention for improving their reliability, decreasing their maintenance cost and unplanned downtimes. There have been various approaches for bearings' prognosis which are mainly for estimation of "Remaining Useful Life (RUL)". However, bearing's RUL estimation is still a challenging task mainly due to not having enough failure data. In this paper, an experimental setup is developed at NTNU in order to perform some accelerated failure tests on some bearings. Vibration data is then collected using two accelerometers mounted horizontally and vertically on each tested bearing. Bearing degradation caused by pouring some "Silicium Carbide" as a contaminant which accelerates the vibration. The collected data is then pre-processed, and some time-domain statistical features are extracted to track the deterioration of the bearings. Furthermore, the extracted features are compared to determine a health indicator for the bearings. Three different time-dependent models and a stochastic process have been applied to the degradation signals. In addition, RUL is predicted using different degradation models and the "Probability Density Function (PDF)" of the "Fist Passage Time (FPT)" is represented for the bearings.

Keywords: Remaining Useful Life, prognosis, feature extraction, vibration signatures, accelerated life tests, rotating machinery, stochastic process.

1. Introduction

Roller bearing is one of the most critical components in rotating machinery. Many faults in rotating machinery are induced by failures in bearings (Khadersab and Shivakumar 2018). Therefore, fault diagnosis and prognosis of bearings have been a concern of researchers for a long time. In order to prevent bearing failure, many effective parameters to measure, have been discussed in the literature such as acoustic temperature, oil analysis, pressure etc. (Tian 2009). However, vibration monitoring is the most widely used technology to analyze the bearing degradation for predicting RUL of the bearing, since it can represent the status of the bearing timely and roundly (Y. Zhang, Zuo, and Bai 2015); (Wu, Li, and Qiu 2017). Vibration signals are buried in noise. Hence it is essential to pre-process the data which consists of data filtering to smooth data while normalizing them to be in the same scale (Miljković 2015).

It is often difficult to monitor the deterioration of bearings using only vibration signals. To tackle this problem, there are three main approaches to extract features, namely, time domain analysis, frequency domain analysis and time and

frequency representation of signals. Time-domain analysis uses statistical properties of the raw signals such as kurtosis, crest factor, Root Mean Square (RMS), impulse factor etc. Some of the features perform well on incipient faults while others are unable to provide meaningful information regarding incipient and local faults (Caesarendra and Tjahjowidodo 2017). Frequency-domain analysis shows raw signals in frequency domain to trend the bearing degradation. The simplest and most widely used approach in industries to perform frequency-domain analysis of bearings vibration is to use Fast Fourier Transform (FFT). FFT helps us examine the high-frequency signals caused by fault in the bearings (Caesarendra and Tjahjowidodo 2017). Comparing different time-domain and frequency-domain features extracted from raw signals, provides us with a health indicator (HI) to monitor the bearing condition. HI is used to model the deterioration of the bearing in order to build a predictive maintenance model to predict RUL to anticipate and avoid failures.

In this paper, we develop a vibration setup at RAMS laboratory at "Norwegian University of

Science and Technology (NTNU)", Trondheim, Norway. The vibration setup is used to perform accelerated experimental tests on two roller bearings that run until failure. The bearings are degraded by particle contamination in lubricants which is one of the major causes of bearing failure. Silicium carbide is the solid particle added to lubricant and poured into the tested bearing. Vibration data is then collected using two accelerometers mounted horizontally and vertically on each tested bearing. The collected data is then pre-processed, and some statistical time-domain features have been extracted. The most appropriate and time-consistent feature has been selected as a health indicator to monitor and inspect the status of the bearings continuously. After selecting the health indicator, some deterministic and a stochastic model have been fitted on the dataset in order to develop a degradation model and predict RUL accordingly.

Validating the proposed models is significantly important. However, due to not having sufficient data, all the data are considered as training dataset and employed to build the model. For further work, a greater number of experimental data will be collected and then categorized into training dataset to create the model and testing dataset to test the model to evaluate the performance of the proposed methodology.

The rest of this paper is organized as follows: Section 2 discusses the theoretical background of the work. The proposed approach is presented in Section 3 and Section 4 is devoted to conclusions.

2. Theoretical Background

2.1 Prognostic and Health Management

Condition-based maintenance (CBM) is a maintenance strategy, helping us optimize the operations cost, increase system reliability and availability, which is based on monitoring the actual condition of the system in order to apply an adequate maintenance action at the right time (Shin and Jun 2015a). Therefore, it requires a condition monitoring system to track the system performance. CBM focuses on detection of faults, as well as failures prediction (Shin and Jun 2015b). The first task, diagnosis, is detection and identification of the root cause of the failure. Whereas, the second task, prognostics, is the process of predicting time-to-failure (TTF) by assessing degradation or deterioration extent of the system from its normal stage (Tsui et al. 2015); (Koons-Stapf 2015).

Prognostics and Health Management (PHM) is used to develop a cost-effective maintenance schedule by monitoring the degradation of engineering systems to figure out when failures may occur (Souto Maior et al. 2019). Three main subjects in PHM that need to be considered include

an estimation of the current health condition of the system, predicting time to failure in the future and identifying the failure's impact on the system performance (Atamuradov et al. 2017).

One of the main critical parameters in prognostics and CBM is RUL which is the time left until failure occurs. Monitoring the system's health status can be based on measuring various parameters such as temperature, vibration, noise level, etc., of which vibration monitoring is of special importance for rotating machinery (Ahmad and Kamaruddin 2012).

Detecting defects and damages using measured vibration data is difficult mainly due to noise in the signals. In this regard, feature extraction is used for preprocessing of the signals and to transform vibration data into relevant knowledge in order to monitor the condition of bearings (Boldt, Rauber, and Varejao 2013); (T.P.K. Nguyen et al. 2018).

2.2 PHM and Feature Extraction

Time-domain features are some statistical features such as kurtosis, crest factor, Root Mean Square (RMS), shape factor etc., some of which such as kurtosis are related to the probability density function (PDF) of the vibration signals. Therefore, if there is a change in vibration signals, PDF of the signals changes as well, and so does the kurtosis (Caesarendra and Tjahjowidodo 2017). Table 1 is a list of some time-domain features together with their formulas. In addition to time-domain features, frequency domain features and time-frequency representation of vibration signals have been described and applied in many articles before (Verma et al. 2012); (Caesarendra and Tjahjowidodo 2017); (Boldt, Rauber, and Varejao 2013); (Beltran-Carbajal 2012). Frequency-domain features and time-frequency representation of vibration signals are not discussed in this paper.

Table 1. Statistical Time-domain Features (Muhammad Masood Tahir 2018)

Time-domain Feature	Formula
Kurtosis	$Ku = \frac{\sum_{i=1}^N (x_i - m)^4}{(N-1)\sigma^4}$
Crest Factor	$CF = \frac{\max x_i }{\sqrt{\frac{1}{N} \sum_{i=1}^N x_i^2}}$
RMS	$RMS = \sqrt{\frac{1}{N} \sum_{i=1}^N x_i^2}$
Shape Factor	$SF = \frac{\sqrt{\frac{1}{N} \sum_{i=1}^N x_i^2}}{\frac{1}{N} \sum_{i=1}^N x_i }$
Impulse Factor	$IF = \frac{\max x_i }{\frac{1}{N} \sum_{i=1}^N x_i }$

Where, x_i is the vibration signal at time i , m and σ are mean and standard deviation of the vibration signals and N is the total number of vibration signals.

2.3 Stochastic Processes

Stochastic processes are popular to describe the deterioration of systems because they can describe the temporal variation of the degradation process in a finite time interval (Liu et al. 2016). Some stochastic processes that have been widely used in degradation modelling are: “Gamma Process” and “Wiener Process”. One of the main properties of Gamma process is monotonicity of the degradation increments. Therefore, wiener process is a more applicable stochastic process applied in this paper.

2.3.1 Wiener Process with Drift and Diffusion Parameters

Brownian Motion or Wiener Process is also a continuous-time stochastic process which is a more popular degradation modelling than Gamma Process. The popularity of this stochastic model is because the degradation increments can vary non-monotonically. Therefore, degradation increments either increase or decrease gradually and accumulatively over time (K.T.P. Nguyen, Fouladirad, and Grall 2018). In general Brownian Motion, the degradation process $\{X_t; t \geq 0\}$ is as follows (Z. Zhang et al. 2018):

$$X_t = X_0 + \eta t + \sigma_B B(t) \quad (1)$$

Where, X_0 is the initial degradation state of the system, η is the drift parameter capturing the degradation rate, σ_B is the diffusion parameter and $\{B(t); T \geq 0\}$ is a standard Brownian motion representing stochastic dynamics of degradation process. A wiener process with drift and scale parameters has the following properties.

- $X_0 = 0$ (with probability 1)
- X has random independent increments. The increments are also stationary.
- X_t is a continuous stochastic process following a Normal distribution with mean ηt and variance $\sigma_B^2 t$ (K.T.P. Nguyen, Fouladirad, and Grall 2018).

In Wiener process with linear drift, the distribution of “First Passage Time (FPT)” can be formulated analytically as “Inverse Gaussian Distribution” with the parameters of $\mu = (\omega - y_t)/\eta$ and $\lambda = (\omega - y_t)^2/\sigma_B^2$ (Rausand and Høyland 2008) where ω is failure threshold and y_t is the degradation level at time t . The FPT distribution can be obtained by utilizing the property that the sum of the Gaussian variables is again

Gaussian distributed. The “Cumulative Distribution Function (CDF)”, mean and variance in “Inverse Gaussian Distribution” is:

$$F_T(t) = \phi\left(\frac{\sqrt{\lambda}}{\mu}\sqrt{t} - \sqrt{\lambda}\frac{1}{\sqrt{t}}\right) + \quad (2)$$

$$\phi\left(-\frac{\sqrt{\lambda}}{\mu}\sqrt{t} - \sqrt{\lambda}\frac{1}{\sqrt{t}}\right)e^{\frac{2\lambda}{\mu}}$$

for $t > 0$, $\mu > 0$ and $\lambda > 0$.

$$E(T) = \mu \quad (3)$$

$$Var(T) = \frac{\mu^3}{\lambda} \quad (4)$$

3. Description of the Proposed Approach

As mentioned above, there are several steps to implement the proposed approach. In this section, the procedure of the proposed method is discussed and shown in Fig. 1. and some theoretical issues based on literature review are introduced in details.

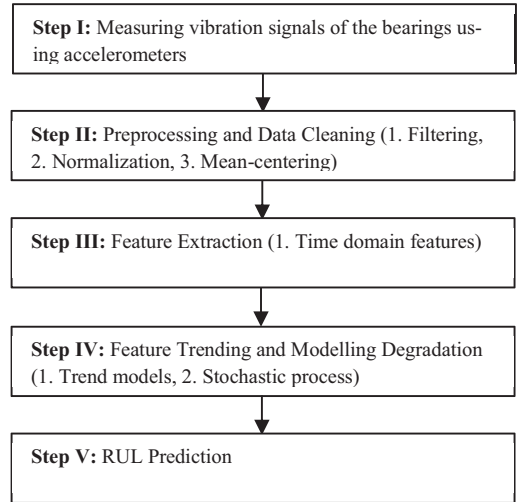


Fig. 1. Flowchart of the proposed approach

3.1 Experimental Setup

As briefly discussed above, an experimental setup called “Bently Nevada (system 1) Rotor Kit, model RK4” is developed at RAMS laboratory at NTNU. The aim of developing this setup is to perform some accelerated “run-to-failure” experimental tests on some roller bearings. The setup consists of some parts such as a rotating part, main part, and a measurement part.

3.1.1 Rotating Part

The rotating part consists of an asynchronous motor as an actuator and two rotor mass wheels. The motor allows the inner race, rollers and the cage of the bearings to rotate through the whole system. The maximum rotational speed of the motor is 10000 revolutions per minute (rpm).

3.1.2 Main Part

The main part has some major components such as a support test bearing shaft (10mm) and two bearing blocks to hold the bearings, mounted on an aluminum frame with a safety cover which is used while running experiments for safety issues.

3.1.3 Measurement Part

The characterization of the bearing degradation is based on vibration sensors. The vibration sensors consist of two sets of miniature accelerometers mounted perpendicular to each other on each bearing. The two accelerometers are placed radially on the external race of the bearings. The data acquisition system aggregates the data from all vibration sensors and transmits them to the central unit in charge of real time data visualization and storage. The amplifier (type 5134B) and accelerometers (type 8702B100) used in the measurement part of this setup are provided by “Kistler” company. Fig. 2 shows an overview of the setup and its different parts. Fig. 3 shows the horizontal and vertical accelerometers together with bearing house, axle and motor.

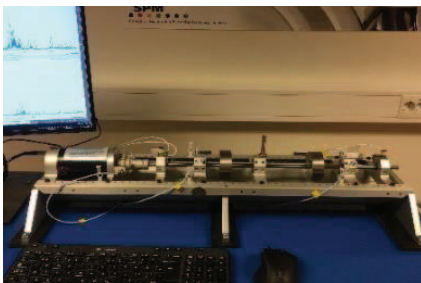


Fig. 2. Vibration Setup

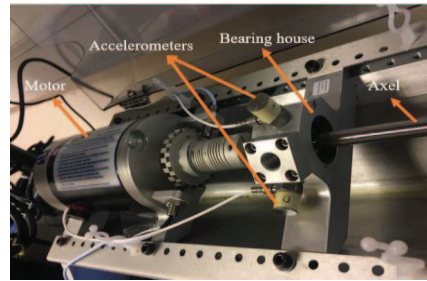


Fig. 3. Main components of the setup

3.2 Data Description

As mentioned before, the acceleration data is collected using two accelerometers mounted horizontally and vertically on each tested bearing. Both experiments were performed under a constant operating condition which has a motor speed of 3050 rpm and room temperature. The sampling frequency is 12860 Hz which means that each sample has a duration of 0.158 seconds and 2032 datapoints. Bearing 1 consists of 86 number of samples, while bearing 2 has 100 samples. The samples are taken every 6 minutes.

Fig. 4 and Fig. 5 show the first and the last samples of raw vibration data of bearing 1. The first sample is for when the bearing is healthy, and the last sample is when it is considered as failed.

Fig. 6 and Fig. 7 present the whole lifetime of bearing 1 and bearing 2 from the healthy state to the failed state. The test is ceased once the vibration level surpasses 7g to prevent damage.

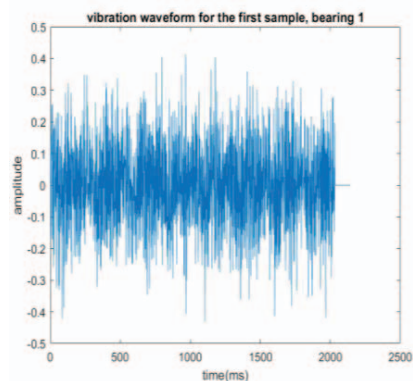


Fig. 4. The first sample of bearing 1

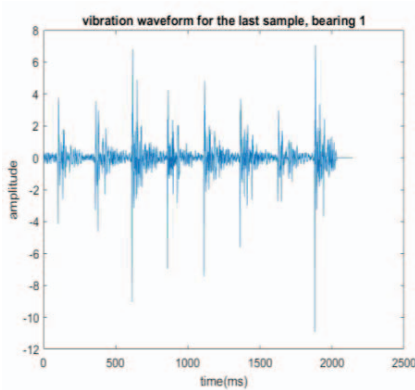


Fig. 5. The last sample of bearing 1

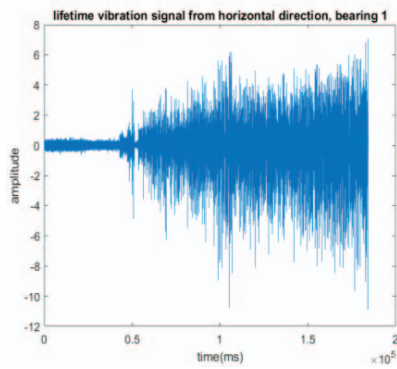


Fig. 6. The lifetime vibration signal from horizontal direction for bearing 1

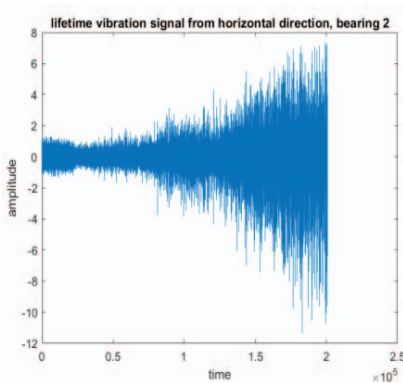


Fig. 7. The lifetime vibration signal from horizontal direction for bearing 2

In addition to vibration data, the bearing geometry data is summarized in Table 2.

Table 2. Specifications of Bearings

Type of Bearing	Open roller/ball bearings
Number of balls	10 Balls
Pitch diameter (B), mm	70
Ball diameter, mm	4.7
Inner diameter (d), mm	15.9
Outer diameter (D), mm	34.9

3.3 Pre-processing and Feature Extraction

In this paper, the vibration signals are mean-centered and normalized in order to be in the same scale. Furthermore, moving-average filter as a filtering method has been applied to normalized data to smooth them. The window size for the moving average is 5 data-points. Extracted features are used to show the status of the bearings' condition. Fig. 8 represents the behaviour of bearing 2 time-domain features calculated using equations presented in Table 1 from the healthy state to the failed state.

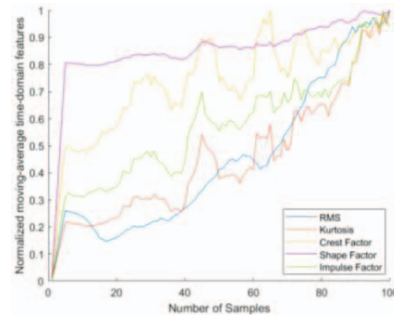


Fig. 8. Time-domain features degradation behaviour, bearing 2

3.4 Health Indicator Selection

The statistical time-domain features extracted before are compared to select the most informative feature as a health indicator. According to the assumption that an ideal degradation path is a monotonic increasing path over time, ‘‘Spearman’s Correlation Coefficient’’ has been calculated for all the features. This is to figure out which features have a very strong relationship with time.

Table 3 represents the Spearman’s correlation coefficients between time and different time-domain features. As it is shown, impulse factor and crest factor have correlation values less than 0.7 and they are not considered for further analysis. Furthermore, ‘‘Principle Component Analysis (PCA)’’ has been performed on the remaining time-domain features to understand how much

they explain the variation of the data. In bearing 1, the first two principle components explain 96 percent of the variance of the data, while in bearing 2, the first principle component explains 94 percent of the data variation. Therefore, sum of loading scores for the first 2 PCs in bearing 1 and the first PC in bearing 2 are calculated to see which feature has a higher impact in explaining the variation of the data. According to Table 4, the three features have almost the same impact in explaining the variance of the data in bearing 2, while in bearing 1, kurtosis is the dominant one. Comparing the results, kurtosis can be selected as the health indicator due to its consistency with time and high influence in explaining the data variation.

Table 3. Spearman's Correlation Coefficients for different time-domain features

Time-domain Features	Bearing 1	Bearing 2
kurtosis	0.7377	0.9124
RMS	0.8917	0.9391
Crest Factor	0.5933	0.7681
Shape Factor	0.8606	0.9318
Impulse Factor	0.6810	0.8814

Table 4. Loading scores for the remaining time-domain features for the two bearings

Loading scores	Bearing 1	Bearing 2
kurtosis	1.3609	0.5737
Shape factor	0.8154	0.5879
RMS	1.1241	0.5703

As mentioned before, kurtosis is a representative of PDF of the vibration signals which increases with the growth of bearing fault (Sutrisno et al. 2012). Fig. 9 represents the normalized moving-average kurtosis as the health indicator over time for the two bearings.

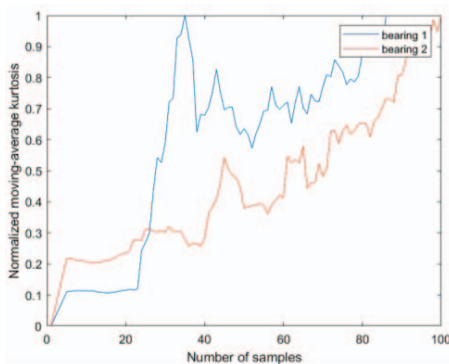


Fig. 9. Normalized Moving-average kurtosis of two bearings

3.5 Feature Trending and Modelling Degradation

In this section, we develop a degradation model to monitor the bearings' behavior to avoid upcoming failures and defects. The bearings' degradation paths are compared by fitting three time-series models. The models $y = aexp(bt)$, $y = aexp(bt^2)$ and $y = at + b$ are fitted on normalized moving-average kurtosis degradation paths of two bearings, where a and b are constants, t is time and y is the degradation level. The R-squared values corresponding to these three models are calculated and presented in Table 5, based on which the goodness-of-fit of the models are compared.

Table 5. Goodness of Fit of Trend Models to Kurtosis of Two Bearings

Deterministic Models	Bearing 1	Bearing 2
$y = aexp(bt)$	0.7902	0.9729
$y = aexp(bt^2)$	0.7006	0.9599
$y = at + b$	0.8488	0.9473

However, stochastic processes are more popular than deterministic models as the deterioration of the bearings has some inherent randomness which can be modelled using stochastic processes. Moreover, deterioration process is not only dependent on the bearing age, but also on current state of the bearings. These make the Brownian motion with linear drift a more suitable and applicable process because of its capabilities in modelling the inherent randomness and non-monotonic property of degradation increments.

Table 6 presents the estimated parameters of the Brownian motion with linear drift using Maximum Likelihood Estimation (MLE). The time unit between either of two consecutive increments is considered one for this probabilistic model.

Table 6. Estimated Coefficients of the Stochastic Process-Brownian Motion with Linear Drift

	Drift Parameter	Diffusion Parameter
Bearing 1	0.0080	0.0553
Bearing 2	0.0101	0.0370

3.6 Estimation of First Passage Time (FPT)

In this section, RUL is predicted using both the deterministic models and the stochastic process.

In deterministic models, different parametric distributions are fitted on models' coefficients to find out which distribution describes the coefficients best. Weibull distribution is selected as to

fit on the coefficients of the three models due to its lowest negative log-likelihood value compared to other distributions. Furthermore, a Monte-Carlo Simulation is applied to simulate a sufficiently large number of degradation paths by generating random samples from the Weibull's Distribution scale and shape parameters in order to predict RUL. The expected value of RUL for the deterministic models are 71, 75 and 69 samples respectively. As already mentioned, the time interval for recording two consecutive signals is 6 minutes. Therefore, RUL can be simply interpreted in terms of time (minutes).

As described before, in Wiener process, the distribution of FPT is analytically formulated as "Inverse Gaussian Distribution".

Fig. 10 depicts the PDFs of the first passage times for bearing 2 at different monitoring samples to show how RUL changes. It indicates that the variance and uncertainty of FPT in bearing 2 decrease at the expense of the number of monitored samples. Fig. 11 shows the CDFs of FPT for the two bearings calculated using Eq. (2). In this analysis, the failure threshold is set to one based on the observation of the kurtosis of the two bearings shown in Fig. 9 and discussion with experts. Therefore, the actual first hitting time is 35 samples for bearing 1 and 100 samples for bearing 2 (see Fig. 9).

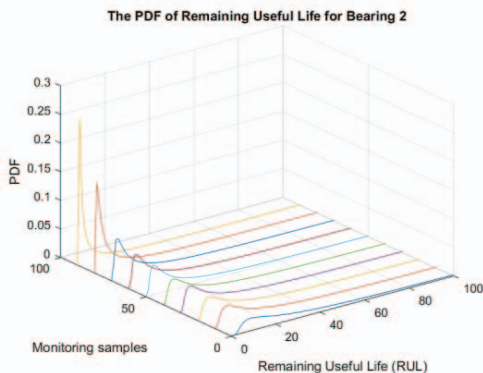


Fig. 10. PDF of FPT for bearing 2

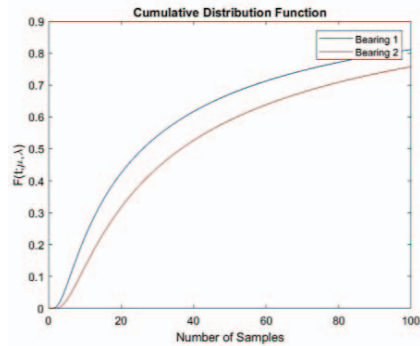


Fig. 11. CDF of FPT for bearings 1 and 2

4. Conclusions

This paper proposes an approach for estimating the RUL of bearings using vibration data collected at RAMS laboratory at NTNU. The approach is based on three deterministic models and a stochastic model to predict the RUL. Several time-domain features were extracted from the dataset. To compare the deterministic models, the R-squared values were presented. The RUL was estimated for either of such deterministic models. Moreover, the CDF of RUL for the bearings was obtained from the stochastic Wiener process which can be used as a preliminary analysis for RUL prediction of roller bearings. A possible solution to improve the result is to include a higher number of run-to-failure experiments of bearings as well as using some advanced signal processing techniques such as Short-Time Fourier Transform (STFT) and wavelet transform of vibration signals (Singleton, Strangas, and Aviyente 2013).

For further work, it is recommended to collect a higher number of experimental vibration data to be able to validate the proposed model and evaluate its performance on unseen data.

References

- Ahmad, Rosmaini, and Shahrul Kamaruddin. 2012. "An overview of time-based and condition-based maintenance in industrial application." *Computers & Industrial Engineering* 63 (1): 135-149.
- Atamuradov, Vepa, Kamal Medjaher, Pierre Dersin, Benjamin Lamoureux, and Nouredine Zerhouni. 2017. "Prognostics and Health Management for Maintenance Practitioners-Review, Implementation and Tools Evaluation." *International Journal of Prognostics and Health Management* 8: 31.
- Beltran-Carbajal, Francisco. 2012. *Advances in Vibration Engineering and Structural Dynamics*.
- Boldt, F de A, Thomas W Rauber, and Flávio M Varejao. 2013. "Feature extraction and selection for automatic fault diagnosis of rotating machinery." *X Encontro Nacional de Inteligencia Artificial e*

- Computacional (ENIAC).*-Fortaleza, Cear : 213-220.
- Caesarendra, Wahyu, and Tegoeh Tjahjowidodo. 2017. "A Review of Feature Extraction Methods in Vibration-Based Condition Monitoring and Its Application for Degradation Trend Estimation of Low-Speed Slew Bearing." *Machines* 5: 21.
- Khadersab, A., and S. Shivakumar. 2018. "Vibration Analysis Techniques for Rotating Machinery and its effect on Bearing Faults." *Procedia Manufacturing* 20: 247-252.
- Koons-Stapf, Amanda. 2015. *Condition Based Maintenance: Theory, Methodology, & Application*.
- Liu, Le, Xiao-Yang Li, Fuqiang Sun, and Ning Wang. 2016. "A General Accelerated Degradation Model Based on the Wiener Process." *Materials* 9: 981.
- Miljkovi , Dubravko. 2015. "Brief Review of Vibration Based Machine Condition Monitoring." *CrSNDT Journal* 5: 14-23.
- Muhammad Masood Tahir, Saeed Badshah, Ayyaz Hussain, Muhammad Adil Khattak. 2018. "Extracting accurate time domain features from vibration signals for reliable classification of bearing faults." *International journal of Advanced and Applied Sciences* 5 (1 (January 2018)): 156-163.
- Nguyen, Khanh T. P., Mitra Fouladirad, and Antoine Grall. 2018. "Model selection for degradation modeling and prognosis with health monitoring data." *Reliability Engineering & System Safety* 169: 105-116.
- Nguyen, Thi Phuong Khanh, Amor Khlaief, Kamal Medjaher, Antoine Picot, Pascal Maussion, Diego Tobon, Bertrand Chauchat, and Regis Cheron. 2018. "Analysis and comparison of multiple features for fault detection and prognostic in ball bearings." Fourth european conference of the prognostics and health management society 2018, Utrecht, Netherlands, 2018-07-01.
- Rausand, Marvin, and Arnljot H yland. 2008. *System Reliability Theory: Models, Statistical Methods, and Applications*. Hoboken, NJ, USA: Hoboken, NJ, USA: John Wiley & Sons, Inc.
- Shin, Jong-Ho, and Hong-Bae Jun. 2015a. "On condition based maintenance policy." *Journal of Computational Design and Engineering* 2 (2): 119-127.
- . 2015b. "On condition based maintenance policy." *Journal of Computational Design and Engineering* 44.
- Singleton, Rodney K, Elias G Strangas, and Selin Aviyente. 2013. "Time-frequency complexity based remaining useful life (RUL) estimation for bearing faults." 2013 9th IEEE International Symposium on Diagnostics for Electric Machines, Power Electronics and Drives (SDEMPED).
- Souto Maior, Caio, Monalisa Santos, Jo o Santana, Ana Negreiros, Marcio Moura, and Isis Lins. 2019. *Convolutional Neural Network for remaining useful life prediction based on vibration signal*.
- Sutrisno, Edwin, Hyunseok Oh, Arvind Vasan, and Michael Pecht. 2012. *Estimation of remaining useful life of ball bearings using data driven methodologies*.
- Tian, Zhigang. 2009. *An artificial neural network method for remaining useful life prediction of equipment subject to condition monitoring*. Vol. 23.
- Tsui, Kwok L., Nan Chen, Qiang Zhou, Yizhen Hai, and Wenbin Wang. 2015. "Prognostics and Health Management: A Review on Data Driven Approaches." *Mathematical Problems in Engineering* 2015: 17.
- Verma, N. K., S. Singh, J. K. Gupta, R. K. Sevakula, S. Dixit, and A. Salour. 2012. "Smartphone application for fault recognition." 2012 Sixth International Conference on Sensing Technology (ICST), 18-21 Dec. 2012.
- Wu, Bo, Wei Li, and Ming-quan Qiu. 2017. "Remaining useful life prediction of bearing with vibration signals based on a novel indicator." *Shock and Vibration* 2017.
- Zhang, Ying, Hongfu Zuo, and Fang Bai. 2015. "Feature extraction for rolling bearing fault diagnosis by electrostatic monitoring sensors." *Proceedings of the Institution of Mechanical Engineers, Part C: Journal of Mechanical Engineering Science* 229 (10): 1887-1903.
- Zhang, Zhengxin, Xiaosheng Si, Changhua Hu, and Yaguo Lei. 2018. "Degradation data analysis and remaining useful life estimation: A review on Wiener-process-based methods." *European Journal of Operational Research* 271 (3): 775-796.

Paper 2

Degradation Modelling of Roller Bearings using Two Different Health Indicators

Bahareh Tajiani

Department of Industrial and Mechanical Engineering, Norwegian University of Science and Technology (NTNU), Norway. E-mail: Bahareh.tajiani@ntnu.no

Jørn Vatn

Department of Industrial and Mechanical Engineering, Norwegian University of Science and Technology (NTNU), Norway. E-mail: jorn.vatn@ntnu.no

The fault detection, diagnostics, and prognostics of bearings play a key role in increasing the reliability, availability, and efficiency of rotating machinery. Signal processing techniques are useful for the health condition monitoring of rotating machinery. Fast-Fourier transformation, Wavelet transformation, and Hilbert-Huang transformation are three main time-frequency techniques to analyze vibration signals and extract representative features to monitor the health status of bearings. Hilbert-Huang transformation has attracted lots of attention due to its advantage in handling non-linear and non-stationary signals. However, identifying an appropriate feature, fault diagnosis, and remaining useful life prediction of roller bearings has remained an open challenge and highly dependent on the applied applications and methods. In this paper, two accelerated failure tests have been conducted on real bearings at NTNU to collect vibration data of bearings from a healthy state to the failed state. The degradation mechanism to degrade the bearings is contamination which is mixing solid particles, i.e., “Silisum Carbide” and a lubricant to pour into the bearing continuously. Empirical Mode Decomposition (EMD) has been applied to decompose the signals into different Intrinsic Mode Functions (IMFs) and the most informative IMF has been selected to extract Hilbert energy as a time-frequency feature for degradation modeling. RMS as an energy representative feature in time-domain has also been employed and compared with Hilbert energy to predict the failure time of the experimental bearings.

Keywords: Remaining Useful Life, Empirical Mode Decomposition, Hilbert-Huang transform, prognosis, accelerated life tests, Wiener process.

1. Introduction

Roller bearings are the critical components in rotating machinery and their health monitoring plays an important role in guaranteeing a safe operation, improving reliability and reducing maintenance costs. Generally, the failure prediction of bearings takes two steps. The first one is selecting an appropriate health indicator (HI) and the second one is how to model the bearings' deterioration. Due to non-stationary, non-linear, and non-Gaussian characteristics of the vibration signals, both time-domain methods and frequency-domain methods are insufficient to obtain the most representative features (Sejdić, Djurović, and Jiang 2009). Since many signals of interest such as vibration signals of roller bearings have changing frequency characteristics, time-frequency analysis has been widely applied in the application of rotating machinery. There have been three main classifications of time-frequency representation techniques which are short-time Fourier transform (STFT), wavelet transform (WT) and Hilbert-Huang transform (HHT). Any of these approaches have their limitations. For instance, wavelet transform is a non-adaptive approach, while STFT has the challenge of window selection size to match with the specific

frequency band which contains fault information of the bearing (Nguyen et al. 2018). Hence, HHT as a self-adaptive method has been known as the most suitable time-frequency approach which is used for analyzing non-stationary and non-linear vibration signals. HHT consists of two different steps: Empirical Mode Decomposition (EMD) and Hilbert spectral analysis.

EMD is used to decompose the signals into a small and finite number of Intrinsic Mode Functions (IMFs) with different frequency ranges ordered from high frequency to low-frequency band within their time scales. In EMD, IMFs need to satisfy two main conditions:

- The number of zero-crossings and extreme values should be equal or differ by one at most.
- The mean envelope which is the average of the high envelope and low envelope at any point in time should be zero.

Proceedings of the 30th European Safety and Reliability Conference and the 15th Probabilistic Safety Assessment and Management Conference.

Edited by Piero Baraldi, Francesco Di Maio and Enrico Zio

Copyright © 2020 by ESREL2020 PSAM 15 Organizers. *Published by* Research Publishing, Singapore
ISBN: 981-973-0000-00-0 :: doi: 10.3850/981-973-0000-00-0 esrel2020psam15-paper

The process to obtain IMFs is called the sifting process which can be described as follows (Soualhi, Medjaher, and Zerhouni 2015).

- (i) Finding all the extreme values (local maxima and minima) and using “cubic spline interpolation” to find the upper and lower envelope of the vibration signals.
- (ii) calculating the mean of upper and lower envelopes (m_1).
- (iii) Subtracting the mean of the higher and lower envelopes from the original vibration signal ($h_1 = x(t) - m_1$). If h_1 meets the two conditions mentioned above, it will be stored as the first IMF (C_1). If not, h_1 will be regarded as the analysis signal and the above steps will be repeated until the obtained IMF satisfies the two conditions.
- (iv) Subtracting C_1 from the original signal ($r_1(t) = x(t) - C_1(t)$).
- (v) $r_1(t)$ will be considered as the original signal and the procedure will be repeated to separate a series of components that meet the IMF conditions.
- (vi) Repeating until the IMF does not satisfy the two conditions anymore. Then, the decomposition procedure stops, and the original signal will be:

$$x(t) = \sum_{i=1}^n c_i(t) + r_n(t) \quad (1)$$

Once the IMFs ($c_i(t)$) have been identified, Hilbert transformation of the IMFs of the vibration signals can be obtained by applying Hilbert transform. The analytic form of IMFs is expressed in Eq. (2) for $1 \leq i \leq n$.

$$C_i^A(t) = C_i(t) + j C_i^H(t) = a_i(t) e^{j\theta_i(t)} \quad (2)$$

Where n is the number of IMFs, $C_i^H(t)$ is the Hilbert transformation of $C_i(t)$. The polar coordinate of the analytic form of IMF gives the possibility to obtain instantaneous amplitude ($a_i(t)$) and instantaneous phase ($\theta_i(t)$).

$$a_i(t) = \sqrt{C_i^2 + C_i^{H^2}} \quad (3)$$

$$\theta_i(t) = \tan^{-1}\left(\frac{C_i^H}{C_i}\right) \quad (4)$$

One can calculate instantaneous frequency based on instantaneous phase which is given below.

$$f_i(t) = \frac{1}{2\pi} \frac{d\theta_i(t)}{dt} \quad (5)$$

The energy of the signals is the sum of squared instantaneous amplitude as a function of both time and frequency and it performs as a time-frequency feature (Yu, YuDejie, and Junsheng 2006).

However, not all the IMFs contain significant information on the fault, and some represent only noise. To identify and select the most informative IMFs, several approaches have been introduced such as energy-based thresholding in (Cho, Shahriar, and Chong 2014) to eliminate physically insignificant IMFs. In this paper, first, the Pearson correlation coefficient between the original signal and each IMF will be calculated and the IMFs with less than 0.1 as their correlation coefficient do not really contain useful information (Li, Yang, and Yang 2018). The second criterion is energy for each IMF (C_i) where $i = 1, 2, 3, \dots, n$ and n is the number of IMFs, the energy can be calculated as:

$$E_i = \sum_{j=1}^N |C_i(j)| \quad (6)$$

Where N is the number of samples in each IMF. The IMFs with a high correlation factor and energy can be identified as the most suitable IMF for feature extraction. However, the first IMF is known as the one with the highest noise which can mislead us in the process of feature extraction and HI selection (Terrien, Marque, and Karlsson 2011).

In addition to time-frequency techniques, time-domain features such as kurtosis, crest factor, Root Mean Square (RMS), shape factor, etc., have the ability to represent the degradation performance of the bearings in one domain (Caesarendra and Tjahjowidodo 2017). However, any of these features have strengths and weaknesses. For instance, kurtosis is employed and used as a health indicator in many published articles and literature reviews. In some cases, kurtosis shows an increasing trend with the degradation of bearing while in some other cases,

it does not perform well when the bearing is approaching the failure threshold and it is more applicable to use in the diagnosis of incipient faults (Wang et al. 2016). Among time-domain features, RMS calculates the energy of the signals in the time domain and therefore this feature is also selected to compare with Hilbert energy (Lei et al. 2008).

3. Modelling

Wiener process as a continuous-time stochastic process has been in favor of many researchers recently. This popularity comes from the fact that the degradation increments in the Wiener process can vary non-monotonically and they can either increase or decrease. Moreover, the degradation level at time zero is zero and the degradation increments are independent of each other.

The general form of the Wiener process with linear drift is represented as follows (Cox and Miller 1965)

$$X_t = X_0 + \mu t + \sigma_B B(t) \quad (7)$$

Where $\{X_t; t \geq 0\}$ is the deterioration process, μ is the drift parameter, σ_B is the diffusion parameter, X_t is the degradation level at time t , and $\{B(t); t \geq 0\}$ is the standard Brownian motion which is representative of the stochastic behavior of the degradation process. In Wiener process with linear drift, X_t follows Normal distribution with the mean of μt and variance of $\sigma_B^2 t$.

The advantage of Wiener process with linear drift is that the First Hitting Time (FHT) distribution is analytically known as Inverse Gaussian distribution with mean value of $\eta = (L - X_t)/\mu$ and $\lambda = (L - X_t)^2/\sigma_B^2$ where L is the failure threshold defined by industrial standards, expert judgement who have enough experiences of working with the system of interest and published articles (Rausand and Høyland 2008). The Cumulative Distribution Function (CDF) of the FHT is obtained by considering the property that the sum of the Gaussian variables is Gaussian distributed. CDF of FHT is presented in Eq. (8).

$$F_T(t) = \phi\left(\frac{\sqrt{\lambda}}{\eta}\sqrt{t} - \sqrt{\lambda}\frac{1}{\sqrt{t}}\right) + \phi\left(-\frac{\sqrt{\lambda}}{\eta}\sqrt{t} - \sqrt{\lambda}\frac{1}{\sqrt{t}}\right)e^{\frac{2\lambda}{\eta}} \quad (8)$$

4. Experimental Setup and Data

The measurement part of the test rig ‘‘Bently Nevada (system 1) Rotor Kit, model RK4’’ is depicted in Fig. 1. It mainly consists of a rotating shaft with the length of 10mm, a motor with the maximum rotation speed of 10000 revolutions per minute (rpm), two accelerometers and a central unit to acquire and visualize the acceleration data. The amplifier (type 5134B) and accelerometers (type 8702B100) used in the measurement part of this setup are provided by ‘‘Kistler’’ company. More details about the vibration setup and the bearings’ physical characteristics can be found in (Tajiani and Vatn 2020). Two accelerated run-to-failure datasets were collected in vertical direction of the two identical bearings operating under the same condition. The motor speed to perform the experiments is 2976 rpm. The degradation mechanism to degrade the bearings is contamination which is mixing silicium carbide particles and grease as a lubricant to pour it into the bearing every 5 samples continuously where the sampling interval is 5 minutes. The experimental tests were terminated when the vertical vibration amplitude reached 12g to prevent damage to the motor and other components. Table 1 shows a brief description of acceleration data. The difference in number of datapoints and sample duration is due to the different sampling frequency for the bearings.

Table 1, Data description of bearing 1 and 2

Bearing	Number of samples	Number of datapoints in each sample	Sample duration (ms)
Bearing 1	104	2064	0.161
Bearing 2	34	8192	0.639

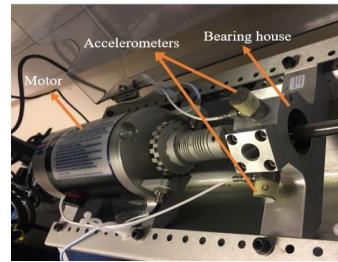


Fig. 1. Measurement part of the setup

5. Results and Discussion

For decomposing the vibration signals into intrinsic mode functions with different frequency bands, EMD was applied on the entire lifetime of the bearings to see how the extracted features

from the IMFs change over time from the healthy state to the failed state.

The analytic form of the IMFs together with their instantaneous amplitudes were calculated using Eq. (2) and Eq. (3) for the two roller bearings. Fig. 2 shows the IMFs and a residue obtained by EMD for bearing 1 when it was in a healthy state as an illustration. In fact, it represents the EMD algorithm applied on the first sample of bearing 1 containing 2064 datapoints.

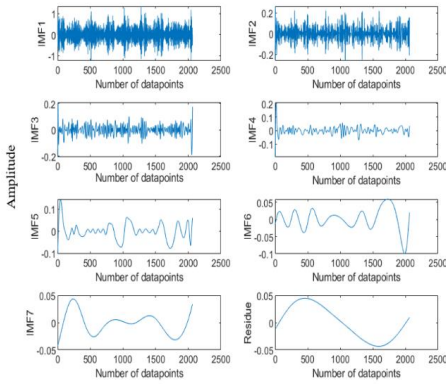


Fig. 2. EMD decomposition of bearing 1, healthy state

The IMFs obtained from the lifetime of bearing 1 and 2 were calculated together with their associated energy and correlation coefficient with the original signal and the result for the first bearing is shown in Table 2. In this paper, the first IMF has the highest energy as well as the highest correlation with the original signal. However, in many published articles, the first IMF is recognized as the IMF with the highest amount of noise and other IMFs were removed since their correlation with the original signal was below 0.1 which means that they do not contain significant information regarding the defect in the bearings. Therefore, the second IMF as the next appropriate one is selected for extracting Hilbert energy as a HI for degradation modelling. In addition, in the EMD scheme, the second IMF is considered providing increased clarity (see Fig. 3 and Fig. 4).

Table 2, Energy and correlation coefficient of each IMF, bearing 1

IMF	Energy	Pearson correlation coefficient
1	3.2e5	0.9460
2	2.5e4	0.2463

3	8.6e3	0.1147
4	1.5e3	0.0189
5	2.9e3	0.06
6	637.13	0.0158
7	130.73	0.0014
8	46.5	0.0014
9	52.15	0.000006

As mentioned before, the Hilbert energy (HE) as a HI was extracted from the second IMF of the vibration samples and it shows an increasing trend with the growth of fault. Fig. 3 and Fig. 4 is an illustration of the HE development over time from the healthy state to the failed state of the bearings calculated using instantaneous amplitude of the signals shown in Eq. (3).

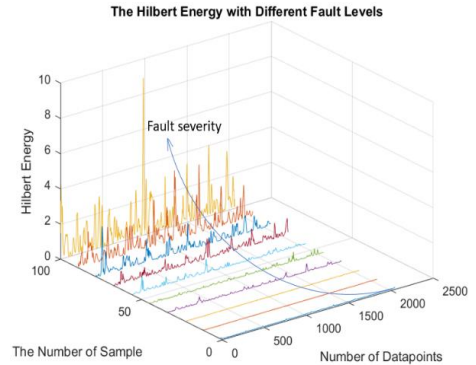


Fig. 3. HE of bearing 1 at different samples with the growth of fault

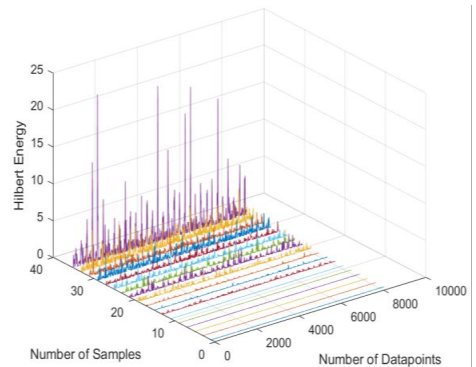


Fig. 4. HE of bearing 2 at different samples with the growth of fault

The main task to develop a deterioration model for the degradation data is to identify a model to

capture the system's behaviour based on the shape and nature of the degradation trajectories as a function of a lifetime. Fig. 5 is an illustration of the degradation paths of bearings 1 and 2 that have an increasing trend over number of samples. The Hilbert energy for each sample is the average of HE at all the datapoints and is defined as the energy extracted from the second IMF of bearings 1 and 2. Fig. 6 represents the time-domain features' performance for bearing 1 over time. As it can be seen, some features such as kurtosis and crest factor have some rises at the beginning which reflects the fact that they are sensitive to faults occurring at the beginning of the bearings' lifetime while they remain stable at the end. On the other hand, RMS which is an energy representative of the signal in time-domain shows an increasing trend during the bearing's lifetime. Time-domain features calculation formulas can be found in (Tajiani and Vatn 2020).

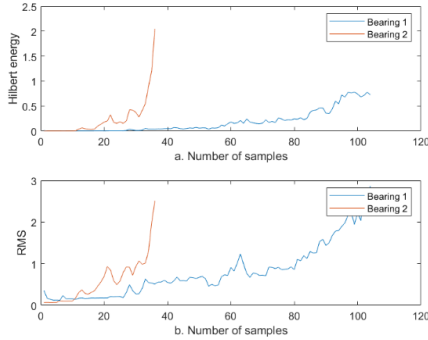


Fig. 5. Degradation trajectories of bearings 1 and 2 showing Hilbert energy and RMS over number of samples from a healthy state to the failed state

The degradation trajectories of bearing 1 and 2 are employed for degradation modelling and failure prediction. As discussed before, the advantage of the Wiener process with linear drift is the analytical solution of first passage time distribution which is “Inverse Gaussian (IG) distribution”. Therefore, if we define failure as the first time that the health indicator value crosses the failure threshold, the CDF of FHT distribution is computed using Eq. (8) depending on η and λ for both bearings. In this paper, based on the observation of Hilbert energy as a HI in Fig. 5 the failure threshold is selected to be at 0.7 for Hilbert energy and 2 for RMS. The drift and diffusion

parameters estimate of the Wiener process using maximum likelihood estimation (MLE) method for the two health indicators for bearing 1 and 2 are listed in Table 3.

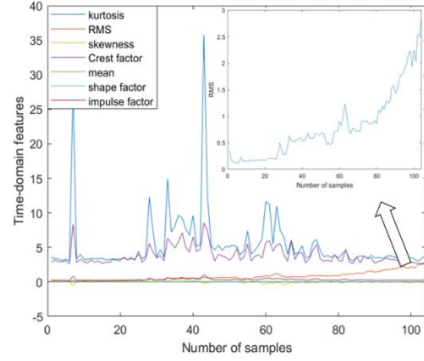


Fig. 6. Time-domain features performance for the lifetime of bearing 1, together with RMS as the energy representative feature in time domain

Table 3. Wiener process parameters using the two health indicators for bearing 1 and 2

	Drift parameter	Diffusion parameter
HE, bearing 1	0.0070	0.0404
HE, bearing 2	0.0584	0.1673
RMS, bearing 1	0.0244	0.1206
RMS, bearing 2	0.0698	0.1751

As it can be observed in Fig. 5a, the bearings work normally for some time and at some point, they start to deteriorate. Hence, one can divide the bearings' lifetime into two health stage and degradation stage in order to apply the Wiener process on the degradation stage which has a constant drift parameter and is of critical importance. Fig. 7 shows the cumulative distribution function of FHT for the two bearings using two health indicators.

Since RUL is a stochastic variable and has distribution at any point of time, one can calculate the expected RUL using the parameters of Inverse Gaussian distribution and the current degradation level at that time. It can be a representation of RUL which is informative and helpful to some extent for comparing the performance of two health indicators in the prediction of failure. The results are quantified by the percentage of expected RUL over the actual RUL. It is shown

that RMS as a time-domain feature is successful in tracking the early degradation of the bearings while it does not provide accurate RUL predictions when it comes to the final stage of the deterioration.

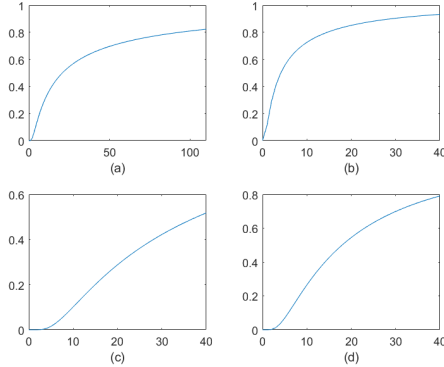


Fig. 7. (a,b) CDF of FHT using HE as a HI for bearings 1 and 2 respectively. (c,d) CDF of FHT using RMS as a HI for bearings 1 and 2 respectively

Hilbert energy which was extracted from the second IMF as a time-frequency feature is performing similar to RMS for bearing 1 which means that usage of HE as a HI may give reasonable RUL prediction at the beginning of the deterioration and it cannot predict well at the end of the degradation stage which is the point of interest for us. It should be noted that, Hilbert energy for bearing 2 does not get close to the actual RUL. This may be due to the fact that the experimental test is rather short and lack of substantial number of samples may result in huge prediction error. Another reason can be the fact that the Hilbert energy for each sample is the average of HE of all the datapoints. Therefore, the degradation trajectories in Fig. 5(a) are a truncated version of the whole lifetime of the bearings which leads to large error in prediction. This is seen in some other papers such as (Singleton, Strangas, and Aviyente 2014) and (Loutas, Roulias, and Georgoulas 2013) which have used Pronostia dataset.

Table 4 shows the comparison in RUL prediction using RMS and HE features as health indicators. The percentage is the division of the expected RUL and the actual RUL multiplied by one

hundred. Therefore, it represents how much the estimated expected RUL is close to the real one.

Table 4. Comparison of the expected RUL divided by actual RUL using RMS versus Hilbert energy at different point of times. The percentage shows the mean RUL divided by the actual RUL

Sample number	RMS, bearing1	RMS, bearing2	HE, bearing1	HE, bearing2
8	84%	97%	86%	46%
10	86%	95%	84%	49%
20	97%	85%	75%	64%
30	94%	39%	65%	71%
40	96%		58%	
50	86%		48%	
60	82%		46%	
70	51%		32%	
80	36%		22%	
90	30%		10%	

6. Conclusion

As presented before, the degradation modelling and RUL prediction depend on health indicator selection and the behaviour of the system of interest. In this paper, the vibration rig at NTNU laboratory was used to run some run to failure experimental tests. EMD is employed to decompose the vibration signals into different frequency bands. The most informative IMF was selected considering the energy and correlation with the original vibration signal. The Hilbert transformation was applied on the selected IMF to extract the Hilbert energy of the signals as a HI. Besides, RMS as a time-domain energy representative feature was also presented and compared with HE for the two bearings. The results were compared and showed that both RMS and HE are more informative at the early stages of the bearings' lifetime. Moreover, the result shows that HE may be dependent on the length of the dataset since it was not able to predict RUL for bearing 2 with 36 samples. Thus, different features may work better depending on the length of the dataset as well as the operating condition. However, further analysis should be conducted regarding the extracted features as well as the prediction model. For instance, Geometric Brownian Motion (GBM) might bring new insights to understand how well the degradation behaviour can be predicted.

As discussed in introduction, although various feature extraction methods, fault detection and prognostics of bearings in rotating machinery have been studied before, one challenge met in this paper is the failure threshold which has not

been studied thoroughly. The vibration threshold to cease the experiments is totally based on the vibration measurements and the vibration measurements have lower prediction capability compared to the extracted features, i.e., Hilbert energy and RMS. On the other hand, there is no constant failure threshold identified for extracted features in reality. Thus, it is challenging to define a failure threshold which has both good failure prediction capability and identified threshold in real-life applications. To overcome this challenge, one can investigate the models with random failure threshold to reduce the uncertainty in degradation modelling. Another limitation is the number of experimental tests. Having sufficient number of experimental tests may show that various features may work better at different time intervals in the bearings' lifetime. Therefore, different features to train the degradation model for different time intervals may be useful to improve the RUL estimation.

For further work, Bayesian approach can be applied to update the Wiener process parameters continuously depending on the historical condition-monitoring data. In addition, the approach can be extended to various sensor data such as the temperature and current of the bearings to improve the RUL prediction accuracy and figure out how RUL can be affected by different types of parameters. A higher number of experimental tests with other causes of failures (radial load, oscillating load and, bearings' current) is suggested to validate the approach and evaluate its performance on unseen data.

References

- Caesarendra, Wahyu, and Tegoeh Tjahjowidodo. 2017. "A Review of Feature Extraction Methods in Vibration-Based Condition Monitoring and Its Application for Degradation Trend Estimation of Low-Speed Slew Bearing." *Machines* 5: 21.
- Cho, Sangjin, Md Rifat Shahriar, and Uipil Chong. 2014. "Identification of significant intrinsic mode functions for the diagnosis of induction motor fault." *The Journal of the Acoustical Society of America* 136: EL72-EL77.
- Cox, D.R., and H.D. Miller. 1965. *The Theory of Stochastic Processes*. Wiley.
- Lei, Yaguo, Zhengjia He, Yanyang Zi, and Xuefeng Chen. 2008. "New clustering algorithm-based fault diagnosis using compensation distance evaluation technique." *Mechanical Systems and Signal Processing* 22 (2): 419-435.
- Li, Guohui, Zhichao Yang, and Hong Yang. 2018. "Noise Reduction Method of Underwater Acoustic Signals Based on Uniform Phase Empirical Mode Decomposition, Amplitude-Aware Permutation Entropy, and Pearson Correlation Coefficient." *Entropy* 20: 918.
- Loutas, Theodoros H, Dimitrios Roulias, and George Georgoulas. 2013. "Remaining useful life estimation in rolling bearings utilizing data-driven probabilistic e-support vectors regression." *IEEE Transactions on Reliability* 62 (4): 821-832.
- Nguyen, Thi Phuong Khanh, Amor Khlaief, Kamal Medjaher, Antoine Picot, Pascal Maussion, Diego Tobon, Bertrand Chauchat, and Regis Cheron. 2018. "Analysis and comparison of multiple features for fault detection and prognostic in ball bearings."
- Rausand, Marvin, and Arnljot Høyland. 2008. *System Reliability Theory: Models, Statistical Methods, and Applications*. Hoboken, NJ, USA: Hoboken, NJ, USA: John Wiley & Sons, Inc.
- Sejdić, Ervin, Igor Djurović, and Jin Jiang. 2009. "Time-frequency feature representation using energy concentration: An overview of recent advances." *Digital signal processing* 19 (1): 153-183.
- Singleton, Rodney K, Elias G Strangas, and Selin Aviyente. 2014. "Extended Kalman filtering for remaining-useful-life estimation of bearings." *IEEE Transactions on Industrial Electronics* 62 (3): 1781-1790.
- Soualhi, A., K. Medjaher, and N. Zerhouni. 2015. "Bearing Health Monitoring Based on Hilbert-Huang Transform, Support Vector Machine, and Regression." *IEEE Transactions on Instrumentation and Measurement* 64 (1): 52-62.
- Tajiani, Bahareh, and Jørn Vatn. 2020. "Remaining Useful Life Estimation Using Vibration-based Degradation Signals." The 30th European Safety and Reliability Conference and 15th Probabilistic Safety Assessment and Management Conference (ESREL2020 PSAM15), Venice, Italy.
- Terrien, jérémy, Catherine Marque, and Brynjar Karlsson. 2011. "Automatic detection of mode mixing in empirical mode decomposition using non-stationarity detection: Application to selecting IMFs of interest and denoising." *EURASIP Journal on Advances in Signal Processing* 2011.
- Wang, Yanxue, Jiawei Xiang, Richard Markert, and Ming Liang. 2016. "Spectral kurtosis for fault detection, diagnosis and prognostics of rotating machines: A review with applications." *Mechanical Systems and Signal Processing* 66-67: 679-698.
- Yu, Yang, YuDejie, and Cheng Junsheng. 2006. "A roller bearing fault diagnosis method based on EMD energy entropy and ANN." *Journal of Sound and Vibration* 294 (1): 269-277.

Paper 3

RUL Prediction of Bearings using Empirical Wavelet Transform and Bayesian Approach

Bahareh Tajjani¹, Jørn Vatn²

Department of Industrial and Mechanical Engineering, Norwegian University of Science and Technology (NTNU), Norway. Email: ¹Bahareh.tajjani@ntnu.no, E-mail: ²jorn.vatn@ntnu.no

Remaining useful life (RUL) is an important requirement for condition-based maintenance specially for critical components whose failures can cause a long unplanned shutdown. Almost 30% of the abnormalities of the rotating machinery are initiated by the bearings' failures. Thus, bearing is considered as one of the most critical components in rotating machinery and it is important to monitor its health condition to be able to avoid the upcoming failures, increase reliability, reduce unplanned shutdowns and maintenance costs. Since the vibration signals in bearings have both nonlinear and nonstationary characteristics, neither of time and frequency-domain approaches can provide reliable and accurate RUL prediction results. For this purpose, most research is based on time-frequency representation techniques such as wavelet transform, Hilbert-Huang transform and Short-time Fourier transform. However, these approaches are more popular within fault detection field, while the combination of these methods as an input for health indicator (HI) construction together with RUL estimation approaches for failure prediction have not been studied thoroughly before. In addition, most research are based on online datasets in which the bearings are only degraded by loading factor. This paper presents a framework using empirical wavelet transform (EWT) for fault detection and HI construction combining with Bayesian inference approach to predict RUL of the bearings. The datasets in this paper are collected by performing several accelerated life tests at NTNU. EWT as an adaptive approach has been employed to decompose the signals into sub-bands to extract different features. The features extracted from the sensitive sub-band are then compared using several performance measures. Afterwards, the Bayesian approach together with Wiener process has been applied on the degradation trajectories to predict RUL efficiently and the framework is validated using the collected experimental datasets.

Keywords: Remaining useful life, Empirical wavelet transform, Condition-based maintenance, bearing, Bayesian inference

1. Introduction

Condition-based maintenance (CBM) is a widely used maintenance strategy which schedules the maintenance of the component or system according to its condition monitoring data such as temperature, current and vibration. Monitoring the health condition of a system can help to detect and identify faults and predict remaining time before a failure occurs which are known as diagnosis and prognosis respectively (Wen, Gao, and Zhang 2018). Remaining useful life (RUL) estimation as an important task in prognostic can provide the basis to implement an effective maintenance optimization model to facilitate the decision-making process in the operation of rotating machinery. Fault diagnosis and failure prediction of Bearings as one of the most frequently used elements in rotating machines has been the main focus of many researchers (Kumar et al. 2018). To prevent a bearing failure, many effective parameters can be measured which have been discussed in literature such as pressure, acoustic temperature, oil analysis and vibration where vibration monitoring is the most widely used technology to analyze bearings degradation and RUL prediction which is due to the fact that vibration is easy to measure and analyze while it can reflect the status of bearings timely and roundly (Tian and Tian 2012)(Wu, Li, and Qiu 2017). In (Y. Zhang, Zuo, and Bai 2015), a new feature extraction method is proposed for fault diagnosis of bearings based on electrostatic monitoring sensors. The dataset in the IEEE 2012 PHM challenge competition is also related to the temperature and vibration of the bearings (Nectoux et al. 2012). When a failure in a bearing occurs, its vibration signals have both nonlinear and nonstationary characteristics (H. Liu and Han 2014). In

addition, they are buried in noise and they do not have a strong failure prediction capability to predict failures appropriately. Therefore, it is necessary to extract representative features using some transformation functions and approaches to create several condition indicators for monitoring bearings. Both time and frequency domain approaches describe the vibration signals as a whole, not at a specific time or frequency range and consequently they can lead to unreliable RUL prediction results. Therefore, time-frequency approaches can be more applicable due to handling nonlinear and nonstationary signals (Q. Zhang et al. 2018). The three main classification of time-frequency approaches are: short-time Fourier transform (STFT), wavelet transform (WT) and Hilbert-Huang transform (HHT) (Caesarendra and Tjahjowidodo 2017). Among the main classification of time-frequency techniques, HHT has the ability to handle nonlinear and nonstationary signals. However, lack of mathematical theory in this approach may lead to erroneous information for fault detection and consequently failure prediction (Huang and Wu 2008). Many articles were published on fault detection of bearings using WT due to its low computational cost as well as its ability to provide time-varying information about the vibration signals (Kankar, Sharma, and Harsha 2011)(Lou and Loparo 2004). WT examines the signals using a set of wavelet functions. The selection of mother wavelet function is challenging and it affects the performance for feature extraction (Ngui et al. 2013). In addition, WT does not perform well on nonlinear signals. However, to tackle this challenge, Gilles (2013) proposed empirical wavelet transform (EWT) which has a solid analytical formulation and can efficiently divide the signals into different

frequency bands. Since in case of a bearing's failure, vibration signals can be both nonlinear and nonstationary, EWT as a full-adoptive approach can be a reasonable candidate for identifying frequency components and extracting features. The main characteristics of EWT inherits the advantage of both WT and EMD (W. Liu and Chen 2019). Table 1 shows a comparison of the three time-frequency signal processing techniques and EWT (W. Liu and Chen 2019).

Table 1. A comparison of Fourier, Wavelet, Hilbert and EWT

	Fourier	Wavelet	Hilbert	EWT
Presentation	Energy-frequency	Energy-time-frequency	Energy-time-frequency	Energy-time-frequency
Nonlinear	No	No	Yes	Yes
Nonstationary	No	Yes	Yes	Yes (to some extent)
Theoretical basis	Theory complete	Theory complete	Empirical	Theory complete

A main challenge of EWT is to select the sub band with the specific frequency which has the hidden defect information of bearings. For this purpose, the statistical condition indicators as well as the EWT energy features can be compared in terms of monotonicity, trendability and prognosability to extract the optimal health indicator (HI) which represents the underlying degradation behavior of the bearings accurately. The HI can then be treated as input to degradation modelling to predict RUL and prevent the failures before occurring. The proposed framework is a multidisciplinary approach which combines data collection, feature extraction, health indicator construction, degradation modeling and failure prediction.

The framework is expected to predict the bearings' failure reasonably well since it attempts to combine the signal-processing technique with nonlinear property and an adaptive approach to update the models' parameters based on the bearings' observed real-time degradation in order to predict the failures optimally.

The rest of this paper is structured as follows. Section 2 presents the proposed framework. In section 3, the experimental vibration setup and data are described. Section 4 demonstrates the results and discussion followed by conclusion in section 5.

2. Proposed Framework

Fig. 1 shows the framework of this paper which consists of four main steps. Since the collected vibration data in step 1 have lots of noise and measurement errors, they do not have

a strong failure prediction capability. Therefore, it is necessary to extract representative features using some transformation functions and techniques for the bearings' condition monitoring. The feature extraction in step 2 has been conducted based on one of the signal processing techniques which is known to handle the bearings vibration signals reasonably well. Thus, it is expected that it provides a clear overview of different frequency components of the signals in order to come up with a HI. In this paper, HI construction using three performance measures (i.e., monotonicity, prognosability and trendability) in step 3 of the framework is mainly based on the methods from literature review. However, the literature review techniques may not provide the optimal HI as an input to adaptive Bayesian approach. One purpose with conducting accelerated life tests can be to test and employ different performance measures or a combination of the existing ones with different weights to ensure that the HI is optimal for prediction stage using Bayesian or to empirically validate the technique in step 3. The idea in step 4 is based on an adaptive stochastic or probabilistic model to be applied on real-time acceleration data. Since, at the beginning of the experiment, there are very few observations available, the stochastic model may not provide very reliable prediction results. Thus, the adaptive approach has been developed to update the parameters continuously, learn from the previous observations and make the prediction model more robust for the future observations.

2.1. Data Acquisition

Degradation modelling and RUL prediction often requires run-to-failure datasets from the operation of the component or the machine which in some cases is difficult to acquire. As described before, temperature and acceleration run-to-failure datasets are the common data for RUL prediction of bearings. More detailed information about the datasets and setup are presented in Section 3.

2.2. EWT

Gilles (2013) proposed EWT to enhance the performance and flexibility of the conventional WT. The basic concept of EWT is to segment the Fourier spectrum of the vibration signal, treated as band-pass filters. For a frequency w , assuming in the normalized Fourier axis of $[0, \pi]$, each segment is defined as $[w_{n-1}, w_n]$, where w_n are the limits between each segments in such a way that $w_0 = 0$ and $w_N = \pi$ or expressed as $\coprod_{n=1}^N [w_{n-1}, w_n] = [0, \pi]$.

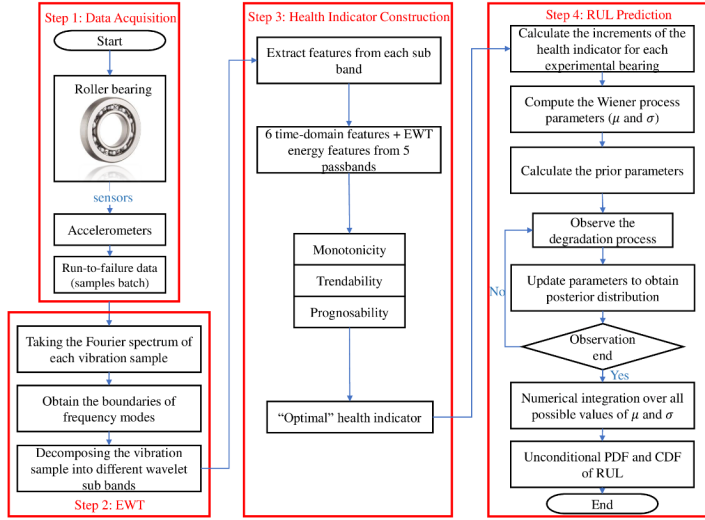


Fig. 1. Flowchart of the proposed framework

The empirical scaling function $\phi_n(w)$ and the empirical wavelets are given by the following expressions:

$$\phi_n(w) = \begin{cases} 1, & |w| \leq (1 - \gamma) w_n \\ \cos \left[\frac{\pi}{2} \beta \left(\frac{1}{2\gamma w_n} (|w| - (1 - \gamma) w_{n+1}) \right) \right], & (1 - \gamma) w_n \leq |w| \leq (1 + \gamma) w_n \\ 0, & \text{otherwise} \end{cases} \quad (1)$$

$$\psi_n(w) = \begin{cases} 1, & (1 + \gamma) w_n \leq |w| \leq (1 - \gamma) w_{n+1} \\ \cos \left[\frac{\pi}{2} \beta \left(\frac{1}{2\gamma w_{n+1}} (|w| - (1 - \gamma) w_{n+1}) \right) \right], & (1 - \gamma) w_{n+1} \leq |w| \leq (1 + \gamma) w_{n+1} \\ \sin \left[\frac{\pi}{2} \beta \left(\frac{1}{2\gamma w_n} (|w| - (1 - \gamma) w_{n+1}) \right) \right], & (1 - \gamma) w_n \leq |w| \leq (1 + \gamma) w_n \\ 0, & \text{otherwise} \end{cases} \quad (2)$$

The function $\beta(w)$ and parameter γ are expressed as $\beta(w) = w^4(35 - 84w + 70w^2 - 20w^3)$ and $\gamma = \min_n \left(\frac{w_{n+1} - w_n}{w_{n+1} + w_n} \right)$. Further, both approximated and detailed coefficients are deduced by the inner products according to classical wavelet theory as shown below:

$$W_f^\varepsilon(0, t) = \langle f | \phi_1 \rangle = \int f(\tau) \phi_1(\tau - t) d\tau \quad (3)$$

$$W_f^\varepsilon(n, t) = \langle f | \psi_n \rangle = \int f(\tau) \psi_n(\tau - t) d\tau \quad (4)$$

Furthermore, the empirical modes are extracted as:

$$f_0(t) = W_f^\varepsilon(0, t) * \phi_1(t) \quad (5)$$

$$f_k(t) = W_f^\varepsilon(k, t) * \psi_k(t) \quad (6)$$

The details of EWT approach can be found in (Gilles 2013). The EWT method shows the multiresolutional analysis of the acceleration data and it is adaptive based on the processed vibration signal. The segmentation of the modes in this method is based on the frequency domain while in empirical mode decomposition (EMD) in HHT, the decomposition is based on the time domain.

EWT approach can decompose the vibration signal into different wavelet windows. At the first step, the Fourier spectrum of the processed vibration signal is obtained while the second step is to separate different portions of Fourier spectrum which correspond to modes centred around a specific frequency. To find the boundaries or portions of the frequency modes in Fourier segmentation, one can apply local maxima method which was the initial Fourier segmentation method in EWT. The local maxima method can be described as follows:

- Finding the local maxima in logarithm of Fourier spectrum
- Sort them in a decreasing order
- Define the boundaries of each segment as the center between two consecutive maxima

Thus, EWT decomposes the signals into different frequency modes or wavelet sub bands using their frequency spectrums.

2.3. HI Construction

The extracted statistical features from each sub band (i.e., kurtosis, Root Mean Square (RMS), crest factor, ...) and their comparison can help to identify the fault-prone sub band and figure out which sub band can reflect the hidden fault information of the bearings. Monotonicity, trendability and prognosability are some performance measures with the range of zero to one which can be used to compare the features (Qiu, Gu, and Chen 2020).

Monotonicity indicates the trend of a feature as the system evolves towards failure due to system cumulative damage. Based on the time series from the beginning to n th HI, the monotonicity is computed by:

$$\text{Monotonicity} = \left| \frac{\text{No.}(\frac{d}{dx} > 0)}{n-1} - \frac{\text{No.}(\frac{d}{dx} < 0)}{n-1} \right| \quad (7)$$

Where n is the number of observation points of a feature and $\frac{\text{No.}(\frac{d}{dx} > 0)}{n-1}$ and $\frac{\text{No.}(\frac{d}{dx} < 0)}{n-1}$ is the average absolute difference of the fraction of positive and negative derivatives for each path.

Trendability provides a measure of similarity between trajectories of a feature measured in multiple run-to-failure experiments. As a system gets progressively closer to failure, a suitable condition indicator is typically highly trendable. Trendability is measured to a certain degree by comparing the fraction of the positive first and second derivatives in each component. This metric is particularly sensitive to noise and can be calculated as follows.

$$\text{Trendability} = 1 - \text{std} \left(\frac{\text{No.}(\frac{d}{dx} > 0)}{n-1} + \frac{\text{No.}(\frac{d^2}{dx^2} > 0)}{n-2} \right) \quad (8)$$

Prognosability shows the variability of a feature. A feature is more prognosable when there is smaller variation between the initial start value and the failure value. Thus, it is calculated as the variation of the final failure values for each degradation path divided by the mean range of the degradation paths (Boukra, Bensafia, and Khettab 2019).

$$\text{Prognosability} = \exp \left(- \frac{\text{std}(\text{failure values})}{\text{mean}(|\text{failure value} - \text{starting value}|)} \right) \quad (9)$$

The features can be compared using the feature selection criteria to create a HI which has a high prediction capability. A suitable HI in this paper is considered the one with the highest monotonicity, trendability and prognosability. The HI can then be utilized as input for modelling degradation and RUL prediction.

2.4. RUL Prediction

In this paper, Wiener process as a continuous-time stochastic process with linear leaning μ and variance σ^2 is considered with the following hypotheses:

- $W_0 = 0$
- Increment law $W(t+h) - W(t)$ is Normal distribution $N(\mu h, \sigma^2 h)$
- If W_0 is a standard Wiener process, i.e. $\mu = 0$ and $\sigma = 1$, then $W(t)$ is a Wiener process with linear drift μ and variance σ^2 .

The first passage time (FPT) of Wiener process with linear drift is analytically known as Inverse Gaussian (IG) distribution with $\nu = \frac{L-W(t)}{\mu}$ and $\lambda = \frac{(L-W(t))^2}{\sigma^2}$, where L is the failure threshold (FT) and $W(t)$ is the degradation level at time t . The cumulative distribution function (CDF) of IG distribution is formulated as follows:

$$F_T(t) = \phi \left(\frac{\sqrt{\lambda}}{\nu} \sqrt{t} - \sqrt{\lambda} \frac{1}{\sqrt{t}} \right) + \phi \left(-\frac{\sqrt{\lambda}}{\nu} \sqrt{t} - \sqrt{\lambda} \frac{1}{\sqrt{t}} \right) e^{\frac{2\lambda}{\nu}} \quad (10)$$

The Bayesian approach is employed to update the Wiener process parameters (i.e., μ and σ^2) resulting in updating IG distribution parameters (i.e., ν and λ) once more observation is available from the degradation process. The prior belief is established based on the analysis of similar systems to build the posterior belief. The conjugate prior distribution is Normal-Gamma distribution as shown below:

$$\begin{aligned} & NG(\mu, \eta | \mu_0, \kappa_0, \alpha_0, \beta_0) \\ & \stackrel{\text{def}}{=} N \left(\mu \middle| \mu_0, \sqrt{\frac{1}{\kappa_0 \eta}} \right) G\alpha(\eta | \alpha_0, \beta_0) \end{aligned} \quad (11)$$

Where, $\mu_0 = \frac{1}{m} \sum_{i=1}^m \mu_i$, $\eta_i = \sum_{i=1}^m \sigma_i^{-2}$ and $\rho_0 = \frac{m}{\sum_{i=1}^m (\mu_i - \mu_0)^2}$ while m is the number of components or systems used as prior knowledge. From the η_i 's, standard maximum likelihood estimation (MLE) can be used to fit a Gamma distribution with calculated shape and scale parameters as α_0 and β_0 respectively. κ_0 can then be calculated as $\kappa_0 = \frac{\rho_0 \beta_0}{(\alpha_0 - 1)}$. By observing the degradation process of a new system i , one can update the posterior distribution which is again a Normal-Gamma distribution with parameters $\mu_n, \kappa_n, \alpha_n$ and β_n . κ_n and α_n are calculated as $\kappa_n = \kappa_0 + n$ and $\alpha_n = \alpha_0 + \frac{n}{2}$, and μ_n and β_n are calculated as follows:

$$\mu_n = \frac{\kappa_0 \mu_0 + n \bar{x}}{\kappa_0 + n} \quad (12)$$

$$\beta_n = \beta_0 + \frac{1}{2} \sum_{i=1}^n (x_i - \bar{x})^2 + \frac{\kappa_0 n (\bar{x} - \mu_0)^2}{2(\kappa_0 + n)} \quad (13)$$

To assess the parameters for each experimental bearing, the other bearings datasets are considered as prior knowledge to be used for estimating the posterior parameters. In case of Wiener process with linear drift, one can obtain the unconditional probability density function (PDF) and CDF of RUL by integrating over all possible values of μ and η

with Normal-Gamma posterior distribution shown in Eq. (14).

$$\Pr(RUL(t|y_t, \mu_n, \kappa_n, \alpha_n, \beta_n) \leq \tau) = \int_0^\infty \int_{-\infty}^\infty F_{IG}(\tau|v, \lambda) f_N\left(\mu \middle| \mu_n, \frac{1}{\kappa_n \eta}\right) f_{GA}(\eta|\alpha_n, \beta_n) d\mu d\eta \quad (14)$$

here F_{IG} is the CDF of IG distribution shown in Eq. (10) with its distribution parameters.

3. Data Collection

The first step of the framework shown on Fig. 1 is described in this section. An experimental setup at RAMS laboratory at NTNU was developed to conduct a number of accelerated life tests on roller bearings. The setup is called “Bently Nevada (system 1) Rotor Kit, model RK4”. The major components of the setup include a bearing shaft with the length of 10 mm, two bearing blocks which are mounted on the two sides of the shaft to hold the two bearings, and the accelerometers. The bearing block located on the left part of the setup contains the experimental bearing which will run until failure, while the other one is only used for balance. The two sets of miniature accelerometers are mounted radially and axially on each bearing to collect the horizontal and vertical acceleration data over time. The collected data will then be transformed into the central system which visualizes the data on the screen. The amplifier (type 5134B) and accelerometers (type 8702B100) used in the measurement part of this setup are provided by “Kistler” company. The rotating part of this setup is an asynchronous motor as an actuator which allows the inner race, rollers and the cage of the bearings to rotate through the whole system. The maximum rotational speed the motor can handle is approximately 10000 revolutions per minute (rpm). The vibration setup is mounted on an aluminium platform with a safety cover which is used while running experiments for safety issues. The degradation mechanism to degrade the bearings is contamination which means mixing Silicium carbide particles (VS 44. D50 – 52 Coultex particles) with a lubricant and pouring into the experimental bearings continuously until the acceleration reading reaches a predefined threshold which in this paper is set as 10g in order to avoid damage to the motor. The overview of the vibration setup can be found in (J. (NTNU) Liu 2020). The collected data is acceleration measurements in both horizontal and vertical directions. Since the vertical acceleration data is under the impact of gravity and they are not so reliable and accurate, the horizontal acceleration data are only considered in this paper. The samples of data are collected every 5 minutes while the mixture of Silicium carbide particles and lubricant are poured with one press of nozzle into the tested bearing every 25 minutes until the acceleration amplitude reaches 10g. The motor speed is 2975 rpm and the sampling frequency is 12820 Hz which means that each sample has a duration of 0.639 seconds and 8192 acceleration readings or datapoints. Table 2 represents the collection of bearings datasets together with the number of samples. The first sample is when the experiment is

healthy, and the last sample is when the bearing is considered as failed.

Table 2. Data description

Bearing	Number of samples collected before reaching the threshold 10g
Bearing 1	110
Bearing 2	35
Bearing 3	146
Bearing 4	106
Bearing 5	77
Bearing 6	248
Bearing 7	150
Bearing 8	143
Bearing 9	114

Table 3. Geometric characteristics of the bearings

Type of bearing	Open roller/ball bearing (R10)
Number of balls	10
Pitch diameter (mm)	70
Ball diameter (mm)	4.7
Inner diameter (mm)	15.9
Outer diameter (mm)	34.9

4. Results and Discussion

In this section, the steps two to four shown on Fig. 1 are represented in more details.

4.1. EWT

The vibration samples of the bearings were decomposed into different modes or wavelet sub bands using EWT approach to filter the irrelevant frequency components and find out the most sensitive frequency band. As the first step to divide the signal into different frequency modes, the Fourier spectrum of the vibration signals are obtained. In this paper, the local minimum method and the global trend removing approach were applied to obtain the boundaries of the frequency modes. The reason to employ these methods is to tackle the two challenges of flat mode issue and global versus local modes. The details of this process and challenges can be found in (Gilles 2013) and (Singh Assistant Professor 2021). Fig. 2 shows the Fourier spectrum, empirical filter bank and the boundaries of the frequency modes for the last sample of bearing 1 as an example. The further details of decomposition is left to the discretion of authors.

Fig. 3 and Fig. 4 show the first and the last raw vibration samples which are decomposed into different mode frequencies or sub bands using EWT approach.

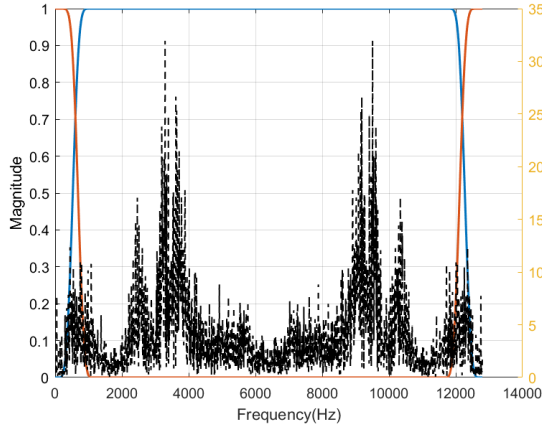


Fig. 2. Fourier spectrum, empirical filter bank and the boundaries of the frequency modes, the last sample, bearing 1

4.2. HI Construction

Once all the vibration samples of all the experimental bearings have been decomposed into sub bands using EWT, one can extract the statistical features from each sub band to detect the sensitive wavelet sub band. The extracted features from all the sub bands of all vibration samples (from a healthy state to the failed state) can be possible condition indicators for the nine experimental bearings. The features are compared in terms of monotonicity, trendability, prognosability using the Eq. (7) to Eq. (9) and Fig. 5 present the results.

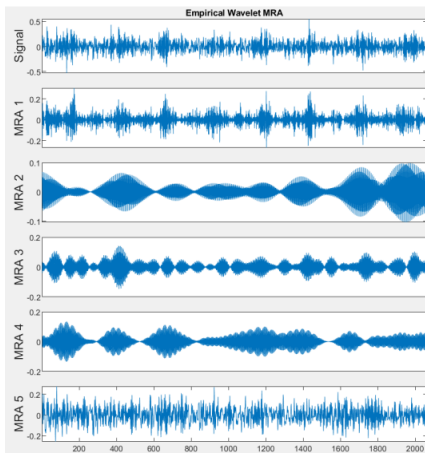


Fig. 3. Sub bands of sample 1 from bearing 1 decomposed using EWT

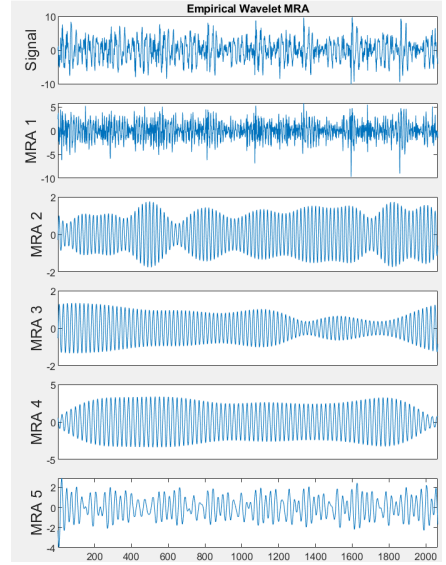


Fig. 4. Sub bands of the last sample from bearing 1 decomposed using EWT

As a result, RMS and energy of the first and fifth sub bands were the condition indicators with the highest prognosability, trendability and monotonicity. Therefore, they can be the candidate HIs for modelling the bearings' degradation. RMS is the dominant among others. Thus, to keep the most information of the signals, RMS of the first sub band of EWT is considered as the optimal HI in this paper. Fig. 6 shows the RMS degradation paths from the first sub band for the nine bearings.

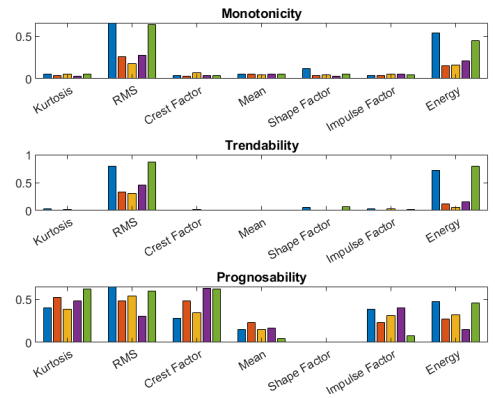


Fig. 5. Monotonicity, trendability and prognosability of the extracted features from different EWT sub bands. The colors from the left show passband 1 to passband 5 respectively.

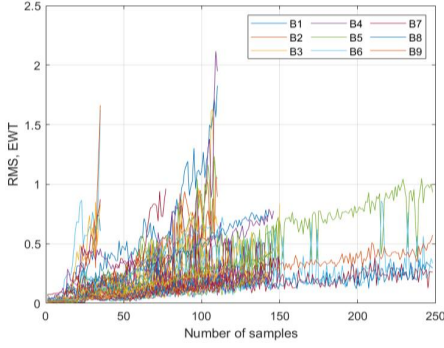


Fig. 6. RMS degradation trajectories

4.3. RUL Prediction

Since the degradation increments vary nonmonotonically and linearly with time, Wiener process with linear drift can be an appropriate model for the bearings’ deterioration modelling. Thus, it has been applied on the degradation trajectories of the bearings while the Bayesian approach has been employed to update the models’ parameters continuously. To obtain the prior parameters for each bearing, the other bearings as reference bearings were considered to build the prior knowledge. Table 4 shows the Wiener process parameters while the time unit is one and Table 5 shows the prior parameters calculated for the bearings using the equations in Section 2.

Table 4. Wiener process parameters

Bearing	Drift	Diffusion
Bearing 1	0.0166	0.0095
Bearing 2	0.0464	0.0216
Bearing 3	0.0053	0.0025
Bearing 4	0.0067	0.0103
Bearing 5	0.0125	0.0035
Bearing 6	0.0038	0.0189
Bearing 7	0.0055	0.0064
Bearing 8	0.0053	0.0019
Bearing 9	0.0058	0.0031

Table 5. Prior parameters of Bayesian approach

Bearing	μ_0	ρ_0	κ_0	α_0	β_0
Bearing 1	0.0114	5533	1.1230e+06	1.6898	139.9798
Bearing 2	0.0077	57688	5.8147e+06	2.1339	114.2874
Bearing 3	0.0128	5635	9.3572e+05	1.7044	116.9613
Bearing 4	0.0127	5563	1.0768e+06	1.7152	138.4383
Bearing 5	0.0119	5444	1.2726e+06	1.5792	135.3935
Bearing 6	0.0130	5740	6.6354e+05	2.0339	119.5008
Bearing 7	0.0128	5622	1.3797e+06	1.5900	144.7833
Bearing 8	0.0128	5633	5.4509e+05	1.9676	93.6280
Bearing 9	0.0128	5610	1.1884e+06	1.6114	129.5126

Fig 7 is a three-dimension plot showing the PDF of RUL of bearing 1 calculated for each sample separately as an

example. In this paper, for simplicity, the failure threshold (L) is defined as the maximum value of the bearing’s degradation trajectory. Once more degradation is observed, one can be more certain of the Wiener process parameters and thus the standard deviation or uncertainty of PDF of RUL will decrease. The red points linked together represent the expected values of PDFs.

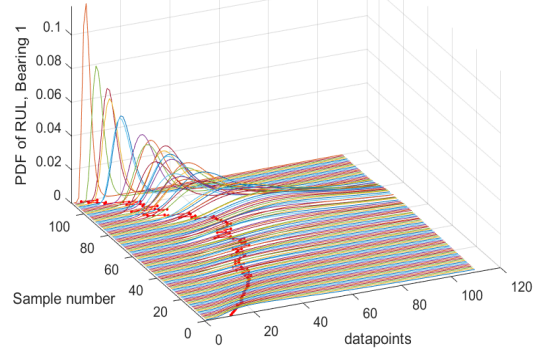


Fig 7. PDF of RUL for bearing 1. The Wiener process parameters are updated continuously from the health state (sample 1) to the failed state (sample 110). The red dots linked together show the expected values of PDFs

The $\alpha - \lambda$ accuracy as a prognostic’s performance metric is employed to show the model’s prediction accuracy for different bearings. $\alpha - \lambda$ accuracy shows whether a prediction result falls into the confidence bound α which is normally specified by analyst at specified time instances. Successful predictions are the ones which are located within the α -bound region. λ range is from 0 to 1 when 0 corresponds to the first time instant and 1 corresponds to a bearing end of lifetime (EOL). The accuracy is then quantified as the difference of the predicted RUL from the actual RUL value. In this paper, the confidence bound α is considered 30% to evaluate the performance of RUL prediction model. Fig 8 shows the 30th percentile of CDFs as a realisation of the estimated RULs together with the actual RULs and their associated confidence bounds.

5. Conclusion

To enhance the performance of scheduling maintenance plan for critical systems in rotating machinery, a framework has been proposed for RUL prediction of bearings. The first stage of this framework is devoted to identifying the fault-prone sub band using empirical wavelet transform which is suitable for handling nonstationary signals and has a strong mathematic background in order to select a feature which represents the underlying degradation behavior of the bearings efficiently. The second stage consists of degradation modelling and RUL prediction by employing Wiener process as a stochastic process in combination with Bayesian inference approach to update the model parameters. The model is able to estimate the health status of the bearings reasonably accurate by using the prior

knowledge of other experimental bearings as similar components.

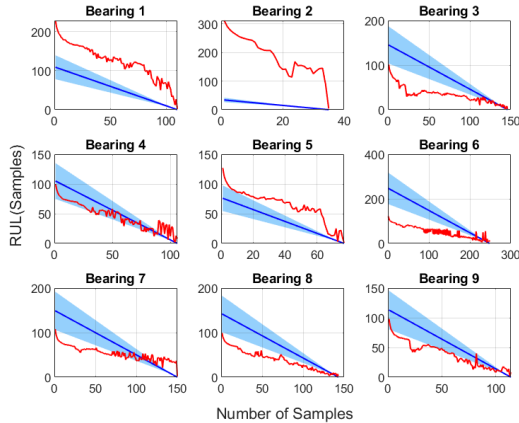


Fig 8. RUL prediction for different bearings. HI is RMS extracted from the first sub band of EWT.

The collected run-to-failure datasets of nine roller bearings are used to validate the effectiveness of the RUL prediction model. The results show that our approach performs rather well on predicting RUL when the bearings are in steady state and close to failure. Furthermore, most of the RUL prediction results fall into the confidence interval range or they are close to the confidence bounds. However, in case of bearing 2, there were some technical problems with the setup or more specifically the accelerometer was not well-attached to the setup. This increased the vibration level in an abnormal way and consequently the acceleration data of bearing 2 were to some extent erroneous and unreliable. This can be the underlying reason why the model does not perform well on bearing 2.

The two important factors influencing the accuracy of RUL prediction results are the selection of the HI and FT.

For further work, combining descriptive features using fusion methods which have different sensitivity to the two stages of the degradation trajectory (i.e., health stage and the deterioration stage) for predicting RUL accurately can be considered. Moreover, with a few numbers of experiments, it is challenging to come up with a strong conclusion. Collecting a greater number of experiments would be of great importance to be able to empirically validate the framework. In more details, the step 3 and 4 in the proposed framework can be combined and inserted in a feedback loop to reflect on different alternative approaches to build the optimal HI and how the models performance change in terms of score, convergence and etc. This makes the framework more robust to provide the optimal feature and optimal probabilistic model as well as the possibility to find specific patterns of features suitable for machine learning techniques in the future. Extending the approach to various sensor data such as temperature can also help to improve the model's robustness. Furthermore, the effect of features on failure thresholds and RUL prediction can be

investigated and used as input for models with random failure threshold.

References

- Boukra, Tahar, Yacine Bensafia, and Khatir Khettab. 2019. "Contribution in Enhancing the Remaining Useful Life Prediction in Abrupt Failures: Bearing Case." *International Journal of Intelligent Engineering and Systems* 12 (3): 156–65.
- Caesarendra, Wahyu, and Tegoeh Tjahjowidodo. 2017. "A Review of Feature Extraction Methods in Vibration-Based Condition Monitoring and Its Application for Degradation Trend Estimation of Low-Speed Slew Bearing." *Machines* 5 (4): 21.
- Gilles, Jerome. 2013. "Empirical Wavelet Transform." *IEEE Transactions on Signal Processing* 61 (16): 3999–4010.
- Huang, Norden E., and Zhao Hua Wu. 2008. "A Review on Hilbert-Huang Transform: Method and Its Applications to Geophysical Studies." *Reviews of Geophysics*. John Wiley & Sons, Ltd.
- Kankar, P. K., Satish C. Sharma, and S. P. Harsha. 2011. "Rolling Element Bearing Fault Diagnosis Using Wavelet Transform." *Neurocomputing* 74 (10): 1638–45.
- Kumar, Sanjay, Deepam Goyal, Rajeev K. Dang, Sukhdeep S. Dhami, and B. S. Pabla. 2018. "Condition Based Maintenance of Bearings and Gears for Fault Detection-A Review." In *Materials Today: Proceedings*, 5:6128–37. Elsevier Ltd.
- Liu, Huanhuan, and Minghong Han. 2014. "A Fault Diagnosis Method Based on Local Mean Decomposition and Multi-Scale Entropy for Roller Bearings." *Mechanism and Machine Theory* 75 (May): 67–78.
- Liu, Wei, and Wei Chen. 2019. "Recent Advancements in Empirical Wavelet Transform and Its Applications." *IEEE Access* 7: 103770–80.
- Lou, Xinsheng, and Kenneth A. Loparo. 2004. "Bearing Fault Diagnosis Based on Wavelet Transform and Fuzzy Inference." *Mechanical Systems and Signal Processing* 18 (5): 1077–95.
- Nectoux, Patrick, Rafael Gouriveau, Kamal Medjaher, Emmanuel Ramasso, Brigitte Chebel-Morello, Noureddine Zerhouni, Christophe Varnier, et al. 2012. "PRONOSTIA: An Experimental Platform for Bearings Accelerated Degradation Tests. PRONOSTIA: An Experimental Platform for Bearings Accelerated Degradation Tests."
- Ngui, W. K., M. Salman Leong, Lim Meng Hee, and Ahmed M. Abdelrhman. 2013. "Wavelet Analysis: Mother Wavelet Selection Methods." In *Applied Mechanics and Materials*, 393:953–58. Trans Tech Publications Ltd.
- Qiu, Guangqi, Yingkui Gu, and Junjie Chen. 2020. "Selective Health Indicator for Bearings Ensemble Remaining Useful Life Prediction with Genetic Algorithm and Weibull Proportional Hazards Model." *Measurement: Journal of the International Measurement Confederation* 150 (January).
- Singh Assistant Professor, Vikramjit. n.d. "Empirical Wavelet Transform & Its Comparison with Empirical Mode Decomposition: A Review." Accessed March 12, 2021. www.ijert.org.
- Tian, Zhigang, and Z Tian. 2012. "An Artificial Neural Network Method for Remaining Useful Life Prediction of Equipment Subject to Condition Monitoring" 23: 227–37.
- Wen, Juan, Hongli Gao, and Jiangquan Zhang. 2018. "Bearing Remaining Useful Life Prediction Based on a Nonlinear Wiener Process Model." *Shock and Vibration* 2018.
- Wu, Bo, Wei Li, and Ming-Quan Qiu. 2017. "Remaining Useful Life Prediction of Bearing with Vibration Signals Based on a Novel Indicator."
- Zhang, Qi, Tian Tian, Guangrui Wen, and Zhifen Zhang. 2018. "A New Modelling and Feature Extraction Method Based on Complex Network and Its Application in Machine Fault Diagnosis." *Shock and Vibration* 2018.
- Zhang, Ying, Hongfu Zuo, and Fang Bai. 2015. "Feature Extraction for Rolling Bearing Fault Diagnosis by Electrostatic Monitoring Sensors." *Mechanical Engineering Science*.

Paper 4



Adaptive remaining useful life prediction framework with stochastic failure threshold for experimental bearings with different lifetimes under contaminated condition

Bahareh Tajiani¹ · Jørn Vatn¹

Received: 11 May 2022 / Revised: 20 April 2023 / Accepted: 3 June 2023
© The Author(s) 2023

Abstract Deterioration modelling and remaining useful life (RUL) prediction of roller bearings is critical to ensure a safe, reliable, and efficient operation of rotating machinery. RUL prediction models in model-based approaches are often based on constant failure threshold and time-domain features for bearings' failure prognosis. Due to nonlinearity of the acceleration signals, noises, and measurement errors, the time-domain features used as condition indicators are unable to track bearings' degradation successfully and they are mostly utilized for fault diagnosis, especially in the fault classification field using machine learning algorithms. This paper proposes an adaptive RUL prediction framework with a stochastic failure threshold which comprises of two main phases of feature extraction and RUL prediction using laboratory-acquired accelerated life test data obtained from contaminated bearings. The first phase is to decompose the empirical input signals into different frequency bands using some time–frequency transformation functions and extract several condition indicators for the second phase. The second phase is based on a stochastic Wiener process while the key parameters of the model are updated iteratively using a Bayesian approach, and RUL at different degradation data-points is computed numerically. The experimental results showed the good performance of the developed framework. Some factors affecting RUL prediction such as the length of bearing samples, and degradation mechanism are highlighted in the result. The results of this paper can be further used for an effective maintenance optimization, determining

an optimal maintenance alarm threshold, improving the reliability and safety of rotating machinery, and reducing the downtime cost.

Keywords Remaining useful life · Bearing · Prognosis · Stochastic modeling · Bayesian inference · Accelerated life tests · Rotating equipment

Abbreviations

ANN	Artificial neural network
CBM	Condition-based maintenance
CDF	Cumulative distribution function
CI	Condition indicator
CNN	Convolutional neural network
CRA	Cumulative relative error
DFT	Discrete Fourier transform
EMD	Empirical mode decomposition
EWT	Empirical wavelet transform
FFT	Fast Fourier transform
FPT	First passage time
FT	Fourier transform
HHT	Hilbert–Huang transform
HI	Health indicator
IMF	Intrinsic mode function
MAE	Mean absolute error
MLE	Maximum likelihood estimation
PDF	Probability density function
PH	Prognostic horizon
RMS	Root mean square
RMSRE	Root mean square relative error
RPM	Revolutions per minute
RUL	Remaining useful life
STFT	Short-time Fourier transform
TFR	Time–frequency representation
TND	Truncated normal distribution

✉ Bahareh Tajiani
bahareh.tajiani@ntnu.no

¹ Department of Mechanical and Industrial Engineering, Norwegian University of Science and Technology (NTNU), 7491 Trondheim, Norway

WPD	Wavelet packet decomposition
WPT	Wavelet packet transform
WT	Wavelet transform

1 Introduction

Roller bearings are one of the most important and sensitive components in rotating machinery in several industries which are widely used in various equipment such as wind turbines, high-speed trains, aeroengines, and vehicles (Yang et al. 2022; Farsi and Masood Hosseini 2019). They are often operated under high stress conditions, which lead to unexpected failures. Such unexpected failures account for 45–55% of motor failures and can cause a breakdown of the entire machine, reducing its productivity, and service lifetime while increasing the unplanned downtime and cost (Xia et al. 2019; Guo et al. 2017; Singleton et al. 2015). Condition monitoring and a precise remaining useful life (RUL) estimation of bearings is required to avoid such sudden failures and catastrophes, improve the reliability, operational safety, and availability of the rotating machinery, and build an effective maintenance schedule (Li et al. 2018a, b; Ravikumar et al. 2021). RUL prediction using the current machine condition and past operating profile, as a key factor in condition-based maintenance (CBM), is defined as the length of the time a system is likely to operate before it fails (Ahmadzadeh and Lundberg 2014; Fornlöf et al. 2016).

Two main challenges in the RUL prediction of roller bearings are health indicator (HI) construction and failure threshold identification. HIs are built based on many features extracted from acceleration signals, which represent the underlying deterioration behavior of the bearings throughout their lifetime. The features are categorized as time-domain features, frequency-domain features, and time–frequency features, which exhibit different failure prediction capabilities and different sensitivities to degradation levels. Frequency-domain and time–frequency domain features are widely used together with data-driven approaches for both fault diagnosis and failure prognostics (Bhattacharya and Dan 2014). The degradation model in data-driven approaches such as machine-learning techniques and artificial neural networks (ANN) is built based on sufficient historical failure data to estimate RUL without any prior knowledge about the system and the physical nature of the system's degradation mechanism (Nguyen and Medjaher 2019).

For instance, Zhu et al. (2019) presented a RUL-estimating approach based on wavelet transform (WT) as a time–frequency representation (TFR) technique and a multiscale convolutional neural network. Liu et al. (2021) proposed a fault prediction method for aero-engine bearings

with multi-stage degradation performance by combining the advantages of long short-term memory network with statistical process analysis. In their study, the time-domain root mean square (RMS) of the raw signals was used as the HI. Li et al. (2018a, b) proposed a novel deep learning-based RUL prediction approach to estimate the machine degradation status. They applied short-time Fourier transform (STFT) on raw acceleration data to obtain time–frequency information of the signals and implemented a multi-scale feature extraction using convolutional neural network (CNN) to improve the learning ability of the algorithm. Li et al. (2018a, b) proposed a new data-driven approach for RUL prediction using deep CNN where the inputs are the normalized raw collected data, and the outputs are the estimated RUL values.

In contrast, model-based approaches use the knowledge of a system's failure mechanism such as the crack growth to build a quantitative mathematical description of the system's deterioration process to estimate its RUL (Liao and Köttig 2016; Salehpour-Oskoue and Pourgol-Mohammad 2017). Among the available model-based approaches, stochastic processes have attracted considerable research interest as they consider random errors in measurements, uncertainties in a working environment, individual variability of components in a larger population, and capture stochastic dynamics in the degradation process (Zhang et al. 2018; Salehpour-Oskoue and Pourgol-Mohammad 2017).

For instance, Liu and Fan (2022) proposed a new stochastic degradation model which integrates the characteristics of multi-stage and multi-variability of degradation trend while the model's parameters are updated using parameters estimation method based on expectation maximization algorithm. To show the effectiveness of their proposed approach, the authors used a real-case bearing dataset where the RMS of vibration signals as a time-domain feature has been used to track the bearings' condition and RUL prediction. In (Wen et al. 2018a, b), the authors employed a multiple change-point Wiener process as a degradation model, applied full Bayesian approach to update the parameters of the model iteratively, and predicted RUL of several bearings using a Monte-Carlo simulation algorithm. The degradation signals in thrust bearings were log transformed vibration signal obtained through accelerated tests. Ahmad et al. (2019) proposed a dimensionless HI, which is the RMS of the vibration signal at any time divided by RMS under a baseline condition and estimated the RUL of bearings using a dynamic regression model. The dynamic regression model was recursively updated to capture the underlying degradation trend of the bearings. Thoppil et al. (2021) proposed an algorithm utilizing principle component analysis (PCA) to reduce the dimensionality of the monitored data and exponential model to construct a HI and estimate RUL. Li et al. (2015) used the kurtosis and RMS of vibration signals as two time-domain

features to track the bearings' degradation in healthy and degraded stages and adopted an improved exponential model for failure prognosis of the bearings. Wen et al. (2018a, b) developed an algorithm to predict the RUL of bearings using the RMS of vibration signals as a time-domain statistical feature and a nonlinear Wiener process with a time-dependent drift parameter. However, in these studies, the frequency domain of vibration signals for failure prognosis has not been thoroughly demonstrated and studied.

As discussed above, much of the available literature on stochastic or statistical models have considered simple time-domain features, which fluctuate significantly in some cases and, thus, are not counted as good indicators for health condition monitoring of rolling components. In contrast, some other studies that considered the frequency domain of the signals, mostly worked with machine learning techniques and neural networks for RUL prediction which may suffer from black box approach and model explainability (Rudin 2019). In other words, the integration of frequency-domain approaches for HI construction and stochastic modeling for failure prediction of bearings has not been fully explored before.

Another key challenge in prognostics is the lack of a pre-determined failure threshold. H. Wang et al. (2021) proposed a dynamic RUL prediction and optimal maintenance time estimation approach where an isotonic regression-based method was used for data preprocessing and a Gamma process was used to predict the bearing RUL. However, in their study, the failure threshold was assumed to be constant through the bearing's lifetime which may not be realistic in practice. Yan et al. (2021) also investigates the degradation modeling and RUL estimation of dependent competing failure processes subject to gradual degradation and random shocks. The failure time in their paper is defined as the first point of time that the system's cumulative damage reaches or exceeds a prespecified failure threshold. Narayanan et al. (2019) defined the failure threshold as the last time instance of running or the last condition-monitoring datapoint and predicted RUL considering kurtosis and RMS as HIs by using a support vector machine. Pan et al. (2017) developed a Wiener process-based reliability estimation approach in which the Wiener process drift parameter follows a truncated normal distribution (TND). The reliability function and probability density function (PDF) of the FPT are both based on a pre-determined failure threshold. While most of the recent literature has studied RUL prediction using a pre-defined fixed threshold, the stochastic failure threshold has not been thoroughly studied. However, in practice, bearings are used by diverse users in various systems. In many cases, the designer of a component might not know with certainty the level at which degradation can explicitly cause failure. In addition, the difference in the scales of features representing

the underlying performance of bearings, as well as the degradation mechanisms, fault location, and some physical characteristics of bearings, yield different failure thresholds (Peng and Coit 2007). These findings emphasize the importance of investigating probabilistic failure thresholds. Tang et al. (2016) are one of the few researchers who developed a Wiener-based RUL prediction model with a stochastic failure threshold following TND. However, the diffusion parameter in the model is assumed to be fixed among all units, which may not be true in some real-life applications.

To address the above issues, this paper proposes a RUL-prediction framework comprising of two main phases of feature extraction using three main time–frequency approaches and an adaptive stochastic model for the RUL prediction of experimental roller bearings under contaminated conditions. The main research contribution is summarized as follows:

- The frequency domain of acceleration signals is accounted for in addition to the time domain by decomposing the signals into various frequency bands using different transformation techniques and extracting statistical features (i.e., condition indicators) from each band for deterioration modeling. The features extracted from such techniques are more sensitive to the degradation stage and thus more suitable for failure prognostics of bearings.
- Since the data of the selected features exhibit a linear non-monotonic degradation trend, a continuous-time stochastic Wiener process is used as the RUL-prediction model. The failure threshold in the model is assumed a probabilistic variable following TND to reflect the threshold variability while the key parameters of the model are also assumed random and updated iteratively when a new observation of the degradation data becomes available. The RUL prediction of the bearings are computed numerically at different degradation datapoints with reasonably high accuracy which helps maintenance managers develop more effective and reliable predictive maintenance policies.
- Some real-time accelerated degradation tests have been conducted on rolling element bearings degraded by particle contamination under laboratory operating condition and the data were collected to present the effectiveness of the proposed framework. Most bearing datasets in literature have been tested under loading effect whereas contamination as a crucial degradation mechanism was not investigated before in existing datasets.

The rest of this paper is structured as follows. Section 2 demonstrates the proposed framework together with the theoretical literature review. Section 3 presents the model development. Section 4 describes the case study to illustrate the

proposed framework, and Sect. 5 presents the discussion and conclusions.

2 Proposed framework for RUL prediction

Figure 1 shows the proposed framework of the paper. Phase 1 of this framework involves feature extraction, where each of the collected raw acceleration signals is decomposed into different frequency bands to filter out all irrelevant frequencies and determine the signature of the fault characteristics of the signals. The decomposition is performed using a number of techniques namely empirical mode decomposition (EMD), empirical wavelet transform (EWT), and fast Fourier transform (FFT). The decomposition in FFT is based on the frequency variation throughout the bearing lifetime. Once the signals have been decomposed into different windows with different frequency ranges, the statistical features as condition indicators including kurtosis, RMS, crest factor, shape factor, impulse factor, skewness, and mean value, are calculated for each window to compare the frequency bands and understand which feature from which band can monitor the health status of the bearings. The condition indicators (CIs) that exhibit a similar trend throughout the lifetime of bearings are then considered as the selected features and used for RUL prediction of bearings in phase 2.

Phase 2 involves degradation modeling and online RUL prediction. A continuous-time stochastic Wiener process is built on the increments of the selected features. The Wiener process parameters are estimated by the maximum likelihood estimation (Si and Zhou 2014). The Bayesian prior knowledge basis for each bearing dataset is obtained from the other bearings' datasets that have been tested under the same laboratory operating condition. The prior distribution for the time-dependent drift and diffusion parameters of the Wiener process is a conjugated normal-gamma distribution (Cowles 2013). The prior distribution parameters, as well as the measurements of the degradation data, are used to update the parameters of the Wiener process and obtain the posterior distribution. The failure threshold is a stochastic variable following TND where the parameters are estimated by fitting a normal distribution on the real failure thresholds observed for each technique. A numerical approximation of RUL with respect to the first passage time (FPT) distribution is obtained for each experimental bearing, and the model is evaluated in terms of score, prediction error, and prognostics horizon (PH). The details of the framework will be discussed further in the following sections.

2.1 Phase 1. Feature extraction

Due to the complicated mechanical structure and nonstationary characteristic of roller bearings, raw acceleration signals may contain massive signal components and they can be contaminated by different kinds of noise during collection and transmission of the signals (Jiao et al. 2019). Thus, they may not be sensitive enough to the bearing's condition and suitable to be directly used for degradation modeling. For this purpose, various methods have been proposed to extract useful information from the acceleration signals in the time domain, frequency domain, and time–frequency domain for both diagnosis and prognosis, which are sensitive to the rotational speed and structural geometry of the bearings (Laala et al. 2020; Kumar et al. 2018). Some of the time-domain features fluctuate significantly, especially at the beginning of the bearing's deterioration, and some are not appropriate for dealing with localized faults (i.e., inner race faults, outer race faults, cage, and roller faults). However, the frequency-domain approaches are more reliable and accurate compared to the time-domain approaches, especially for fault diagnosis, as different types of bearing faults correspond to different frequency characteristics (Wang et al. 2014a; b). Time–frequency signal-processing techniques provide the opportunity to identify components carrying important diagnostic information for further processing (Kumar et al. 2018).

The three main classifications of TFR techniques are Fourier transform (FT), WT, and Hilbert–Huang transform (HHT) (Cooley and Tukey 1965; Ricker 1940; Huang 2005). Among these, HHT as an adaptive data-driven approach performs well on both nonlinear and nonstationary vibration signals. However, it is an empirical approach and lacks an underlying solid mathematical theory (Boashash et al. 2016). In contrast, WT is based on a solid mathematical theory and can handle nonlinear signals and, in some cases, nonstationary signals. However, it is still based on a prescribed division mechanism for analyzing vibration signals (Bessous et al. 2016). FT faces the challenge of frequency band selection and does not perform effectively on nonstationary signals where different frequency components exist at different intervals of time (Kumar et al. 2022). In this study, the above three approaches are used to decompose the experimental signals into several frequency frames to understand how the features extracted from the decomposed signals using these techniques can differ in monitoring the underlying degradation process of the bearings and perform in combination with stochastic-threshold Wiener process for failure prognostics.

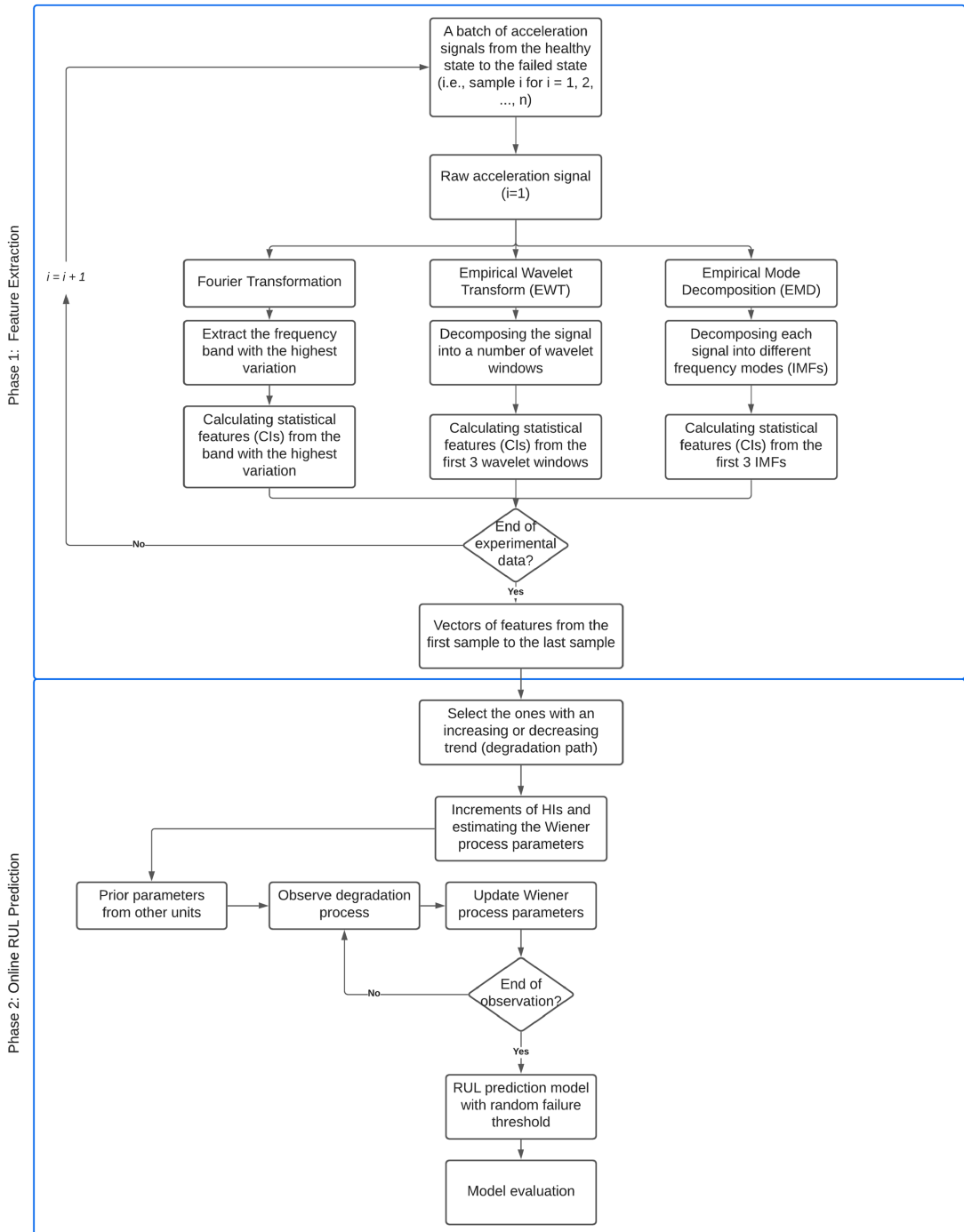


Fig. 1 Proposed framework for RUL prediction

2.1.1 Fast Fourier transform

In this paper, FFT is applied to each acceleration signal taken within regular time frames, assuming that they are stationary. The FFT algorithm is used to compute the discrete Fourier transform (DFT) and its inverse. The k -point DFT converts a time-domain signal into a frequency-domain signal. The FFT of a signal is defined as $Y = FFT(x)$, where x is the raw acceleration signal and Y is the Fourier-transformed vector of the acceleration signal calculated using Eq. (1) (Zhang et al. 2013):

$$Y(k) = \sum_{j=1}^M x_j e^{\frac{-2\pi i}{M}(j-1)(k-1)} \quad (1)$$

where M is the total number of acceleration readings in one acceleration sample or the signal length, $e^{\frac{-2\pi i}{M}}$ is the M th root of unity, and k is the number of points in DFT, or the new length of the Fourier-transformed signal, which is obtained from $2^{2^k \geq |M|}$ and is used to improve the visual frequency resolution and performance of FFT. $Y(k)$ is the k th Fourier coefficient, which is a complex number comprising an imaginary part and a real part. One of the challenges with FT is the selection of the frequency band of interest. This selection can be based on the frequency variation of the frequency components in the Fourier spectrum of the signals, which can show the signal energy distribution as a function of frequency. This can be recognized by plotting the power spectral density or square of the magnitude part of the Fourier vector over the frequency vector to determine the dominant frequency of the data. Equation (2) calculates this mathematically by computing the difference between the accumulated amplitude difference of the FFT spectra on each frequency line (Wu et al. 2017):

$$f_{diff}(k) = \sum_{i=2}^N |f_i(k) - f_{i-1}(k)| \quad (2)$$

where $f_i(k)$ is the squared amplitude of $Y(k)$ for the i th acceleration sample. N is the number of FFT spectra, which is equal to the number of acceleration samples from the healthy state to the failed state. $f_{diff}(k)$ indicates the variation in each frequency line throughout the lifetime of the bearings. Based on $f_{diff}(k)$, the indicator $H(g)$ is calculated using Eq. (3), which indicates the accumulated sum of $f_{diff}(k)$ and stands for the total difference from the first frequency line to the g th frequency line.

$$H(g) = \sum_{k=1}^g f_{diff}(k) \quad (3)$$

If the differences in the corresponding frequency line amplitudes along with lifetime are small, then the change

in $H(g)$ will be smooth. Otherwise, the value of $H(g)$ will change rapidly and $H(g)$ will have a large slope (Wu et al. 2017). The objective here is to find the range of g values (i.e., frequencies) where $H(g)$ changes rapidly and has a large slope. This yields the optimal frequency band, where there is the highest variation in frequency throughout the bearing lifetime. The optimal frequency band can then be used to filter the signals and extract features from the filtered signals. The selected feature, which has a common increasing trend among all bearings, can then be used as an HI to model the bearing degradation and RUL prediction as it will reveal the underlying degradation performance of the bearing. In this study, the other frequency ranges that are close to the optimal frequency band are also used to filter the signals and, consequently, feature extraction, and RUL prediction performance.

2.1.2 Hilbert–Huang transform

The basis of HHT is empirical mode decomposition (EMD), which decomposes the signals based on their time-domain characteristics and uses the envelopes defined by the local maxima and minima. Through EMD, the time-based signals are decomposed into different segments called intrinsic mode functions (IMFs), ordered from high frequency to low frequency, as presented in Eq. (4). An IMF must satisfy two conditions. First, the number of local extrema and the number of zero crossings must differ at most by one. Second, at any point in the IMF, the mean value of the local minima and local maxima must be zero (Zhang et al. 2019).

$$x(t) = \sum_{i=1}^n c_i(t) + r(t) \quad (4)$$

where t is the time within each sample, $x(t)$ is the original time-domain signal, $c_i(t)$ is the i th IMF, n is the number of IMFs extracted from an acceleration signal, and $r(t)$ is the residual signal, which is the mean trend of $x(t)$. The algorithm used to extract these IMFs is summarized below.

1. Initialize with the input signal $x(t)$.
2. Find the extrema (local minima and maxima points).
3. Use pchip interpolation to determine the mean of the upper and lower envelopes: $(m_1(t))$ and $h_1(t) = x(t) - m_1(t)$.
4. $h_1(t)$ is regarded as the 1st IMF ($c_1(t)$) if the two IMF conditions are met; if not, steps 2 to 3 are repeated on $h_1(t)$ until the conditions are satisfied and the 1st IMF is obtained.
5. Once $c_1(t)$ is determined, steps 2 to 4 are repeated on the residue, $r(t) = x(t) - c_1(t)$, to determine other IMFs. There are various stopping criteria to stop the procedure, such as the Cauchy-type criterion, the mean value crite-

rion, and the maximum number of IMF criteria (Wang et al. 2010). Once one of these criteria is met, the algorithm stops and provides a set of IMFs together with the residue signal. As the original acceleration signals are not smoothed, pchip interpolation was selected to determine the mean of local extrema.

The details of the process are provided in the literature (Huang et al. 1998; Lei et al. 2012). In this section, the acceleration signals are decomposed into a number of IMFs. The statistical features are calculated from each of these IMFs and compared to determine which feature from which IMF is suitable for deterioration modeling and failure prognostics.

2.1.3 Empirical wavelet transform

Wavelet transform examines acceleration signals using several wavelet basis functions. The selection of this function and the number of decomposition levels in the denoising process are crucial factors for extracting the fault features, which affect the performance of the fault detection process (Lin and Qu 2000). EWT is developed to overcome some of these shortcomings and to improve the flexibility and decomposition performance of conventional WT. The process of signal segmentation in EWT is conducted using the Fourier spectrum of the signal, which is important to make the wavelet adaptive to the signal (Chen et al. 2016). However, the main challenge is still to select the most sensitive fault-prone sub-band, which contains the hidden defect information of the bearings. The analysis of inappropriate sub-bands can lead to misleading frequency ranges and negatively affect fault detection and failure prediction.

The general idea of EWT is to segment the Fourier spectrum of the acceleration signal by obtaining band-pass filters. For a frequency w , assumed in the normalized Fourier axis of $[0, \pi]$, each segment is defined as $[w_{n-1}, w_n]$, where w_n is the limit between the segments such that $w_0 = 0$ and $w_n = \pi$ or expressed as $\coprod_{n=1}^N [w_{n-1}, w_n] = [0, \pi]$. In this paper, the EWT function is applied to each signal (i.e., acceleration sample) to obtain the EWT coefficients and multiresolution analysis (MRA) of the signals.

The model segmentation in this method is based on the frequency domain, while in EMD, the decomposition is based on the time domain. Thus, the first step is to obtain the Fourier spectrum of the acceleration signal, and the second step is to separate different portions of the spectrum that correspond to modes centered around a specific frequency. To determine these boundaries or portions of the frequency modes in Fourier segmentation, the local minima method of the Fourier spectrum's logarithm of the processed signal is used. This is to address the two challenges namely flat picked modes and global-versus-local modes described by Lei et al. (2012). In this paper, EWT obtains the MRA of

each acceleration signal by using the five largest peaks, while the first local minimum is located between adjacent peaks.

The objective of EWT implementation on the acceleration signals is to break them down into different sub-bands based on their frequency domain. The statistical features are calculated from each of the first three sub-bands and compared to identify which feature from which band is the most informative for failure prognosis.

Table 1 presents the features and their calculation formulae.

If the time-domain acceleration signals are directly used for feature extraction without accounting for the frequency domain, then x_i indicates the acceleration measurements. However, if the signals are processed by FFT, EMD, and EWT, x_i can be the measurements of the processed signal. The variables m , σ , and M indicate the mean, standard deviation, and the number of measurements in a signal respectively.

Several performance measures in literature have been discussed for selecting more appropriate degradation indicators, such as monotonicity, prognosability, and trendability (Boukra et al. 2019; Thoppil et al. 2021). They are used to measure the suitability of a candidate for RUL estimation. However, in this paper, a broader perspective is considered, which means that the RUL of bearings is predicted using all features that have a similar trend over the bearings' lifetimes.

2.2 Phase 2. Modeling and evaluation of the model

To capture the stochasticity of the bearings degradation, a Wiener process as a continuous-time stochastic process with a stochastic failure threshold is employed to model the health status of the bearings and predict their RUL. The Wiener process is selected because the observed experimental degradation trajectories exhibit linear and nonmonotonic

Table 1 Statistical features (Caesarendra and Tjahjowidodo 2017)

Features	Formula
Kurtosis	$K = \frac{\sum_{i=1}^M (x_i - m)^4}{(M-1)\sigma^4}$
RMS	$RMS = \sqrt{\frac{1}{M} \sum_{i=1}^M x_i^2}$
Crest factor	$CF = \frac{\max(x_i)}{\sqrt{\frac{1}{M} \sum_{i=1}^M x_i^2}}$
Skewness	$S = \frac{\sum_{i=1}^M (x_i - m)^3}{(M-1)\sigma^3}$
Mean	$Mean = \frac{1}{M} \sum_{i=1}^M x_i$
Shape factor	$SF = \frac{\sqrt{\frac{1}{M} \sum_{i=1}^M x_i^2}}{\frac{1}{M} \sum_{i=1}^M x_i }$
Impulse factor	$IF = \frac{\max x_i }{\frac{1}{M} \sum_{i=1}^M x_i }$

behavior over the components' lifetimes. In this model, the drift and diffusion parameters are updated iteratively using the Bayesian inference approach once more observations are available in order to make the model adaptive and consider the uncertainty of the model's parameters. As mentioned before, the failure thresholds in different experiments are treated as stochastic variables following TND to involve the uncertainty of the thresholds.

2.2.1 Wiener process with stochastic failure threshold

A general format of Wiener process as a widely used stochastic process, is given in Eq. (5). One main assumption in this model is that the degradation increments are assumed to be independent and normally distributed with the mean and standard deviation μt and $\sigma^2 t$, respectively, while t is the time unit. In the conventional Wiener process, the degradation process $(X(t))$ is modeled as follows (Wang et al. 2014a, b):

$$X(t) = x_0 + \mu t + \sigma_B B(t) \tag{5}$$

where x_0 is the initial degradation state of the system of interest, μ is the drift coefficient capturing the degradation rate, σ_B is the diffusion coefficient, and $B(t)$ while $t \geq 0$ is the standard Brownian motion that represents the stochastic dynamics of the degradation process.

Assuming that RUL is interpreted as FPT or the first time that the degradation state has passed the failure threshold, FPT distribution is analytically proved to be an inverse gaussian (IG) distributed with the parameters $\nu_n = \frac{L-X_t}{\mu_n}$ and $\lambda_n = \frac{(L-X_t)^2}{\sigma_n^2}$, where L is the failure threshold, X_t is the degradation status at time t , and μ_n and σ_n are the drift and diffusion coefficients of the Wiener process, respectively (Zhang et al. 2018).

2.2.2 Bayesian inference—Wiener process

The mean (μ) and precision parameters ($\frac{1}{\sigma_B^2}$) as the two uncertain factors affecting the bearing degradation process, are the two examples of random variables that are unknown in reality. Expert knowledge, theoretical analyses, and historical data can be used to obtain preliminary information regarding these uncertain factors and their associated probability distributions (Gao et al. 2020). In this paper, to obtain the prior distribution parameters, b datasets are divided into two portions, which include the bearing of interest whose parameters need to be estimated and the $b - 1$ other datasets treated as historical data. Since a Wiener process is used to model the degradation processes and future increments are assumed to follow a normal distribution with unknown mean and precision parameters, the

conjugate prior distribution is a normal-gamma distribution, as presented in Eq. (6):

$$NG(\mu, \eta | \mu_0, \eta_0, \kappa_0, \alpha_0, \beta_0) \sim Normal\left(\mu | \mu_0, \frac{1}{\kappa_0 \eta}\right) Gamma(\eta | \alpha_0, \beta_0) \tag{6}$$

Let us consider b units (i.e., experimental bearings), and μ_l, σ_l , and η_l for $l = 1, 2, \dots, b$ are the mean, standard deviation, and precision parameters of the measurements of bearing l respectively, then the prior distribution parameters of bearing j , where $j \in [1, 2, \dots, b]$, are calculated as below (Cowles 2013):

- α_0 and β_0 are the maximum likelihood estimated shape and scale parameters of fitted Gamma distribution on η_l values, where $l = 1, 2, \dots, b$ and $j \notin l$. The PDF of Gamma distribution is:

$$f(x|k, \theta) = \frac{1}{\theta^k \Gamma(k)} x^{k-1} e^{-\frac{x}{\theta}}$$

where $\Gamma(\cdot)$ is the Gamma function, k and θ are the shape and scale parameters respectively (Cowles 2013).

- $\rho_0 = \frac{b}{\sum_{l=1}^{j-1} (\mu_l - \mu_0)^2 + \sum_{l=j+1}^b (\mu_l - \mu_0)^2}$
- $\kappa_0 = \frac{\rho_0 \beta_0}{(\alpha_0 - 1)}$

Once the prior distribution parameters are computed, the degradation observations of bearing j , $(x_1, x_2, x_3, \dots, x_n)$, at different samples, together with the existing prior distribution information, can be used to update the posterior distribution of the uncertain variables for bearing j . Equations (7–10) present how to calculate the posterior distribution parameters, which is also a normal-gamma distribution. The increments in the degradation observations (x_i 's) are both measurements from time-domain features and the measurements from the features obtained with three other techniques (i.e., FFT, EMD, and EWT). The large uncertainty regarding the μ and η parameters at the beginning of the procedure, when the prior distribution is only available, can lead to a large uncertainty in RUL prediction. However, as new observations are gradually obtained, the updated posterior distribution approaches the real distribution, the uncertainty of μ and η decreases, and the uncertainty of RUL prediction reduces as well. This provides an updated RUL distribution for each sample; however, RUL is still affected by the stochastic nature of the degradation process:

$$\mu_n = \frac{\kappa_0 \mu_0 + n \bar{x}}{\kappa_0 + n} \tag{7}$$

$$\beta_n = \beta_0 + \frac{1}{2} \sum_{i=1}^b (x_i - \bar{x})^2 + \frac{\kappa_0 n (\bar{x} - \mu_0)^2}{2(\kappa_0 + n)} \tag{8}$$

$$\alpha_n = \alpha_0 + \frac{n}{2} \tag{9}$$

$$\kappa_n = \kappa_0 + n \tag{10}$$

In addition to μ and η parameters, the failure threshold (L) is another uncertain variable in the model. In real-life applications, the failure threshold is not a fixed value, which varies among different components and users. Moreover, there is uncertainty of threshold with respect to the failure time in historical data, while the degradation level that can cause failure is also uncertain. If the considered failure threshold is larger than the real failure threshold, it will lead to an unexpected failure, a less reliable system, and a delay in maintenance time. In contrast, if it is smaller than the real failure threshold, it will cause premature maintenance. In this paper, the failure threshold is a stochastic variable following TND. The mean (μ_L) and standard deviation (σ_L) of TND are obtained by fitting normal distribution on the real observed failure thresholds for the features that have a trend over time in each technique (i.e., FFT, EMD, and EWT).

Using the law of total probability (Cowles 2013), the unconditional cumulative distribution function (CDF) of RUL of bearings can be calculated numerically, as presented in Eq. (11). The numerical solution is determined by integrating the multiplication of IG distribution, conjugate normal-gamma distribution, and TND over all possible values of μ , η , and L . The reason to choose TND to model the failure threshold is that the observed thresholds in features among different bearings follow a normal distribution. A truncated version of normal distribution is considered, as L and IG distribution parameters are positive values (i.e., $L > 0$, $\nu_n = \frac{L - X_i}{\mu_n} > 0$, $\lambda_n = \frac{(L - X_i)^2}{\sigma_n^2} > 0$). As the Wiener process parameters (μ_n and σ_n^2) are also positive, $L - X_i$ should be above zero. Thus, the TND domain is $[X_i, +\infty]$, which means that only L values greater than X_i are taken into account for modeling.

$$P(RUL(t|y_t, \mu_n, \kappa_n, \alpha_n, \beta_n) \leq \tau) = \int_0^\infty \int_0^\infty \int_0^\infty F_{IG}(\tau|v, \lambda) f_N\left(\mu|\mu_n, \frac{1}{\kappa_n \eta}\right) f_{GA}(\eta|\alpha_n, \beta_n) f_{L,TND}(L|\mu_L, \sigma_L) d\mu d\eta dL \tag{11}$$

where $F_{IG}(\tau|v, \lambda)$ is the CDF of IG distribution with $\nu_n = \frac{L - X_i}{\mu_n}$ and $\lambda_n = \frac{(L - X_i)^2}{\sigma_n^2}$, $f_N\left(\mu|\mu_n, \frac{1}{\kappa_n \eta}\right)$ is the normal PDF of μ , and $f_{GA}(\eta|\alpha_n, \beta_n)$ is the PDF of η , which is

gamma-distributed. The result of Eq. (11) is the CDF and PDF of RUL at different samples of the experimental bearings.

The multidimensional composite midterm rule (Cowles 2013) can then be employed to solve numerical integration along each dimension. For this purpose, the three intervals are divided into n subintervals so that the entire 3D support is divided into small rectangular solids, and the integral can be solved numerically, although it becomes computationally expensive, depending on the number of subintervals.

To address this problem, it is proposed to find the areas of each subfunction that have non-zero values at different subintervals. As the main total function is a multiplication of the three distributions over μ , η and L , if one subfunction is equal to zero, the total function will also be equal to zero, and such intervals can be disregarded to have a more efficient and faster computation. For this purpose, the 0.025th and 99.975th percentiles are calculated for each subfunction, and the values in between are extracted as meaningful non-zero intervals. The non-zero intervals can then be divided into subintervals to calculate the integration using the multidimensional composite midterm rule.

2.2.3 Model evaluation

To evaluate the model, the relative error denoted by Er_i in Eq. (12) is calculated at the i th prediction point by comparing the actual observed value of RUL, denoted by RUL , and its predicted value, denoted by \widehat{RUL} .

$$\%Er_i = \frac{RUL_i - \widehat{RUL}_i}{RUL_i} \times 100 \tag{12}$$

There are various performance metrics to evaluate the model's accuracy and how well it can predict future condition of the system. In this paper, several prognostic metrics are used for the model's evaluation. The score of a model is a measure of its accuracy and is estimated by the weighted average of penalty function, using Eq. (13). The weighted score function assigns a higher weight to the recent RUL predictions, as it corresponds to the severe degradation

stage of the bearings when failure prediction is vital. The weights increase linearly from the first datapoint to the last one. The highest weight is assigned to the last prediction, and then descends linearly based on the number of predicted

datapoints. Thus, the n th prediction value has a weight of n and the first prediction datapoint has a weight of 1.

$$Score = \frac{\sum_{i=1}^n w_i \times A_i}{\sum_{i=1}^n w_i} \tag{13}$$

The penalty function presented in Eq. (14), is adopted from IEEE PHM 2012 prognostics challenge datasets to distinguish between the overestimation and underestimation of RUL (Necoux et al. 2012).

$$A_i = \begin{cases} \exp^{(-\ln 0.5) \cdot \left(\frac{Er_i}{5}\right)} & \text{if } Er_i \leq 0 \\ \exp^{(+\ln 0.5) \cdot \left(\frac{Er_i}{20}\right)} & \text{if } Er_i > 0 \end{cases} \tag{14}$$

Equation (14) means that there is a higher penalty with respect to the estimated RULs that exceed the actual RUL and a lesser penalty where the estimated RULs are lower than the actual ones.

Equation (15) gives the Cumulative relative accuracy (CRA) which is defined as the average relative error between the predicted and actual values of RUL at all prediction points.

$$CRA = \frac{1}{n} \sum_{i=1}^n 1 - |Er_i| \tag{15}$$

Prognostics horizon (PH) in Eq. (16) estimates the first time that the prognostics algorithm gives its prediction within the confidence bound interval (i.e., $\alpha \in [0, 1]$) (Yuan et al. 2019):

$$PH = n - i \widehat{RUL}_i \in [RUL_i \cdot (1 - \alpha), RUL_i \cdot (1 + \alpha)] \tag{16}$$

where n represents the prediction number. A larger PH exhibits a better prediction performance, which results in an earlier end of life prediction with more reliability.

Equations (17) and (18) give the root mean square relative error (RMSRE) and mean absolute error (MAE) of the predicted and actual lifetimes, respectively.

$$RMSRE = \sqrt{\frac{1}{n} \sum_{i=1}^n \left(\frac{RUL_i - \widehat{RUL}_i}{RUL_i} \right)^2} \tag{17}$$

$$MAE = \frac{1}{n} \sum_{i=1}^n |RUL_i - \widehat{RUL}_i| \tag{18}$$

Higher values of *score*, *PH*, and *CRA* and lower values of *RMSRE* and *MAE* indicate that the model exhibits a better prognostics capability for RUL prediction (Wu et al. 2017).

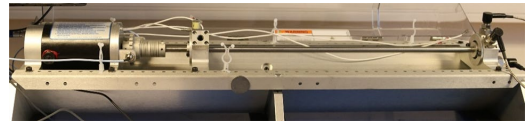


Fig. 2 Overview of the vibration setup (Liu et al. 2022)

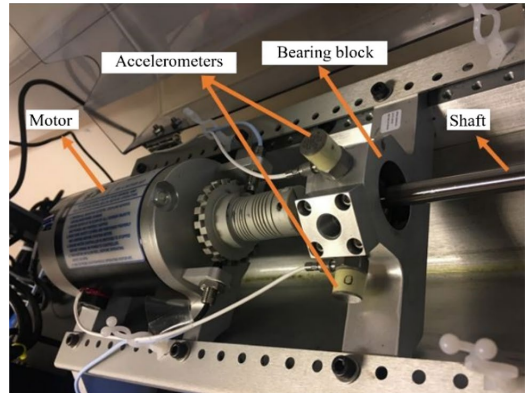


Fig. 3 Main components of the vibration setup

3 Case study

In this section, an experimental dataset is used to illustrate the proposed framework. The data are the acceleration of rotational bearings in the horizontal direction collected under laboratory operating condition. A detailed description of the experimental setup and the data are given in the following sections.

3.1 Laboratory setup design and data description

3.1.1 Laboratory setup design

An experimental setup at the Reliability, Availability, Maintainability, and Safety (RAMS) laboratory at NTNU is developed to conduct numerous accelerated life tests on roller bearings. The setup is called the “Bently Nevada (system 1) Rotor Kit, model RK4” depicted in Fig. 2. The major components of the setup include a horizontal bearing shaft, bearing blocks mounted on the two sides of the shaft to hold the bearings, and the accelerometers shown in Fig. 3. The bearing block located on the left part of the setup contains the experimental bearing which runs until its acceleration amplitude crosses 10 g. The two sets of

miniature accelerometers are mounted radially and axially on each bearing to collect the horizontal and vertical acceleration data over time. The collected data are then transformed into the central system, which visualizes the data on the screen. The amplifier (type 5134B) and accelerometers (type 8702B100), used in the measurement part of this setup are provided by the “Kistler” company. The rotating part of this setup is an asynchronous motor, which is used as an actuator that allows the inner race, rollers, and the bearing cage to rotate. The maximum rotational speed of the motor is approximately 10,000 revolutions per minute (rpm). The vibration setup is mounted on an aluminum platform with a safety cover, which is used while running experiments to ensure the safety of the operator.

Lubrication and contamination are the two most important failure modes (Lee and Choi 2020). However, in this study, contamination is selected as the degradation mechanism, since it can speed up the experiment process. To this aim, the bearing degradation mechanism is achieved by mixing solid Silicon carbide particles (called BW F240, Coulter particles, with the average size of 50–52 μm) with a lubricant and pouring the same amount of this mixture with one press of nozzle into the experimental bearing at predetermined time intervals (i.e., every 25 min) until the acceleration reading reaches a predefined threshold.

3.1.2 Data description

The output data are stored in CSV files and include horizontal and vertical acceleration, together with motor speed and the date and time of data collection. As the vertical acceleration data are under the impact of gravity and are not reliable and accurate enough, only the horizontal acceleration data are considered in this paper. Table 2 presents the geometric characteristics of the bearings.

The lifetime of a bearing consists of a number of acceleration samples which are obtained every 5 min. Figure 4 presents the lifetime of B1 for illustration.

Table 3 summarizes the collected acceleration data in the horizontal direction and the number of samples for each bearing. The motor speed is 2975 rpm, the sampling

Table 2 Geometric characteristics of the bearings

Type of bearing	Open roller/ ball bearing (R10)
Number of balls	10
Pitch diameter (mm)	70
Ball diameter (mm)	4.7
Inner diameter (mm)	15.9
Outer diameter (mm)	34.9

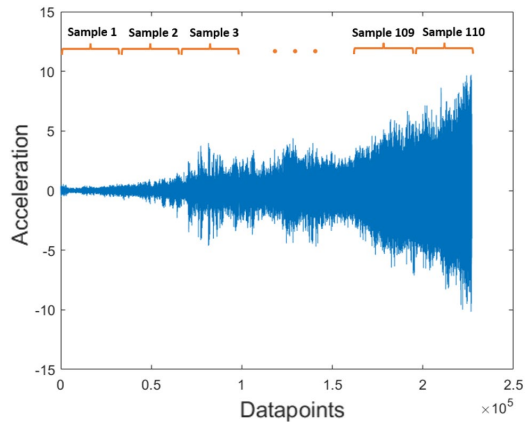


Fig. 4 Lifetime of B1

frequency for bearing B1 is 12,806 Hz, and for the rest of this dataset is 12,802 Hz. Each sample lasts 0.639 s, which means B1 has 2064 and the other bearings have 8192 datapoints. To prevent motor damage, the experimental tests are stopped once the amplitude of the acceleration surpasses 10 g.

For illustration purpose, Fig. 5 shows the first sample of bearing B1 when the bearing is healthy and the last sample (i.e., sample number 110) when the acceleration amplitude is above 10 g and the test is stopped.

3.2 Feature extraction and HI construction

After collecting the data as a batch of acceleration samples, the three techniques of FFT, EMD, and EWT as given in Sects. 2.1.1, 2.1.2, and 2.1.3 are employed to decompose the signals into different frequency bands and filter the signals. In the FT approach, the frequency spectrum of

Table 3 Number of samples per bearing

Type of bearing	Open roller/ ball bearing (R10)
B1	110
B2	35
B3	146
B4	106
B5	77
B6	248
B7	150
B8	143
B9	114
B10	115

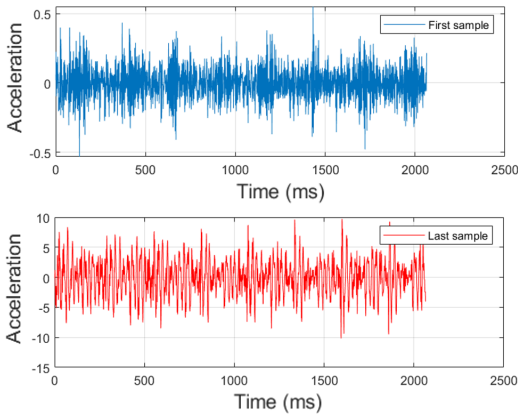


Fig. 5 First and last samples of bearing B1

the acceleration signals corresponding to the failure state of the bearings is obtained. As stated before, one major challenge in FT is to determine the fault-prone frequency band that contains the bearing’s defect information. The

development of frequency spectra shows the variation in frequency over the bearing’s lifetime, which evolves gradually at the beginning and dramatically at the end. The frequency band with the highest variation is mathematically computed using Eq. (3).

Figures 6 and 7 show $f_{diff}(k)$ and $H(g)$ given in Eqs. (2) and (3), respectively, for the 10 experimental bearings tested in the laboratory. The optimal frequency band for all bearings is marked with red dashed lines. The frequency band of [50, 2000] Hz has the maximum variation in all bearings and the bearings show a severe degradation within this frequency band interval. Thus, it is selected as optimal frequency band for feature extraction and degradation modeling. In addition to the optimal frequency band, the frequencies of [50, 2500], and [50, 3000] Hz are also used for feature extraction and their RUL prediction performance is presented in Appendix 1, Table 11.

The statistical features are calculated for the Fourier optimal frequency band and the frequencies of [50, 2500] and [50, 3000] Hz using the mathematical expressions in Table 1.

Figure 8 shows the features calculated for the optimal frequency band (i.e., [50, 2000] Hz) over the bearings’

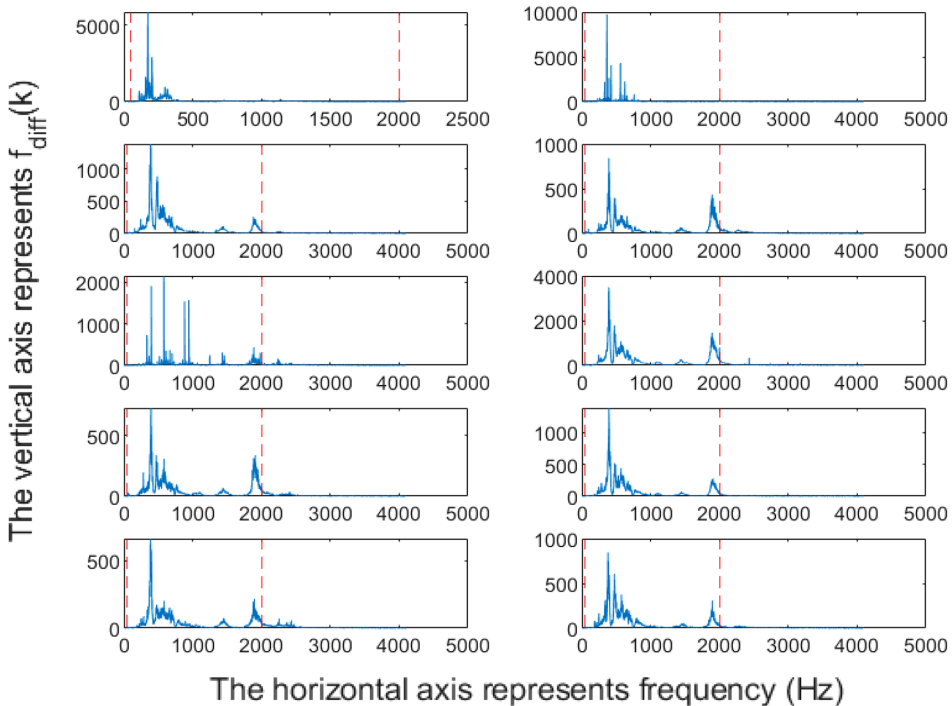


Fig. 6 The frequency variation throughout the bearings lifetime using FFT

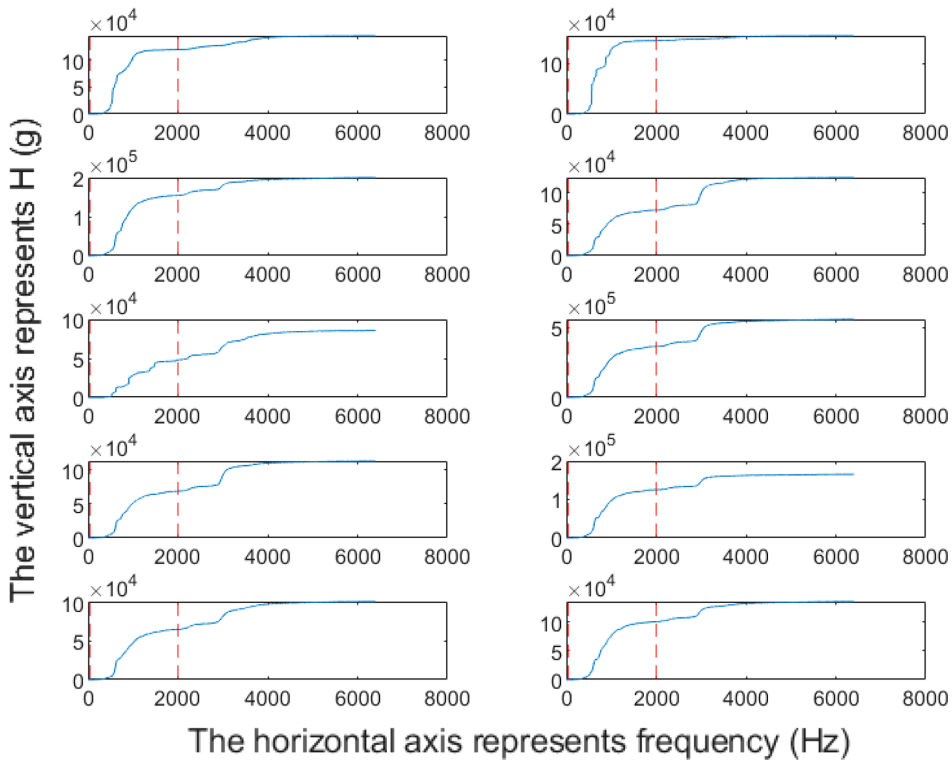


Fig. 7 The optimal frequency band for different bearings using FFT

lifetime. As shown in this Figure, the RMS energy-representative feature exhibits a similar increasing trend over the bearings' lifetime, while the other features do not show a common increasing or decreasing trend. Thus, RMS feature is selected as the degradation indicator since it can provide more relevant information for degradation modeling while it is simple to extract. The same argument applies to the other tested frequencies.

To obtain the optimal HIs from the EMD and EWT approaches, each acceleration sample is decomposed into different modes. The decomposition process in EWT is based on the local minimum approach to avoid the challenge of flat-picked modes, while the logarithm of the frequency spectrum of the signals is taken into account, instead of the frequency spectrum, to address the challenge of global-versus-local modes. Similar to FT, the features are calculated for each of the first three EWT sub-bands and are compared to identify the most informative HI for deterioration modeling and RUL prediction. In EMD, as a method with a time-based decomposition procedure, the first three IMFs of each acceleration signal are extracted, and their statistical features are calculated and compared. The first IMFs mainly consists

of high-frequency components, they are more informative, however they contain more noise compared to the last IMFs (Zhang et al. 2020).

Figure 9 presents the RMS energy degradation trajectories of the FT optimal frequency band, the first IMF of EMD, and the first MRA of EWT, as well as the time-domain approach. The RMS starts from zero where the experiment has started, and it ends when the acceleration amplitude surpasses 10 g.

4 Results and discussion

The increments in the different degradation trajectories of the bearings' datasets are used to estimate the drift and diffusion parameters of the Wiener process. The prior parameters and observation measurements of the degradation process are used to update the parameters continuously at each sample. In this model, the stochastic failure threshold (L), denoted by $L \sim TND(\mu_L, \sigma_L)$, follows a TND with mean (μ_L) and standard deviation (σ_L). μ_L and σ_L are estimated by fitting a normal distribution to the maximum degradation

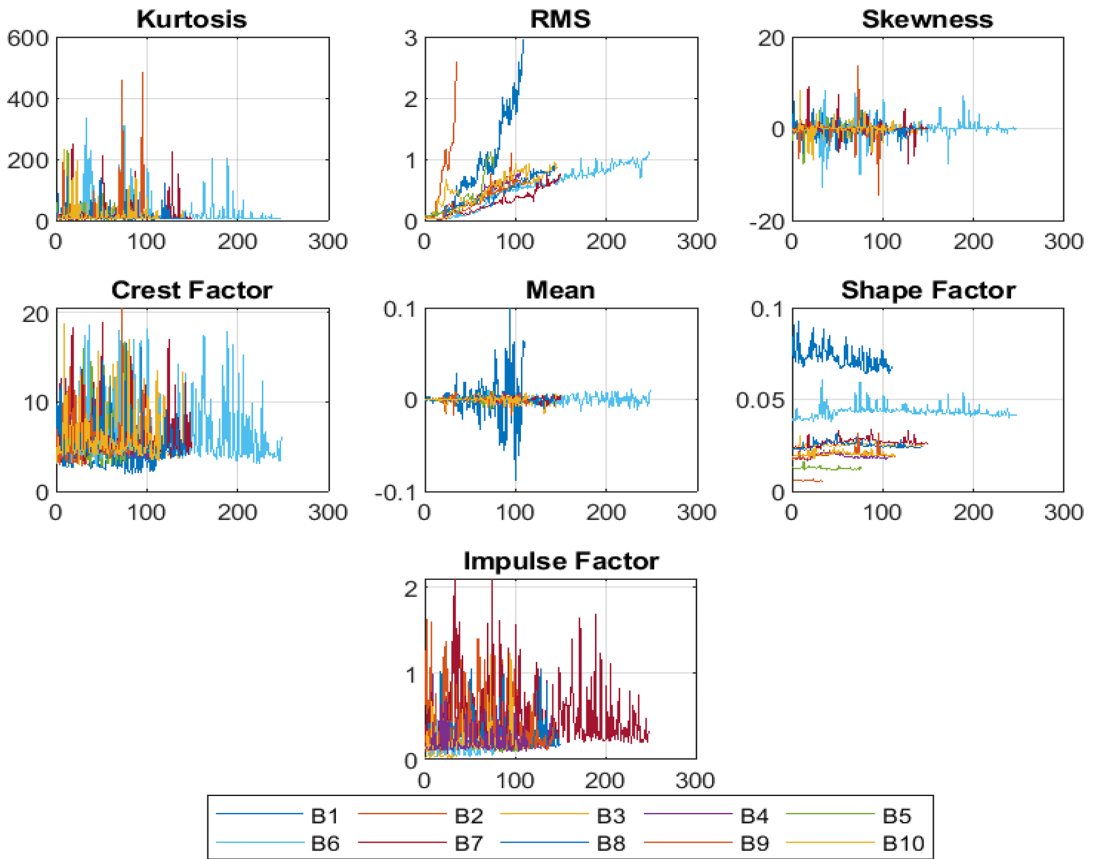


Fig. 8 Feature path for different bearings

levels of different bearings which vary between 0.5 and 3.0 as seen in Fig. 9. Table 4 presents the TND parameters of the failure thresholds.

Table 5 presents the drift and diffusion parameters of the Wiener process for B1 using different approaches. It also presents the prior parameters, denoted by $\mu_0, \sigma_0, \rho_0, \alpha_0, \beta_0, \kappa_0$ for B1. The parameters for other bearings are available in Appendix 1, Tables 8, 9 and 10. The parameters are also calculated for frequency windows [50, 2500] Hz, [50, 3000] Hz in FT, IMF 2 and IMF 3 in EMD, MRA 2 and MRA 3 in EWT, presented in Appendix 1, Table 11, and will be further used for RUL estimation.

Several performance measures are utilized to evaluate the model performance in RUL prediction. The $\alpha - \lambda$ performance metric, given in Eq. (19), evaluates whether the prediction accuracy at time t falls within the confidence bounds of α , which are expressed as a percentage of the

actual RUL values (Saxena et al. 2010). In other words, it measures whether the predictions stay within a cone of accuracy. That is, the accuracy bounds shrink over time. In this paper, the $\alpha - \lambda$ prognostic metric is used to illustrate the predicted RUL values at different sample numbers over the bearing lifetime.

Figures 10 and 11 present the $\alpha - \lambda$ accuracy plot of RUL predictions with a stochastic and constant failure threshold, respectively, where the HI is the RMS feature extracted from the time domain, FT [50–2000] Hz, EMD (IMF1), and EWT (MRA 1). α in $\alpha - \lambda$ approach is a goal threshold which is normally specified by an analyst considering the accuracy required to fulfill user specific criteria for success (Lall et al. 2013). In this paper, α is selected arbitrarily as 30% for performance validation. In Fig. 11, the constant failure thresholds are equal to the maximum degradation level of the bearings.

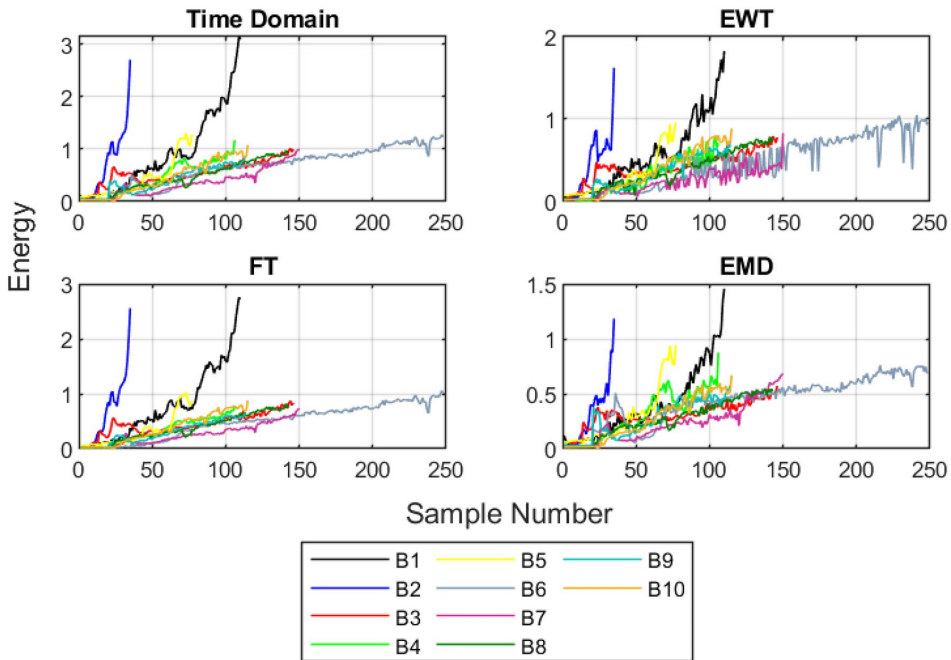


Fig. 9 RMS Energy degradation trajectories of the bearings using the FT optimal frequency band, the 1st IMF of EMD, and the 1st MRA of EWT

Table 4 Normal distribution parameters of stochastic failure threshold, L

	EWT (MRA 1)	EMD (IMF 1)	FT [50–2000] Hz	Time domain
μ_L	1.0470	0.8570	1.3350	1.4540
σ_L	0.3871	0.2975	0.7891	0.7510

$$\alpha - \lambda = \begin{cases} 1, & \text{if } (1 - \alpha)\hat{y}_i < y_i < (1 + \alpha)\hat{y}_i \\ 0, & \text{Otherwise} \end{cases} \quad (19)$$

As it can be seen in Fig. 10, the estimation results of the model are close to the actual RUL values in most of the bearing datasets, especially, for the ones that have an average number

of samples (e.g., 100–150 samples), such as B1, B4, and B9. In these cases, approximately 80% of the prediction results fall within 30% confidence bound intervals or are close to the confidence bounds. However, for the bearings that have a short lifetime with a few samples (e.g., 35 samples), such as B2, the model does not predict an acceptable RUL and there is a high prediction error. B2 has an abnormal lifetime, and there might be technical issues or external factors affecting the experiment that cause a shock in the acceleration amplitudes. Thus, the amplitude is recorded as over 10 g while the bearing is still in a normal operating mode. The technical problem can be induced by the accelerometers not being well-attached to the bearings resulting in erroneous signals. What is common among all datasets is that

Table 5 Wiener process parameters and prior parameters for bearing B1

	EWT (MRA 1)	EMD (IMF 1)	FT [50–2000] Hz	Time domain
μ	0.0166	0.0132	0.0270	0.0280
σ_B	0.0976	0.0599	0.1823	0.0884
μ_0	0.0110	0.0089	0.0144	0.0163
σ_0	0.0127	0.0092	0.0213	0.0218
$\rho_0 (\times 10^4)$	0.6174	1.1736	0.2200	0.2110
α_0	1.7926	3.6000	2.9186	2.5573
β_0	142.2290	176.3439	109.5286	179.5783
$\kappa_0 (\times 10^5)$	11.078	7.9595	1.2562	2.4337

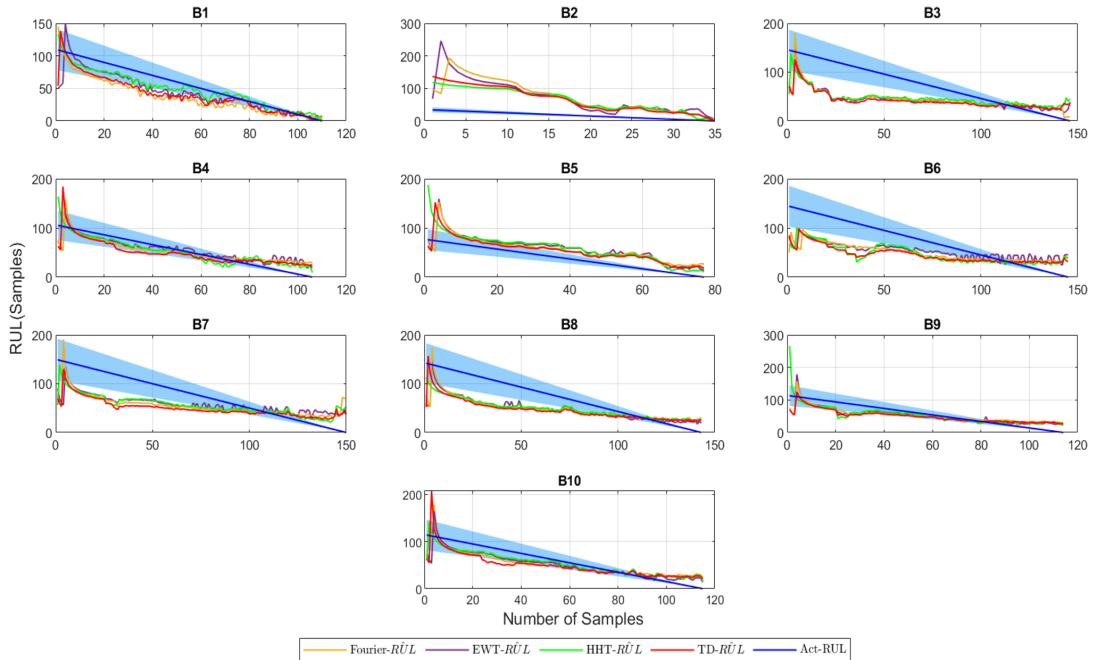


Fig. 10 $\alpha - \lambda$ accuracy plot ($\alpha = 30\%$) with a stochastic failure threshold, where HI is the RMS feature of the four approaches

at the beginning of the bearing lifetime, the model has a larger prediction error, which is due to high uncertainties associated with the underlying model parameters (μ , σ , L). However, the uncertainties reduce with time and the model yields a more reliable RUL prediction as more degradation measurements are observed and used to update the model parameters.

Figure 11 shows the RUL prediction results assuming a constant failure threshold throughout the lifetime of bearings. The constant failure threshold is assumed to be equal to the maximum degradation level of the bearing. Compared to the stochastic threshold case, the model has negligible prediction error in the second half of the bearing lifetimes (i.e., deterioration stage), which is significantly important in terms of predictive maintenance scheduling and decision-making. This indicates that, in the first half of the bearing lifetimes (i.e., normal stage), there is a higher variation in the failure threshold compared to the second half (i.e., deterioration stage). Moreover, in deterioration stage, with both constant and stochastic failure thresholds, the time–frequency approaches (FT, EMD, and EWT) fluctuate more and show higher variation and sensitivity to noise compared to the simple time-domain technique.

In order to evaluate the prediction performance of the model with both constant and stochastic failure threshold, the performance metrics given in Eqs. (12–18) have been calculated for each approach. Tables 6 and 7 present the

average of performance metrics such as MAE, RMSRE, and the model score, of all the bearings for the model with stochastic and constant failure threshold, respectively.

As it can be seen from Table 6, the RMS from EMD as the HI, has less RUL prediction error compared to others in terms of the average CRA, RMSRE, and MAE metrics. This means that it is a better health indicator for reflecting the deterioration process of roller bearings throughout their lifetime. The RMS extracted from the [50–2000] Hz frequency band in FT, has larger average PH value compared to the other methods. This states that the \widehat{RUL} falls within the confidence bound at an earlier point of time in the degradation process compared to other methods. A better performance of the different methods is presented in bold.

According to Tables 6 and 7, taking the uncertainty of failure threshold into account in addition to other model parameters has reduced the prediction error significantly and improved the result, although the score of the model in both cases (i.e., stochastic and constant failure threshold) did not have a noticeable change. Additionally, the model with stochastic failure threshold has larger values of PH which means the model can predict within the desired accuracy sufficiently prior to the end of bearings life.

As it is presented in Table 10 in Appendix 1, for the bearings with short lifetime (i.e., those with few samples) and a different RUL prediction pattern, such as B2, the EMD

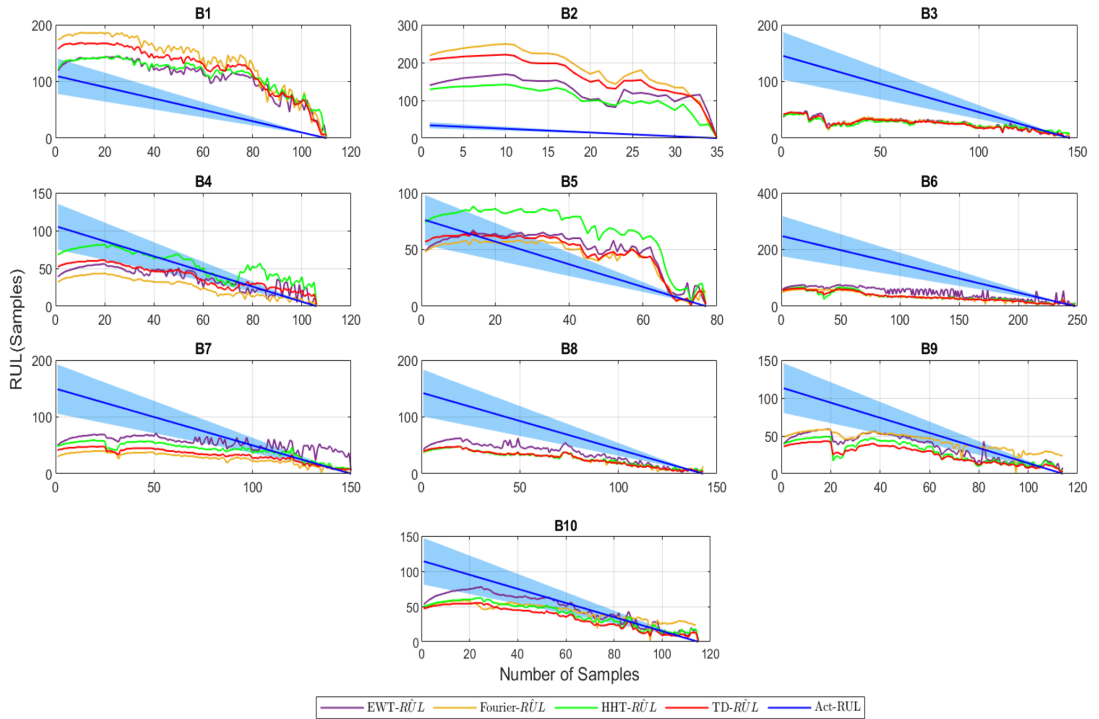


Fig. 11 α - l accuracy plot ($\alpha = 30\%$) with a constant failure threshold, where HI is the RMS feature of the four approaches

Table 6 The average of performance metrics for the model with stochastic failure threshold

	EWT (MRA1)	EMD (IMF1)	FT [50–2000] Hz	Time-domain
Avg. score	0.8555	0.8606	0.8508	0.8614
Avg. PH	101.2	107.3	107.5	106.2
Avg. CRA	-0.1826	-0.0337	-0.2348	-0.1028
Avg. RMSRE	2.9436	2.6301	3.2524	2.7418
Avg. MAE	25.0961	22.8285	26.3968	25.5910

Table 7 The average of performance metrics for the model with Constant failure threshold

	EWT (MRA1)	EMD (IMF1)	FT [50–2000] Hz	Time-domain
Avg. score	0.8716	0.8675	0.8605	0.8670
Avg. PH	71.6000	50.7000	28.8000	32.5000
Avg. CRA	-0.9183	-0.6729	-1.2009	-1.0287
Avg. RMSRE	3.2942	2.6809	2.9738	2.7555
Avg. MAE	42.7139	45.6410	56.6450	52.8345

approach outperforms the other methods. In other words, the RMS value extracted from IMF 1 is a more informative and suitable HI for condition monitoring of bearings compared to the simple time-domain approach, even for the bearings with an abnormal period of life. In contrast, for the bearings with long lifetime (i.e., those with more than 200 samples), such as B6, the EWT and time-domain approaches perform better than EMD. For the bearings with an average lifetime

(i.e., 100 to 150 samples), the RUL predictions fall within the 30% confidence bounds after approximately 20 samples. This means that in both the early stage of bearing lifetime and in the deterioration stage, RUL can be predicted based on the prior knowledge obtained from similar bearings and the current condition-monitoring data using this framework.

Overall, by considering the uncertainty of different parameters such as failure threshold, and the parameters of

the degradation model, the performance of the framework has improved significantly. The prediction error has been lowered, and the PH value has increased. In addition, combining the RMS feature extracted from EMD method with this framework, will provide the possibility of estimating RUL of roller bearings which have different length of lifetime and the same degradation mechanism.

5 Conclusions and recommendations

This paper proposes an adaptive RUL prediction framework for experimental roller bearings degraded by contamination using Silicon carbide particles. The framework comprises of two main phases of feature extraction and degradation modeling, with both constant and stochastic failure thresholds. The feature extraction phase focuses on the decomposition of the raw acceleration signals and extracting statistical features to understand which frequencies and which features are the most relevant for degradation modeling. In order to propose the effectiveness of the proposed framework, it is applied to 10 run-to-failure experimental tests of bearings conducted at RAMS laboratory at NTNU.

To this aim, the $\alpha - \lambda$ accuracy plot with $\alpha = 30\%$ is presented to show whether the predicted RUL values fall within the specified α bounds. The results show that the RUL prediction depends heavily on the failure threshold and duration of the bearing lifetime. According to the results, the optimal features (HIs) can successfully capture the evolving trend of bearing lifetime, especially within the steady-state and degradation stage. Moreover, the RMS feature from IMF 1 in EMD method has the best performance, and, therefore, it is a more suitable feature for tracking and representing the bearing deterioration process.

By considering the failure threshold as a stochastic variable, the RUL prediction performance of the model has improved significantly compared to the model with constant failure threshold. The prediction results, especially at the

deterioration stage, were within the desired accuracy sufficiently in advance to the bearing end of life.

To improve the prediction results, future studies can focus on the fusion of HIs and a mixed-threshold RUL prediction model. In addition, data-driven approaches such as machine learning algorithms can be investigated to compare the performance of RUL prediction with respect to the mathematical complexity, computational time, and prediction accuracy at different health stages of bearings. Furthermore, the framework can be extended to various sensor data including temperature and different degradation mechanisms such as overloading.

Funding Open access funding provided by NTNU Norwegian University of Science and Technology (incl St. Olavs Hospital - Trondheim University Hospital). The research received no funding from any funding agency.

Declarations

Conflict of interest We, the authors of this manuscript have no conflicts of interest to disclose.

Human participants and/or animals We, the authors ensure that no human or animal participation is involved in this research.

Informed consent We haven't used human participation or other personal information, informed consent is not required.

Open Access This article is licensed under a Creative Commons Attribution 4.0 International License, which permits use, sharing, adaptation, distribution and reproduction in any medium or format, as long as you give appropriate credit to the original author(s) and the source, provide a link to the Creative Commons licence, and indicate if changes were made. The images or other third party material in this article are included in the article's Creative Commons licence, unless indicated otherwise in a credit line to the material. If material is not included in the article's Creative Commons licence and your intended use is not permitted by statutory regulation or exceeds the permitted use, you will need to obtain permission directly from the copyright holder. To view a copy of this licence, visit <http://creativecommons.org/licenses/by/4.0/>.

Appendix 1

See Tables 8, 9, 10 and 11.w

Table 8 Wiener process parameters of experimental bearings using EWT, EMD, FT, and time-domain approach

	Time Domain		EWT (MRA 1)		EMD (IMF 1)		FT [50–2000] Hz	
	μ	σ_B	μ	σ_B	μ	σ_B	μ	σ_B
Bearing 1	0.0280	0.0884	0.0166	0.0976	0.0132	0.0599	0.0270	0.1823
Bearing 2	0.0771	0.1455	0.0469	0.1471	0.0338	0.0823	0.0744	0.1387
Bearing 3	0.0068	0.0502	0.0053	0.0498	0.0039	0.0353	0.0060	0.0515
Bearing 4	0.0110	0.0501	0.0067	0.1012	0.0082	0.0535	0.0077	0.0441
Bearing 5	0.0166	0.0531	0.0125	0.0591	0.0123	0.0440	0.0118	0.0560
Bearing 6	0.0049	0.0481	0.0038	0.1376	0.0028	0.0407	0.0043	0.0647
Bearing 7	0.0066	0.0412	0.0055	0.0802	0.0045	0.0342	0.0051	0.0454
Bearing 8	0.0065	0.0316	0.0053	0.0437	0.0037	0.0277	0.0063	0.0467
Bearing 9	0.0075	0.0448	0.0058	0.0552	0.0050	0.0455	0.0060	0.0861
Bearing 10	0.0093	0.0491	0.0077	0.0498	0.0058	0.0391	0.0082	0.0582

Table 9 Prior parameters of the extracted RMS feature from EMD (IMF1), TD, FT [50–2000] Hz, EWT (MRA 1)

	Technique	Prior parameters					
		μ_0	σ_0	$\rho_0(\times 10^4)$	α_0	β_0	$\kappa_0(\times 10^5)$
Bearing 1	EMD	0.0089	0.0092	1.1736	3.6000	176.3439	7.9595
	TD	0.0163	0.0218	0.2110	2.5573	179.5783	2.4337
	FT	0.0144	0.0213	0.2200	2.9186	109.5286	1.2562
	EWT	0.0110	0.0127	0.6174	1.7926	142.2290	11.078
Bearing 2	EMD	0.0066	0.0036	7.6918	5.2965	122.6066	21.950
	TD	0.0108	0.0069	2.0975	4.4443	105.3500	6.4156
	FT	0.0092	0.0066	2.2807	2.2886	138.6192	20.453
	EWT	0.0077	0.0039	6.4899	2.2507	116.1787	60.287
Bearing 3	EMD	0.0099	0.0091	1.1979	3.1558	182.7352	10.154
	TD	0.0186	0.0218	0.2111	2.0264	211.8509	4.3572
	FT	0.0168	0.0214	0.2181	1.6468	170.6680	5.7540
	EWT	0.0123	0.0127	0.6238	1.7370	127.7462	10.811
Bearing 4	EMD	0.0095	0.0093	1.1501	3.3222	188.7196	9.3468
	TD	0.0182	0.0220	0.2073	2.0264	211.8365	4.2776
	FT	0.0166	0.0215	0.2163	1.7503	151.8795	4.3787
	EWT	0.0121	0.0127	0.6166	1.8196	140.5640	10.574
Bearing 5	EMD	0.0090	0.0093	1.1626	3.0738	197.9012	11.095
	TD	0.0175	0.0221	0.2051	2.0381	212.9584	4.2079
	FT	0.0161	0.0216	0.2136	1.6280	176.6502	6.0069
	EWT	0.0115	0.0128	0.6060	1.6470	142.5430	13.350
Bearing 6	EMD	0.0101	0.0090	1.2232	3.0525	196.1508	11.690
	TD	0.0188	0.0216	0.2136	2.0245	210.1352	4.3803
	FT	0.0169	0.0213	0.2201	1.6353	181.2757	6.2813
	EWT	0.0124	0.0126	0.6344	2.1492	121.3209	6.6973
Bearing 7	EMD	0.0099	0.0092	1.1869	3.2149	177.5171	9.5125
	TD	0.0187	0.0218	0.2114	2.0785	196.2891	3.8464
	FT	0.0169	0.0214	0.2191	1.7215	156.3092	4.7464
	EWT	0.0122	0.0127	0.6224	1.6829	148.1481	13.502
Bearing 8	EMD	0.0100	0.0091	1.2030	4.3556	119.6225	4.2885
	TD	0.0187	0.0217	0.2115	2.6634	135.9930	1.7291
	FT	0.0167	0.0214	0.2178	1.6990	160.0851	4.9881
	EWT	0.0122	0.0127	0.6235	1.9270	108.1766	7.2764
Bearing 9	EMD	0.0098	0.0092	1.1794	3.0982	197.6008	11.108
	TD	0.0186	0.0218	0.2104	2.0361	205.2817	4.1677
	FT	0.0168	0.0214	0.2180	1.7580	175.2130	5.0401
	EWT	0.0122	0.0127	0.6212	1.6689	137.9410	12.811
Bearing 10	EMD	0.0097	0.0093	1.1686	3.0607	193.7904	10.990
	TD	0.0183	0.0219	0.2085	2.0247	211.1045	4.2962
	FT	0.0165	0.0215	0.2159	1.6257	178.5130	6.1591
	EWT	0.0120	0.0128	0.6124	1.7369	127.7606	10.617

Table 10 The performance metrics using the RMS features extracted from EMD (IMF1), TD, FT [50–2000] Hz, EWT (MRA1), for the model with stochastic failure threshold

	Score	PH	CRA	RMSRE	MAE
<i>Time domain</i>					
B1	0.9694	105	0.7184	0.3425	14.1111
B2	0.5830	0	-2.3007	3.7021	48.3143
B3	0.8948	139	0.0806	2.8988	35.3357
B4	0.8634	102	0.1169	2.7829	14.4528
B5	0.8093	76	-0.1391	2.9057	16.6883
B6	0.9636	17	0.3041	0.7195	89.6774
B7	0.8855	141	0.0578	3.2148	30.6345
B8	0.9026	141	0.1937	2.4839	30.3147
B9	0.8630	110	0.0531	3.1401	16.5263
B10	0.8800	111	0.1488	2.9390	16.8261
Average	0.8614	106.2	-0.1028	2.7418	25.5910
<i>EMD, IMF1</i>					
B1	0.9457	109	0.7290	0.7083	8.6000
B2	0.5894	0	-2.1738	3.4497	47.0857
B3	0.8858	142	0.0392	3.1285	32.6181
B4	0.8721	104	0.2286	2.5727	10.2925
B5	0.8242	70	0.0158	1.8738	20.9481
B6	0.9500	17	0.2000	1.0984	92.0685
B7	0.8872	143	0.1793	3.0590	25.2276
B8	0.8998	142	0.2124	2.4433	27.6783
B9	0.8677	112	0.1257	2.9005	14.3860
B10	0.8842	113	0.2146	3.1035	11.0435
Average	0.8606	107.3	-0.0337	2.6301	22.8285
<i>EWT, MRA1</i>					
B1	0.9580	105	0.7083	0.5222	12.4727
B2	0.5399	0	-3.1444	5.4074	55.7714
B3	0.9086	142	0.2242	2.2248	34.3288
B4	0.8513	101	0.1087	2.8689	11.1792
B5	0.7925	76	-0.2254	2.5853	20.9870
B6	0.9515	108	0.3313	0.8873	83.7137
B7	0.8646	145	-0.1436	4.3370	29.3333
B8	0.9145	139	0.3070	2.1424	27.4685
B9	0.8756	109	0.1880	2.7349	13.8947
B10	0.8979	110	0.3324	2.4558	12.2609
Average	0.8555	101.2	-0.1826	2.9436	25.0961
<i>FT [50–2000] Hz</i>					
B1	0.9510	108	0.5820	0.5354	18.5636
B2	0.5540	0	-2.7268	4.0675	57.3429
B3	0.9129	142	0.3599	1.0817	33.8014
B4	0.8492	105	-0.0131	3.5169	12.8396
B5	0.7852	76	-0.3695	3.5509	19.1818
B6	0.9562	9	0.2510	0.8704	89.1613
B7	0.8784	145	-0.3597	6.5093	31.3200
B8	0.8961	139	0.1537	2.7539	28.9790
B9	0.8542	109	-0.0164	3.4248	15.9298
B10	0.8711	114	0.0877	3.2245	15.3826
Average	0.8508	107.5	-0.2348	3.2524	26.3968

For each bearing, the bold values represent the better performance of different processing methods

Table 11 Average of the performance metrics considering the RMS feature extracted from FT ([50, 2500], [50, 3000]Hz), IMF 2 and IMF 3 in EMD, and MRA 2 and MRA 3 in EWT

	Score	PH	CRA	RMSRE	MAE
EWT, MRA 2	0.7780	104.5	-0.8759	5.5245	33.5402
EWT, MRA 3	0.6864	117.8	-2.0026	7.8742	48.3223
EMD, IMF 2	0.8409	95.9	-0.3505	2.8673	32.9210
EMD, IMF 3	0.8022	87.3	-0.98	3.3660	38.8116
FT [50–2500] Hz	0.8421	68.4	-0.2631	3.2697	35.5931
FT [50–3000] Hz	0.8325	55.4	-0.4479	3.8044	38.8071

References

- Ahmad W, Khan SA, Islam MMM, Kim JM (2019) A reliable technique for remaining useful life estimation of rolling element bearings using dynamic regression models. *Reliab Eng Syst Saf* 184(April):67–76. <https://doi.org/10.1016/J.RESS.2018.02.003>
- Ahmadzadeh F, Lundberg J (2014) Remaining useful life estimation: review. *Int J Syst Assur Eng Manag* 5(4):461–474. <https://doi.org/10.1007/S13198-013-0195-0/FIGURES/1>
- Bessou N, Zouzou SE, Bentrach W, Sbaa S, Sahraoui M (2016) Diagnosis of bearing defects in induction motors using discrete wavelet transform. *Int J Syst Assur Eng Manag*. <https://doi.org/10.1007/s13198-016-0459-6>
- Bhattacharya A, Dan PK (2014) Recent trend in condition monitoring for equipment fault diagnosis. *Int J Syst Assur Eng Manag* 5(3):230–244. <https://doi.org/10.1007/S13198-013-0151-Z/FIGURES/6>
- Boashash B, Touati S, Flandrin P, Hlawatsch F, Tauböck G, Oliveira PM, Barroso V et al (2016) Advanced time-frequency signal and system analysis. In: Boashash B (ed) *Time-frequency signal analysis and processing: a comprehensive reference*. Elsevier Inc., pp 141–236. <https://doi.org/10.1016/B978-0-12-398499-9.00004-2>
- Boukra T, Bensafia Y, Khettab K (2019) Contribution in enhancing the remaining useful life prediction in abrupt failures: bearing case. *Int J Intell Eng Syst* 12(3):156–165. <https://doi.org/10.22266/ijies.2019.0630.17>
- Caesarendra W, Tjahjowidodo T (2017) A review of feature extraction methods in vibration-based condition monitoring and its application for degradation trend estimation of low-speed slew bearing. *Machines*. <https://doi.org/10.3390/machines5040021>
- Chen J, Pan J, Li Z, Zi Y, Chen X (2016) Generator bearing fault diagnosis for wind turbine via empirical wavelet transform using measured vibration signals. *Renew Energy* 89(April):80–92. <https://doi.org/10.1016/J.RENENE.2015.12.010>
- Cooley JW, Tukey JW (1965) An algorithm for the machine calculation of complex Fourier series. *Math Comput* 19(90):297–301. <https://doi.org/10.1090/S0025-5718-1965-0178586-1>
- Cowles MK (2013) *Applied Bayesian statistics: with R and OpenBUGS examples*, vol 232. https://books.google.com/books/about/Applied_Bayesian_Statistics.html?id=iVxDAAQAQBAJ
- Farsi MA, Masood Hosseini S (2019) Statistical distributions comparison for remaining useful life prediction of components via ANN. *Int J Syst Assur Eng Manag* 10(3):429–436. <https://doi.org/10.1007/S13198-019-00813-W>
- Fornlöf V, Galar D, Syberfeldt A, Almgren T (2016) RUL estimation and maintenance optimization for aircraft engines: a system of system approach. *Int J Syst Assur Eng Manag* 7(4):450–461. <https://doi.org/10.1007/S13198-016-0509-0/FIGURES/12>

- Gao T, Li Y, Huang X, Wang C (2020) Data-driven method for predicting remaining useful life of bearing based on Bayesian theory. *Sensors* 21(1):182. <https://doi.org/10.3390/S21010182>
- Guo L, Li N, Jia F, Lei Y, Lin J (2017) A recurrent neural network based health indicator for remaining useful life prediction of bearings. *Neurocomputing* 240(May):98–109. <https://doi.org/10.1016/j.neucom.2017.02.045>
- Huang NE, Shen Z, Long SR, Wu MC, Snin HH, Zheng Q, Yen NC, Tung CC, Liu HH (1998) The empirical mode decomposition and the Hilbert spectrum for nonlinear and non-stationary time series analysis. *Proc R Soc A Math Phys Eng Sci* 454(1971):903–995. <https://doi.org/10.1098/RSPA.1998.0193>
- Huang NE (2005) Introduction to the Hilbert–Huang transform and its related mathematical problems. 1–26. World Scientific Publishing Co. https://doi.org/10.1142/9789812703347_0001
- Jiao J, Zhao M, Lin J, Liang K (2019) Hierarchical discriminating sparse coding for weak fault feature extraction of rolling bearings. *Reliab Eng Syst Saf* 184(April):41–54. <https://doi.org/10.1016/j.RESS.2018.02.010>
- Kumar S, Goyal D, Dang RK, Dhani SS, Pabla BS (2018) Condition based maintenance of bearings and gears for fault detection: a review. *Mater Today Proc* 5(2):6128–6137. <https://doi.org/10.1016/J.MATPR.2017.12.219>
- Kumar V, Parida MK, Albert SK (2022) The state-of-the-art methodologies for quality analysis of arc welding process using weld data acquisition and analysis techniques. *Int J Syst Assur Eng Manag* 13(1):34–56. <https://doi.org/10.1007/S13198-021-01282-W/FIGURES/13>
- Laala W, Guedidi A, Guettaf A (2020) Bearing faults classification based on wavelet transform and artificial neural network. *Int J Syst Assur Eng Manag*. <https://doi.org/10.1007/S13198-020-01039-X/FIGURES/14>
- Lall P, Lowe R, Goebel K (2013) Prognostic health monitoring for a micro-coil spring interconnect subjected to drop impacts. In: PHM 2013—2013 IEEE international conference on prognostics and health management, conference proceedings. <https://doi.org/10.1109/ICPHM.2013.6621458>
- Lee D, Choi D (2020) Analysis of the reliability of a starter-generator using a dynamic Bayesian network. *Reliab Eng Syst Saf* 195:106628. <https://doi.org/10.1016/J.RESS.2019.106628>
- Lei Y, Lin J, He Z, Zuo MJ (2012) A review on empirical mode decomposition in fault diagnosis of rotating machinery. *Mech Syst Signal Process*. <https://doi.org/10.1016/j.ymsp.2012.09.015>
- Li X, Ding Q, Sun JQ (2018a) Remaining useful life estimation in prognostics using deep convolution neural networks. *Reliab Eng Syst Saf* 172(April):1–11. <https://doi.org/10.1016/J.RESS.2017.11.021>
- Li N, Lei Y, Lin J, Ding SX (2015) An improved exponential model for predicting remaining useful life of rolling element bearings. *IEEE Trans Ind Electron* 62(12):7762–7773. <https://doi.org/10.1109/TIE.2015.2455055>
- Li X, Zhang W, Ding Q (2018b) Deep learning-based remaining useful life estimation of bearings using multi-scale feature extraction. *Reliab Eng Syst Saf*. <https://doi.org/10.1016/j.res.2018.11.011>
- Liao L, Köttig F (2016) A hybrid framework combining data-driven and model-based methods for system remaining useful life prediction. *Appl Soft Comput* 44(July):191–199. <https://doi.org/10.1016/J.ASOC.2016.03.013>
- Lin J, Qu L (2000) Feature extraction based on Morlet wavelet and its application for mechanical fault diagnosis. *J Sound Vib* 234(1):135–148. <https://doi.org/10.1006/JSVI.2000.2864>
- Liu S, Fan L (2022) An adaptive prediction approach for rolling bearing remaining useful life based on multistage model with three-source variability. *Reliab Eng Syst Saf* 218(February):108182. <https://doi.org/10.1016/J.RESS.2021.108182>
- Liu J, Pan C, Lei F, Hu D, Zuo H (2021) Fault prediction of bearings based on LSTM and statistical process analysis. *Reliab Eng Syst Saf* 214(October):107646. <https://doi.org/10.1016/J.RESS.2021.107646>
- Liu J, Vatn J, Pedersen VGB, Yin S, Tajiani B (2022) A comparison study for bearing remaining useful life prediction by using standard stochastic approach and digital twin. https://www.researchgate.net/publication/363346096_A_comparison_study_for_bearing_remaining_useful_life_prediction_by_using_standard_stochastic_approach_and_digital_twin
- Narayanan R, Halawa E, Jain S (2019) Remaining useful life prediction of rolling element bearings using supervised machine learning. *Energies* 12(14):2705. <https://doi.org/10.3390/EN12142705>
- Nectoux P, Gouriveau R, Medjaher K, Ramasso E, Chebel-Morello B, Zerhouni N, Varnier C et al (2012) PRONOSTIA: an experimental platform for bearings accelerated degradation tests, pp 1–8. <https://hal.archives-ouvertes.fr/hal-00719503>
- Nguyen KTP, Medjaher K (2019) A new dynamic predictive maintenance framework using deep learning for failure prognostics. *Reliab Eng Syst Saf* 188(August):251–262. <https://doi.org/10.1016/J.RESS.2019.03.018>
- Pan D, Liu JB, Huang F, Cao J, Alsaeidi A (2017) A Wiener process model with truncated normal distribution for reliability analysis. *Appl Math Model* 50(October):333–346. <https://doi.org/10.1016/J.APM.2017.05.049>
- Peng W, Coit DW (2007) Reliability and degradation modeling with random or uncertain failure threshold. In: 2007 proceedings—annual reliability and maintainability symposium, RAMS, pp 392–97. <https://doi.org/10.1109/RAMS.2007.328107>
- Ravikumar KN, Aralikatti SS, Kumar H, Kumar GN, Gangadharan KV (2021) Fault diagnosis of antifriction bearing in internal combustion engine gearbox using data mining techniques. *Int J Syst Assur Eng Manag*. <https://doi.org/10.1007/S13198-021-01407-1/TABLES/7>
- Ricker NH (1940) The form and nature of seismic waves and the structure of seismograms. *Geophysics* 5(4):348–366. <https://doi.org/10.1190/1.1441816>
- Rudin C (2019) Stop explaining black box machine learning models for high stakes decisions and use interpretable models instead. *Nature.Com*. <https://www.nature.com/articles/s42256-019-0048-x?fbclid=IwAR3156gP-ntoAyw2sHTXo0Z8H9p-2wBKe5jqitsMCdf7xA0P766QvStHFs&ref=https://githubhelp.com>
- Salehpour-Oskouei F, Pourgol-Mohammad M (2017) Risk assessment of sensor failures in a condition monitoring process; degradation-based failure probability determination. *Int J Syst Assur Eng Manag*. <https://doi.org/10.1007/s13198-017-0573-0>
- Saxena A, Celaya J, Saha B, Saha S, Goebel K (2010) Metrics for offline evaluation of prognostic performance. *Int J Progn Health Manag*. <https://doi.org/10.36001/IJPHM.2010.V111.1336>
- Si XS, Zhou D (2014) A generalized result for degradation model-based reliability estimation. *IEEE Trans Autom Sci Eng* 11(2):632–637. <https://doi.org/10.1109/TASE.2013.2260740>
- Singleton RK, Strangas EG, Aviyente S (2015) Extended Kalman filtering for remaining-useful-life estimation of bearings. *IEEE Trans Ind Electron* 62(3):1781–1790. <https://doi.org/10.1109/TIE.2014.2336616>
- Tang S-J, Yu C-Q, Feng Y-B, Xie J, Gao Q-H, Si X-S (2016) Remaining useful life estimation based on wiener degradation processes with random failure threshold. *J Cent South Univ* 23(9):2230–2241. <https://doi.org/10.1007/S11771-016-3281-Z>

- Thoppil NM, Vasu V, Rao CSP (2021) Health indicator construction and remaining useful life estimation for mechanical systems using vibration signal prognostics. *Int J Syst Assur Eng Manag* 12(5):1001–1010. <https://doi.org/10.1007/S13198-021-01190-Z/FIGURES/6>
- Wang G, Chen XY, Qiao FL, Zhaohua Wu, Huang NE (2010) On intrinsic mode function. *Adv Adapt Data Anal* 2(3):277–293. <https://doi.org/10.1142/S1793536910000549>
- Wang F, Chen S, Sun J, Yan D, Wang L, Zhang L (2014a) Time-frequency fault feature extraction for rolling bearing based on the tensor manifold method. *Math Probl Eng*. <https://doi.org/10.1155/2014/198362>
- Wang X, Jiang P, Guo Bo, Cheng Z (2014b) Real-time reliability evaluation with a general wiener process-based degradation model. *Qual Reliab Eng Int* 30(2):205–220. <https://doi.org/10.1002/QRE.1489>
- Wang H, Liao H, Ma X, Bao R (2021) Remaining useful life prediction and optimal maintenance time determination for a single unit using isotonic regression and gamma process model. *Reliab Eng Syst Saf* 210(June):107504. <https://doi.org/10.1016/J.RESS.2021.107504>
- Wen J, Gao H, Zhang J (2018a) Bearing remaining useful life prediction based on a nonlinear wiener process model. *Shock Vib*. <https://doi.org/10.1155/2018/4068431>
- Wen Y, Wu J, Das D, Tseng TLB (2018b) Degradation modeling and rul prediction using wiener process subject to multiple change points and unit heterogeneity. *Reliab Eng Syst Saf* 176(August):113–124. <https://doi.org/10.1016/J.RESS.2018.04.005>
- Wu B, Li W, Qiu MQ (2017) Remaining useful life prediction of bearing with vibration signals based on a novel indicator. *Shock Vib*. <https://doi.org/10.1155/2017/8927937>
- Xia M, Li T, Shu T, Wan J, De Silva CW, Wang Z (2019) A two-stage approach for the remaining useful life prediction of bearings using deep neural networks. *IEEE Trans Ind Inform* 15(6):3703–3711. <https://doi.org/10.1109/TII.2018.2868687>
- Yan T, Lei Y, Li N, Wang B, Wang W (2021) Degradation modeling and remaining useful life prediction for dependent competing failure processes. *Reliab Eng Syst Saf* 212(August):107638. <https://doi.org/10.1016/J.RESS.2021.107638>
- Yang C, Ma J, Wang X, Li X, Li Z, Luo T (2022) A novel based-performance degradation indicator RUL prediction model and its application in rolling bearing. *ISA Trans* 121:349–364. <https://doi.org/10.1016/j.isatra.2021.03.045>
- Yuan MJ, Wang MK, Welte TM (2019) Twin Exponential degradation model for online remaining useful life prediction
- Zhang Z, Si X, Changhua Hu, Lei Y (2018) Degradation data analysis and remaining useful life estimation: a review on Wiener-process-based methods. *Eur J Oper Res* 271(3):775–796. <https://doi.org/10.1016/J.EJOR.2018.02.033>
- Zhang J, Soangra R, Lockhart TE (2020) A comparison of denoising methods in onset determination in medial gastrocnemius muscle activations during stance. *Sci* 2(3):53. <https://doi.org/10.3390/SCI2030053>
- Zhang Z, Wang Yi, Wang K (2013) Fault diagnosis and prognosis using wavelet packet decomposition, Fourier transform and artificial neural network. *J Intell Manuf* 24(6):1213–1227. <https://doi.org/10.1007/s10845-012-0657-2>
- Zhang X, Zhao J, Ni X, Sun F, Ge H (2019) Fault diagnosis for gearbox based on EMD-MOMEDA. *Int J Syst Assur Eng Manag*. <https://doi.org/10.1007/s13198-019-00818-5>
- Zhu J, Chen N, Peng W (2019) Estimation of bearing remaining useful life based on multiscale convolutional neural network. *IEEE Trans Ind Electron* 66(4):3208–3216. <https://doi.org/10.1109/TIE.2018.2844856>

Publisher's Note Springer Nature remains neutral with regard to jurisdictional claims in published maps and institutional affiliations.

Paper 5

Maintenance Optimization of Systems with Lead Time Subject to Natural degradation and Stochastic Shocks

Bahareh Tajjani^{1*}, Jørn Vatn¹, Masoud Naseri²

¹ Department of Mechanical and Industrial Engineering, Norwegian University of Science & Technology (NTNU), 7491, Trondheim, Norway

² Department of Technology and Safety, UiT The Arctic University of Norway, 9037, Tromsø, Norway

Abstract

Shocks have attracted considerable interest in reliability and maintenance engineering because of their impact on vulnerable systems. Most industrial systems suffer from both internal degradation caused by fatigue and wear-out, and external shocks that often occur randomly due to harsh weather condition, overloading, etc. Developing maintenance optimization models without taking these stochastic shocks into account is often ineffective. This paper develops a model to optimize maintenance alarm threshold for a single-component continuously-monitored system which is exposed to both fatal and non-fatal shocks in presence of lead time for hard time maintenance. The shocks occur randomly according to a homogeneous Poisson process during the whole degradation process and have a stochastic impact on degradation level and the probability of shock occurrence increases as the system approaches failure. We propose a new numerical maintenance optimization model to find the solution without Monte-Carlo simulation and the model is compared with Wiener process. A numerical example and a real-time experimental case study on roller bearings are used to demonstrate the effectiveness of the model. The results show that the model is capable to improve maintenance decision-making in terms of failure probability and risk perspective.

This paper is submitted for publication and is therefore not included.

Paper 6

Optimized Random Forest Model for Remaining Useful Life Prediction of Experimental Bearings

Muhammad Gibran Alfarizi¹, Bahareh Tajjani, Jørn Vatn, and Shen Yin^{1b}, *Senior Member, IEEE*

Abstract—Bearings are essential to the reliable operation of rotating machinery in manufacturing processes. There is a rising demand for accurate bearing remaining useful life (RUL) predictions. The data-driven technique for predicting RUL of bearing has demonstrated promising prospects to facilitate intelligent prognostics. This article proposes a new data-driven prediction framework for bearing RUL utilizing an integration of empirical mode decomposition, random forest (RF), and Bayesian optimization. The proposed framework consists of two main phases: 1) feature extraction and 2) RUL prediction. The first phase of this framework focused on decomposing the empirical input signals using empirical mode decomposition into distinct frequency bands to filter out irrelevant frequencies and determine the fault characteristics of the signals. In the second phase, the RUL prediction is then carried out by an RFs-based model with its hyperparameters tuned by Bayesian optimization. The proposed approach is validated using datasets obtained from an actual run-to-failure experiment of roller bearings. The experiment results significantly improved compared to the standard data-driven and stochastic approaches.

Index Terms—Bayesian optimization, empirical mode decomposition (EMD), random forest (RF), remaining useful life (RUL) prediction, roller bearings.

I. INTRODUCTION

ROLLING bearings are vital in ensuring a stable operation in many industrial mechanical drive systems, such as aero engines, high-speed trains, and wind turbines. However, the operation of bearings may encounter many unexpected failures due to lack of lubrication, overload, and inappropriate installation. To avoid undesired consequences due to bearings failure, researchers have developed several remaining useful life (RUL) prediction methods to estimate the failure of the rolling bearings in advance and to schedule proper maintenance actions [1], [2]. RUL prediction is an efficient tool to improve the overall system's reliability and reduce maintenance expenses. However, the challenge remains in describing the degradation trend of rolling bearings due to unknown external circumstances,

such as ambient noise and rotational speed, which can produce a significant discrepancy between actual rolling bearing life and theoretical calculating value.

In recent years, many approaches have been proposed to predict the RUL of bearings. These approaches can be mainly classified into model-based, data-driven, or a combination of both. Model-based approaches use mathematical functions or mappings to represent the physical nature of the failure [3]. Most model-based approaches use the crack growth curves to describe the degradation of rolling bearing, such as the Marco–Starkey theory [4], where statistical estimation methods are applied, e.g., extended Kalman filtering (EKF) [5], to update the prediction over time. Some researchers have favored stochastic processes within model-based approaches because random errors in measurements, working environment uncertainties, and stochastic dynamics in the degradation process could be considered [6]. However, several other variables will influence the final prediction findings, such as fatigue theory, computation method, materials, fracture, and vibration, resulting in a lack of extensibility. Therefore, an increasing number of researchers pay more attention to the data-driven approaches, which use historical failure data to build the degradation model without knowing the physical failure mechanism of the system. A recent review of data-driven methods for RUL prediction can be found in [7].

Data-driven approaches for bearing RUL prediction can be broadly divided into health indicator (HI)-based and direct prediction methods. Using similarity-based interpolation techniques, the first category generates a synthetic HI that depicts the level of system degradation from sensor data. For instance, Huang et al. [8] employed a similarity weighting technique based on Euclidean distance for RUL estimation. They also produced confidence intervals for the predicted RULs using an adaptive kernel density estimation method for managing uncertainty. Likewise, Wang et al. [9] suggested HI curve modeling for online RUL prediction based on sparse Bayesian learning. Yu et al. [10] used a similarity-based HI curve matching method for RUL prediction and a bidirectional recurrent-neural-network-based autoencoder to construct HIs. Although the capability of this group of ways to incorporate new instances is beneficial, the system degradation patterns could be distorted by the data-fusion techniques used to simulate HIs [11].

Machine learning models are explicitly utilized for RUL prediction in direct prediction methods. According to recent studies, HIs are just rescaled RULs and are directly predicted rather than RULs [12], [13]. Recent advances in deep learning have led to the development of numerous direct prediction algorithms.

Manuscript received 22 June 2022; revised 9 August 2022 and 22 August 2022; accepted 4 September 2022. Date of publication 13 September 2022; date of current version 24 May 2023. Paper no. TII-22-2667. (Corresponding author: Muhammad Gibran Alfarizi.)

The authors are with the Department of Mechanical and Industrial Engineering, Faculty of Engineering, Norwegian University of Science and Technology, 7491 Trondheim, Norway (e-mail: muhammad.g.alfarizi@ntnu.no; bahareh.tajjani@ntnu.no; jorn.vatn@ntnu.no; shen.yin@ntnu.no).

Color versions of one or more figures in this article are available at <https://doi.org/10.1109/TII.2022.3206339>.

Digital Object Identifier 10.1109/TII.2022.3206339

Using a deep belief network, Deutsch and He [14] have created RUL prediction models for gears. Li et al. [15] showed that convolutional neural networks perform better than conventional shallow machine learning models when used to predict the RULs of aircraft engines. Wu et al. [16] show that long short-term memory can predict the RULs of aviation engines.

Despite the effectiveness of deep learning models in various prognostics and health management tasks, the lack of datasets makes it difficult to increase the RUL prediction performance [17]. A significant number of parameters must be modified during the training phases of deep learning models. Deep learning models can offer excellent prediction performance on test samples with good generalization abilities when sufficient data are available. In the case of inadequately labeled historical data, training may result in unsatisfactory model parameters that only apply to the information upon which models were trained [18]. In addition, deep learning requires relatively high computational cost and lengthy training time [19]. Other algorithms, such as the random forest (RF) method, can be utilized to overcome the drawbacks of deep learning.

Developed by Breiman (in 2001) [20], RF is an ensemble machine-learning technique. It is a bagging-based approach that integrates many predictors (regression trees) generated randomly using the bootstrapping method. Multiple predictors can minimize complexity and yield superior performance compared to a single predictor. RFs can handle discrete and continuous variables without making assumptions about their distribution and are not susceptible to overfitting [21]. Moreover, the RFs approach minimizes complexity in the following three different ways.

- 1) It keeps complexity low by constructing submodels from sample subsets using the bootstrap.
- 2) It keeps computation speedy by using a parallel ensemble to create submodels on each sample.
- 3) It has fewer hyperparameters to tune in comparison to deep learning [22].

The hyperparameters must be determined optimally to predict the RUL of bearings using RFs. Hyperparameter optimization identifies a set of hyperparameters that minimizes a predetermined loss function when applied to a group of independent data. One approach to optimizing hyperparameters is the grid search approach, which is an exhaustive search over a manually chosen subset of a learning algorithm's hyperparameters space. Another approach, random search, is an improvement relative to grid search because it replaces the exhaustive enumeration of all combinations by randomly selecting them. When only a small number of hyperparameters influences the machine learning algorithm's performance, it can outperform grid search [23]. However, these two approaches are relatively inefficient since they do not select the next hyperparameters to assess depending on the outcomes of the prior evaluations. Previous evaluations do not influence the grid and random searches. They frequently spend a lot of time analyzing "bad" hyperparameters.

For noisy black-box functions, there is a global optimization technique called Bayesian optimization [24]. The Bayesian approach remembers the outcomes of earlier analyses, unlike random or grid search. Using these data, they create a probabilistic model that connects hyperparameters to the probability

of a score on the objective function $P(\text{score} \mid \text{hyperparameters})$. Bayesian hyperparameters optimization is used because it can identify better model configurations in fewer iterations than random search by assessing hyperparameters that appear more promising based on the previous iteration.

The main objective of this article is to assess how accurately the proposed approach can predict the RUL of rolling bearings. The Bayesian optimization algorithm is used to optimize the hyperparameters of the RFs model. To validate the performance of the proposed method, the authors conducted a run-to-failure experiment of rolling bearings and collected the raw acceleration signals. The natural signals are then decomposed into several HIs using the empirical mode decomposition (EMD) [25]. The most significant advantage of the EMD method is that it is adaptive and data-driven, without the need for *a priori* basis function selection for signal decomposition. In addition, EMD, as a widely used signal processing approach, can also analyze nonlinear and non-stationary vibration signals. These HIs are then selected using feature importance from the RFs algorithm and inputted to the RFs-based Bayesian model. Its performance is compared with support vector regression (SVR), LASSO regression, artificial neural networks (ANNs), and conventional RFs. Additionally, the performance of the proposed model is compared with a model-based approach using the Wiener process.

The main contributions of this article can be summarized as follows.

- 1) A framework to construct HIs is proposed by applying EMD and selecting them using feature importance to determine the best feature for RUL prediction.
- 2) A novel data-driven approach is proposed by utilizing the proposed HI framework, RF, and Bayesian optimization to offer precise RUL prediction to overcome the drawbacks of deep learning (e.g., high computational cost and lengthy training time) and improve prediction accuracy.
- 3) The proposed RUL prediction approach is verified by real-world datasets obtained from a run-to-failure experiment of rolling bearings. Furthermore, the performance of the proposed model has been investigated and compared with other data-driven and model-based approaches for RUL prediction of bearings.

The remainder of this article is organized as follows. Section II presents the proposed framework and the preliminaries of our approach. Section III describes the data used in the case study. Section IV discusses the performance of the proposed model in real-world datasets. Section V concludes this article.

II. PROPOSED METHOD

A. Framework of the Proposed Method

Fig. 1 depicts the framework of the proposed method. The initial phase of this framework is focused on feature extraction, in which each of the gathered raw acceleration signals is decomposed into distinct frequency bands to filter out irrelevant frequencies and determine the fault characteristics of the signals. The signal decomposition is performed with EMD. The EMD decomposition is based on the variation in frequency over the bearings' lifespan. The statistical features as indicators (i.e.,

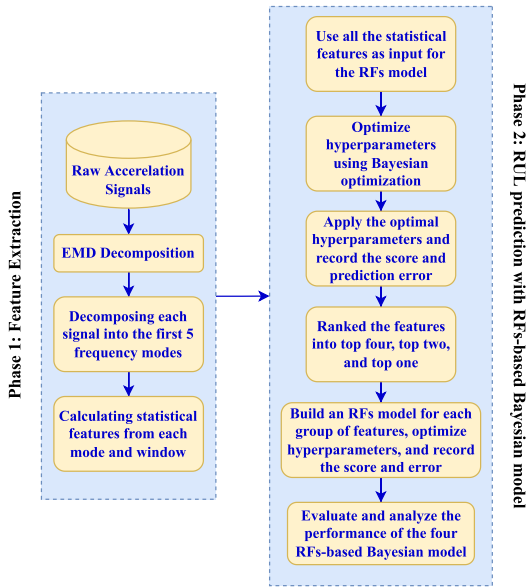


Fig. 1. Framework of the proposed method.

kurtosis, RMS, crest factor, shape factor, impulse factor, skewness, and mean value) are calculated for each intrinsic mode function (IMF) to compare the frequency bands and determine which feature from which band is suitable for predicting RUL of bearings. The EMD decomposition is further elaborated in Section II-B.

The second phase is related to the RUL prediction. The bearing datasets have been obtained by an experimental laboratory with the same operating condition. The statistical features from other bearings' datasets are used as input basis for the RFs-based model to predict the RUL of the current bearing of interest. The hyperparameters of concern (the number of trees in the forest, the maximum depth of the tree, and the minimum number of samples required to be at a leaf node) of every RFs-based model are optimized using Bayesian optimization. The features are then ranked and divided into four groups based on their importance, which results in groups containing all, top four, top two, and top one features. The RFs-based model considers every feature group as the input to predict the RUL of the current bearing of interest. The RUL prediction of every bearing is evaluated based on its score and prediction error. The details of each step will be further elaborated in Section II-F.

B. Empirical Mode Decomposition

Traditional signal-processing techniques assume that the signals are linear or stationary. Thus, they may result in false information and erroneous results. However, among various time-frequency methods, the Hilbert–Huang transform (HHT) is an empirical approach that can analyze stationary and nonstationary signals for fault detection, condition monitoring, and failure prognosis of bearings [25]. HHT is an adaptive data-driven

Algorithm 1: Empirical Mode Decomposition.

Input: Acceleration signal $y(t)$

Identify all local maxima and minima of $y(t)$

for $i = 1$ **to** n **do**

while $j \leq k$ **do**

The upper and lower envelopes, y_u^t and y_l^t , are formed by connecting all local maxima and minima with a cubic spline line, respectively

Calculate the mean of y_u^t , y_l^t , as $m_{i1}^t = (y_u^t + y_l^t)/2$, and $h_{i1}^t = y(t) - m_{i1}^t$

The above sifting process is repeated several times as $h_{ij}^t = h_{i(j-1)}^t - m_{ij}^t$

end while

h_{1k}^t satisfies the definition of IMF and the stopping

condition, SD, where $SD = \sum_{t=0}^T \left(\frac{|h_{i(k-1)}^t - h_{i(k)}^t|}{h_{i(k-1)}^t} \right)^2$,

it becomes IMF, that is, $c_1 = h_{jk}^t$

A new signal, x_1 , is generated by $x_1 = y(t) - c_1$

Repeat above steps as $x_i = x_{i-1} - c_i$

end for

Output: The original signal is decomposed into n IMFs, and one residual x_n

approach that can also handle the nonlinearity of the signals [26]. The first step in HHT is EMD, which decomposes the signals into different segments called IMFs based on their time-domain characteristics. The process of carrying out an EMD approach on an acceleration signal is summarized in Algorithm 1.

C. Random Forests

The RFs algorithm is based on a collection of predictors influenced by each forest tree's random value. To observe the modeling of RFs, input datasets are extracted from a group and then randomized. The higher success of the RFs algorithm is attributable to its efficient handling of big datasets, rapid operational speed, and lack of predictor overfitting [27].

The forest in RFs is built using the p dimension input vector of $X = x_1, x_2, \dots, x_p$. Then, a set of K trees $\{T_1(x), T_2(x), \dots, T_k(x)\}$ is developed inside the forest. Each tree determines its output value, represented as $\hat{Y}_1 = T_1(X), \dots, \hat{Y}_m = T_m(X)$, where $m = 1, \dots, K$. The overall output of the RFs is calculated by the estimation of an average of all tree predictors, mathematically expressed as

$$\text{Predict}_{\text{RFs}}(X) = \frac{1}{K} \sum_{m=1}^K \hat{Y}_m(X). \quad (1)$$

The training dataset $D = D_1, D_2, \dots, D_n = \{(x_1, y_1), (x_2, y_2), \dots, (x_n, y_n)\}$ is taken independently from input and output, where $x_i, i = 1, \dots, n$ denotes the input vector training dataset and $y_i, i = 1, \dots, n$ denotes the output vector training dataset. From the original sample set D , the RF randomly creates K tree sample sets using the bootstrap resampling technique. Approximately one-third of the data in the original sample set D is not drawn in bootstrap samples;

Algorithm 2: Random Forest.

Input: Training samples $D = \{(x_1, y_1), \dots, (x_n, y_n)\}$, testing samples x_t

for $m = 1$ to K **do**

Construct the bootstrap sample D_m randomly from the original training set D with replacement

Create a nonpruning decision tree \hat{Y}_m through D_m

Pick n_{try} features at random from N features

Choose the best feature from each node's n_{try} features to split

Split the tree until it reaches its maximum size

end for

Output: A set of decision trees $\{\hat{Y}_m, m = 1, 2, \dots, K\}$.

The decision tree \hat{Y}_m generates the predictor $\hat{Y}_m(x_t)$ for the testing samples. The overall output of the RFs is calculated as in (1)

these data are known as out-of-bag (OOB) data, whereas the remaining data are known as in-bag data. Pseudocode of the RF algorithm [20] is described in Algorithm 2.

As stated previously, the growth of each tree depends on a bootstrap sample containing almost two-thirds of the training data. Testing is done with the remaining training data (OOB). As shown in the following equation, the MSE of the OOB error is derived by deducting the predicted values from the reference values

$$\text{MSE} \approx \text{MSE}^{\text{OOB}} = \frac{1}{N} \sum_{i=1}^N (\hat{Y}(X_i) - Y_i)^2 \quad (2)$$

where $\hat{Y}(X_i)$ denotes the predicted output, Y_i denotes the observed output, and N represents the total number of samples.

D. Bayesian Optimization

Bayesian optimization produces a probabilistic model of the function mapping from hyperparameter values to the objective as evaluated by a validation set when used for hyperparameter optimization. Bayesian optimization is an iterative procedure that involves two fundamental components: 1) a probabilistic surrogate model and 2) an acquisition function to determine the next point to examine. In each iteration, the surrogate model is fitted to all previous observations of the target function. After that, the acquisition function, which utilizes the probabilistic model's predictive distribution, decides the utility of various prospective spots while balancing exploitation and exploration. The acquisition function can be thoroughly tuned because it is inexpensive to compute compared to assessing the costly black-box process.

A visual representation of Bayesian optimization is shown in Fig. 2. After two evaluations, the black line represents the surrogate model's initial estimate, with the related uncertainty shown in gray. The surrogate model falls short of the actual objective function shown in red.

The surrogate function after eight evaluations is shown in Fig. 3. The real objection function is now matched with the surrogate function. In light of this, the hyperparameters that

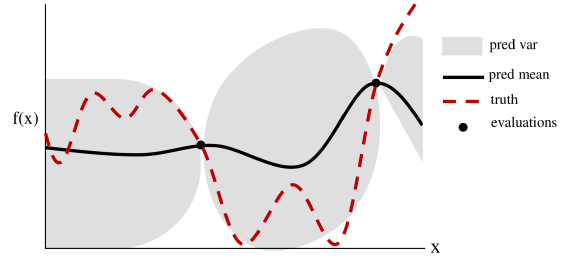


Fig. 2. Bayesian optimization run after two evaluations. Modified from Snoek et al. [28].

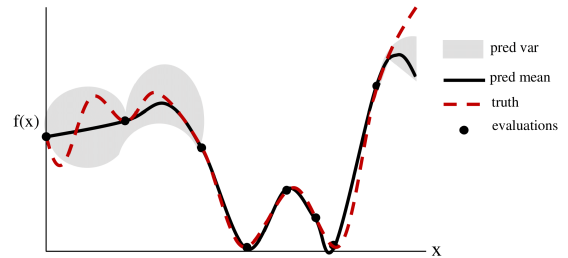


Fig. 3. Bayesian optimization run after eight evaluations. Modified from Snoek et al. [28].

maximize the surrogate will also optimize the actual objective function.

One of the acquisition functions is expected improvement (EI)

$$\text{EI}_{y^*}(x) = \int_{-\infty}^{y^*} (y^* - y)p(y|x)dy \quad (3)$$

where y^* is the objective function's threshold value, the objective function value y is calculated using the hyperparameters x and the surrogate probability model $p(y|x)$ expresses the probability that y will occur given x . The goal is to maximize the EI concerning x .

The tree-structured Parzen estimator applies the Bayes rule, which is expressed as

$$p(y|x) = \frac{p(x|y) * p(y)}{p(x)} \quad (4)$$

to construct a model where the probability of the hyperparameters given the score on the objective function is denoted by $p(x|y)$, which may be written as

$$p(x|y) = \begin{cases} l(x) & \text{if } y < y^* \\ g(x) & \text{if } y \geq y^* \end{cases} \quad (5)$$

where $y < y^*$ denotes an objective function value below the threshold. According to this equation, there are two possible distributions for the hyperparameters: One in which the objective function value is lower than the threshold ($l(x)$) and another in which it is greater ($g(x)$).

Since the $l(x)$ distribution only includes x that resulted in scores below the threshold, draw values of x from this distribution are superior. Bayes' rule also supports it since the EI

Algorithm 3: Bayesian Hyperparameter Optimization.

Input: (hyperparameter space Θ , Target score function $H(\theta)$, max number of evaluation n_{\max})
 Select an initial configuration $\theta_0 \in \Theta$
 Evaluate the initial score $y_0 = H(\theta_0)$
 Set $\theta^* = \theta_0, y^* = H(\theta_0)$, and $S_0 = \{\theta_0, y_0\}$
for $n = 1$ **to** n_{\max} **do**
 Select a new hyperparameter configuration $\theta_n \in \Theta$ by maximizing EI in (6)
 Evaluate H in θ_n to obtain a new numeric score $y_n = H(\theta_n)$
 Augment the data $S_n = S_{n-1} \cup \{\theta_n, y_n\}$
 Update the surrogate model
 if $y_n < F^*$ **then**
 $\theta^* = \theta_n$ and $y^* = y_n$
 end if
end for
Output: θ^* and y^*

equation becomes

$$\text{EI}_{y^*}(x) = \frac{\gamma y^* l(x) - l(x) \int_{-\infty}^{y^*} p(y) dy}{\gamma l(x) + (1 - \gamma) g(x)} \propto \left(\gamma + \frac{g(x)}{l(x)} (1 - \gamma) \right)^{-1} \quad (6)$$

which states that the EI is inversely proportional to $\frac{l(x)}{g(x)}$. Therefore, this ratio will be maximized when values for x are taken from $l(x)$, increasing the EI. The variable γ represents the quantile of the negative accuracy scores (observed thus far), used as a cutoff point, and defines the threshold y^* . This user-defined cutoff point is often set at 15% by default.

Before saving the results and scores, the algorithm compares each new set of hyperparameters it proposes with the real objective function. The algorithm builds a probabilistic model that gets better with each iteration by computing $l(x)$ and $g(x)$ using the account of the objective function.

In conclusion, a preliminary estimate of the surrogate function is developed and modified as new information becomes available. When there are enough evaluations of surrogate functions, the objective function will eventually be adequately reflected. The objective function would also be maximized by the same hyperparameters that maximize the EI. The pseudocode for Bayesian hyperparameter optimization is presented in Algorithm 3.

E. Model Evaluation

A score function is defined to evaluate the model's performance by comparing the actual and predicted RUL of bearings. The score function is based on the percent errors of predictions, which is defined as

$$\% \text{Error} = 100 \times \frac{\text{Act RUL} - \widehat{\text{RUL}}}{\text{Act RUL}}. \quad (7)$$

The early prediction of RUL (i.e., cases where $\% \text{Error} > 0$) and late prediction of RUL (i.e., cases where $\% \text{Error} \leq 0$) will be

TABLE I
INITIAL HYPERPARAMETERS AND THEIR SEARCH RANGE

Hyperparameter	Initial Value	Search Space
The number of trees	100	[10:500]
The maximum depth of tree	50	[2:100]
The minimum leaf per tree	1	[1:50]

treated differently. Thus, a penalty function, expressed in (8), is introduced, which penalizes late RUL predictions more than early ones. Late RUL predictions might result in more severe consequences and are more crucial than early ones [29]

$$A_i = \begin{cases} \exp(-\ln(0.5) \cdot (\% \text{Error}/5)) & \text{if } \% \text{Error} \leq 0 \\ \exp(+\ln(0.5) \cdot (\% \text{Error}/20)) & \text{if } \% \text{Error} > 0. \end{cases} \quad (8)$$

Moreover, accurate RUL predictions at the later stage of a bearing's lifetime are more vital than predictions at the early stage. So, higher weights are given to the predictions near the bearing's time to failure. The weight is assigned linearly as the first prediction data point weights 1, and the n th prediction weights n . The score function is then defined as

$$\text{Score} = \frac{\sum_{i=1}^n w_i \times A_i}{\sum_{i=1}^n w_i} \quad (9)$$

where n is the number of samples, and w_i is the weight of i th prediction.

In addition to the score function, the root-mean-square relative error (RMSRE) is also calculated. RMSRE is expressed as

$$\text{RMSRE} = \sqrt{\frac{1}{n} \sum_{i=1}^n \left(\frac{\text{Act RUL} - \widehat{\text{RUL}}}{\text{Act RUL}} \right)^2}. \quad (10)$$

A higher score and lower RMSRE values indicate that the model's predictive abilities for RUL prediction are superior.

F. Framework of the Proposed RFs-Based Bayesian Model

The proposed model's objective is to accurately predict the RUL of rolling bearings. The RFs regression model is responsible for predicting the RUL while Bayesian optimization will optimize the RFs model's hyperparameters to increase its prediction accuracy. The RUL prediction of bearings begins with specifying the input sample, the features, and the hyperparameters' initial values. The initial hyperparameters and their search range are summarized in Table I.

The optimal hyperparameter settings will decrease prediction error [30]. According to the literature, no analytical formula exists to find the optimum set of hyperparameters [31]. Thus, Bayesian optimization is combined with the RFs model to determine the optimal hyperparameter settings, resulting in lower prediction error. The objective of the optimization is to minimize the MSE of the RFs model. The flowchart of the proposed RFs-based Bayesian model is shown in phase 2 of Fig. 1.

The steps involved in phase 2 of the flowchart are explained as follows.

TABLE II
BEARINGS AND THEIR NUMBER OF SAMPLES

Bearing	B1	B2	B3	B4	B5
Number of samples	110	35	146	106	77
Bearing	B6	B7	B8	B9	B10
Number of samples	248	150	143	114	115

- 1) The samples and features are obtained from the feature extraction phase with EMD decomposition using other bearings' data for each bearing. The features used for input are kurtosis, RMS, crest factor, shape factor, impulse factor, skewness, and mean value. The output is the RUL of bearings for every timestep.
- 2) The hyperparameters (see Table I) are set to the initial values and then optimized using Bayesian optimization. It was observed that most of the time, the value of the surrogate function does not improve after 40 evaluations; the maximum number of evaluations is set to 50.
- 3) The optimal set of hyperparameters is applied to the RFs model, and the score and the RMSRE are recorded for model evaluation.
- 4) The features are ranked based on their importance in predicting the RUL of bearings using RFs feature importance and SHAP importance analysis. The best 50% of the features are selected and then ranked again. The process is repeated, and as a result, the features are divided into the top four, the top two, and the top one.
- 5) Build an RFs model for each group of features and repeat steps 2 and 3. In total, there are four different RFs models for each bearing.
- 6) Evaluate and analyze the performance of the four RFs-based Bayesian models.

III. CASE STUDY

A. Data Description

A set of run-to-failure experimental tests on roller bearings is designed to illustrate the effectiveness of the proposed approach. The bearings are operated under similar laboratory conditions with the same motor speed of 2975 r/min. The original data are a batch of acceleration signals in the horizontal direction collected from the bearings' healthy state until the acceleration amplitude crosses the level of $10g$ where the experiments ceased. The bearings are degraded by contamination, i.e., pouring a mixture of Silicon carbide solid particles and lubricant onto the bearing at regular intervals until the stopping threshold (i.e., $10g$) is reached. Table II lists the number of samples of different bearings from a healthy state to a failed state. The details of the data and the vibration setup used to conduct the experiments can be found in [32].

B. Health Indicator

In this section, EMD is implemented to decompose each horizontal acceleration signal over different frequency ranges according to the signal's time-scale characteristics resulting in

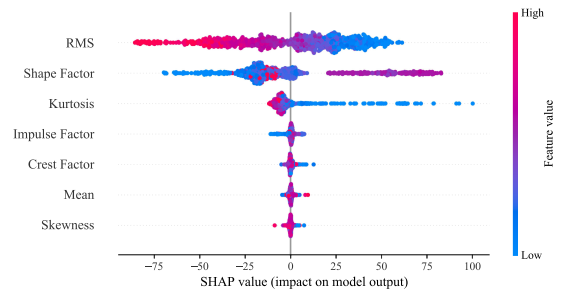


Fig. 4. SHAP variable importance plot for B10.

a series of IMFs. Comparing different IMFs with their feature scales for each signal gives insights into the relevant or informative frequencies and features concerning the bearings' faults. The statistical features will then be calculated from each of the first 5 IMFs of the acceleration signals. The first IMF in EMD is the dominant feature among all with the highest value of fitness function (i.e., metric that combines monotonicity, trendability, and prognosability). It is thus chosen for the HIs. Table III shows how to calculate the statistical features where M is the number of measurements in one sample, c_i is the processed signal measurements obtained by the EMD algorithm, and the mean and standard deviation are m and σ , respectively.

In every bearing, the RMS feature has the highest value in monotonicity, prognosability, and trendability, which means it is the essential feature for RUL prediction. The RFs feature importance and SHAP importance analysis also corroborate this finding, as RMS is the critical feature for every bearing. RMS is also the only feature that visually trends upward as time passes, indicating higher degradation over time until bearing failure. However, the value of RMS in one bearing cannot be compared to other bearings, as the RMS value at failure time is different in every bearing. Thus, the RMS feature must be considered individually.

IV. EXPERIMENT RESULTS AND ANALYSIS

A. Model Results

Fig. 4 shows the SHAP variable importance plot for B10. The plot shows that the RUL prediction depends on the RMS feature. Moreover, the RMS is negatively correlated with the RUL value, which means that the higher the RMS value, the lower the RUL value. This correlation makes sense since higher RMS indicates higher degradation, which means lower the RUL of the bearing. The SHAP variable importance plot shows similar results for other bearings.

Tables IV and V show the score and RMSRE of the RFs-based Bayesian model for every bearing after hyperparameters optimization is applied to every group of features. Fig. 5 shows the RUL prediction for every bearing with the best score.

Tables IV and V show that the proposed model, on average, produces the highest score and lowest RMSRE when using only the top two features. However, the differences in score and error are only significant when using only one feature and insignificant

TABLE III
FORMULA FOR STATISTICAL FEATURES

Feature	Kurtosis	RMS	Crest factor	Skewness
Formula	$K = \frac{\sum_{i=1}^M (c_i - m)^4}{(M-1)\sigma^4}$	$RMS = \sqrt{\frac{1}{M} \sum_{i=1}^M c_i^2}$	$CF = \frac{\max(c_i)}{\sqrt{\frac{1}{M} \sum_{i=1}^M c_i^2}}$	$S = \frac{\sum_{i=1}^M (c_i - m)^3}{(M-1)\sigma^3}$
Feature	Mean	Shape factor	Impulse factor	
Formula	$Mean = \frac{1}{M} \sum_{i=1}^M c_i$	$SF = \frac{\sqrt{\frac{1}{M} \sum_{i=1}^M c_i^2}}{\frac{1}{M} \sum_{i=1}^M c_i }$	$IF = \frac{\max c_i }{\frac{1}{M} \sum_{i=1}^M c_i }$	

TABLE IV
SCORE OF RUL PREDICTIONS FOR EVERY BEARING

Score	B1	B2	B3	B4	B5	B6	B7	B8	B9	B10	Average
All features	0.7621	0.7950	0.9277	0.9533	0.8760	0.9648	0.8809	0.9516	0.9094	0.9461	0.8967
4 features	0.7636	0.7853	0.9307	0.9580	0.8643	0.9634	0.8972	0.9537	0.9164	0.9487	0.8981
2 features	0.7761	0.8597	0.9362	0.9612	0.9329	0.9641	0.8447	0.9603	0.9135	0.9429	0.9092
1 feature	0.9536	0.6414	0.8151	0.8413	0.8096	0.9645	0.8532	0.8266	0.7917	0.8306	0.8328

TABLE V
RMSRE OF RUL PREDICTIONS FOR EVERY BEARING

RMSRE	B1	B2	B3	B4	B5	B6	B7	B8	B9	B10	Average
All features	2.6739	2.2487	1.3654	0.7220	1.1861	0.8493	1.4983	0.8499	1.4479	0.9599	1.3801
4 features	2.6187	2.2637	1.0971	0.6671	1.4759	0.9307	1.3785	0.8547	1.4315	0.8149	1.3533
2 features	2.3878	1.3728	1.2691	0.6417	0.7147	0.8891	1.8001	0.7249	1.2908	1.1332	1.2224
1 feature	0.5278	4.2387	4.3198	3.4316	1.7146	0.8916	1.8849	5.5522	7.3177	2.9226	3.2802

otherwise. The top feature here is the RMS feature. This difference suggests that using multiple HIs is beneficial for predicting RUL values. Many HIs can provide better information about the bearing's health condition than only one. The proposed model also runs efficiently due to the use of Bayesian optimization to update parameters, which avoids the high computational cost and lengthy training time.

There are differences between the proposed method as a data-driven approach and the Wiener process as a stochastic approach. In the Wiener process, the underlying randomness or the probabilistic behavior in the bearings' degradation is considered while the uncertainty of the failure threshold is also considered at each timestep. On the other hand, the proposed method can provide better RUL prediction results regarding score and error without determining a failure threshold.

Fig. 5 shows that the prediction results of the proposed model are close to the actual RUL values in most of the bearings, especially near the end of the bearings' lifetime, where the RUL prediction matters most. Generally, the proposed model performs better when the bearing has an average number of samples (i.e., 100–110 samples) like bearing 1, 4, 9, and 10. However, the model does not give an accurate RUL prediction when the bearing only has a small number of samples (i.e., short lifetime), such as bearing 2 and 5. According to the manufacturer, the average lifespan of such bearings is between 8 and 12 hours. Consequently, bearing 2 and 5 are atypical, and there may be technical problems in conducting experiments. The technical issue may be caused by the accelerometers not being correctly mounted to the bearings, resulting in erroneous signals. In addition, the predictions of bearing 6 perform poorly compared to the other bearings. Its inferior prediction could be due to its higher number of samples (248) than others.

Because the RFs model learned from other bearings datasets to make predictions, it has not seen samples higher than 200 and, therefore, makes outrageous predictions.

Generally, at the beginning of a bearing's lifespan, the model has a more considerable prediction error, and this is due to some uncertainty in the input data. At the middle and deterioration stages, when the bearings are approaching failure, the uncertainty has decreased because more degradation data have been seen and utilized to capture the degradation trend, resulting in a more accurate RUL prediction.

B. Results Validation

A comparison with other data-driven algorithms is made to corroborate the proposed model's performance, including conventional RFs, ANNs [33], SVR [34], and LASSO regression [35]. The hyperparameters of ANN (number of layers, hidden unit, and learning rate), SVR (gamma and C), and LASSO (alpha) are optimized with Bayesian hyperparameters optimization. Moreover, the performance of the proposed model is also compared with a model-based approach using the Wiener process. The average score and RMSRE are recorded for every method and summarized in Table VI. The proposed method results are bolded in Table VI.

Based on the score and RMSRE in Table VI, the proposed method outperforms all other ways to predict the RUL of bearings. Compared to conventional RFs, the proposed model has improved the average score by 3% and reduced the average error by 9%. Furthermore, compared to the Wiener process, the proposed model has enhanced the average score by 6% and reduced the average error by 54%. A higher score and lower

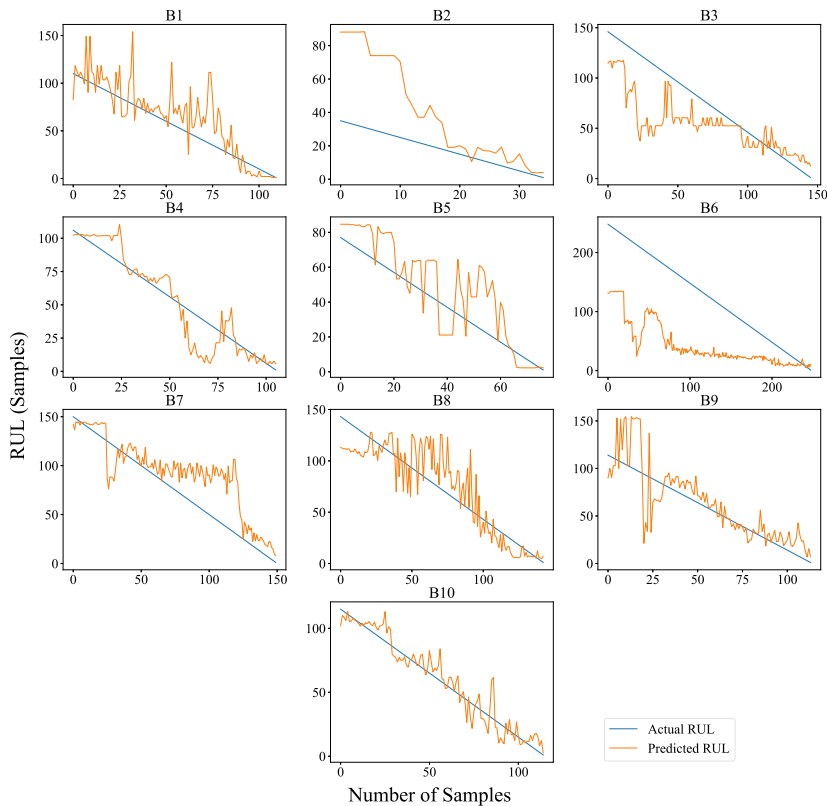


Fig. 5. Best RUL prediction of every bearing.

TABLE VI
SCORE AND RMSRE OF ALL METHODS

Method	Avg. Score	Avg. RMSRE
Proposed method	0.9092	1.2224
Conventional RFs	0.8856	1.3375
ANN	0.7735	6.5496
SVR	0.7581	7.5216
LASSO	0.8196	3.6325
Wiener process	0.8606	2.6301

RMSRE values imply that the model's predictive capabilities for RUL prediction are superior.

V. CONCLUSION

This article proposes a data-driven framework for predicting the RUL of bearings. The framework consists of the feature extraction phase and RUL prediction phase. EMD performed the feature extraction to decompose input signals into different frequency bands to identify signal fault characteristics. Then, an RFs-based model combined with Bayesian hyperparameters optimization was developed to predict the RUL of bearings. A run-to-failure experiment of roller bearings was performed to validate the proposed method. Score function and RMSRE were used to evaluate the method's performance. The proposed

method outperforms other data-driven and model-based approaches in terms of score and error. Additionally, the proposed approach requires relatively low computational cost and fast training time compared to the deep learning approach. However, like any RFs-based method, one has to find a tradeoff between the training time and prediction accuracy. RF is also a black box algorithm, so the results are not easily interpretable, i.e., it does not provide complete visibility into the coefficients like linear regression.

For further research, a more detailed investigation is required to compare the proposed method and the stochastic Wiener process depending on the decision context, the length of the dataset or the bearing's lifetime, accuracy of the prediction results on the two distinct healthy stages, and deterioration stage of bearings, as well as their mathematical complexity and computational time.

REFERENCES

- [1] W. Mao, J. Chen, J. Liu, and X. Liang, "Self-supervised deep domain-adversarial regression adaptation for online remaining useful life prediction of rolling bearing under unknown working condition," *IEEE Trans. Ind. Informat.*, 2022, doi: [10.1109/TII.2022.3172704](https://doi.org/10.1109/TII.2022.3172704).
- [2] Y. Qin, D. Chen, S. Xiang, and C. Zhu, "Gated dual attention unit neural networks for remaining useful life prediction of rolling bearings," *IEEE Trans. Ind. Informat.*, vol. 17, no. 9, pp. 6438–6447, Sep. 2021.

- [3] M. G. Alfarizi, J. Vatn, and S. Yin, "An extreme gradient boosting aided fault diagnosis approach: A case study of fuse test bench," *IEEE Trans. Artif. Intell.*, 2022, doi: [10.1109/TAI.2022.316137](https://doi.org/10.1109/TAI.2022.316137).
- [4] L. Cortese, F. Nalli, and M. Rossi, "A nonlinear model for ductile damage accumulation under multiaxial non-proportional loading conditions," *Int. J. Plast.*, vol. 85, pp. 77–92, 2016.
- [5] L. Cui, X. Wang, Y. Xu, H. Jiang, and J. Zhou, "A novel switching unscented Kalman filter method for remaining useful life prediction of rolling bearing," *Measurement*, vol. 135, pp. 678–684, 2019.
- [6] Z. Zhang, X. Si, C. Hu, and Y. Lei, "Degradation data analysis and remaining useful life estimation: A review on wiener-process-based methods," *Eur. J. Oper. Res.*, vol. 271, no. 3, pp. 775–796, 2018.
- [7] Y. Lei, N. Li, L. Guo, N. Li, T. Yan, and J. Lin, "Machinery health prognostics: A systematic review from data acquisition to RUL prediction," *Mech. Syst. Signal Process.*, vol. 104, pp. 799–834, 2018.
- [8] C.-G. Huang, H.-Z. Huang, W. Peng, and T. Huang, "Improved trajectory similarity-based approach for turbofan engine prognostics," *J. Mech. Sci. Technol.*, vol. 33, no. 10, pp. 4877–4890, 2019.
- [9] P. Wang, B. D. Youn, and C. Hu, "A generic probabilistic framework for structural health prognostics and uncertainty management," *Mech. Syst. Signal Process.*, vol. 28, pp. 622–637, 2012.
- [10] W. Yu, I. Y. Kim, and C. Mechefske, "An improved similarity-based prognostic algorithm for RUL estimation using an RNN autoencoder scheme," *Rel. Eng. Syst. Saf.*, vol. 199, 2020, Art. no. 106926.
- [11] R. Khelif, S. Malinowski, B. Chebel-Morello, and N. Zerhouni, "RUL prediction based on a new similarity-instance based approach," in *Proc. IEEE 23rd Int. Symp. Ind. Electron.*, 2014, pp. 2463–2468.
- [12] J. Zhang, Y. Jiang, S. Wu, X. Li, H. Luo, and S. Yin, "Prediction of remaining useful life based on bidirectional gated recurrent unit with temporal self-attention mechanism," *Rel. Eng. Syst. Saf.*, vol. 221, 2022, Art. no. 108297.
- [13] J. Zhang, Y. Jiang, X. Li, M. Huo, H. Luo, and S. Yin, "An adaptive remaining useful life prediction approach for single battery with unlabeled small sample data and parameter uncertainty," *Rel. Eng. Syst. Saf.*, vol. 222, 2022, Art. no. 108357.
- [14] J. Deutsch and D. He, "Using deep learning-based approach to predict remaining useful life of rotating components," *IEEE Trans. Syst., Man, Cybern. Syst.*, vol. 48, no. 1, pp. 11–20, Jan. 2018.
- [15] X. Li, Q. Ding, and J.-Q. Sun, "Remaining useful life estimation in prognostics using deep convolution neural networks," *Rel. Eng. Syst. Saf.*, vol. 172, pp. 1–11, 2018.
- [16] Y. Wu, M. Yuan, S. Dong, L. Lin, and Y. Liu, "Remaining useful life estimation of engineered systems using vanilla LSTM neural networks," *Neurocomputing*, vol. 275, pp. 167–179, 2018.
- [17] C. Sun, M. Ma, Z. Zhao, S. Tian, R. Yan, and X. Chen, "Deep transfer learning based on sparse autoencoder for remaining useful life prediction of tool in manufacturing," *IEEE Trans. Ind. Informat.*, vol. 15, no. 4, pp. 2416–2425, Apr. 2019.
- [18] D. Yoo, H. Fan, V. Boddeti, and K. Kitani, "Efficient k-shot learning with regularized deep networks," in *Proc. AAAI Conf. Artif. Intell.*, vol. 32, no. 1, 2018, pp. 4382–4389.
- [19] C. Ferreira and G. Gonçalves, "Remaining useful life prediction and challenges: A literature review on the use of machine learning methods," *J. Manuf. Syst.*, vol. 63, pp. 550–562, 2022.
- [20] L. Breiman, "Random forests," *Mach. Learn.*, vol. 45, no. 1, pp. 5–32, 2001.
- [21] C. Lei et al., "A comparison of random forest and support vector machine approaches to predict coal spontaneous combustion in gob," *Fuel*, vol. 239, pp. 297–311, 2019.
- [22] I. A. Ibrahim and T. Khatib, "A novel hybrid model for hourly global solar radiation prediction using random forests technique and firefly algorithm," *Energy Convers. Manage.*, vol. 138, pp. 413–425, 2017.
- [23] J. Bergstra and Y. Bengio, "Random search for hyper-parameter optimization," *J. Mach. Learn. Res.*, vol. 13, no. 2, pp. 281–305, Feb. 2012.
- [24] J. Mockus, *Bayesian Approach to Global Optimization: Theory and Applications*. Berlin, Germany: Springer, 2012, vol. 37.
- [25] Y. Lei, J. Lin, Z. He, and M. J. Zuo, "A review on empirical mode decomposition in fault diagnosis of rotating machinery," *Mech. Syst. Signal Process.*, vol. 35, no. 1/2, pp. 108–126, 2013.
- [26] Q. Miao, D. Wang, and M. Pecht, "Rolling element bearing fault feature extraction using EMD-based independent component analysis," in *Proc. IEEE Conf. Prognostics Health Manage.*, 2011, pp. 1–6.
- [27] M. H. Lipu et al., "Real-time state of charge estimation of lithium-ion batteries using optimized random forest regression algorithm," *IEEE Trans. Intell. Veh.*, 2022, doi: [10.1109/TIV.2022.3161301](https://doi.org/10.1109/TIV.2022.3161301).
- [28] J. Snoek, H. Larochelle, and R. P. Adams, "Practical Bayesian optimization of machine learning algorithms," in *Proc. 25th Int. Conf. Neural Inf. Process. Syst.*, Red Hook, NY, USA, 2012, vol. 2, pp. 2951–2959.
- [29] P. Nectoux et al., "Pronosta: An experimental platform for bearings accelerated degradation tests," in *Proc. IEEE Int. Conf. Prognostics Health Manage.*, 2012, pp. 1–8.
- [30] I. A. Ibrahim, M. Hossain, and B. C. Duck, "An optimized offline random forests-based model for ultra-short-term prediction of PV characteristics," *IEEE Trans. Ind. Informat.*, vol. 16, no. 1, pp. 202–214, Jan. 2020.
- [31] A. Liaw et al., "Classification and regression by RandomForest," *R News*, vol. 2, no. 3, pp. 18–22, 2002.
- [32] B. Tajiani and J. Vatn, "RUL prediction of bearings using empirical wavelet transform and Bayesian approach," in *Proc. 31st Eur. Saf. Rel. Conf.*, 2021, pp. 2006–2013.
- [33] A. Krogh, "What are artificial neural networks?," *Nature Biotechnol.*, vol. 26, no. 2, pp. 195–197, 2008.
- [34] M. Awad and R. Khanna, "Support vector regression," in *Efficient Learning Machines*. Berlin, Germany: Springer, 2015, pp. 67–80.
- [35] L. Meier, S. Van De Geer, and P. Bühlmann, "The group LASSO for logistic regression," *J. Roy. Stat. Soc.: Ser. B (Stat. Methodol.)*, vol. 70, no. 1, pp. 53–71, 2008.



Muhammad Gibran Alfarizi received the B.Sc. degree from the Bandung Institute of Technology, Bandung, Indonesia, in 2017, and the M.Sc. degree from the Norwegian University of Science and Technology, Trondheim, Norway, in 2020, both in petroleum engineering. He is currently working toward the Ph.D. degree in reliability, availability, maintainability, and safety with the Norwegian University of Science and Technology.



Bahareh Tajiani received the bachelor's degree in industrial engineering from the University of Tehran, Tehran, Iran, in 2016, and the master's degree in reliability, availability, maintenance, and safety (RAMS) from the Norwegian University of Science and Technology (NTNU), Trondheim, Norway, in 2019. She is currently working toward the Ph.D. degree with RAMS group, NTNU.

Her main research interests include stochastic modeling, accelerated life tests, and signal processing.



Jorn Vatn received the M.Sc. degree in mathematical statistics and the Ph.D. degree with a dissertation on maintenance optimization from the Norwegian University of Science and Technology (NTNU), Trondheim, Norway, in 1986 and 1996, respectively.

He has more than 30 years of experience as a Researcher with SINTEF. He is currently a Professor with Department of Mechanical and Industrial Engineering, Norwegian University of Science and Technology, Trondheim, Norway.



Shen Yin (Senior Member, IEEE) received the M.Sc. degree in control and information system and Ph.D. (Dr.-Ing.) degree in electrical engineering and information technology from the University of Duisburg-Essen, Duisburg, Germany, in 2007 and 2012, respectively.

He is currently a Full Professor (DNV-GL Professor) with the Department of Mechanical and Industrial Engineering, Norwegian University of Science and Technology, Trondheim, Norway. His research interests include fault diagnosis/prognosis and fault-tolerance strategy, safety, reliability, and security of complicated systems, system and control theory, data-driven and machine learning approaches, and applications in health diagnosis and cyber-physical systems.

ISBN 978-82-326-7610-1 (printed ver.)
ISBN 978-82-326-7609-5 (electronic ver.)
ISSN 1503-8181 (printed ver.)
ISSN 2703-8084 (online ver.)



NTNU

Norwegian University of
Science and Technology